



LUND UNIVERSITY

Development of Spatial Sequencing Methods and Applications for Brain Circuit Repair in Parkinson's Disease

Rajova, Jana

2023

Document Version:

Publisher's PDF, also known as Version of record

[Link to publication](#)

Citation for published version (APA):

Rajova, J. (2023). *Development of Spatial Sequencing Methods and Applications for Brain Circuit Repair in Parkinson's Disease*. [Doctoral Thesis (compilation), Department of Experimental Medical Science]. Lund University, Faculty of Medicine.

Total number of authors:

1

General rights

Unless other specific re-use rights are stated the following general rights apply:

Copyright and moral rights for the publications made accessible in the public portal are retained by the authors and/or other copyright owners and it is a condition of accessing publications that users recognise and abide by the legal requirements associated with these rights.

- Users may download and print one copy of any publication from the public portal for the purpose of private study or research.
- You may not further distribute the material or use it for any profit-making activity or commercial gain
- You may freely distribute the URL identifying the publication in the public portal

Read more about Creative commons licenses: <https://creativecommons.org/licenses/>

Take down policy

If you believe that this document breaches copyright please contact us providing details, and we will remove access to the work immediately and investigate your claim.

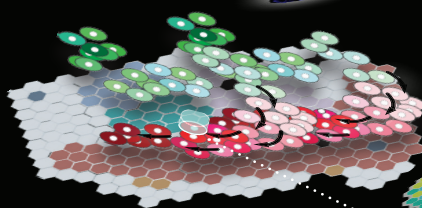
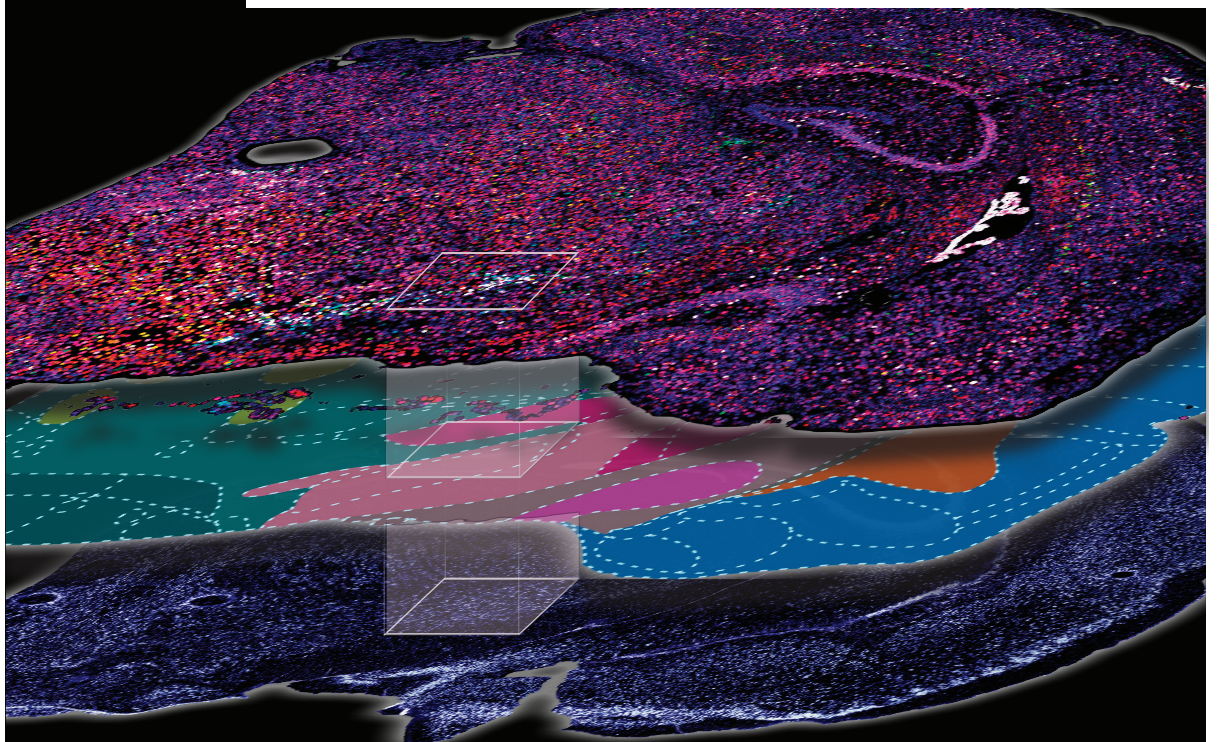
LUND UNIVERSITY

PO Box 117
221 00 Lund
+46 46-222 00 00

Development of Spatial Sequencing Methods and Applications for Brain Circuit Repair in Parkinson's Disease

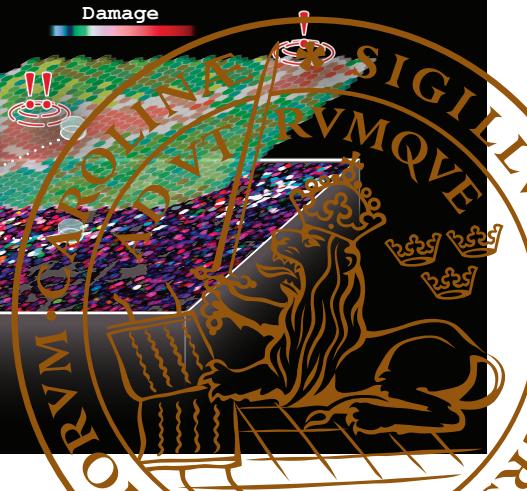
JANA RÁJOVÁ

EXPERIMENTAL MEDICAL SCIENCES | FACULTY OF MEDICINE | LUND UNIVERSITY



DAergic Neuron

Area: SN - A9
Coordinates: (2.8, -4,5, 7.9)
Identifier: TH, GIRK2
Status: Dying



Development of Spatial Sequencing Methods and Applications for Brain Circuit Repair in Parkinson's Disease

Jana Rájová



LUND
UNIVERSITY

DOCTORAL DISSERTATION

By due permission of Faculty of Medicine of Lund University, this thesis will be publicly defended on 23rd of October at 9.00 in Segerfalksalen, BMC A10 Klinikgatan 32, Lund, Sweden

Thesis advisor:

Prof. Tomas Björklund

Faculty opponent:

Prof. Sten Linnarsson

Karolinska Institute
Stockholm, Sweden

Organization: LUND UNIVERSITY
Department of Experimental Medical Science
Box 118
SE-221 00 LUND
Sweden

Document name: DOCTORAL DISSERTATION

Date of issue:2023-10-23

Sponsoring organization:Lund University

Author:

Jana Rájová

Title and subtitle:

Development of Spatial Sequencing Methods and Applications for Brain Circuit Repair in Parkinson's Disease

Abstract

Tools for transcriptional analysis have claimed their place as some of the most ubiquitously used methods for profiling cells and tissues. However, many of these tools currently depend on tissue dissociation, losing out on broader patterns. While a deeper understanding of the cellular components and their relatedness brought vast knowledge about the individual tissue constituents, much information is left untapped. This thesis presents tools that can tap into some of these additional informational layers and expand the view in which many conditions are understood.

A primary focus of this thesis lies within the context of spatial transcriptome analysis. To this end, we began by showcasing the utility of this approach by exploring the transcriptomic landscape of hESC-derived dopaminergic transplants. With profiling of the tissue transcriptome down to 100 μm , we can take a deeper look into the transcriptional patterns of the underlying cellular populations, revealing a large number of dopaminergic neurons resembling those native to substantia nigra, coexisting with a robust glial cell population. We further relate these findings to a published single-cell RNA sequencing analysis, revealing overlap of the vast majority of the cellular populations, and through immunohistological analysis, we bring the focus back into the tissue and confirm that the picture given by spatial transcriptomics provides quantitatively accurate information.

Inspired by this finding, we continue our investigation in the spatial transcriptomics area. Moving from unbiased capture to targeted transcript detection, we take on the task of providing large and easy-to-scale-and-generate probe libraries for the legion of incoming transcriptome analysis methods utilizing hefty collections of padlock probes and modified cDNA primers. We demonstrate the generation of these libraries by employing a minimal amount of a highly diverse construct array, its amplification to a milligram scale, and a release of the target sequences into a ready-to-use library. We follow this with a demonstration of the resulting library on gene expression profiling in rodent brain.

In the latter part, we switch focus to another goal, the analysis of cellular trajectories throughout pathology progression. We demonstrate this by modeling transcriptional changes associated with the transition from the healthy state into the early stages of pathology brought on by an overload of α -synuclein, a protein heavily implicated in Parkinson's disease. Lastly, this thesis explores a hypothesis of inter-neuronal transport of the retrotransposon ARC protein *in vivo*. To this end, we employ an extensive toolkit for monitoring of *Arc* expression and its protein movement and interactions, ultimately reinforcing the ARC inter-neuronal transport hypothesis.

Key words

spatial transcriptomics, pseudotime, method development, RCA, *in situ* sequencing, tissue analysis, Parkinson's Disease

Classification system and/or index terms (if any):

Supplementary bibliographical information:

Lund University, Faculty of Medicine Doctoral Dissertation Series 2023:123

Language:

English

ISSN and key title:

1652-8220

ISBN:

978-91-8021-464-3

Recipient's notes:

Number of pages:

119

Price

Security classification:

I, the undersigned, being the copyright owner of the abstract of the above-mentioned dissertation, hereby grant to all reference sources the permission to publish and disseminate the abstract of the above-mentioned dissertation.

Signature

Date 2023-9-11

Development of Spatial Sequencing Methods and Applications for Brain Circuit Repair in Parkinson's Disease

Jana Rájová



LUND
UNIVERSITY

from

MOLECULAR NEUROMODULATION

Department of Experimental Medical Science, Faculty of Medicine

Lund University, Lund, Sweden

Thesis cover conceptualized and drawn by Jana Rájová depicts the fusion of several layers on information enabled both by improvement in spatial information preservation and in computational methods, integrating all data sources and providing a more holistic view of the tissue.

Coverphoto by Jana Rájová
Copyright pp 1-119 Jana Rájová

Paper 1 © Molecular Therapy: Methods & Clinical Development
Paper 2 © by the Authors (Manuscript unpublished)
Paper 3 © by the Authors (Manuscript unpublished)
Paper 4 © Frontiers in Molecular Neuroscience

Faculty of Medicine
Department of Experimental Medical Sciences

ISBN 978-91-8021-464-3
ISSN 1652-8220
Printed in Sweden by Media-Tryck, Lund University
Lund 2023



Media-Tryck is a Nordic Swan Ecolabel certified provider of printed material. Read more about our environmental work at www.mediatryck.lu.se

MADE IN SWEDEN 

To my grandmother

If one has really technically penetrated a subject,
things that previously seemed in complete contrast,
might be purely mathematical transformations of each other.

John von Neumann

Journalist:

This ship that was involved in the incident
off Western Australia this week...

Senator Collins:

Yeah, the one the front fell off?

Journalist:

Yeah

Senator Collins:

Yeah, that's not very typical,
I'd like to make that point

Clarke & Dawe

Contents

Original Papers	i
Lay summary	ii
Populärvetenskaplig sammanfattning	iv
Populárně-vědecké shrnutí	vi
Abbreviations	viii
Introduction	1
Cells and Their Identity	2
RNA: From DNA to Protein	3
Sequencing	4
From Short Reads to Genome	5
Towards Single Cells	7
Single-Cell RNA-seq Analysis	11
Exploring the Transcriptome	12
Spatial Transcriptomics and 10X Visium	12
Slide-seq	14
Seq-Scope	14
Stereo-seq	15
Deconvolution Methods	16
The Evolution of FISH	16
Molecular Toolbox: Padlock Probes and Rolling Circle Amplification	17
FISSEQ and ExSEQ	18
In Situ Sequencing	19
BaristaSeq	20

BARseq	20
RNA Detection Methods	21
Parkinson's Disease	24
Pathological Mechanisms	25
Genetic and Environmental Influences	25
Basal Ganglia and its Dysregulation in PD	26
Therapies	27
Animal Models	32
The Biology of α -Synuclein	34
Molecular Tools for Gene Therapy	35
AAV basics	35
Gene Editing in the Brain	35
Aims	38
Summary of Key Results	39
Paper I	39
hESC-Derived Transplants	39
Removing Batch Effect from Spatial Transcriptomics Data	39
Identification of Human Tissue and Anatomical Regions	41
Deconvolution of ST Features with an External scRNA-seq Dataset	41
Comparison of Transplant scRNA-seq vs ST Analysis	42
Paper II	45
PCR Probe Amplification	45
Rolling Circle Amplification	45
Transcript Detection with RCA-synthesized Probes	47
Lock-seq Introduction	50
Paper III	52
Experimental Setup	52
Nuclei Extraction and Sorting	53
Cell Type Assignment	54

AAV Gene Expression	55
AAV Barcode Isolation	55
Regression Analysis of AAV-Related Gene Expression	57
Pseudotime Analysis	58
Paper IV	60
Targeting HITI System to the Arc 5' ORF Leads to In-Frame Knock-in	60
Regional Potentiation Induces ARC-mCherry Expression in Dentate Gyrus	61
ARC-mCherry Protein Preserves ARC's Interaction with Synaptic Modules	62
Key Methodology	67
Methods for Spatial Transcriptome Analysis	67
Spatial Transcriptomics	67
BARseq2	68
Lock-seq	68
Molecular Techniques	69
PCR Template Amplification and Product Processing	69
RCA and Product Processing	69
Circular ssDNA Template Generation	70
Bioinformatic analyses	71
Spatial Transcriptome Data Analysis - Normalization and Batch correction	71
Anatomical Region Assignment	72
Differential Gene Expression	72
Deconvolution	73
scRNA-seq Analysis	73
Pseudotime Analysis	73
Discussion and Future Perspectives	75
References	79
Acknowledgement	117

APPENDIX (Papers I-IV)

Paper I: Deconvolution of spatial sequencing provides accurate characterization of hESC-derived DA transplants in vivo	
Paper II: Scaling Gene Detection in situ by array synthesis and isothermal probe amplification	
Paper III: Engineered retrogradely transported, barcoded AAVs elucidate molecular pathways involved in the pathogenesis in Parkinson's disease	
Paper IV: Visualizing Arc protein dynamics and localization in the mammalian brain using AAV-mediated in situ gene labeling	

Original Papers

Papers included in this thesis:

Paper I

Deconvolution of spatial sequencing provides accurate characterization of hESC-derived DA transplants in vivo

J. Rájová, M. Davidsson, M. Avallone, M. Hartnor, P. Aldrin-Kirk, T. Cardoso, S. Nolbrant, A. Mollbrink, P. Storm, A. Heuer, M. Parmar and T. Björklund

Molecular Therapy - Methods & Clinical Development 29 (June 8, 2023): 381–94

Paper II

Scaling Gene Detection in situ by array synthesis and isothermal probe amplification

J. Rájová, S. Palo, C. Mirabello, M. Avallone and T. Björklund

Manuscript in preparation

Paper III

Engineered retrogradely transported, barcoded AAVs elucidate molecular pathways involved in the pathogenesis in Parkinson's disease

M. Avallone, J. Pardo, S. Palo, J. Rájová, A. Hammarberg, J. Johansson, A. Fiorenzano and T. Björklund

Manuscript in preparation

Paper IV

Visualizing Arc protein dynamics and localization in the mammalian brain using AAV-mediated in situ gene labeling

M. Avallone, J. Pardo, T.F Mergiya, J. Rájová, A. Räsänen, M. Davidsson, M. Åkerblom, L. Quintino, D. Kumar, C.E Braham and T. Björklund

Frontiers in Molecular Neuroscience 16 (2023): 1140785

Lay summary

This thesis explores the intricate world of cells within tissues, exploring their environment and interactions. Nowhere is this more relevant than in the brain, where billions of neurons constantly communicate, supported by countless other cells that handle various tasks, such as recycling neurotransmitters, facilitating information transfer, and protecting the brain's vital functions.

To understand the complexity of this organ and its inner workings, we need advanced tools capable of examining the multitude of cellular players. Technological advancements often lead to exciting discoveries, and while the biological findings in this thesis might seem rather loosely related, they collectively highlight the vast potential of cutting-edge methodologies and the exciting possibilities they offer for future research.

First, let us introduce spatial transcriptomics, a method that prompts cells to reveal information about their currently active genes, labeling them with a location-based tag. This approach sheds light on the state of individual cells and their interactions within the tissue. In the initial application of this thesis, spatial transcriptomics was employed to understand cell-based therapy for Parkinson's disease. It unveiled the spatial distribution of cellular components, their identities, and the overall state of the tissue community.

However, like any early method, spatial transcriptomics had limitations, particularly its relatively low resolution, which required computational estimations for cellular-level details. Recognizing this gap, several research groups sought to enhance the resolution, leading to numerous tools for directly analyzing gene expression in cells and tissues. These tools typically use a large number of DNA probes to pinpoint specific genes. While impressive, their adoption in most laboratories could be challenging due to the resources they demand. In response, a method presented in the second paper of this thesis aims to lower the initial barriers to entry into the spatial transcriptome analysis domain. It demonstrates that with common reagents and equipment and a modest investment, a comprehensive library that visualizes the activity of hundreds of genes can be generated. Alternatively, it offers a method able to visualize gene expression with higher sensitivity and lower probe requirements.

The tools explored in the later publications allowed us to establish a model of Parkinson's disease using viral vectors, specifically adeno-associated viral vectors. These vectors are very apt at delivering a small cargo to a desired cell population while leaving a traceable infection mark. The implemented technological advancements enabled us to profile thousands of rare cells while assessing their levels of PD-related protein load. This, in turn, allowed us to map out the landscape of cellular changes associated with the transition from a healthy to a diseased population.

Finally, we present a toolset for investigating the proposed transmission of the Arc gene among neuronal cells. This toolset enables us to tag individual ARC molecules by creating a fusion protein and observing its interactions with synaptic proteins. The resulting images of cellular communication confirmed previously known interactions and provided additional evidence supporting the idea of ARC molecule trafficking as previously suggested.

In closing, this journey through advanced methodologies and their application in understanding the intricate workings of cells and tissues offers a glimpse into the possibilities of modern technologies. As we venture deeper into the world of cellular interactions, we uncover new layers of knowledge that hold the potential to revolutionize our understanding of diseases, therapies, and the complexities of the human body. The tools and insights presented in this thesis attempt to do their share in broadening our scientific horizons and hopefully encourage future research, leading to even more discoveries.

Populärvetenskaplig sammanfattning

Denna avhandling utforskar den intrikata världen av celler inom vävnader och deras omgivning och interaktioner. Ingenstans är detta mer relevant än i hjärnan, där miljarder nervceller konstant kommunicerar. För att denna kommunikation skall fungera så krävs stöd av otaliga andra celler som utför specifika uppgifter, såsom återvinning av signalsubstanser, underlättande av informationsöverföring och skydd av hjärnans vitala funktioner.

För att förstå komplexiteten i detta organ och dess inre funktioner behöver vi avancerade verktyg som är kapabla att undersöka den mångfald av celler som är inblandade. Teknologiska framsteg leder ofta till spännande upptäckter. De biologiska resultaten i denna avhandling kanske verkar löst relaterade men tillsammans belyser de den enorma potentialen hos toppmoderna metoder och de spännande möjligheter som de erbjuder för framtida forskning.

Först låt mig introducera spatial transkriptomik, en metod som får celler att avslöja information om sina för närvarande aktiva gener genom att märka dem med en platsbaserad etikett. Denna metod ger insikt om individuella cellers tillstånd och deras interaktioner inom vävnaden. I denna avhandling användes spatial transkriptomik för att förstå cellbaserad terapi för Parkinsons sjukdom. Det avslöjade den spatiala distributionen av cellkomponenter, deras identiteter och vävnadens övergripande tillstånd.

Men precis som alla tidiga metoder hade spatial transkriptomik sina begränsningar, särskilt dess relativt låga upplösning, som krävde beräkningsmässiga uppskattningar för detaljer på cellnivå. Flera forskargrupper har arbetat med att förbättra upplösningen, vilket lett till många verktyg för direkt analys av genuttryck i celler och vävnader. Dessa verktyg använder vanligtvis ett stort antal DNA-prober för att exakt lokalisera specifika gener. Även om de är imponerande så kan deras användning vara utmanande för de flesta laboratorier på grund av att de är så resurskrävande. Som svar på detta syftar en metod som presenteras i den andra artikeln av denna avhandling till att sänka trösklarna för inträde inom området spatial transkriptomik. Den visar att med vanliga reagenser och utrustning samt en måttlig investering vi visualisera aktiviteten hos hundratals gener. Den erbjuder också visualisering av genuttryck med högre känslighet och lägre behov av prober.

De verktyg som utforskas i den tredje publikationen möjliggjorde uppbyggnaden av en modell för Parkinsons sjukdom med hjälp av virala vektorer. Dessa vektorer är väl lämpade för att leverera nya gener till en önskad cellpopulation och samtidigt lämna en spårbar infektionsmarkör. De implementerade teknologiska framstegen möjliggjorde profileringen av tusentals sällsynta celler samtidigt som deras nivåer av PD-relaterad proteinbelastning bedömdes. Detta gjorde det möjligt för oss att kartlägga landskapet av cellulära förändringar som är förknippade med övergången från en frisk till en sjuk nervcell.

Slutligen presenterar vi ett verktyglåda för att undersöka den föreslagna överföringen av Arc-genen mellan nervceller. Denna verktyglåda möjliggör märkning av enskilda ARC-molekyler genom att skapa ett fusionsprotein och observera dess interaktioner med synaptiska proteiner. De resulterande bilderna av cellkommunikation bekräftade tidigare kända interaktioner och tillhandahöll ytterligare bevis som stöder hypotesen om ARC-molekylens transport, som tidigare föreslagits.

Avslutningsvis erbjuder denna resa genom avancerade metoder en glimt av deras potential och tillämpningarna fördjupar vår förståelse kring cellers och vävnaders intrikata funktioner. När vi utforskar djupare in i världen av cellulära interaktioner avslöjar vi nya kunskapslager som har potential att revolutionera vår förståelse av sjukdomar, terapier och komplexiteten i den mänskliga kroppen. De verktyg och insikter som presenteras i denna avhandling försöker göra sitt bidrag till att bredda vår vetenskapliga horisont och förhoppningsvis uppmuntra framtida forskning, vilket leder till ännu fler upptäckter.

Populárně-vědecké shrnutí

Tato práce zkoumá složitý svět buněk a tkáních, jejich prostředí a interakce. Nikde není tato problematika relevantnější než v mozku, kde miliardy neuronů neustále komunikují, podporovány nespočetnými dalšími buňkami, které plní různé úkoly, jako je recyklace neurotransmiterů, usnadňování přenosu informací a ochrana vitálních funkcí mozku.

Abychom pochopili složitost tohoto orgánu a jeho vnitřních mechanismů, potřebujeme pokročilé metody schopné zkoumat značné množství buněk. Technologické pokroky často vedou k převratným objevům, a i když se biologická zjištění v této práci mohou zdát spíše volně související, dohromady ukazují obrovský potenciál nejmodernějších metodik a nové možnosti, které nabízejí pro budoucí výzkum.

Nejprve se pojďme seznámit s metodou profilování prostorového transkriptomu, která zpřístupňuje buněčné informace o aktuálně aktivních genech a označí je štítkem signalizujícím jejich polohu. Tento přístup osvětluje stavy jednotlivých buněk a jejich interakce v tkáních. V počáteční aplikaci této práce byla tato metoda použita k porozumění buněčné terapie pro Parkinsonovu chorobu. S pomocí této metody jsme tak objasnili prostorové rozložení buněk, jejich identitu a celkový stav tkáňového společenství.

Avšak jako každá raná metoda měla i prostorová transkriptomika svá omezení, zejména její relativně nízké rozlišení, které vyžadovalo výpočetní techniku pro detaily na úrovni jednotlivých buněk. Rozpoznávajíc toto omezení, mnoho výzkumných skupin se rozhodlo zvýšit rozlišení, což vedlo k vytvoření mnoha metod pro přímou analýzu vyjádření genů v buňkách a tkáních. Tyto nástroje obvykle používají velké množství DNA sond k přesnému lokalizování konkrétních genů a i když jsou tyto nástroje impozantní, jejich použití většinou vyžaduje značné zdroje. Metoda prezentovaná ve druhém článku této práce, si proto klade za cíl snížit vstupní bariéry pro analýzu transkriptomu v prostoru. Ukazuje, že s běžnými chemikáliemi, enzymy a vybavením a rozumnou investicí lze vytvořit komplexní knihovnu, která dokáže zobrazit aktivitu stovek genů. Alternativně nabízí metodu schopnou analyzovat vyjádření genů s vyšší citlivostí a nižšími požadavky na sondy.

Nástroje zkoumané v pozdějších publikacích nám umožnily vytvořit model Parkinsonovy choroby pomocí virových vektorů, konkrétně adenoasociovaných virových vektorů. Tyto vektory jsou schopné doručovat malý genový náklad do požadované populace buněk a zároveň zanechávat stopy infekce, které lze sledovat. Implementované technologické pokroky nám umožnily profilovat tisíce vzácných buněk a současně hodnotit jejich úroveň zatížení doručným proteinem, který je v Parkinsonově chorobě implikovaný. Tato studie nám umožnila mapovat soubor buněčných změn spojených s přechodem od zdravé k nemocné populaci.

Nakonec představujeme soubor nástrojů pro zkoumání hypotetizovaného přenosu proteinu ARC mezi nervovými buňkami. Tento soubor nástrojů nám umožňuje označit jednotlivé molekuly tohoto proteinu skrze fúzi s fluorescenčním reportérem a pozorovat jejich interakce se synaptickými proteiny. Výsledné obrazy buněčné komunikace potvrdily dříve známé interakce a poskytly další důkazy, které podporují hypotézu transportu molekul ARC, jak bylo dříve navrženo.

Závěrečně, tato cesta skrze pokročilé metodiky a jejich aplikace pro pochopení složitých funkcí buněk a tkání nabízí pohled na možnosti moderních technologií. Čím více se ponořujeme do světa buněčných interakcí, tím více nových vrstev znalostí ojevujeme. Informace, které tyto vrstvy nesou, mají potenciál změnit naše chápání nemocí, terapií a komplexity lidského těla. Nástroje a poznatky představené v této práci se takto pokoušejí přispět k rozšíření našich vědeckých obzorů a doufejme, že podnítí i budoucí výzkum, který povede k dalším objevům.

Abbreviations

α Syn	α -synuclein
6-OHDA	6-hydroxydopamine
AADC	aromatic L-amino acid decarboxylase
AAV	adeno-associated virus
AC	anterior commissure
ADORA2A	adenosin A2A-receptor
AFAP1L1	actin filament associated protein 1 like 1
ANOVA	analysis of variance
AQP4	aquaporin-4
ARC	activity-regulated cytoskeleton-associated protein
ASIC2	acid-sensing ion channel subunit 2
BC	barcode
Cas9	CRISPR associated protein 9
CC	corpus callosum
COL1A1	collagen type I alpha 1 chain
CRISPR	clustered regularly interspaced short palindromic repeats
Ctx	cortex
DAPI	4',6-diamidino-2-phenylindole
DARPP-32	dopamine- and cAMP-regulated neuronal phosphoprotein
DAT	dopamine transporter
DBS	deep brain stimulation
DG	dentate gyrus
DLB	dementia with Lewy bodies
SDB	double-strand break
DNA	deoxyribonucleic acid
cDNA	complementary DNA
circDNA	circular DNA
dsDNA	double stranded DNA
ssDNA	single stranded DNA
DOCK6	dedicator of cytokinesis protein 6
FANS	fluorescent-activated nuclei sorting
fEPSPs	field evoked postsynaptic potential
FISH	fluorescence <i>in situ</i> hybridization
FISSEQ	fluorescent <i>in situ</i> sequencing

FSC	forward scatter
GABA	gamma-aminobutyric acid
GAMR	guided attention model for (visual) reasoning
GCH1	GTP cyclohydrolase 1
GDNF	glial cell-derived neurotrophic factor
GFP	green fluorescent protein
GID	graft-induced dyskinesias
GMP	good manufacturing practice
GOI	gene of interest
GP	globus pallidus
GPe	external globus pallidus
GPi	internal globus pallidus
GTPase	guanine nucleotide-binding protein
HBSS	Hanks' Balanced Salt Solution
hESC	human embryonic stem cells
HITI	homology-independent targeted integration
HSF	high-frequency stimulation
Hipp	hippocampus
IHC	immunohistochemistry
ISH	<i>in situ</i> hybridization
ISS	<i>in situ</i> sequencing
ITGA6	integrin subunit alpha 6
L-DOPA	levodopa
LSF	low-frequency stimuli
LTP	long-term potentiation
MFB	medial forebrain bundle
MPTP	1-methyl-4-phenyl-1,2,3,6-tetrahydropyridin
MSA	multiple system atrophy
MSNs	medium spiny neurons
NAC	non-amyloid component
NEB	New England Biolabs
NGS	next-generation sequencing
NHEJ	non-homologous end joining
NHS	N-Hydroxysuccinimide
NURR1	nuclear receptor 4A2
ORF	open reading frames
PAF	pure autonomic failure
PCA	principal component analysis
PCR	polymerase chain reaction
PD	Parkinson's disease
PENK	proenkefalin
PFA	paraformaldehyde
PFFs	preformed fibrils
PLA	proximity ligation assay
PLEKHG1	pleckstrin homology and rhoGEF domain containing G1

RBD	REM behavior disorder
RCA	rolling circle amplification
RET	rearranged during transfection protein
RNA	ribonucleic acid
mRNA	messenger RNA
ROI	region of interest
RSPO2	r-spondin 2
scRNA-seq	single-cell RNA sequencing
sgRNA	single guide RNA
SLC6A3	solute carrier family 6 member 3
SN	substantia nigra
SNc	substantia nigra pars compacta
SNr	substantia nigra pars reticulata
SNP	single-nucleotide polymorphism
snRNA-seq	single nuclei RNA sequencing
SOLiD	sequencing by oligonucleotide ligation and detection
SOX9	SRY-Box transcription factor 9
SSC	saline-sodium citrate
ST	Spatial Transcriptomics
STN	subthalamic nucleus
SNCA	α -synuclein
Str	striatum
TH	tyrosine hydroxylase
tSNE	t-distributed stochastic neighbor embedding
TX	transplant
TENM4	teneurin transmembrane protein 4
Tukey's HSD	Tukey's honestly significant difference
UMAP	uniform manifold approximation and projection
UMI	unique molecular identifiers
UTR	untranslated region
VLMC	vascular and leptomeningeal cell
VLPs	virus-like particles
VTA	ventral tegmental area

Introduction

The quest to understand the intricate workings of animal bodies has been the central aspiration of biological sciences since their conception. These systems, evolving from a single cell, encompass a multitude of interacting components across various spatial and temporal scales. These components interact within themselves and with the dynamic ecosystems they inhabit. Even at lower scales, on the tissue communities level, the interactions' complexity is still astounding. A comprehensive understanding of these communities demands advanced methodologies offering high-resolution and multiplexed capabilities. Additionally, it necessitates the application of sophisticated computational approaches to make sense of the acquired data. Recent decades have witnessed the emergence of methods capable of analyzing tissues with remarkable detail, shedding light on events within tissues during both health and disease (Gyllborg et al., 2020; Svedlund et al., 2019; The Tabula Sapiens Consortium, 2022). This thesis focuses on the development and application of select tools within this transformative landscape.

The journey of every animal begins with a single fertilized egg, rapidly dividing into a myriad of daughter cells. Each of these cells embarks on its unique developmental path, pushed on by the signals it receives from its environment in the growing embryo. Throughout gestation, cells migrate to their destinations, often specializing in their gene expression programs. This specialization enables them and their descendants to seamlessly integrate into the broader biological communities. In this manner, the body's organs emerge and gradually assume their functions, contributing to the organism's autonomy. While changes continue during an animal's growth and development, adult cells have to maintain their identities stable. A serious deviation from this equilibrium presents a risk for the organism as a whole, as observed in pathological states. Throughout an organism's lifespan, inevitable damage accumulates within its DNA and other cellular components. This accumulation ultimately leads to pathological conditions, exemplified by the increased likelihood of cancer or neurodegenerative diseases with advancing age, ultimately leading to the organism's death.

To truly grasp the symphony of a living organism, it is necessary to identify the performers, their roles, and their locations within the orchestra. Extensive efforts have been dedicated to characterizing cells from both animal models and humans, shedding light on the inhabitants of various tissues. Most of these endeavors categorize cells based on their gene expression patterns, facilitated by the rapid advancements in DNA and RNA profiling techniques. The field has evolved significantly from the initial conception of DNA sequencing methods, such as the Maxam-Gilbert method, to today's high-throughput next-generation sequencing. We have transitioned from sequencing large cell populations to profiling individual cells and have expanded our capabilities

to capture multiple modalities simultaneously (Stoeckius et al., 2017; Vandereyken et al., 2023; Vickovic et al., 2022).

Modern high-throughput methods, like single-cell and single-nucleus RNA sequencing (scRNA-seq and snRNA-seq, respectively), have significantly enriched our understanding of tissue composition. However, within an organism, cells are interdependent, and comprehending these intricate relationships necessitates insight not only into their inner states but also into their temporal and spatial relationships. This thesis aims to explore a subset of these complexities, specifically focusing on understanding various aspects of brain function in both healthy and diseased states.

Cells and Their Identity

As cells evolved from solitary entities into integrated components of complex organisms, they diversified their functions and properties, gaining a collective survival advantage. Similarly, during an organism's development from a fertilized egg, various developmental pathways are activated within embryonic cells, gradually establishing the complete cell type repertoire of the organism. These cells can be categorized based on numerous properties (Regev et al., 2017), including morphology (Ghanegolmohammadi et al., 2022; Peng et al., 2021; K. Yao et al., 2019), molecular compositions such as the proteome (Pontén et al., 2009), transcriptome (La Manno et al., 2021; Vinsland & Linnarsson, 2022), epigenome (Bakken et al., 2021; Rahmani et al., 2019), metabolome (Gebert et al., 2021), and various other physiological properties or so-called "omes", such as distinct electrophysiological properties of neuronal cells (Callaway et al., 2021; Somogyi & Klausberger, 2005).

Quantifying cellular diversity within the human body has garnered significant attention in recent decades. Due to technological advancements, cell typing based on transcriptomic signatures has emerged as a prominent approach, particularly in recent years. However, defining the boundaries of a "cell type" remains a topic of debate (Clevers et al., 2017; Doyle, 2022; Miao et al., 2020; Trapnell, 2015). Most publications focused on higher animals generally settle on the existence of several hundred cell types (Domínguez Conde et al., 2022; Eraslan et al., 2022; La Manno et al., 2021; Svensson et al., 2020; The Tabula Sapiens Consortium, 2022; Vickaryous & Hall, 2006). Nevertheless, studies with a deeper focus on specific organs can yield significantly higher estimates. For example, in a recent study, the brain was classified into well over 400 further divisible cellular classes (Siletti et al., 2022). While uncertainties persist regarding the total number of relevant categories, the brain consistently stands out as one of the most diverse organs (Siletti et al., 2022; Vickaryous & Hall, 2006). It has also been the most extensively profiled organ using single-cell technologies (Svensson et al., 2020).

With its unparalleled complexity and cellular diversity (Siletti et al., 2022), the adult brain hosts a multitude of diverse neuronal classes, various glial cell categories (e.g., oligodendrocytes, astrocytes, microglia, and ependymal cells), as well as several vasculature-related cells (La Manno et al., 2021; Z. Yao et al., 2023). Profiling the entire brain, which comprises hundreds of millions of diverse cells in mice (Herculano-Houzel et al., 2006) and billions in humans (Azevedo et al., 2009), presents an ambitious process at the very least. This magnitude led to many studies

focusing on specific brain regions (Bakken et al., 2021; Callaway et al., 2021; Svensson et al., 2020), while also giving rise to more extensive efforts pursuing the profiling the entire brain or the central nervous system (CNS) (La Manno et al., 2021; Siletti et al., 2022; Z. Yao et al., 2023; Zeisel et al., 2018).

Despite the growing number of cells profiled through single-cell sequencing, a limitation of this method is the loss of spatial distribution information, rendering it more an encyclopedia than an atlas. Several atlases have emerged in recent years, providing gene expression data with associated spatial information, many of which will be detailed in this thesis. Notable examples include the Allen Brain Atlas (Lein et al., 2007), which offers gene expression data throughout the mouse brain for thousands of genes. However, profiling one gene at a time is time, tissue, and reagent-intensive. Consequently, various methods attempting to capture as much of the transcriptome as possible have emerged. Among fluorescence *in situ* hybridization (FISH)-based methods, notable examples include seqFISH, showcased through a map of mouse hippocampus (Shah et al., 2016), followed by osmFISH (Codeluppi et al., 2018) presenting a detailed description of the mouse somatosensory cortex or MERFISH (Y. Zhang et al., 2020), introduced with analysis of mouse motor cortex and hypothalamus (Moffitt et al., 2018). While highly sensitive, profiling with FISH methods is resource-intensive, particularly in terms of time and expensive fluorescent reagents. Some challenges have been addressed with EEL-FISH (Borm et al., 2023), which reduces background noise and the z-dimension through mRNA pull-down onto a glass; this is, however, at the cost of some signal loss.

Efforts to map tissues using non-FISH methods include padlock probe-based approaches (X. Chen et al., 2018; Y. Chen et al., 2022; Ke et al., 2013; H. Lee et al., 2022; S. Liu et al., 2021; Lohoff et al., 2022; Y.-C. Sun et al., 2021; Svedlund et al., 2019; Vicari et al., 2023), solid-phase capture of mRNA sequences as seen in Spatial Transcriptomics-based methods (Hahn et al., 2023; Ortiz et al., 2020; Ståhl et al., 2016; Vickovic et al., 2019) or Slide-seq (Stickels et al., 2021), and commercialized implementations such as 10X Visium, Xenium or Curio Seeker solutions. Other noteworthy approaches include Stereo-seq (Y. Chen et al., 2022), which provided an atlas of mouse organogenesis, or Geo-seq (J. Chen et al., 2017).

Finally, all these methodologies, in conjunction with information already gleaned from single-cell datasets, have the potential to contribute to the creation of maps of tissues complementary to those annotated based on anatomical structures and enrich them with a functional rather than geographical component.

RNA: From DNA to Protein

Genes and functional sequences are stored on large DNA molecules within the cell nucleus. In the human genome, the average size is approximately 6.3 - 6.4 billion bases per diploid genome (range is caused by the difference in the lengths of X and Y chromosomes), with around 19,000 protein-coding genes (Piovesan et al., 2019). To be actuated as proteins, genes have to be transcribed into messenger RNA (mRNA), transported into the cytoplasm, translated with the ribosomal

machinery into an amino acid sequence, and assume a functional conformation. This flow of genetic information through the layers is better known as the central dogma of biology.

Gene transcription initiates when a transcription factor locates its transcription regulator sequence (Orphanides & Reinberg, 2002). Once bound, this protein regulates access to other translation machinery components and assists in recruiting RNA polymerase (Karin, 1990; Latchman, 1993; Nikolov & Burley, 1997; Riggs et al., 1970; Tafvizi et al., 2011; Zrimec et al., 2021). Transcription initiation is followed by the addition of a 5' cap to protect the transcript from degradation, followed by the mRNA elongation. The newly synthesized mRNA molecules initially include many intronic sequences, which must be removed for the protein to reach its functional form. This splicing out of introns begins already during elongation (Fong & Zhou, 2001; Hirose & Manley, 2000; Orphanides & Reinberg, 2002; G. Zhang et al., 1994). After the translation stop codon, the 3' untranslated region (UTR) with functional sequences begins, among others, guiding the polyA tail addition (Connelly & Manley, 1988; Logan et al., 1987). Once all steps are completed, the molecule's journey out of the nucleus and toward its translation inside a ribosomal complex begins. The collection of all proteins produced in the cell gives the cell its functionality and recognizable phenotypic features.

Sequencing

Since the discovery of DNA's structure in 1953 (Watson & Crick, 1953), extensive efforts have been made to analyze its protein-coding sequences in various organisms, and thousands of small steps have been made toward understanding genome functional elements. The first-generation DNA sequencing methods began with the success of the chemical degradation-based Maxam-Gilbert sequencing (Maxam & Gilbert, 1977), published in 1977 in the Proceedings of the National Academy of Sciences (PNAS), followed by Sanger sequencing (Sanger et al., 1977) introduced in the journal's last issue the same year. Both these methods, while groundbreaking, are limited to relatively short reads, with the Maxam-Gilbert method limited to stretches of 100 - 200 nucleotides and Sanger sequencing up to 1000. While initially tedious, Sanger sequencing was the method of choice during the times of the first human genome sequencing, and its automated version is still widely used today (Aach et al., 2001; Lander et al., 2001; Venter et al., 2001).

The advent of second-generation sequencing marked a significant leap in throughput and cost efficiency. This technology, built on the foundation of millions of short reads, moved away from the electrophoresis readout. Notable approaches within this generation included pyrosequencing (Nyren et al., 1993; Ronaghi et al., 1996; Uhlen, 1989), Solexa sequencing by synthesis (Balasubramanian et al., 2007), and SOLiD sequencing by ligation. These innovations shifted towards optical readout techniques. In contrast, Ion Torrent (Rusk, 2011) adopted a novel approach, relying on detecting pH changes following nucleotide incorporation. While Ion Torrent offered the advantage of sequencing longer molecules and bypassed the need for costly optical equipment and fluorescent dyes, it faced challenges with homopolymer reads (Loman et al., 2012). Notably, Solexa, later acquired by Illumina, emerged as one of the most prevalent and widely used sequencing methods, as evidenced by its remarkable 4 billion in revenue in 2022 ("Illumina reports financial results for fourth quarter and fiscal year 2022", n.d.).

In contrast to DNA, which is found nearly identical in all somatic cells of an organism, the range of mRNA expression patterns among diverged cellular populations is extensive. The quest to analyze mRNA molecules across diverse cell types has been fueled by the continual advancement of DNA sequencing methods over the past three decades. This journey's beginnings saw the rise of the microarray-based methods (Bertone et al., 2004; Carninci et al., 2005), rapidly followed by the advent of Illumina-based sequencing (Nagalakshmi et al., 2008). To make mRNA compatible with DNA sequencing, these methods entail transcribing mRNA into complementary DNA (cDNA) using an RNA-dependent DNA polymerase (Temin & Mizutani, 1970). Following this step, the cDNA is amplified and can be processed in a manner specific to the chosen method, involving either fluorescent labeling or adapter ligation.

From Short Reads to Genome

In the realm of second-generation sequencing, with Illumina as a prominent example, short reads have proven invaluable for unraveling the intricate complexities of genomes. These reads, although relatively short, ranging from 50 bases for small RNA sequencing kits to a maximum of 300 bases, offer a wealth of information. However, due to the complex nature of genomes, riddled with repetitive sequences and the inescapability of sequencing errors, the endeavor of *de novo* genome assembly using these short reads has proven not only impractical but nearly unattainable for routine analysis. As a pragmatic alternative, researchers turn to read alignment against a known reference genome, a computational process that introduces polynomial time complexity (Baichoo & Ouzounis, 2017; Canzar & Salzberg, 2017), a significant departure from the more complicated nature of *de novo* assembly (Liao et al., 2019). This alignment task comes with its own set of challenges. The reference genome may be incomplete or contain gaps, or, at the opposite end, reads may map to multiple locations throughout the genome. Furthermore, addressing possible strand bias in the reads adds another layer of processing. Over 100 read alignment algorithms have emerged throughout the years to tackle the technology-associated obstacles, offering a plethora of strategies (Alser et al., 2021).

The prevailing sequencing technologies profoundly shape the development and suitability of these alignment algorithms. Initially, the read numbers of early methods were quite limited in comparison to today's throughput, allowing for algorithms less optimized for this variable. However, transitioning to a massive quantity of short reads with relatively low error rates compelled the aligner development community to adopt a more parallel approach. In recent years, yet another shift has occurred with the advent of technologies capable of generating long reads, extending up to several megabases in length, albeit with higher error rates (Lu et al., 2016; L. Wang et al., 2020). This shift has introduced a completely new set of computational requirements, further diversifying the landscape of read alignment methodologies.

With the unprecedented progress in RNA sequencing (RNA-seq) technologies, specialized aligners have emerged to address the unique challenges the mRNA molecules' specifics brought on. Unlike DNA, RNA-seq provides insights into gene expression levels and isoform diversity. Aligning RNA-seq reads is inherently more complex due to splicing events, where exons can be arranged in various combinations to produce diverse transcripts. To navigate this task efficiently, specialized aligners have evolved to incorporate spliced alignments, enabling precise gene expression and isoform abundance quantification. Two predominant strategies for transcript alignment have emerged: the read-to-genome approach, employed by algorithms such as STAR (Dobin et al., 2013), Bowtie (Langmead & Salzberg, 2012), and BWA (H. Li & Durbin, 2009), which aligns reads directly to the genome. STAR, for instance, is a popular splice-aware approach known for its widespread application in both bulk and single-cell RNA-seq studies. It employs a two-step mapping process that initially aligns reads to the genome and subsequently identifies splice junctions, providing read-to-gene mapping and a comprehensive view of splicing events. The second strategy is adopted by a range of pseudoaligners, including Kallisto (Bray et al., 2016; Du et al., 2020) and Salmon (Patro et al., 2017). These pseudoaligners eschew genome alignment in favor of alignment to a transcriptome reference, streamlining transcript quantification and significantly reducing computational demands.

While second-generation sequencing is the popular choice for transcriptome profiling, it falls short when it comes to sequencing entire genomes, particularly in regions with long repeat sequences. Third-generation sequencing emerged as an alternative solution to address this limitation, eliminating the need for library amplification and fragmentation and enabling the sequencing of reads up to tens of kilobases in length. Two prominent approaches have emerged, led by PacBio's single-molecule sequencing technology (Travers et al., 2010) and Oxford Nanopore (ONT). However, the early versions of these technologies exhibited a considerably higher error rate (around 14%) (Workman et al., 2019) compared to second-generation sequencing (which can be generally assumed to lie between 0.1-1.5%). To mitigate this challenge, several studies showed a workaround with a combination of the two approaches (Berbers et al., 2020). To reduce this error rate, PacBio and ONT took on two different approaches, both promising over 99% accuracy (Sahlin & Medvedev, 2021; Wenger et al., 2019). PacBio, using the fact that the errors are randomly distributed, introduced a circular consensus sequencing in 2019, which allowed for a significant bump up in the accuracy of the method with circular consensus sequencing, and ONT presented a computational isONcorrect method.

Sequencing Nucleic Acids with Illumina

Sequencing nucleic acids using Illumina technology involves a series of steps that transform the DNA or RNA into a platform-specific library format. When sequencing DNA, the first essential task is fragmentation, which can be achieved either mechanically or enzymatically through transposases. The latter method has the advantage of labeling the cut sites with molecular identifier "tag" sequences, a process known as tagmentation. Subsequently, index-carrying primers are incorporated into the DNA sequences in a polymerase chain reaction (PCR) amplification. The resulting sequences of appropriate lengths are then purified using Solid Phase Reversible Immobilization (SPRI) beads. In cases involving multiple libraries, various indexes can be employed to separate the data during subsequent analysis. Once these steps are completed, the library is denatured, and an adapter-ligated library of the Φ -X 174 bacteriophage genome is introduced as an internal sequencing control. The prepared libraries are then applied to the sequencing chip, where they become anchored to the surface through adapter sequences introduced during the indexing PCR. At the beginning of the sequencing process, uniform sequence clusters are generated from hybridized molecules through bridge amplification. These local clusters are subjected to a series of cycles involving the addition of fluorescently labeled 3'-capped nucleotides, fluorescence imaging after their incorporation, and finally nucleotide de-blocking to enable further extension. The final sequence is established through the consensus fluorescence data obtained from these local clusters and is then aligned to the genome, following the previously described procedures. The overview of the Illumina sequencing approach is further illustrated in figure 1.

When profiling RNA molecules in a sample, the protocol requires specific modifications before the transcriptome can be sequenced. First, the mRNAs within the sample must be reverse-transcribed into complementary DNA (cDNA). This crucial step introduces priming sequences containing indexes that can differentiate molecule identities at the end of the sequencing run. After cDNA synthesis, the mRNA is removed and replaced with a complementary DNA strand. The resulting samples are equipped with Illumina-compatible anchors and the library can be amplified, fragmented, purified, and sequenced in a manner similar to that employed for DNA libraries.

Towards Single Cells

Transitioning from RNA-seq of bulk tissues to the single-cell level marked a significant breakthrough in molecular biology. Initially, RNA-seq demanded an amount of RNA equivalent to hundreds or thousands of cells, obscuring the intricacies of cellular dynamics and heterogeneity. This limitation rendered the method impractical for scenarios where only a handful of cells were available, such as in the study of developing embryos. Notably, a pivotal 2009 study using SOLiD sequencing managed to analyze the RNA content of a single blastomere cell (Tang et al., 2009), demonstrating the power of sequencing at the single-cell level.

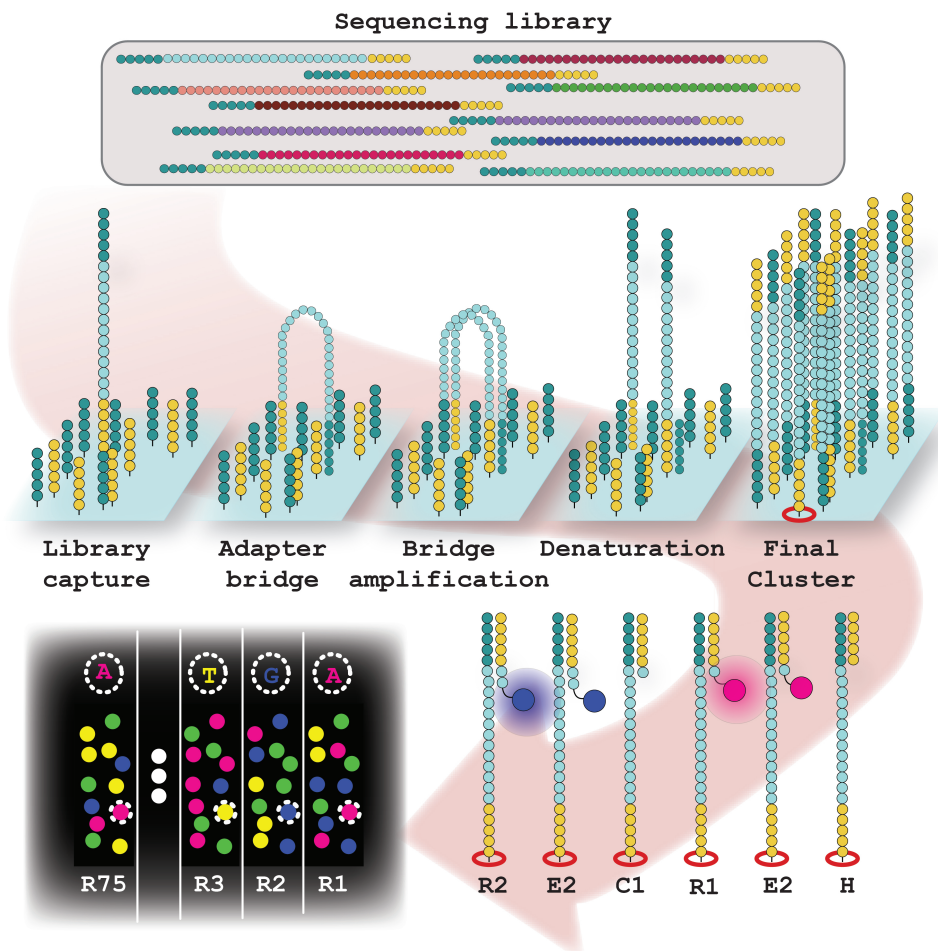


Figure 1: Illumina sequencing by synthesis approach. The denatured sequencing library is loaded onto the flow cell, where it hybridizes to adapters. Library fragments are amplified through binding, synthesis, and release cycles, creating local clusters. DNA in these is then read with sequencing by synthesis, where each round, the hybridized (H) sequencing adapter is extended (E) by fluorescently labeled and cap-protected nucleotide, which is imaged (R), deprotected (C) and then further extended repeating the cycle. The consensus sequence of each cluster's library fragment is assembled from fluorescent signals coregistered through the sequencing rounds.

However, to comprehensively understand cellular diversity in animals, profiling on an entirely different scale was required to capture representative snapshots of cellular populations. Before the advent of DNA sequencing, cell analysis primarily relied on low-throughput methods, including cell staining to visualize morphology, immunohistochemistry to detect protein presence (Jones et al., 1941), and fluorescence *in situ* hybridization (FISH) to identify known DNA and RNA sequences (Langer-Safer et al., 1982). Initial attempts at single-cell RNA sequencing (scRNA-seq) increased the number of genes or features detected within a cell but remained limited in throughput and involved substantial manual labor. This landscape evolved with the emergence of numerous new methods.

An early milestone involved profiling the transcriptome of 92 mouse cells using Illumina sequencing and plate-based cell barcoding (Islam et al., 2011), marking a significant leap in the number of cells that could be profiled. Methods such as CEL-seq (Hashimshony et al., 2012) and Smart-seq2 (Picelli et al., 2013) further expanded the range to hundreds or even a thousand of cells. Automation contributed to this scalability as seen in the MARS-seq system (Jaitin et al., 2014). A pivotal moment for the field was the simultaneous publication of droplet-based scRNA-seq techniques (A. M. Klein et al., 2015; Macosko et al., 2015), which allowed the processing of thousands of cells by enclosing them in tiny droplets containing barcode-labelled reverse transcription reaction. These barcodes are added to each captured molecule transcribed into cDNA and retain information about a molecule's cellular origin throughout library preparation and sequencing, enabling the simultaneous profiling and later demultiplexing of thousands of single cells. This method was later commercialized as the 10X Chromium, making it accessible and convenient for widespread adoption (figure 2).

Despite its impressive capabilities, scRNA-seq has several limitations. One drawback is the damage a cell can sustain with the processing of its whole cell body. While this can be advantageous as the intact cell membrane allows for protein detection or further multiplexing of several samples (Stoeckius et al., 2017), several studies have reported discrepancies in cellular proportions between expected and obtained values, particularly for cell types with complex morphology (Andrews et al., 2022; Santiago et al., 2023). Dissociation protocols in scRNA-seq have been found to alter gene expression patterns, especially for stress-response genes, potentially affecting the evaluation of pathological conditions and cellular responses to experimental conditions (Adam et al., 2017; Denisenko et al., 2020; Truong et al., 2023). These issues and the technical difficulties of obtaining fresh tissues desirable in scRNA-seq have led to the development of snRNA-seq as an alternative. Comparisons between scRNA-seq and snRNA-seq have revealed that the former tends to deplete cells with complex or interconnected morphologies while preserving the proportions of the mostly free cells, such as immune cells (Gaedcke et al., 2022; Santiago et al., 2023; Slyper et al., 2020; Wen et al., 2022). Functionally, snRNA-seq appears mostly equivalent to scRNA-seq for the majority of the transcriptome (Lake et al., 2017). However, studies highlighted differences have appeared, such as disparate profiles of microglial activation in Thrupp et al., 2020 and mitochondrial-related gene enrichment in scRNA-seq compared to snRNA-seq in Gaedcke et al., 2022. As briefly mentioned, an advantage of snRNA-seq is its independence from fresh frozen tissue, allowing the analysis of samples that are no longer viable for scRNA-seq (Martelotto et al., 2017).

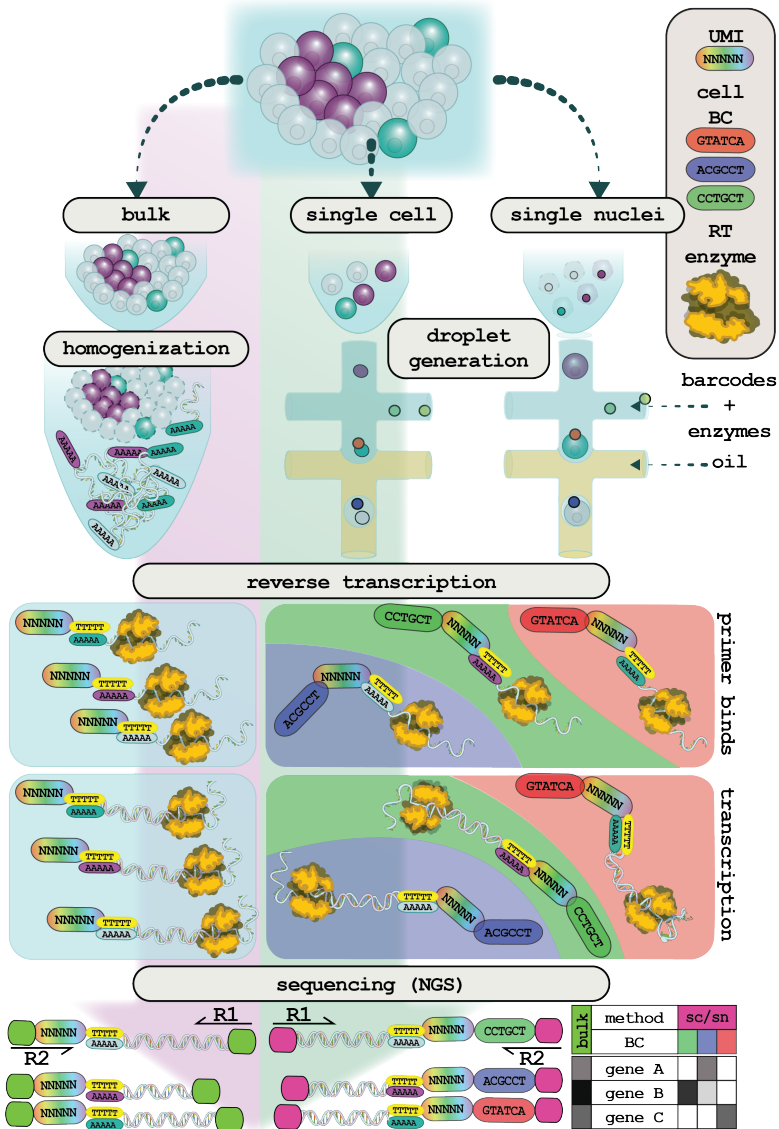


Figure 2: Comparison of bulk and single-cell resolution methods (scRNA-seq and sn-RNAseq). Tissue (top) processing is shown with the bulk (left) and single-cell and nuclei approaches. For bulk processing is shown tissue homogenization and RNA release, followed with reverse transcription (RT) initiated by oligo-dT probes with UMIs, and sequencing. In single-cell and nuclei approaches, cells are encapsulated in droplets in oil with oligo-dT probes carrying a unique barcode (BC) and UMI, as well as all enzymes and reagents for RT. RT is performed in these droplets, labeling all cDNAs with a barcode. Following sequencing, this BC assigns a cell identity to all transcripts.

Single-Cell RNA-seq Analysis

Several reviews documenting best practices for scRNA-seq have been published and updated, offering a step-by-step explanation of all analysis steps (Heumos et al., 2023; Luecken & Theis, 2019). This toolbox provides a rudimentary description of the basic workflow. The reviews mentioned above provide a wealth of information for those interested in more detail.

Although bulk RNA-seq and scRNA-seq share many similarities, the latter requires specialized tools to address its unique characteristics. Notably, scRNA-seq data tends to be sparse due to the sampling of individual cells. While gene count matrices would ideally still exhibit sparsity, technical dropouts, where lowly expressed genes are missed despite their presence, introduce noise into the data. This issue is less prominent in bulk samples, where profiles are averaged across multiple cells (Hicks et al., 2018; Ziegenhain et al., 2022). The sparsity of single-cell data has also prompted scrutiny of the suitability of methods designed for bulk sequencing (Gagnon et al., 2022; Y. Liu et al., 2023; Squir et al., 2021).

In standard scRNA-seq processing, cells undergo quality control, typically involving a three-part assessment of mitochondrial content, read count, and the number of genes per cell (Griffiths et al., 2018; Ilicic et al., 2016). This quality control stage also addresses several other factors specific to scRNA-seq. Sparsity in gene counts is one concern; steps are also taken to correct for "multiplet" events originating from cell droplet creation in cases where more than one cell is enclosed in a barcoded droplet. These events can lead to mixed cell types, necessitating tools to distinguish between single, empty, and mixed droplets (Bais & Kostka, 2020; DePasquale et al., 2019; McGinnis et al., 2019; Wolock et al., 2019). Additionally, ambient RNA from lysed cells in the sample, which released their content in the surrounding reaction, should be considered (Caglayan et al., 2022; Lun et al., 2019; Muskovic & Powell, 2021; Yang et al., 2020; Young & Behjati, 2020).

Following quality control, read counts from qualifying cells undergo normalization to account for read depth and sampling effects (Babcock et al., 2021; Boeshaghi et al., 2022; Hafemeister & Satija, 2019; Vallejos et al., 2017). Given the consensus of no one-size-fits-all approach, normalization methods should be selected based on a per-dataset basis (Cole et al., 2019).

While normalization addresses some sources of non-biological variability, other factors, such as batch effects or cell cycle variations, can still obscure cellular transcriptome patterns. To mitigate these unwanted variations, comprehensive RNA-seq processing tools like Seurat (Butler et al., 2018) and Scanpy (Wolf et al., 2018) offer tools for regressing these factors out. Cell cycle effects are typically corrected using curated gene lists from the literature (Macosko et al., 2015). Batch effects, which can stem from differences in cell source, processing, or technology, can be further removed using an array of batch correction tools (Butler et al., 2018; Hie et al., 2019; Korsunsky et al., 2019; X. Li et al., 2020).

Integrated and batch-corrected datasets still contain tens of thousands of genes, only a subset informative of the population-level patterns. A subset of 1,000-5,000 highly variable genes is typically selected to enhance data interpretability, increasing the informational density. Cells characterized by these highly variable genes are subjected to dimensionality reduction techniques, which provide a compact representation of cellular profiles and facilitate visualization. Commonly used techniques include principal component analysis (PCA) (Pearson, 1901), t-distributed stochastic neighbor embedding (t-SNE) (Hinton & Roweis, 2002), and uniform manifold approximation and projection (UMAP) (McInnes et al., 2020). Following dimensionality reduction, data can undergo clustering (Altman & Krzywinski, 2017), pseudotime inference (Deconinck et al., 2021; Van den Berge et al., 2020) or analysis of RNA velocity (Bergen et al., 2020; La Manno et al., 2018; H. Li et al., 2023), compositional landscape (Cao et al., 2019), or differential gene expression (Das et al., 2022; Gagnon et al., 2022) to unveil valuable insights.

Exploring the Transcriptome

While scRNA-seq has revolutionized the analysis of the tissue's constituents, it is essential to recognize that extensive tissue processing and dissociation can introduce biases while also discarding the information about the spatial relationships in which cells function. Numerous methods have been developed to bridge this gap to preserve spatial information in various ways. Historically, spatially-resolved transcriptome methods were low-throughput, often relying on fluorescently labeled oligonucleotide probes or antibodies, making a comprehensive understanding of tissues hard to come by. In this section, I will introduce several pivotal methods in the field, some crucial to the experiments presented in later chapters. These methods can be categorized based on the portion of the transcriptome they capture, as well as their general approach to gene detection.

When it comes to transcriptome profiling, methods can be broadly divided into two categories based on multiple characteristics. Some of these are the nature of the mRNA capture or readout modality. Capture modes dividing methods into unbiased profiling, which aims to profile all transcripts equally, and targeted profiling, which detects only a subset of the transcriptome relevant to the specific research question. Readout modality methods can be further partitioned into ones that use optical *in situ* readout or are the ones that label transcript positions and map them back after *ex situ* sequencing.

Spatial Transcriptomics and 10X Visium

Spatial Transcriptomics (ST), published in 2016 (Ståhl et al., 2016), was one of the pioneering unbiased spatial methods for profiling the transcriptome while preserving the spatial positions of transcripts within $\sim 100 \mu\text{m}$. This method utilized slides with immobilized probes carrying oligo-dT sequences, spatial barcodes, unique molecular identifiers (UMIs), and detachment handles. Over a thousand batches of probes, each with a position-unique barcode, were deposited onto a slide in a microarray format and covalently linked. This created thousands of spots or

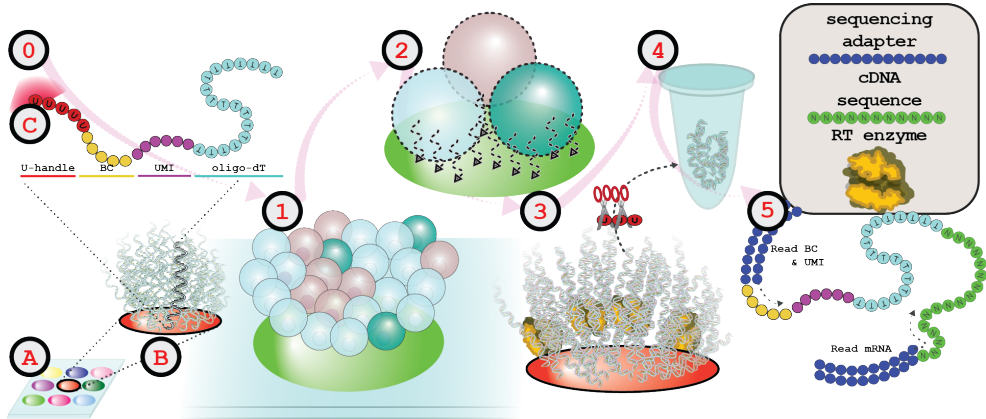


Figure 3: Illustration of ST transcriptome analysis. (0) ST feature array (A) with a feature detail in (B) and an example of a capture probe on its surface in (C) with uracil handle (U-handle), location-specific barcode (BC), UMI and oligo-dT capture sequence. (1) Tissue is placed on the array, (2) permeabilized, releasing mRNA, which is transcribed into cDNA from the feature's probes (3). Uracil stretch is then digested, releasing cDNA (4), which can be sequenced with paired-end sequencing (5).

"features" that captured mRNA molecules following tissue permeabilization brought on by the tissue's partial digestion. These spots also served as priming sites for reverse transcription, irreversibly linking mRNA sequences to the solid-phase bound spatial probe. After removing the surrounding tissue material, the barcoded transcriptome could be detached through hydrolysis of the detachment handle and processed into a sequencing library. Paired-end sequencing enabled the readout of both the spatial barcode and UMI from one end and the transcript sequence from the other, allowing mapping onto its corresponding position on the array (figure 3). As no genes were pre-selected, this method captured a sample of the whole transcriptome, enabling exploratory analysis.

This approach gained significant success and was later acquired by 10X Genomics, transforming ST to the 10X Visium platform, leading to standardization, user-friendliness improvements, and increased resolution from 100 μm to 50 μm . Since their introduction, ST and 10X Visium have reached significant popularity and have been extensively used in hundreds of studies, with tumor and brain biology being the most commonly explored areas ("Publications", n.d.).

Further advancements in resolution were achieved by the founding group in 2019 with High-Definition Spatial Transcriptomics (HDST) (Vickovic et al., 2019). This method iteration reached an impressive 2 μm resolution by employing split-and-pool barcoded beads distributed into plates covered with hexagonal wells. The barcode-position association was first decoded through sequential hybridization. From this point, the process mirrored the original ST, with barcode reads from RNA-seq matched to the initial barcode-position mapping.

An intriguing advancement that has pushed the boundaries of resolution involves the fusion of expansion microscopy with ST methodology, as shown in a recent study by Fan et al. (Fan et al., 2023). While many research endeavors aim to shrink feature sizes to increase resolution, expansion microscopy takes the opposite route by reducing the number of cells per unit area. This unique approach results in an increase in resolution proportional to the expansion of the tissue. However, it is important to note that this approach also has its limitations, particularly in relation to the standardized capture area sizes used in Visium. Consequently, the size of the specimen that can be effectively analyzed diminishes as the expansion factor increases.

Slide-seq

Slide-seq represents another approach to unbiased solid-phase capture methods, employing split-and-pool barcoded beads with a size of 5 μ m. In this method, the tiny beads are randomly distributed on a tape, creating a base for mRNA capture. Slide-seq2, an improved version of Slide-seq, significantly enhances capture efficiency, making it a noteworthy advancement in the field (Rodrigues et al., 2019; Stickels et al., 2021). Slide-seq2 has also demonstrated higher sensitivity compared to methods based on Spatial Transcriptomics (ST).

The key components of Slide-seq beads include spatial barcodes, unique molecular identifiers (UMIs), and capture probes targeting the polyadenylated (polyA) tail of mRNA molecules. Spatial barcodes, later used for mapping barcode-position pairs, are sequenced with *in situ* sequencing techniques. After obtaining these mappings, the tissue is placed and permeabilized to enable mRNA binding to the immobilized probes on the beads. Reverse transcription is then performed, effectively anchoring the mRNA sequences to the beads. Subsequently, Slide-seq dissociates the beads from the slide and processes the sequences, ultimately generating an Illumina-compatible library for downstream analysis (figure 4).

Seq-Scope

The Seq-Scope method employs direct amplification on a MiSeq Illumina chip, which grants it an impressive resolution of approximately 0.5 - 0.7 μ m and a respectable coverage of around 4,700 profiled transcripts per cell. The creation of a transcriptome map using this method involves a two-step process.

In the initial step, barcoded oligonucleotide probes are strategically distributed across the chip's surface. Oligonucleotide clusters sharing a common spatial barcode sequence are then created through a local bridge PCR. Subsequently, the spatial barcode sequences are read via sequencing by synthesis, and the resulting molecules are cleaved to expose an mRNA capture sequence. The tissue of interest is then carefully placed on the chip, permeabilized to facilitate mRNA binding, and the captured mRNA is transcribed into cDNA. This cDNA is subsequently indexed, processed into a library format, and subjected to sequencing, following which reads can be mapped back onto the tissue.

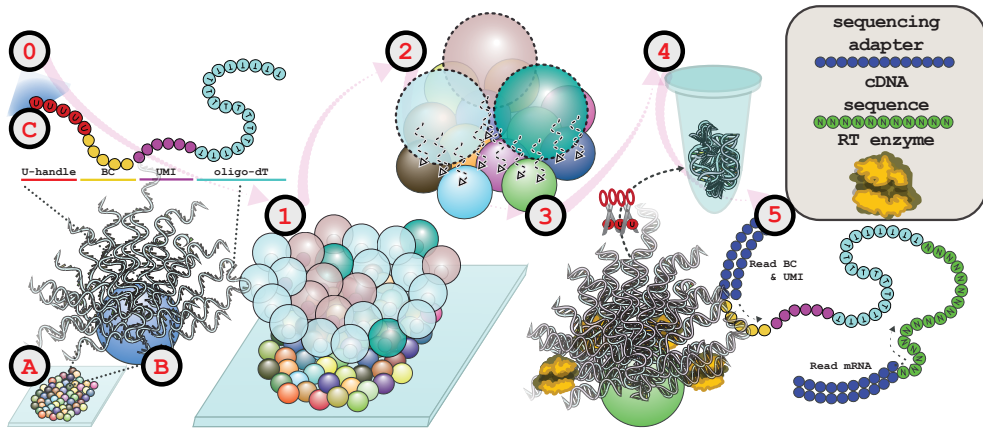


Figure 4: Illustration of Slide-seq transcriptome analysis. (0) Slide-seq bead array (A) with a bead detail in (B) and an example of a capture probe on its surface in (C) with uracil handle (U-handle), bead-specific barcode (BC), UMI and oligo-dT capture sequence. (1) Tissue is placed on the array, (2) permeabilized, releasing mRNA, which is transcribed into cDNA on the beads (3). Uracil stretch is then digested, releasing cDNA (4), which can be sequenced with paired-end sequencing.

Stereo-seq

Stereo-seq is a remarkable method that relies on lithography chips featuring wells with diameters ranging from 500 to 715 nm and DNA nanoballs (A. Chen et al., 2022). In this method, each feature on the chip is assigned a precise spatial coordinate by distributing randomly labeled circular templates onto the chip's surface. These templates are then transformed into DNA nanoballs using a technique called rolling circle amplification (RCA).

Subsequently, capture probes are ligated onto these nanoballs, which merge oligo-dT probes with spatial identifier sequences. To profile the transcriptome of a tissue sample, the tissue is placed onto this prepared array. A series of permeabilization steps releases the mRNA from the tissue, allowing it to bind to the capture probes on the nanoballs. This mRNA is then transcribed into cDNA. The resulting cDNA is removed from the array and used to prepare a sequencing library. After sequencing, the reads can be accurately mapped back to their respective nanoball positions on the chip.

Stereo-seq has demonstrated outstanding efficiency, capturing approximately 20,000 transcripts per well while maintaining a relatively large overall area of 200 mm²—an achievement in the realm of unbiased spatial sequencing.

The method was demonstrated by creating an impressive map of the developmental processes in a developing mouse embryo, spanning from E9.5 to E16.5. Only several months later, the method was used to map the axolotl brain with single-cell resolution (Wei et al., 2022), with a focus on

ependymogial cells. This study provided valuable insights into the transcriptional states of these cells during both development and regeneration.

Deconvolution Methods

The advent of various spatial transcriptomics methods has expanded our ability to profile tissue at high resolution. However, many of these methods still need to achieve single-cell resolution. To this end, computational deconvolution methods have emerged to bridge this gap and extract cellular-level information from spatial data. As several deconvolution methods have been previously used to deconvolve bulk RNA-seq composition into its cellular constituents (B. Chen et al., 2018; Monaco et al., 2019; Steen et al., 2020), their adaptation for spatial transcriptomics was a natural progression.

Many of these deconvolution methods utilize scRNA-seq data as a reference for deconvolving the spatially resolved bulk features (Andersson et al., 2020; Biancalani et al., 2021; Cable et al., 2022; Danaher et al., 2022; Kleshchevnikov et al., 2022; Y. Liu et al., 2023; Lopez et al., 2022; Song & Su, 2021; D. Sun et al., 2022). This approach is excellent for experimental setups profiling tissues with both spatial and single-cell resolution or, optionally, with a suitable external single-cell reference available. Nevertheless, it is not always feasible to have a cellular-level reference, prompting some methods to focus on either including an internal reference (Y. Ma & Zhou, 2022) or identifying underlying transcriptionally similar cell populations through probabilistic modeling (H. Zhang et al., 2023).

Many new approaches to transferring the successes of other fields to biology have also been published. Among them, for example, a novel, unsupervised, reference-free deconvolution approach emerging from the natural language processing domain, featuring the latent Dirichlet allocation (LDA) model (Miller et al., 2022).

With an abundance of available models, selecting the most suitable one for a specific dataset and tissue type can be challenging. Several review articles have been published to assist researchers in this task, benchmarking these methods on numerous high-quality datasets (H. Li et al., 2023; Yan & Sun, 2023), thus facilitating the selection of appropriate method-application combinations.

The Evolution of FISH

The use of FISH methods for RNA species detection dates back to the early 1980s, with the first publication on transcript detection through radiolabeled *in situ* hybridization (ISH) in 1973 (Harrison et al., 1973). Subsequently, fluorescently labeled versions emerged in the following decades. A pivotal moment in FISH technology was a precursor to seqFISH, which surfaced in 2012 with the detection of 32 genes facilitated by super-resolution microscopy. SeqFISH, employing multiple rounds of fluorescent probe hybridization, showcased the potential to label the transcriptome with increasing granularity (Lubeck et al., 2014). This method was later refined by

introducing error correction techniques (Shah et al., 2016). It evolved into RNA SPOTs and seqFISH+, both demonstrating the detection of over 10,000 transcripts, a substantial advancement from their predecessors (Eng et al., 2019; Eng et al., 2017).

The subsequent development of multiplexed error-robust FISH (MERFISH) introduced the encoding of transcripts in a fluorescent binary code while also streamlining the detection process by eliminating only the fluorescent component of the detection ensemble (K. H. Chen et al., 2015). This innovation led to extensive transcriptome profiling capabilities (Xia et al., 2019). In 2018, the implementation of cyclic transcript labeling further improved the method, offering a clever solution to mitigate optical crowding and overcome the minimum transcript length limitations present in seqFISH and MERFISH with osmFISH (Codeluppi et al., 2018).

Advancements in FISH techniques continued to improve the methods further. An improvement in the signal-to-noise ratio was achieved through the incorporation of rolling circle amplification (RCA) into the workflow (Gyllborg et al., 2020; Jang et al., 2023), as well as the utilization of branched DNA (Battich et al., 2013) and hybridization chain reactions (Choi et al., 2014; Jang et al., 2023; Shah et al., 2016). Additionally, innovations emerged through the implementation of tissue clearing (X. Wang et al., 2018) and expansion methodologies (F. Chen et al., 2016). These collective developments have significantly expanded the capabilities and resolution of FISH techniques for transcriptome analysis.

Molecular Toolbox: Padlock Probes and Rolling Circle Amplification

The molecular toolbox employed in the *in situ* sequencing methods described in this thesis predominantly relies on padlock probes and RCA for gene detection, sequence capture, and sequencing. This section aims to provide a foundational understanding of these methodologies.

Padlock probes are single-stranded DNA molecules featuring hybridization arms at their 3' and 5' ends, typically spanning 15 to 20 bases each. These arms are designed to be complementary to the target transcript of interest. Complementarity of the arms is the most crucial at the arm junction as a non-matching base would cause a failure of the arms to be ligated together; however, this effect tapers towards the non-ligating ends of the padlock probes. When the arms of a padlock probe successfully ligate, they form a circular molecule that serves as a template for RCA. This concept has been widely applied in single nucleotide polymorphism (SNP) detection (Edwards et al., 2009; Krzywkowski & Nilsson, 2018). In addition to the hybridization arms, padlock probes typically feature a backbone that constitutes about 60% of the probe's length. This backbone can incorporate various functional elements, such as a detection site compatible with fluorescent *in situ* hybridization, primer binding sites for sequencing or gene/transcript identifier sequences (X. Chen et al., 2019; Ke et al., 2013; X. Wang et al., 2018) (figure 5).

Initially, padlock probes were limited to targeting only DNA molecules due to constraints of the available ligase enzymes. However, the advent of ligases that accept RNA:DNA hybrid

molecules has enabled methods to directly target RNA without the need for reverse transcription (H. Lee et al., 2022; S. Liu et al., 2021). This approach offers several advantages: it eliminates the efficiency loss associated with reverse transcription, reduces costs (as reverse transcriptases are often costlier enzymes used in higher concentrations), and decreases time requirements.

RCA has gathered significant attention in recent years due to its ability to generate an exceptional amount of product. The primary enzyme involved in this reaction, Φ 29 (Phi29) polymerase, can synthesize kilobases of a concatemeric product from a single primed circular molecule due to its unparalleled processivity. This makes it an excellent choice for applications requiring the synthesis of a large quantity of DNA. In addition to *in situ* sequencing approaches, RCA has found applications in viral genome synthesis (Barreira et al., 2023), DNA sequencing (Dean et al., 2002; English et al., 2012) and spatial transcriptomics methods, such as Stereo-seq (Wei et al., 2022) mentioned earlier. An even more processive variant of Phi29 polymerase has been developed by ThermoFisher Scientific, which claims faster reaction times and improved yields while maintaining a constant error rate. Apart from DNA synthesis and displacement properties, Phi29 has been reported to possess a 3'-5' exonuclease activity (X.-Y. Li et al., 2017) and restricted reverse transcription activity (Krzywkowski et al., 2018), rendering it a versatile enzyme.

FISSEQ and ExSEQ

The FISSEQ (Fluorescent In Situ Sequencing) method presents a unique approach to RNA sequencing. It employs the Circligase enzyme after cDNA reverse transcription, effectively transforming the cDNA itself into a RCA amplification template. This distinctive method was first introduced in 2003 (Mitra et al., 2003). What sets FISSEQ apart is its aim to provide an unbiased approach, which is less common in RCA-based methods. However, this unbiased nature comes with the drawback of a significant proportion of reads originating from ribosomal RNA, reaching up to 81.6% (J. H. Lee et al., 2014). Despite this limitation, FISSEQ offers extensive readout capabilities, particularly when combined with SOLiD sequencing, allowing for the sequencing of a 28-base-long stretch with minimal cross-talk.

FISSEQ was further integrated as an untargeted component of an expansion microscopy-based method, ExSeq, designed for extensive transcriptome analysis (Alon et al., 2021). Expansion chemistry not only enhances resolution but also makes RNAs more accessible to reagents. While retaining the *in situ* sequencing component, ExSeq expands and adds an *ex situ* sequencing step in the final phase, utilizing *in situ* sequencing as a mapping tool back to the tissue. The targeted branch of ExSeq relies on padlock probes that hybridize directly to RNA molecules, providing an excellent counterpart to FISSEQ.

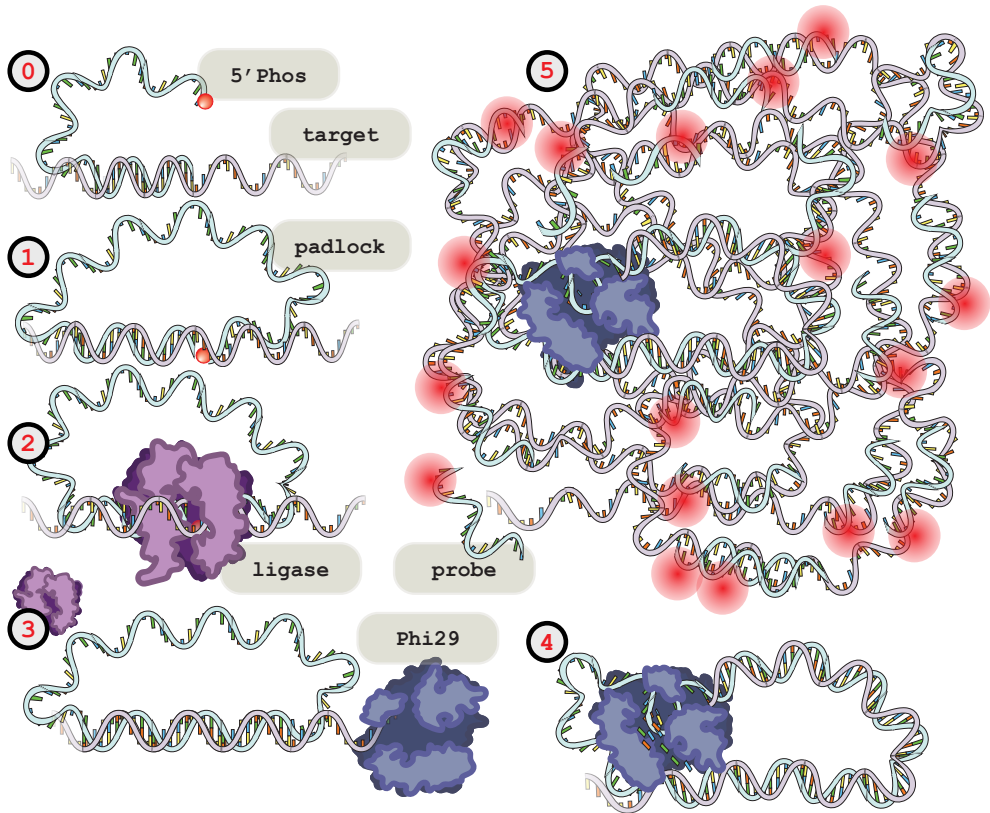


Figure 5: Schematic illustration of RCA of the padlock probe signal. (0) A padlock probe with a phosphate molecule at 5' end (5'Phos) finds its target transcript. (1) Padlock probe fully hybridized to its target with gaps between the hybridization arms. (2) Ligase joining the gap. (3) Phi29 digesting away DNA from the 3' end until dsDNA region. (4) Phi29 switching into its polymerase mode and synthesizing a complementary strand to the padlock probe. (5) With a strong strand displacement activity, Phi29 copies over the circularized probe thousands of times, creating a concatemeric molecule, a "rolony", containing the detection site of every padlock probe copy.

In Situ Sequencing

The ISS (in situ sequencing) method, which was later commercialized into the Cartana system (H. Lee et al., 2022) and subsequently acquired by 10X Genomics, represents one of the early *in situ* sequencing approaches. In their 2013 publication (Ke et al., 2013), the research group introduced a padlock probe-based strategy for gene detection. This method involves tissue fixation and permeabilization, followed by cDNA synthesis and the removal of template RNA to create a binding site for the padlock probe. For transcript detection using padlock probes, the molecules

are allowed to hybridize, and their arms are ligated. Subsequently, RCA is performed, with cDNA serving as the priming site for the reaction. The resulting product, known as a "rolony", is then anchored in the tissue, and the barcode embedded in the template padlock probe backbone is read through sequencing by ligation.

In the case of padlock probes designed for sequence capture, the probe is designed to bind the hybridization arms around a sequence of interest. Once the arms hybridize, a polymerase without strand-displacement activity is employed to fill in the gap; in this case, the Stoffel fragment was used. The remaining gap is ligated, and the circular molecule is transformed into a rolony sequenced as in the gene targeting approach. The difference lies in the fact that a binding arm sequence is used as a priming site for sequencing.

Through this approach, Ke et al. demonstrated a high accuracy rate of 98.1% for gap-filling sequencing, which was applied to sequence four bases in the human β -actin gene. Additionally, they successfully targeted 35 transcripts associated with breast cancer prognosis using gene targeting with padlock probes (Ke et al., 2013).

BaristaSeq

The gap-filling approach has been significantly improved in the BaristaSeq method (X. Chen et al., 2018). While the study by Ke et al. used the Stoffel fragment to fill in the gap between the arms, a more detailed investigation in the BaristaSeq group revealed a notable issue with over-extended products, making the ligation of padlock probes infeasible in many cases. To address this challenge, a search for a polymerase lacking strand displacement activity was conducted, and it was found that Phusion polymerase produced the lowest amount of incorrectly sized products, making it the most suitable enzyme among those tested. Subsequent optimization of reaction conditions further improved the yield, resulting in slightly over half of all padlock probes generating the correctly sized product. This represents a significant enhancement over the original implementation while maintaining a low rate of false positives (X. Chen et al., 2018).

In addition to optimizing gap-filling, BaristaSeq replaced the sequencing-by-ligation method with sequencing-by-synthesis by adapting Illumina sequencing chemistry. This change improved signal-to-noise ratio and demonstrated minimal signal loss for sequences up to 15 bases (X. Chen et al., 2018).

BARseq

BARseq is a method that followed MAPseq's publication (X. Chen et al., 2019). MAPseq was initially designed for projection mapping through cell barcoding with a Sindbis virus carrying a presynaptic protein capable of binding to a transcript consisting of a boxB sequence, along with a reporter protein and a barcode sequence (Kebschull et al., 2016). Like many other RNA-seq methods, MAPseq requires tissue homogenization, which results in a loss of cellular resolution and limits its applicability to dissectable areas. In the years following, other connectivity mapping methods were published (Huang et al., 2020; Peikon et al., 2017; Wu et al., 2021), with BARseq being one of them.

BARseq utilizes the MAPseq approach, where cells in a source node are infected with the previously described Sindbis virus, which is then trafficked to the presynaptic sites of these cells. However, unlike MAPseq, BARseq focuses on analyzing the area at the injection site with single-cell resolution. This method has demonstrated higher sensitivity compared to standard projection tracing approaches, such as contralateral projection tracing using retrograde cholera toxin subunit B. Sindbis-delivered cellular barcodes are read using the BaristaSeq approach, which also enables the assignment of cell type transcriptional identity through compatible methods like marker-based *Cre* driver lines or FISH. Both approaches were validated in the founding study. First, through the use of the *Fezf2* driven *Cre*, allowing for *dTomato* expression that was mainly confined to five PT-I cell populations (Tasic et al., 2018). Second, with FISH detection of the *Slc17a7* gene (a marker for excitatory neurons) and *Gad2* (marking inhibitory neurons). Both cell labeling methods revealed population-level patterns in projection preferences, underscoring the added value of the BARseq approach over MAPseq.

Classification based on endogenous genes assumes that infection with the Sindbis virus used to drive strong cellular barcode expression does not interfere with the gene expression of the cells. The performed experiments indicated that this may not be the case, as the overall endogenous expression was lower in barcoded sites over the intact. Luckily, the relative levels of transcripts were found unchanged, leaving the type-specific expression patterns as informative as in an intact tissue. The BARseq method has since been implemented in numerous connectomic studies (X. Chen et al., 2019; Muñoz-Castañeda et al., 2021).

Following the initial BARseq implementation, an improved follow-up method was published in 2021 (Y.-C. Sun et al., 2021). This iteration retained its potential for projection mapping while also introducing a targeted padlock approach for cell-type profiling. This advancement allowed for a detailed mapping of cortical neurons and their projections (figure 6). A third iteration, Axonal BARseq, is currently in development, promising even finer resolution of axonal projections and their interactions (Yuan et al., 2023).

RNA Detection Methods

After cDNA-based approaches, several notable methods have emerged, which target RNA directly, moving away from the use of cDNA (R. Deng et al., 2018; H. Lee et al., 2022; S. Liu et al., 2021; Sountoulidis et al., 2020). Some noteworthy methods in recent years include SeqEA (R. Deng et al., 2018), STARmap (X. Wang et al., 2018), SCRINSHOT (Sountoulidis et al., 2020), BOLORAMIS (S. Liu et al., 2021), and dRNA-ISS (H. Lee et al., 2022).

SeqEA is based on a rolony-type approach with DNA probes being ligated directly on RNA with SplintR ligase, which operates about 100 times faster on RNA:DNA molecules than T4 ligases (Ho et al., 1997; Jin et al., 2016). It was introduced in 2018 and offered a unique approach by detecting variations not only in fluorophores but also in the effectiveness of probe hybridization. This effectively expanded the detection capabilities, demonstrated through the detection of 36 distinct barcodes using only two different fluorophores.

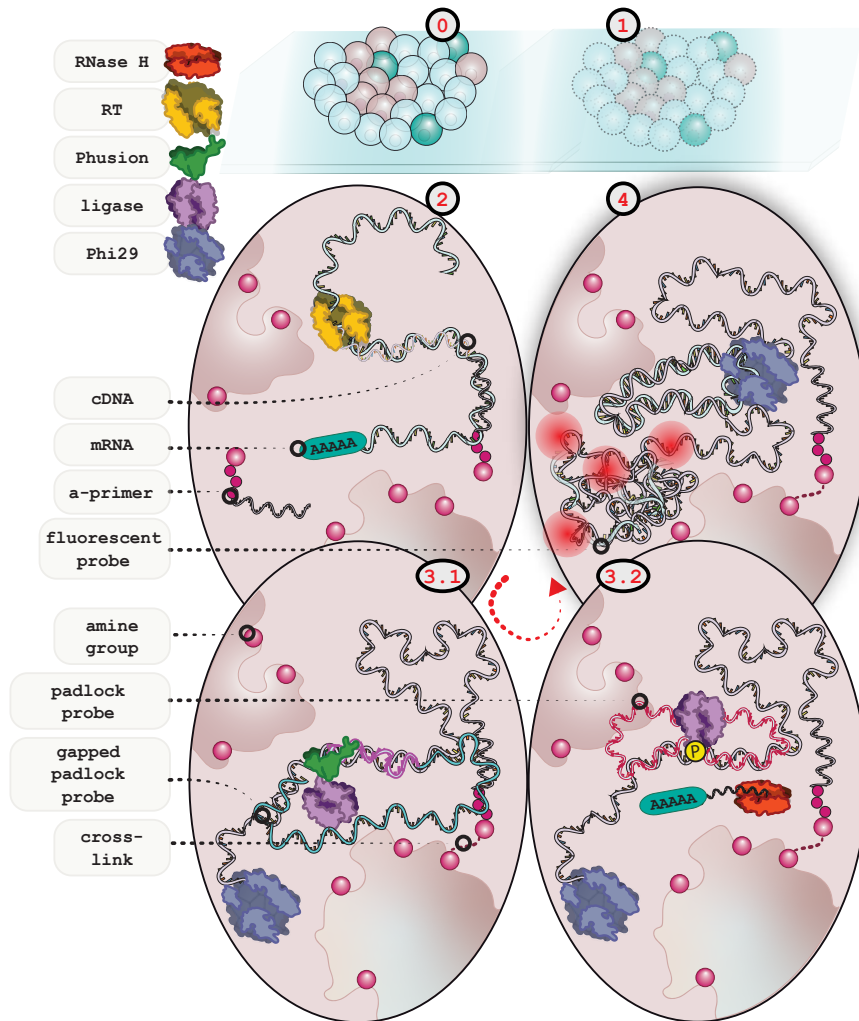


Figure 6: Illustration of the BARseq method for transcript detection and analysis. (0) Cut tissue placed on a slide. (1) permeabilized tissue. (2-4) Details of sequence capture in tissue from (2) cDNA synthesis, to (3.1) crosslinking and sequence capture with a gapped padlock probe, (3.2) gene detection with a padlock probe and finally (4) RCA. RT - reverse transcriptase; a-primer - 5'-aminoallyl-modified-primer.

STARmap presents one of the most extensive RCA-based transcriptome profiling efforts up to date with the successful detection of 1024 genes in a mouse brain tissue. Unlike the vast majority of padlock-based methods targeting mRNAs, STARmap achieves gene detection without using SplintR ligase by moving the ligation sequence outside the hybridization segment. Specificity is maintained by including a double-purpose splint oligonucleotide that allows probe ligation and primes the RCA reaction after hybridizing to its mRNA target (figure 7). As tissue imaging can be complicated by its background signal, STARmap uses tissue-hydrogel chemistry to remove all background. The padlock barcode is then sequenced through sequencing with error-reduction by dynamic annealing and ligation (SEDAL), which has both good efficiency and error-checking qualities by querying two bases at a time. It is an excellent alternative to replace SOLiD chemistry and simultaneously overcome errors, which are difficult to detect in single-base querying methods such as cPAL (Drmanac et al., 2010). A follow-up method, STARmap PLUS, has shown its utility by extensively monitoring Alzheimer's disease pathology in animal models and creating detailed mouse CNS single-cell resolution maps. While the core concepts of the method remained, this expanded version extended the barcode from 5 to 10 bases and included protein detection (H. Shi et al., 2022; Zeng et al., 2023).

SCRINSHOT uses DNA padlock probes that directly hybridize to mRNA and are ligated using the SplintR ligase (Jin et al., 2016; Sountoulidis et al., 2020). Due to the reported low selectivity of SplintR ligase and its reported ability to ligate despite a mismatched site (Krzykowski & Nilsson, 2017), the group focused on defining stringent conditions for the hybridization reaction. It showed the detection of 30 mRNA species in mouse lungs and submucosa.

BOLORAMIS achieves the direct detection of 96 genes from mRNA using SplintR ligase. This method features 60-nt long padlock probes, which are over 30% shorter than those used in comparable methods (typically 90 bases). Optimization of the 5' arm length effect on true detection rates is carried out, interestingly resulting in arm asymmetry. After the rolon synthesis, the padlock barcode recovery is demonstrated using both FISH and a previously published ISS method (Shendure et al., 2005). Notably, in BOLORAMIS, no significant advantage in using more than 5-10 probes per gene was seen compared to other padlock-based methods employing up to 30 probes per mRNA, which at a scale vastly decreases the number of necessary probes. While the authors aimed to detect 77 miRNAs, barcode recovery for miRNAs was found to be insufficient, necessitating further protocol optimization for miRNA detection.

dRNA-HybISS provides a commercial kit alternative to methods where individual components need to be implemented by the adopting lab. This method exhibits superior sensitivity compared to the cDNA-HybISS approach and has been benchmarked against osmFISH. While osmFISH proved to be more sensitive overall, dRNA-HybISS demonstrated the ability to categorize underlying cell populations with similar resolution (H. Lee et al., 2022).

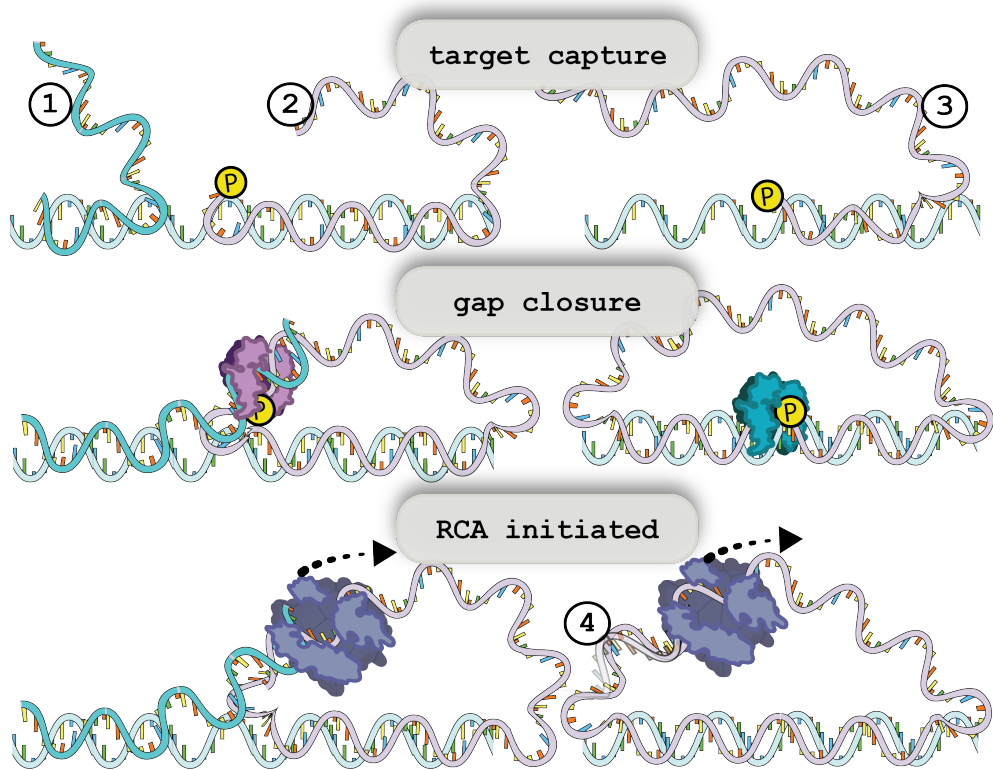


Figure 7: Illustration of the STARmap employing its SNAIL probe mechanism compared to padlock probe ligated directly on RNA (as seen in SCRINSHOT, BOLORAMIS and dRNA-HybISS). (1) SNAIL probe splint oligonucleotide, (2) SNAIL probe, (3) padlock probe. DNA ligase is in magenta, SplintR ligase in teal and Phi29 polymerase in dark blue.

Parkinson's Disease

Parkinson's Disease (PD) stands as the second most prevalent neurodegenerative disorder, affecting approximately 2-3% of individuals above the age of 65 (Dorsey et al., 2007; Pringsheim et al., 2014; Savica et al., 2013; Twelves et al., 2003; Van Den Eeden et al., 2003), while it remains relatively rare among those under 50 years old. Its prevalence is expected to increase in parallel with the aging population. Interestingly, PD exhibits a significant gender bias, affecting men nearly twice as often as women in many populations, a trend curiously opposite to Alzheimer's disease (Elbaz et al., 2016). The clinical diagnosis of PD is primarily based on the presence of bradykinesia and other motor symptoms, often with an asymmetrical presentation (Kalia & Lang,

2015). However, non-motor symptoms such as cognitive impairment, sleep disorders, impaired sense of smell, and psychiatric symptoms like anxiety and depression significantly impact the patient's quality of life. They can precede the onset of motor symptoms by several years or even decades (Chaudhuri & Schapira, 2009). James Parkinson officially described the disease in 1817 as a 'shaking palsy,' emphasizing its prominent motor component (Parkinson, 2002).

Pathological Mechanisms

The majority of motor symptoms of Parkinson's Disease result from the degeneration of dopaminergic neurons in the substantia nigra (SN), leading to dopamine depletion in striatal structures and aberrant functioning of the surviving dopaminergic neurons. The disease is also characterized by the presence of Lewy bodies and α -Synuclein (α Syn) positive aggregates (Dickson et al., 2009; Halliday et al., 2011). PD primarily affects specific cell types and brain regions unlike other neurodegenerative diseases. In the early stages, the damage is confined to the ventrolateral SN (Damier et al., 1999; Fearnley & Lees, 1991), gradually spreading in later stages. Minimal symptoms can be observed in the prodromal stage of degeneration (Dijkstra et al., 2014). The oncoming Lewy pathology in PD is initially localized to the cholinergic and monoaminergic neurons of the brainstem and olfactory system, in contrast to Alzheimer's disease with a center in the limbic areas (Iacono et al., 2015).

Genetic and Environmental Influences

PD has a genetic component, with several genes having a strong effect and causing early-onset PD and many newly discovered genes showing much lower penetrance (C. Klein & Westenberger, 2012; Nalls et al., 2014). Mutations in several genes are associated with familial forms of PD, including SNCA, VPS35, and LRRK2, which are linked to autosomal-dominant transmission, and PARKIN, PINK1, DJ-1, and DNAJC6 are associated with recessive forms. Genetic variation among ethnic populations may explain some disparities in PD risk, such as certain LRRK2 and GBA gene variants over-represented in Ashkenazi Jews, associated with an increased risk of PD (Chillag-Talmor et al., 2011). Increased prevalence has also been observed in other ethnic groups (Gordon et al., 2012). However, disentangling the contributions of genetic, societal, and environmental factors has proven challenging.

As only about 10% of PD cases can be attributed to a genetic burden, roughly 90% of cases are likely caused by other factors (C. Klein & Westenberger, 2012). Many studies have focused on the relationship between the environment and the disease development and progression (Ascherio & Schwarzschild, 2016). Some examples of factors influencing PD are exposure to pesticides, history of melanoma or brain injury, or consumption of dairy products, which increase the risk of diagnosis and physical activity, caffeine and nicotine usage as well as the use of several anti-inflammatory medications, which are associated with a lower risk. (Ascherio & Schwarzschild, 2016; Paul et al., 2023). The lifestyle within the so-called Western nations also seems to carry a risk factor for the disease onset, as demonstrated by a study involving American men of Japanese ancestry, who experienced an increased risk of PD after moving to the United States compared to most Asian countries (Morens et al., 1996).

During the course of PD, numerous cellular processes are disrupted, including α Syn proteostasis, mitochondrial function, oxidative stress pathways, calcium homeostasis, axonal transport, lysosome-dependent degradation, and neuroinflammation (Nalls et al., 2014).

Basal Ganglia and its Dysregulation in PD

The basal ganglia constitute a complex network of subcortical nuclei, with critical hubs including the striatum, globus pallidus (GP), substantia nigra (SN), and subthalamic nucleus (STN), which output to the thalamus (figure 8). Dysfunctional interactions within this network play a pivotal role in manifesting motor symptoms associated with Parkinson's Disease (PD).

Historically, various models of basal ganglia function have been proposed (McGregor & Nelson, 2019). Here, we will introduce the classical model, widely accepted in the field as a reasonable simplification. According to this model, two major pathways (see figure 9), distinguished by their unique populations of striatal medium spiny neurons (MSNs), govern motor behavior. These pathways are the direct and indirect pathways, with the hyperdirect pathway from the cortex to the subthalamic nucleus being included additionally. (Nambu et al., 2000).

The direct pathway is primarily associated with the initiation of movement. It involves the D1 receptor-expressing MSN population in the striatum, which projects to the internal GP (GPi) and SNr. Activation of this pathway inhibits the GPi and SNr, subsequently disinhibiting the thalamus. This disinhibition leads to the activation of thalamic glutamatergic neurons, ultimately initiating motor movements (Albin et al., 1989; Alexander & Crutcher, 1990; DeLong, 1990; Y.-P. Deng et al., 2006; Gerfen et al., 1990; Moore & Bloom, 1978).

Conversely, the indirect pathway is primarily involved in inhibiting non-target motor movements. It originates with the D2 receptor-carrying MSNs, which are inhibited by dopamine. These neurons project into the external segment of GP, whose neurons, in turn, influence the STN, further supporting the baseline thalamus inhibition from SNr and GPi. The activation of this pathway increases thalamic inhibition and prevents signal transmission to the cortex. Additionally, the hyperdirect pathway from the cortex to the subthalamic nucleus has been proposed to play a role in preventing premature responses by strengthening the indirect pathway (Frank et al., 2007).

In Parkinson's Disease, this delicate balance within the basal ganglia system is disrupted. Dopamine depletion in the striatum, a hallmark of PD, leads to an overall increase in the inhibition of thalamus. This heightened inhibition of the excitatory thalamocortical projections ultimately results in the lack of excitation of the upper motor neurons, contributing to the motor deficits characteristic of the disease (McGregor & Nelson, 2019). The dysregulation of the basal ganglia circuitry underscores the fundamental role of these subcortical structures in motor control and the pathophysiology of PD. But additionally, besides basal ganglia imbalances, other complex changes in information processing are suggested to be involved in the PD pathology, such as cortico-subcortical communication or the interaction between basal ganglia and cerebellum (Dirkx et al., 2016; Kühn et al., 2008).

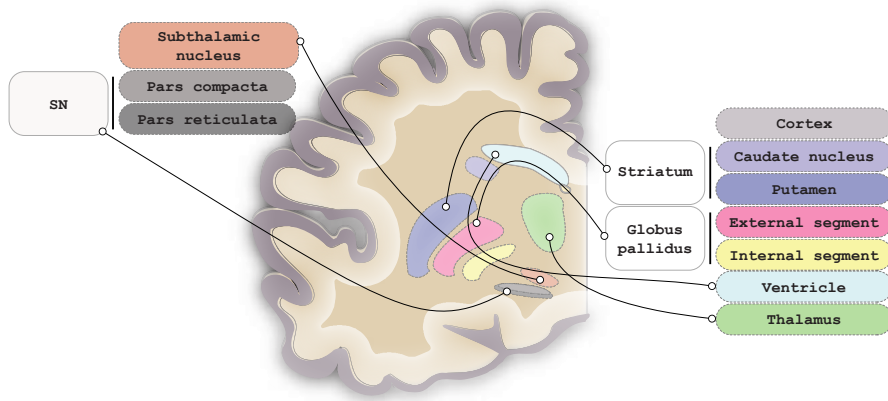


Figure 8: Main anatomical structures of the basal ganglia

Therapies

Pharmacological Solutions

One of the oldest drugs for PD, the dopamine precursor L-DOPA, has been on the market for over 50 years. As many of the PD symptoms arise from the lack of dopamine in the striatum, systemic administration of L-DOPA, which crosses the blood-brain barrier and can be converted into dopamine (LeWitt & Fahn, 2016) is a widely used solution (figure 10). It comes, however, with the caveat that its long-term usage leads to side effects, mostly in the form of involuntary movements, so called dyskinesias. While the cause of these side effects is not fully understood, one of the key players is the discontinuous delivery of the shortly-lived L-DOPA, inherent to the standard delivery methods, together with the variability in its absorption and transport (Poewe & Antonini, 2015). Correspondingly, improvements in the continuity of the delivery ameliorate the effects (Foltynie et al., 2013; Olanow et al., 2014).

Other dopamine targeting solutions include catechol-O-methyltransferase (COMT) inhibitors, frequently co-administered with L-DOPA, which inhibit the metabolizing of dopamine, effectively increasing its bioavailability (Ferreira et al., 2016). Additionally, monoamine oxidase type B (MAO-B) inhibitors extend dopamine synaptic concentrations by inhibiting its processing into an inactive metabolite (Schapira, 2011). Further, dopamine agonists, acting on medium spiny neurons' D1 and D2 receptors, are also employed (Connolly & Lang, 2014; Fox et al., 2011). Some agonistic drugs have demonstrated efficacy comparable to L-DOPA while causing fewer dyskinesic side effects. However, a drawback of this class is the potential stimulation of D3 receptors in the ventral striatum, which can lead to excessive activation of brain reward centers and result in impulse control issues or drowsiness (Weintraub et al., 2010).

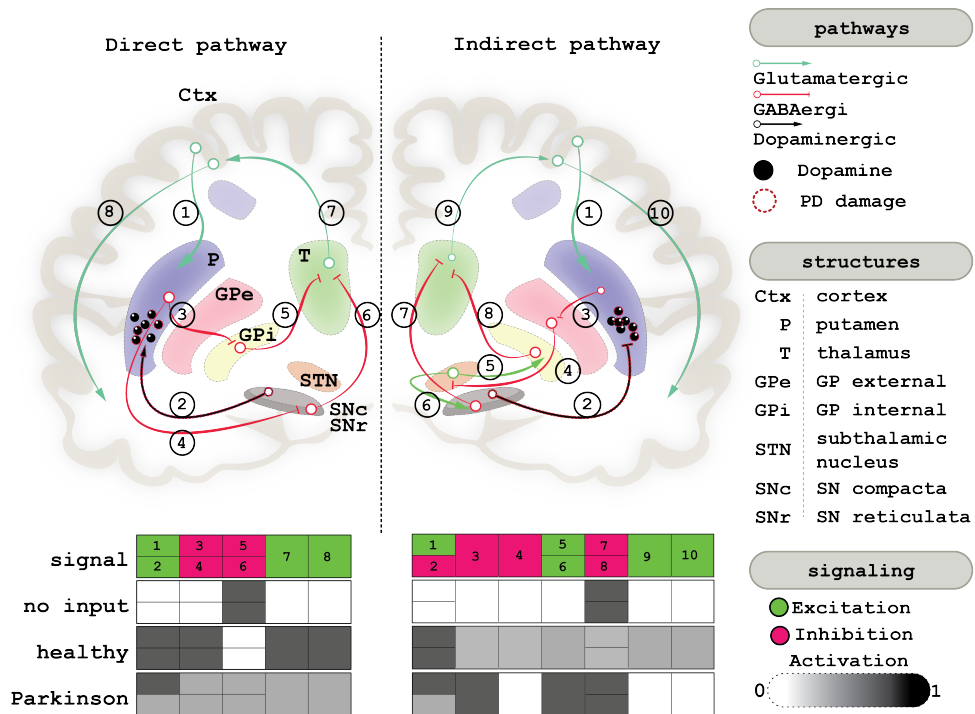


Figure 9: Schematic illustration of the direct and indirect pathways. Green arrows depict pathways with glutamatergic signal, red with GABAergic, and black with dopaminergic. Pathways degenerated in PD are shown with a dashed red border. The table below shows whether a signal from the structure is excitatory or inhibitory, as well as activation patterns in a healthy subject versus in a Parkinson's disease patient

Deep Brain Stimulation

Deep Brain Stimulation (DBS) for PD has its roots dating back to 1993 when the subthalamic nucleus (STN) was identified as a viable target for PD treatment (Limousin et al., 1995). Following the discovery that high-frequency stimulation can mimic lesioning, electrode implantation was employed to modulate the subthalamic nucleus, a practice still in use today for managing advanced PD symptoms (Fox et al., 2011). This treatment is typically reserved for patients who initially responded well to L-DOPA but have exhausted its effectiveness and do not exhibit severe psychiatric symptoms (Bronstein et al., 2011). Young-onset PD patients are a common group eligible for this surgical intervention (Deuschl & Agid, 2013). While dopaminergic medication is not entirely discontinued after the surgery, its reduction by approximately 60% reduces dyskinesic events by a similar rate, markedly improving patients' quality of life. Apart from the STN, another target of DBS is the internal segment of the globus pallidus (GPi). However, at best,

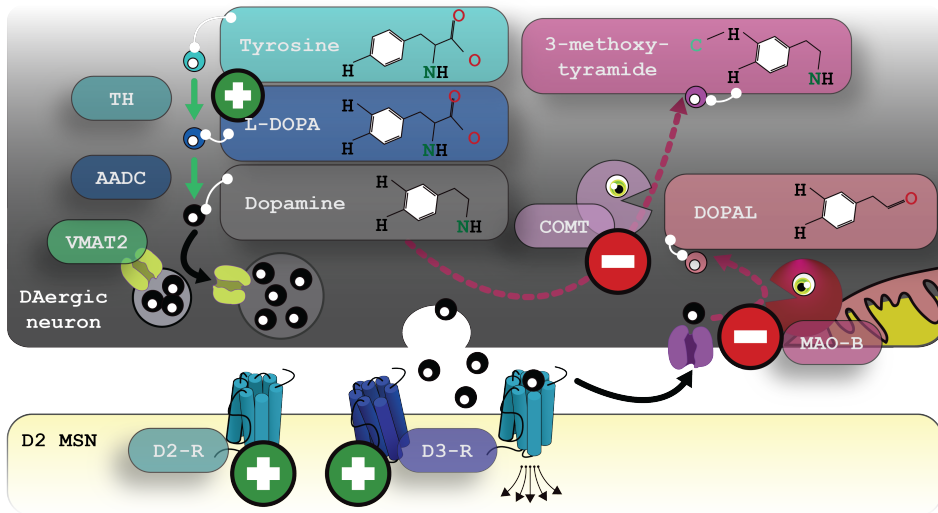


Figure 10: Pharmacological targets of PD therapy. Synthesis pathways are shown in green, degradation pathways are in red, and transport pathways are in black. TH - Tyrosine hydroxylase, AADC - aromatic L-amino acid decarboxylase, DOPAL - 3,4-dihydroxyphenylacetaldehyde, D2-R - D2 receptor, D3-R - D3 receptor

long-term outcomes of GPi targeting appear to be equivalent to STN targeting (Odekerken et al., 2016).

Gene Therapy

Gene therapy in the context of PD can be categorized into three main approaches: neurotrophic factor delivery, dopamine restoration through enzyme delivery, and basal ganglia modulation agents.

In the realm of neurotrophic factor delivery, members of the glial cell line-derived neurotrophic factor (GDNF) family have shown promise in animal models of PD (Kordower et al., 2006). While initial trials with GDNF delivery into the putamen have shown promise in symptom and L-DOPA side effects reduction, the benefit was later not shown in a more extensive study, which compared GDNF to a placebo infusion (Lang et al., 2006). Later, this lack of results was theorized to be potentially caused by a lack of GDNF spread throughout the tissue.

To improve delivery, viral vectors, such as Adeno-associated virus serotype 2 (AAV2), were employed. Trials documented the delivery of neurturin (NTN), a close analog of GDNF, using AAV2. NTN-based therapy showed a positive trend in a preliminary study with very few human subjects, where the therapy diminished the level of dyskinesias, improved functional scores, and had very few side effects (Marks et al., 2008). A more extensive trial, unfortunately, did not

show significant symptomatic relief despite the encouraging initial studies, even as it showed good tolerability, observed in most AAV2-based gene therapies (Marks et al., 2010). Post-mortem investigation revealed that AAV2 successfully transduced cells were mainly by the injection tract and weren't especially numerous (Bartus & Johnson Jr, 2017). Other factors explored included cerebral dopamine neurotrophic factor, brain-derived neurotrophic factor, and vascular endothelial growth factor (Lindholm et al., 2007; Tsukahara et al., 1995; Yasuhara et al., 2004).

The second approach focuses on the delivery of dopamine-modifying enzymes. Numerous clinical trials, many utilizing AAV2 as the delivery vector, have been initiated (Kozłowska et al., 2023). Among completed studies, many have focused on the delivery of genes related to dopamine restoration, including tyrosine hydroxylase (*TH*), L-amino acid decarboxylase (*AADC*), and GTP cyclohydrolase 1 (*GCHI*) (Carlsson et al., 2005; Jarraya et al., 2009). Some of these studies have shown promising results in animal models for dopamine restoration. A 2012 study using an AAV2 vector carrying the *AADC* gene (Mittermeyer et al., 2012) exhibited a good safety profile and tolerance. Prior studies had demonstrated the restorative effect of *AADC* in animal models (Sánchez-Pernaute et al., 2001), and this study showed AAV2-delivered *AADC* to remain active four years post-surgery. Symptomatic relief was observed in the first 12 months post-surgery; however, it appeared to deteriorate afterward. Another AAV2-based trial focused on the striatal delivery of *AADC* genes and, when followed for 36 months, allowed for a reduction in L-DOPA dose of up to 30% (Christine et al., 2022). Oxford Biomedica explored a tri-enzyme approach involving the delivery of *TH*, *AADC*, and *GCHI* directly into the striatum using a lentiviral vector (Palfi et al., 2014). This approach was necessitated by the cargo size, which exceeded the AAV size limit. A non-human primate study using this construct demonstrated good tolerability, symptomatic improvement, and the absence of dyskinesias following treatment (Jarraya et al., 2009). The positive outcome prompted a human trial, where patients' progress was monitored for 12 months. Similar to other attempts, the treatment was well tolerated but resulted in only modest yet reliable motor recovery (Palfi et al., 2014). Glutamic acid decarboxylase, which modulates basal ganglia activity, was also shown to be well tolerated and in human trials and studies performed up to date shows a promise with a decrease in motor symptoms over the course of 12 months (Niethammer et al., 2017).

Lastly, among the basal ganglia activity modulation category. Among its members is glutamic acid decarboxylase, which has shown to be well tolerated and, in human trials and studies performed up to date, shows a promise with a decrease in motor symptoms over the course of 12 months (Niethammer et al., 2017).

Cell-Based Therapy

Cell-based therapy aims to replace not only the dopamine-related components but also the entire dopaminergic cell population that degenerates during the course of PD. The journey of cell-based therapies for PD dates back to the 1970s and 1980s when preclinical studies were initiated. The first human trial occurred in 1982, involving two patients who received adrenal medullary tissue. This tissue produces catecholamines and, to a lesser extent, dopamine (Backlund et al., 1985). Unfortunately, these grafts did not demonstrate clinical benefits (W. J. Freed et al., 1990). However, in 1987, a study claimed symptom alleviation in two patients following medullary transplantation

(Madrazo et al., 1987), leading to a wave of transplantations based on somewhat dubious foundations and with inconsistent results (Allen et al., 1989; Hurtig et al., 1989; Jankovic et al., 1989), ultimately resulting in the abandonment of this approach. Apart from adrenal medullary tissue, human retinal pigment epithelium (hRPE), autologous carotid body, and embryonic porcine ventral mesencephalic cells were also explored (Gross et al., 2011; Mínguez-Castellanos et al., 2007; Schumacher et al., 2000).

Early efforts leading up to fetal dopaminergic graft transplantation emerged in the 1990s from a search for new ways to restore the dopamine release in the striatum (Björklund et al., 1980; Björklund & Stenevi, 1979). These early studies performed experiments using rat embryos between E16-E19 for the collection of ventral mesencephalic tegmentum, later developing into SN and VTA areas, and their transplantation into the dorsal striatum of the 6-OHDA rat model of PD. While the resulting number of grafted dopaminergic neurons was quite variable, these studies laid the foundation for the field's progress by proving a functional integration of these neurons through neuronal outgrowth and corresponding levels of motor recovery. First human trials were initiated not only due to the potential shown by early studies but also due to a sudden availability of aborted fetal tissue brought on by a change in Swedish law regarding its use for medical purposes. After initial studies with human material, confirming the presence of surviving dopaminergic neurons in grafts from ventral mesencephalic tissue from embryos aged 6.5 - 9 weeks (Brundin et al., 1986). First human trials began rather swiftly, and the first two patients and their progress was reported in 1989 (Lindvall et al., 1989).

During the 1990s, fetal dopamine neuron studies gained momentum. While initial patient data was suboptimal (Lindvall et al., 1989), subsequent attempts demonstrated more promise (Lindvall et al., 1990). These findings led to larger-scale efforts, which, despite variable outcomes, consistently showed overall symptom improvement (Brundin et al., 2000; C. R. Freed et al., 2001; Lindvall et al., 1994; Wenning et al., 1997). Notably, these therapies were more effective for patients in the early stages of the disease (Olanow et al., 2003). Long-term monitoring of transplant activity confirmed the durability of the graft over decades (Kefalopoulou et al., 2014; Olanow et al., 2003; Piccini et al., 2000). However, the use of fetal cells had its drawbacks, including limited availability of suitable donor material, the development of severe graft-induced dyskinesias (GID), and the challenge of achieving a homogeneous cell population (C. R. Freed et al., 2001; Y. Ma et al., 2002). Subsequent research attributed GID to the presence of contaminating serotonergic neurons, prompting the search for a more controllable population (Lane et al., 2006; Mendez et al., 2005; Politis et al., 2010). Another possible issue presented the discovery of Lewy pathology in transplants in post-mortem examinations (J.-Y. Li et al., 2008; J.-Y. Li et al., 2010); however, as the proportion of infected cells did not exceed 15%, and the transplants demonstrated decade-long survival, the positive outcomes of transplantation outweighed the eventual impermanence (Guo & Lee, 2014; Hallett et al., 2014).

As fetal cells posed scalability challenges, the field gradually shifted toward human embryonic stem cells (hESC), showing initial promise (Barker, 2014). With the development of protocols for generating dopaminergic neurons from embryonic cells, animal models swiftly followed and demonstrated the viability of transplanted cells (Cooper et al., 2010; Park et al., 2005; Roy et al., 2006). After developing protocols for generating dopaminergic neurons from embryonic cells, the first animal models transplantation did not wait long. It showed a population that

survives transplantation (Cooper et al., 2010; Park et al., 2005; Roy et al., 2006). Shortly after, the generation of pluripotent stem cells through a combination of four transcription factors was announced (Takahashi et al., 2007). Soon, these induced pluripotent stem cells (iPSCs) were subjected to differentiation towards dopaminergic fate similar to hESC, generating early successes (Chambers et al., 2009; Kikuchi et al., 2011; Soldner et al., 2009; Tabar & Studer, 2014). A deeper understanding of the origin of dopamine-producing neurons (Arenas et al., 2015; Kirkeby et al., 2012) and studies highlighting the similarity between hESC and fetal cell-derived neurons (Grealish et al., 2014) further accelerated progress in the field.

As the product is meant for eventual clinical use, a Good Manufacturing Practice (GMP)-compliant protocol was published for the cell generation (Nolbrant et al., 2017). The cells have been shown to display evidence of fiber outgrowth (Adler et al., 2019; Grealish et al., 2015), indicating integration into the host tissue.

The identity of the grafts was initially assessed with immunohistochemistry as well as RNA-seq (Adler et al., 2019; Kirkeby et al., 2017). Higher resolution analysis on the single-cell level was published in 2020 (Tiklová et al., 2020) and the spatial transcriptome was assessed in **paper I** of this thesis.

Animal Models

Numerous animal models have been established to replicate the key features of PD. Rodents, in particular, have become a favored choice due to their ease of handling and highly similar cortico-basal ganglia-thalamocortical circuits compared to humans (Reiner et al., 1998). In both human and rodent models, motor symptoms of PD begin to manifest when approximately 50% of dopaminergic connections to the striatum are lost (Boix et al., 2018; Fearnley & Lees, 1991). These symptoms reach their full potential when approximately 80% of these connections are lost (Francardo et al., 2011). Several strategies have been established to replicate degeneration of the nigrostriatal pathway in an animal model, including toxin-based, proteasome inhibitor-based, and α Syn based models (Cenci & Björklund, 2020).

Toxin-Based Lesion Models Toxin models primarily involve inducing chemical damage to dopaminergic populations. Some of the most widely used toxins include 6-hydroxydopamine (6-OHDA) (Ungerstedt, 1968), 1-methyl-4-phenyl-1,2,3,6-tetrahydropyridine (MPTP) (Langston et al., 1983), and environmental toxins such as Paraquat (Powers et al., 2017).

The 6-OHDA model, first described in 1968, has persisted due to its ease of generation and ability to induce robust dopaminergic cell death (Ungerstedt, 1968). 6-OHDA, a dopamine analog, triggers oxidative damage and glial inflammation upon entry into a cell, leading to neuron death (Kuter et al., 2020; Rotman & Creveling, 1976). Since 6-OHDA cannot cross the blood-brain barrier, it must be injected directly into the brain, typically into the substantia nigra (SN), medial forebrain bundle (MFB), or the striatum. While this model offers stable and controllable pathology, it fails to capture the systemic nature of PD, strictly targeting dopaminergic cells and lacking the characteristic Lewy pathology, necessitating its combination with other methods to represent various aspects of PD.

Proteasome Inhibitor Models Models based on proteasome inhibitors focus on deficits in protein degradation, which play a role in PD pathology development and are linked to α Syn aggregation (Xilouri et al., 2013). These models involve injecting irreversible proteasome inhibitors into the SN or MFB. The severity of resulting damage is dose-dependent (Xie et al., 2010), and the motor deficits can be reduced with L-DOPA administration (Konieczny et al., 2014). Unlike toxin-based models, proteasome inhibitor models exhibit progressive extranigral pathology (Ding et al., 2004; Vernon et al., 2011), with observable α Syn inclusions in affected regions (Elson et al., 2016).

α Syn-Based Models α Syn, a protein long and closely associated with PD pathology, has been extensively studied due to its involvement in familial forms of PD (Polymeropoulos et al., 1997). At the same time, a PD-like disorder was also seen in individuals with more than one copy (Chartier-Harlin et al., 2004). Models based on α Syn can be created using transgenic models, viral delivery (commonly using an AAV or lentivirus), or injecting pre-formed fibrils. These models offer the advantage of replicating progressive pathology and more accurately modeling protein misfolding, a hallmark of PD (Cenci & Björklund, 2020). While transgenic models provide insight into systemic pathology, viral delivery offers a more targeted approach.

One popular method for delivering α Syn is through AAV vectors, which are stereotactically injected to target brain regions. AAV-based delivery is highly efficient, resulting in an extensive pathology and spreading throughout multiple stages of degeneration, allowing for the study of early PD phases as well (Kordower & Björklund, 2013). This method provides a pathology at the cellular level that is more similar to PD, including early axonal pathology and striatal dopaminergic dysfunction, further supporting the feasibility of the study of very early PD-associated changes (Thomsen et al., 2021). Over the years, AAV vectors used to deliver α Syn have undergone significant improvements in efficiency, selectivity, and spread, making them highly tunable tools for mimicking PD pathology (Davidsson et al., 2019; Kirik et al., 2002; Volpicelli-Daley et al., 2011). While this approach presents technical challenges related to titer variability, transduction efficiency, and vector serotype-specific action, AAV-based α Syn models appear to be among the most faithful representations of PD pathology (Cenci & Björklund, 2020).

The ability of α Syn pre-formed fibrils (PFFs) to induce further oligomerization of available monomeric α Syn has been well documented (Cenci & Björklund, 2020; Volpicelli-Daley et al., 2011). In fibril-based animal models, the PD-like disease is initiated primarily by recruiting endogenous α Syn by these PFFs rather than the fibrils' toxicity. This is supported by the lack of pathogenicity observed in the absence of α Syn (Peelaerts et al., 2015).

When PFFs are injected into the brain, they lead to the extensive formation of α Syn-positive aggregates. These aggregates are heavily phosphorylated, insoluble, and ubiquitinated, similar to Lewy inclusions found in PD. However, the development of pathology in PFF-induced models is relatively slow compared to other methods, with significant neurodegenerative changes typically appearing around six months after the injection into brain regions such as the SN, striatum, or cortex (Luk et al., 2012; Osterberg et al., 2015; Paumier et al., 2015).

While PFFs can spread from the injection site, their propagation tends to taper off around the 1-year mark, making this model less stable over time (Rey et al., 2016; Rey et al., 2018). Due to

their complementary qualities, researchers often use the AAV-induced α Syn and PFFs approaches together. Increased α Syn production from AAV further stimulates fibril formation, allowing the separation of the disease process into well-defined stages resembling PD progression. Additionally, this combination model can maintain lower overall α Syn levels compared to AAV-only models, where α Syn needs to be severely upregulated to induce pathology (Faustini et al., 2018).

Several studies have demonstrated that the combination of PFFs and AAV-delivered α Syn leads to severe and progressive pathology, resembling many molecular and symptomatic aspects of PD. This includes inflammation, phosphorylated α Syn inclusions, extensive loss of dopaminergic cells at the tissue level, as well as behavioral impairments in working memory, attention, inhibition, and motor function (Espa et al., 2019; Hoban et al., 2020; Negrini et al., 2022; Thakur et al., 2017).

The Biology of α -Synuclein

α -synuclein is a 140-amino-acid-long acidic protein consisting of three functional domains (Fusco et al., 2014).

- The first domain, located at the N terminus (amino acids 1-60), forms an α -helical structure crucial for the protein's interaction with cellular membranes (Vamvaca et al., 2009).
- The second domain (amino acids 61-95), known as the non-amyloid- β component (NAC region), is the region most prone to aggregation.
- The final region is negatively charged, possesses chaperone-like activity and can bind Ca^{2+} , which facilitates interactions with cellular membranes (Lautenschläger et al., 2018; Nielsen et al., 2001).

In Parkinson's disease (PD), α -synuclein aggregates into β -sheet conformations that can recruit additional monomers, leading to extensive aggregation. In healthy individuals, α -synuclein is mainly found at presynaptic sites, where it plays a role in membrane stabilization, neurotransmitter trafficking, and storage (Burré et al., 2010; Shen et al., 2012). It also modulates dopamine storage in synaptic vesicles through interaction with vesicular monoamine transporter 2 (*VMAT2*), preventing damage caused by dopamine metabolites (González-Hernández et al., 2004). In PD, α -synuclein aggregation also disrupts cellular transport between the cell body and terminals (Volpicelli-Daley, 2017; Volpicelli-Daley et al., 2014).

Apart from PD, α -synuclein pathology is typical in other synucleinopathies (Calabresi et al., 2023). These include dementia with Lewy bodies (DLB), characterized by inflammatory processes initiated by α -synuclein, amyloid, and tau aggregates (Amin et al., 2022). Multiple system atrophy (MSA), featuring α -synuclein aggregation in oligodendrocytes (Kiely

et al., 2018) and pure autonomic failure (PAF) or REM behavior disorder (RBD), often observed in patients who later develop PD or, more rarely, other synucleinopathies (Stokholm et al., 2017).

Molecular Tools for Gene Therapy

AAV basics

AAVs are non-enveloped viruses with a capsid comprised of 60 subunits and a diameter of approximately 25 nm. They rely on co-infection with other viruses, such as adenoviruses or herpes simplex viruses, for replication (Hocquemiller et al., 2016; D. Klein et al., 2023; Naso et al., 2017).

The wild-type AAV (wtAAV) genome is approximately 4.7 kb in length and includes sequences for polyadenylation, promoters, replication, structural capsid, and assembly activation protein genes. The genome is flanked by inverse terminal repeats (ITRs), which are essential for viral replication. When using AAV for gene therapy, the viral genes are replaced with a therapeutic gene of interest (D. Klein et al., 2023).

Modification of the capsid coat has received a lot of attention in recent decades as the need for precise cell targeting became apparent, and many cell-specific vectors have been discovered (Agbandje-McKenna & Kleinschmidt, 2011; Denard et al., 2018; O'Carroll et al., 2021). Various naturally occurring capsid variants have been discovered (Hsu et al., 2020), but efforts have also been made to design capsids rationally or evolve them to improve targeting (Agbandje-McKenna & Kleinschmidt, 2011; Dalkara et al., 2013; Denard et al., 2018; Deverman et al., 2016; O'Carroll et al., 2021; Santiago-Ortiz et al., 2015). In addition to capsid optimization, cassette engineering has been a focus of AAV research. Self-complementary AAV, for example, has been developed to increase transduction efficiency (McCarty et al., 2003; Mendell et al., 2017; Z. Wang et al., 2003). Promoter selection is another important aspect of AAV research, as it can modify transgene expression and restrict it to specific cell types (Sack & Herzog, 2009).

Gene Editing in the Brain

Gene editing methods, such as those using CRISPR/Cas9, carry tremendous potential for therapy for genetic disorders and innumerable applications in biological research. Despite great potential, CRISPR/Cas systems have various limitations, efficiency, and poor function in non-dividing cells being one of them. Many of the cells desirable as targets of gene therapy, neuronal cells being a prime example, are not actively dividing, relegating gene therapy to the more dynamic populations. This limitation is primarily connected to the homology-directed repair (HDR) pathway, which becomes active during the G2/S cell cycle phase (Iyama & Wilson, 2013; Orthwein et al., 2015). HDR has been successfully used to correct both loss-of-function and gain-of-function

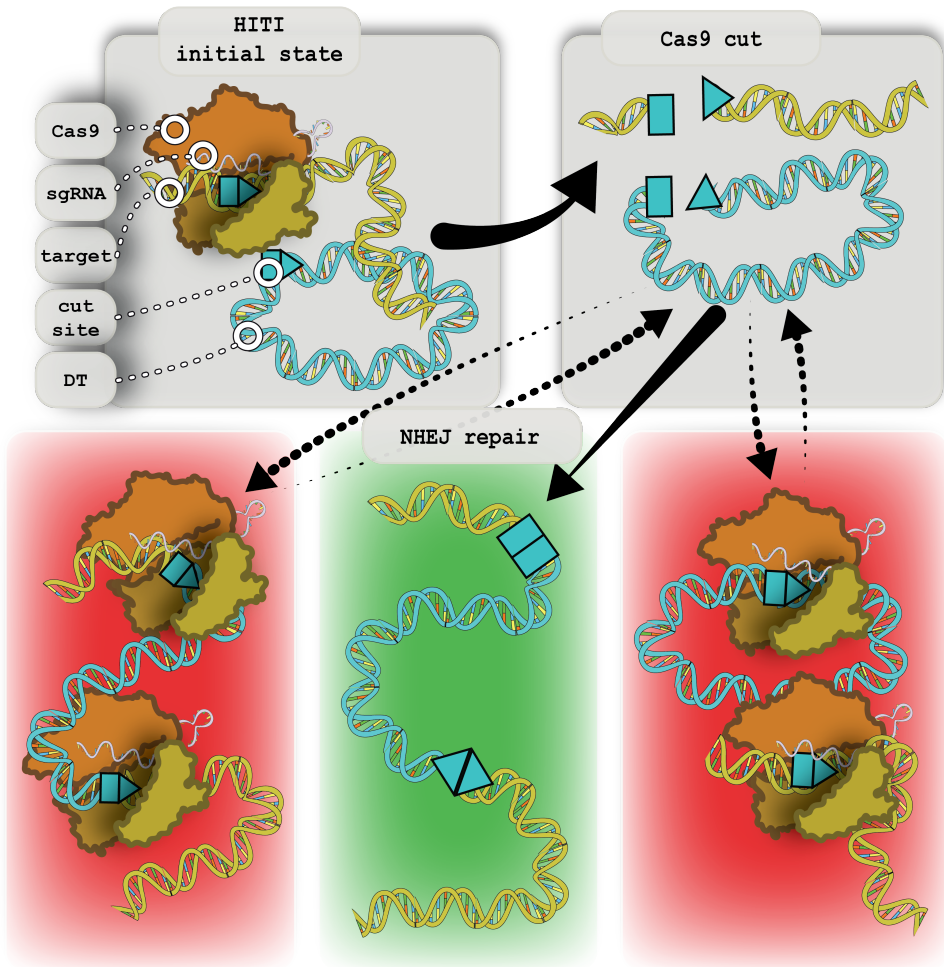


Figure 11: Illustration of the mechanism of HITI gene knock in. Initial state shows target with a cut site as well as a circular donor template with the same sequence. CRISPR/Cas9 system targets both and only in the case of correct insertion is the Cas9 unable to cut either construct.

alleles, and despite its relatively low efficiency, it has been shown to successfully target hematopoietic cells and repair X-linked severe combined immunodeficiency caused by a mutation in *IL2RG* (Genovese et al., 2014).

The other major pathway for repairing double-strand breaks (DSBs) is the non-homologous end joining (NHEJ) pathway, which ligates the DNA ends directly and is active throughout the cell cycle (Lieber, 2010). Homology-independent targeted insertion (HITI) is a method with a focus on highly efficient transgene delivery and integration into non-dividing cells (Suzuki et al., 2016).

As the name suggests, it uses the NHEJ mechanism to extend its target niche. While previous attempts have been made to utilize NHEJ for transgene insertion (Auer et al., 2014; J. Li et al., 2015; Z. Shi et al., 2015), due to the nature of the NHEJ pathway repair mechanism, the direction of the insertion cannot be controlled. HITI takes advantage of the CRISPR/Cas9 system to create a DSB at the locus of interest and further supplies a circular donor template with a target for the single guide RNA (sgRNA) used. Consequently, after CRISPR/Cas9 system cuts the donor template, NHEJ can integrate it into the DSB. In the case of reverse orientation integration, the partial sgRNA complementary sequences will restore the cut target site at both ends of the newly integrated sequence, encouraging its excision and re-integration. Following an integration in the correct direction, the cutting site is not regenerated, cementing the insert in its place (figure 11). The rationale of this design was largely confirmed in the founding study, where the insert was found in the incorrect orientation only 2% of the time. Further, compared to HITI, HDR only amounted to ~10%

An area of NHEJ repair that still needs further exploration is its proneness to insertions and deletions (indel) (W. Chen et al., 2019). While most integrations in Suzuki et al., 2016 were error-free, indel frequency remained non-negligible. This feature is advantageous when the desired outcome is gene knockout (J. Li et al., 2015; Min et al., 2019). In cases where flawless insertion is the goal, significant effort must be made to limit the indel rate. To this end, new tools are continuously emerging, improving indel prediction (Konstantakos et al., 2022; X. Liu et al., 2022) and detection (Bennett et al., 2020) alongside many other aspects of the gene editing process.

Aims

The major focus of my thesis was the development and application of novel tools, with the aim to expand our understanding of events happening in various stages of Parkinson's pathology and attempts at its reversal. Within the scope of the papers presented in this thesis, the aims are the following:

I. Analysis of the composition of several human embryonic stem cell-based dopaminergic transplants in an animal model with Spatial Transcriptomics (ST). Of specific interest is its comparison to a preceding single-cell RNA sequencing analysis.

II. Development of a method able to generate diverse probe and modified cDNA primer libraries in large amounts for targeted spatial transcriptomics methods.

III. Analysis of transcriptional changes in dopaminergic neurons associated with α Syn overexpression. For this, barcoded Cre-dependent α Syn-carrying expression cassettes were delivered by an MNM008 AAV capsid into the cells and the effects were assessed through single nuclei RNA sequencing.

IV. Investigation into the transmission of the Arc retrotransposon among cells in the mouse brain. AAV capsids delivered CRISPR/Cas9 and mCherry cassettes and HITI system was deployed to integrate mCherry into the 5' region of the Arc gene.

Summary of Key Results

Paper I

Cell therapy aimed at replacing dopaminergic cells lost to PD has started entering the clinic in recent years and has shown great promise with symptomatic relief. However, an unbiased analysis of the graft composition has been mostly lacking. To probe the transplant composition in an unbiased manner and with spatial information, we explored the transcriptomic landscape of dopaminergic transplants aimed to supplement the dopamine lost in the striatum of Parkinson's patients in animal models of PD. To this aim, we analyzed the transcriptome patterns of three grafts and compared the cellular proportions in the deconvolved spatial features to a previously published single-cell RNA sequencing analysis (Tiklová et al., 2020).

hESC-Derived Transplants

To obtain the dopamine-producing cells to implant into the striatum, human embryonic stem cells (hESC) were differentiated towards ventral midbrain (VM) fate according to a previously published protocol (Nolbrant et al., 2017). When cells reached a level of phenotypic maturity, they were transplanted into a striatum of immunocompromised PD rat model, with parkinsonism caused by a unilateral lesioning of SN. The implanted cells were left to integrate and mature for six up to 15 months, after which the animals were sacrificed, and their brains were preserved and sectioned. Up to 6 transplant-containing sections were analyzed per animal with spatial transcriptomics (ST) (figure 12A, B).

Removing Batch Effect from Spatial Transcriptomics Data

The resulting sequencing data from transplanted and control sections was subjected to quality control and normalization. From dimensional reduction analysis, it became clear that a strong batch effect was present as even tissues from the same animal failed to co-register (see figure 12C-C'). As most batch correction algorithms were developed for scRNA-seq or bulk sequencing data, we tested three batch correction algorithms to find the best fit for our dataset: Seurat, Scanorama, and autoencoder-based DESC. Out of all the algorithms tested, Seurat showed the highest preservation of patterns found within unique sections and known anatomical regions, including the separation of the cortical area into layers (figure 12F-F'). Scanorama performed well

within a single animal but failed to remove differences among them. Notably, the transplanted area was detected as a unique region throughout (figure 12D-D'). While DESC separated the majority of the tissue well, many outlier features were left unintegrated into the tissue as a whole, creating their own micro-communities (figure 12E-E'). While there has been plenty of debate as to which method is superior, in our case, Seurat integration performed most in line with the biological ground truth and was used in downstream analysis.

Identification of Human Tissue and Anatomical Regions

In summary, to get a good understanding of the tissues, we annotated the observed clusters by their content of uniquely human or rat transcripts and assigned them to anatomical areas through their associated cell populations' marker gene expression whenever possible. Analysis for species assignment made use of species-specific transcripts. Through their distribution in the tissue, human clusters clearly stood out from the rest (figure 13B-B"). and the surrounding striatum was unanimously identified through its medium spiny neurons population marker genes (figure 13C-C"). A closer look at genes differentially expressed in the transplant in comparison to the surrounding striatum indicated the presence of a dopaminergic population with many of the dopaminergic neuron markers robustly expressed in both transplants and SN (figure 13D-F). Further, the distribution of species-specific marker gene transcripts also pointed at dopaminergic neuron markers, such as *TH*, dopamine transported gene (*DAT*) and *VMAT2* captured inside the transplant to be of human origin. In contrast, the opposite is true for the rat substantia nigra areas, which show only rat-specific transcript presence.

Deconvolution of ST Features with an External scRNA-seq Dataset

As ST features are 100 μm in diameter, about ten times that of a reference mammalian cell, computational approaches had to detangle the cellular signal from a single feature. This was done through a combination of information from the ST dataset together with a scRNA-seq reference (figure 14A) from relevant areas of a mouse brain atlas (Zeisel et al., 2018). These were integrated with the cell2location algorithm, which estimated the proportions of the cells from scRNA-seq reference within the ST features. Another method, stereoscope, was also assessed but showed worse performance based on the known distribution of human and host-associated cell types. The final deconvolution results showed a high concordance of the predicted host cell type distribution with the current knowledge, supporting the suitability of the deconvolution design. The transplanted brain section areas showed the presence of a sizeable dopaminergic population as well as a smaller neuroblast and astrocytic ones (figure 14B-E). This dopaminergic population was unique to the transplant within the grafted sections, and linear regression analysis confirmed a high correlation between human and dopaminergic content of a feature, providing further support for the human origin. To verify these results in tissue, markers for the most prominent transplant cell populations were analyzed in tissue sections, recapitulating their localization in the transplant. *TH* was used for dopaminergic neurons, *GFAP* for astrocytes, *COL1A1* for vascular leptomeningeal cells (VLMCs), and *HuNu* to highlight cells of human origin (figure 15).

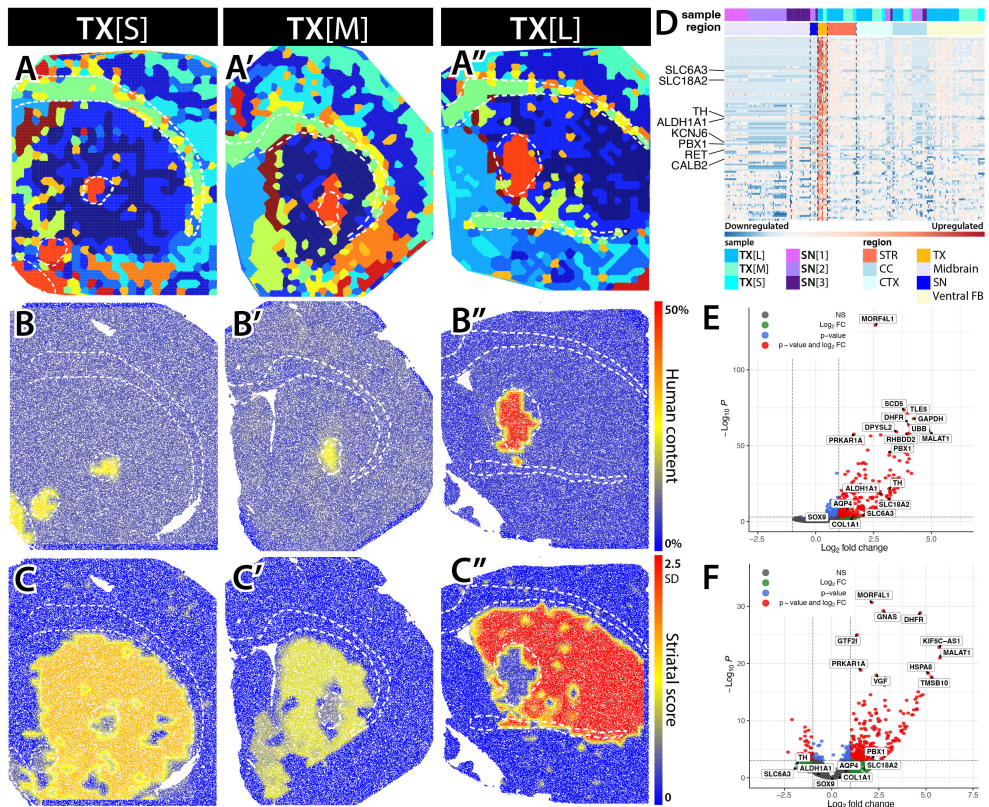


Figure 13: (A–A'') Seurat-assigned clusters in tissues with transplants and their respective scores for (B–B'') human transcript content and (C–C'') MSN-associated gene content. (D) Heatmap of genes most differentially expressed between striatum and transplant regions and their expression in the remaining regions of the ST processed tissues. (E) Genes found differentially expressed between the transplants and the remainder of the grafted tissues. (F) Differentially expressed genes between the substantia nigra and the transplants.

Comparison of Transplant scRNA-seq vs ST Analysis

A dopaminergic transplant of the same kind was previously analyzed with scRNA-seq and results were reported in Tiklová et al., 2020. In this publication, cells were annotated on a cluster basis through the observed marker genes and correlation analysis with an available mouse scRNA-seq dataset (Zeisel et al., 2018). We noticed that the clusters showed high similarities to multiple finer cell types within a larger category (e.g., cluster with high neuronal marker expression showed high correlation with not only dopaminergic but also peptidergic, cholinergic, and other neuronal subtypes), and the clusters did not seem to show a unanimous marker gene expression. We,

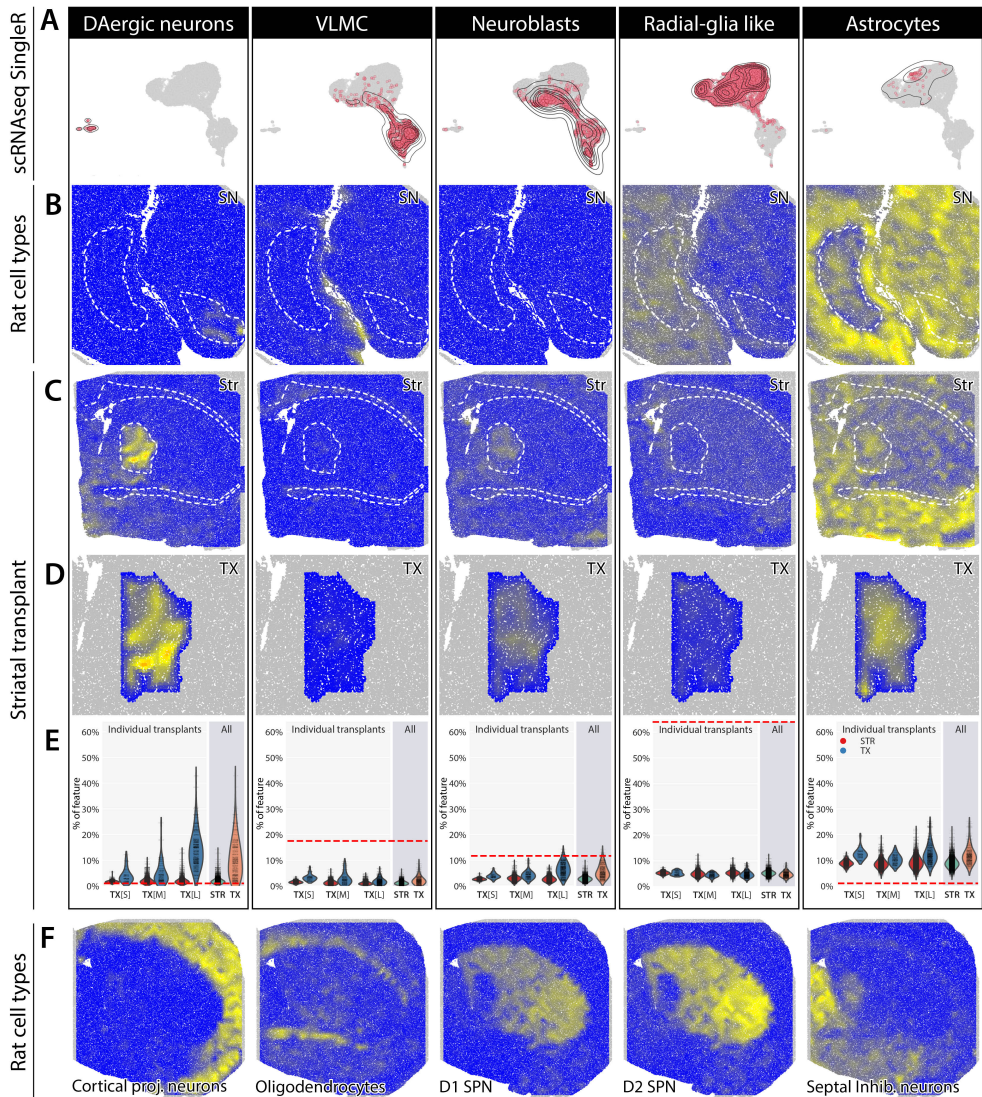


Figure 14: (A) Distribution of the most abundant cell types as assigned by SingleR throughout the scRNA-seq UMAP representation. (B) Deconvolution of a host SN-containing tissue and the distribution of the detected cell types. (C) Distribution of cell types in the grafted striatal sections, with a detailed look at the transplant area alone (D). (E) The proportion of cell types in the transplant area versus in the striatum as assessed by the deconvolution of the ST sections compared to the proportion of the cell types in the scRNA-seq dataset (dashed red line signifies percentage in scRNA-seq). (F) Distribution of control host populations in the grafted tissue. Str, striatum; TX, transplant; Ctx, cortex; CC, corpus callosum; Hipp, hippocampus; AC, anterior commissure.

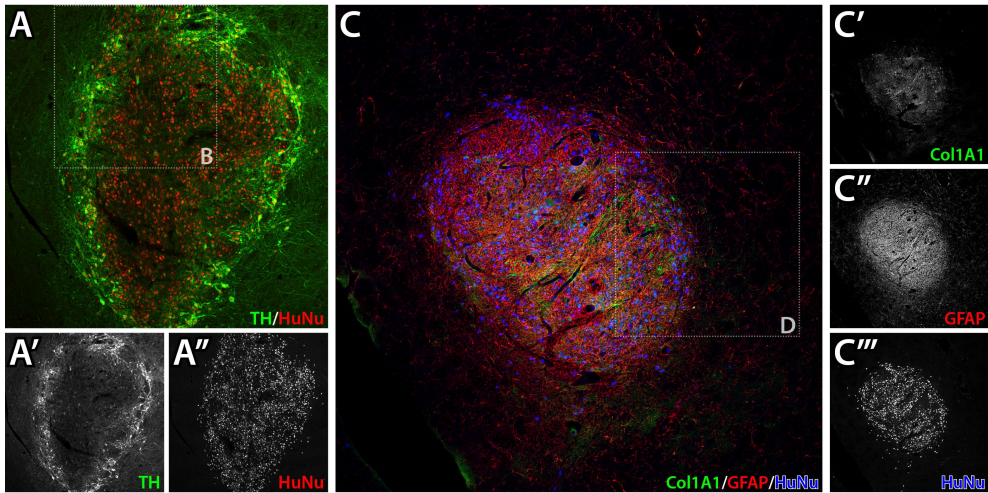


Figure 15: (A) Co-registration of IHC signal from TH and human nuclear antigen (HuNu) in a dopaminergic transplant. B Co-localization of IHC signal from COL1A1, GFAP and HuNu.

therefore, decided to assess the cell identity with SingleR, which attempts to assign the identity to each cell separately by comparison to a reference dataset, overcoming the averaging of expression values within a cluster. This assessment assigned cells into additional cell-type classes, especially within the neuronal cluster. A further look into the assignment probabilities patterns showed a congruent story, with high uncertainty on lower levels compared to a clear differentiation between cells assigned into the glial and neuronal populations (figure 15A).

The difference between the datasets standing out the most is the proportion of neuronal to non-neuronal cells. While in the scRNA-seq dataset, neuronal populations assume less than a percent of all analyzed cells, in spatial analysis, this climbs to 11.3%, making it the most prominent transplant population. The overall percentage might go even higher with a higher-resolution method due to the small size of the grafts and relatively large spatial features, which causes a strong partial volume effect, clearly observable through the intermingling of dopaminergic and medium spiny neuron marker genes and a gradient of the human-specific transcripts percentage, decaying towards the edges of the transplant.

Paper II

In the past years, many methods have appeared in the field of spatial transcriptome profiling. Many of them dependent on a large amount of probes to mark transcript positions (X. Chen et al., 2018; Gyllborg et al., 2020; Jang et al., 2023; Ke et al., 2013; S. Liu et al., 2021; Sountoulidis et al., 2020; Y.-C. Sun et al., 2021; X. Wang et al., 2018). While offering flexible gene detection, the number of oligonucleotides that must be purchased for effective tissue analysis is usually in hundreds to thousands and only increases in methods that necessitate cDNA synthesis. This amount of sequences can present a challenge to handle as well as a financial hurdle for laboratories. To address these obstacles, we have developed a method for the synthesis of a large number of complex libraries from minimal material ordered in the convenient form of oligonucleotide arrays. These offer huge variety (usually up to 100,000 unique sequences) but make up for it in the total amount, which can be limited to as little as 10 pmol.

We decided to showcase the BARseq2 approach as it is easily implemented in most laboratory settings and also introduce a modified method with high sensitivity and independent of cDNA primers.

PCR Probe Amplification

The first approach for probe amplification we present is a proof of concept utilizing PCR. This experiment showed the feasibility of sequence amplification in a construct and proved that the resulting product is at least as functional as a product synthesized in its final form.

To allow amplification, padlock probe sequences generated through this approach were initially embedded in a construct with PCR amplification primers on the 3' end and 5' end. The construct was given binding sites for universal primers used for general library upkeep as well as sublibrary-specific primers, which allow for a selection of a subset of padlock probes (figure 16A-B). The functionality of the probes has been shown through the detection of DARPP-32 transcript throughout the tissue, corresponding to the pattern documented in Allen Brain Atlas (figure 16C-C"). Due to the digestion process design, 5' phosphate, which has to be added otherwise, is already present due to USER enzyme digestion. This has shown to be advantageous in comparison with enzymatic phosphate addition with T4 polynucleotide kinase, as the PCR probe resulted in a higher signal in comparison with a synthesized and additionally phosphorylated probe. Measuring signal number in a striatal sample, the PCR probe gave, on average, 2,180 rolonies per mm² compared to 1,552 rolonies per mm² for the synthesized.

Rolling Circle Amplification

To avoid PCR amplification bias (Aird et al., 2011) and to reach a much larger amplification scale, we tested a follow-up approach utilizing a rolling circle amplification approach. For the amplification to start, the backbone enzyme of the reaction, ϕ 29 polymerase, has to find a single-stranded circular template molecule and a bound primer, which allows the enzyme to copy the

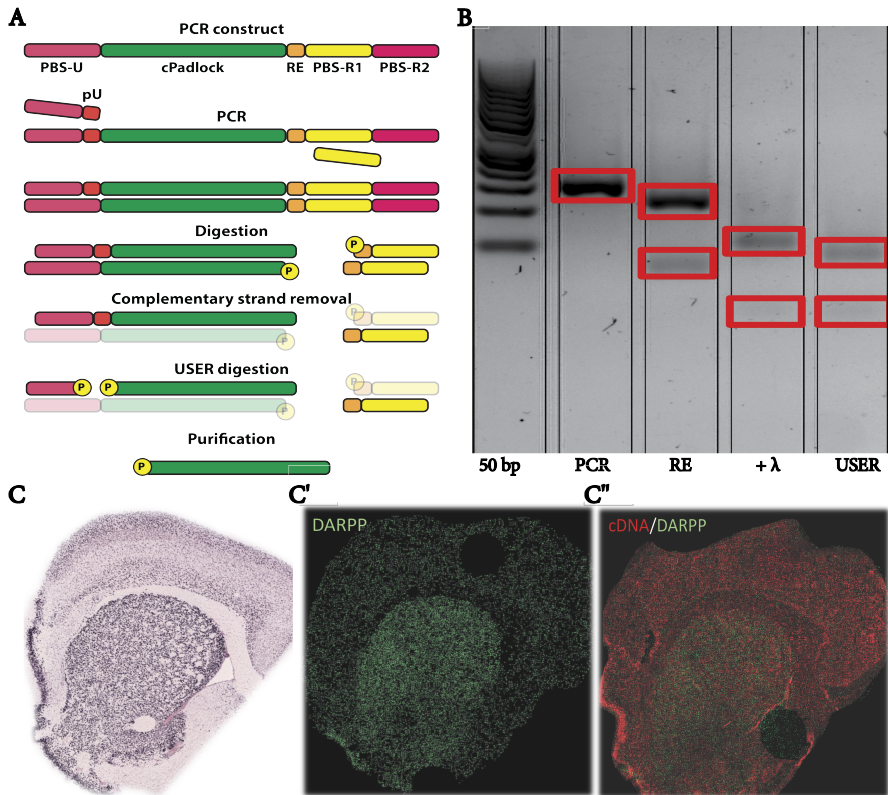


Figure 16: (A) PCR padlock processing steps from a gene array construct to a functional padlock probe. (B) Corresponding digestion steps are shown parallelly in a scheme and on gel electrophoresis. (C) *Darpp-32* detection in a striatal tissue with a PCR-prepared probe, mouse atlas image from <http://mouse.brainmap.org/experiment/show/73732146>.

circular molecule, displace the synthesized strand upon meeting it and continue strand synthesis (figure 17A-B). As we also provide a reverse primer, complementary strands to the newly created are constantly synthesized. Due to the abundance of the primer in the reaction, a large amount of concatemers of various sizes is created, and we have observed the synthesis of up to $800 \text{ ng } \mu\text{L}^{-1}$ of product. This product can be digested into units containing a single copy of the final product and further processed to remove all supporting sequences (figure 17C-E). For cDNA primer synthesis, we have slightly modified the protocol to include 25% amine-modified dUTP in the RCA reaction, which will be incorporated instead of dTTP and is used to crosslink the resulting cDNA to the protein scaffold.(figure 17E-F)

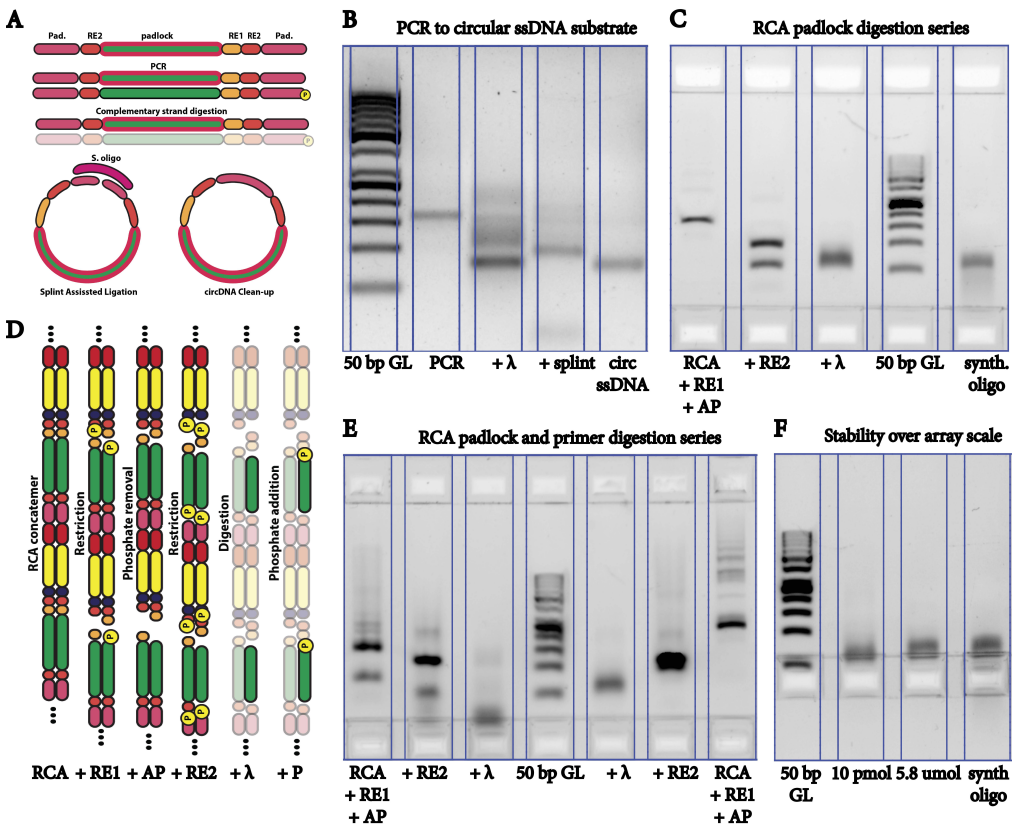


Figure 17: RCA padlock processing steps from a gene array construct to a functional padlock probe. (A) Scheme of the process from a ssDNA oligonucleotide to a circDNA through PCR amplification. (B) The steps of creating a circular RCA template are shown on a 3% agarose gel. Starting from the PCR product follows the removal of the reverse strand, the addition of splint oligonucleotide bringing the arms of the forward strand together, and finally, the ligated circular product. (C) Padlock probe library digestion series and final product comparison to a synthesized probe. (D) Schematic drawing of RCA digestion steps. (E) Digestion series for cDNA primers and padlock probes synthesized from an oligonucleotide gene library. (F) Comparison of the final product from several sources.

Transcript Detection with RCA-synthesized Probes

After verification of the functionality of RCA-synthesized probes on one gene sample, we moved on to an array containing constructs carrying four different padlock probes for 63 genes. A unique combination of fluorophore-labelled probes labeled each of the genes. During this first array test, we used probes synthesized from a library, which initially contained 5.8 μmol of probes, a

scale larger than the final array would have. This array was amplified and processed as shown in figure 17A and D and used on a tissue processed with the BARseq2 approach. This yielded a large number of rolonies, labeled by the expected a large number of fluorophore combinations as shown in figure 18A-A', with unique anatomical areas showing distinct fluorescent signatures. Figure 18B shows a detailed example from the SN region. DAT is shown in Cy5. Cy3 and AlexaFluor 750 channels further separate into VTA and ST.

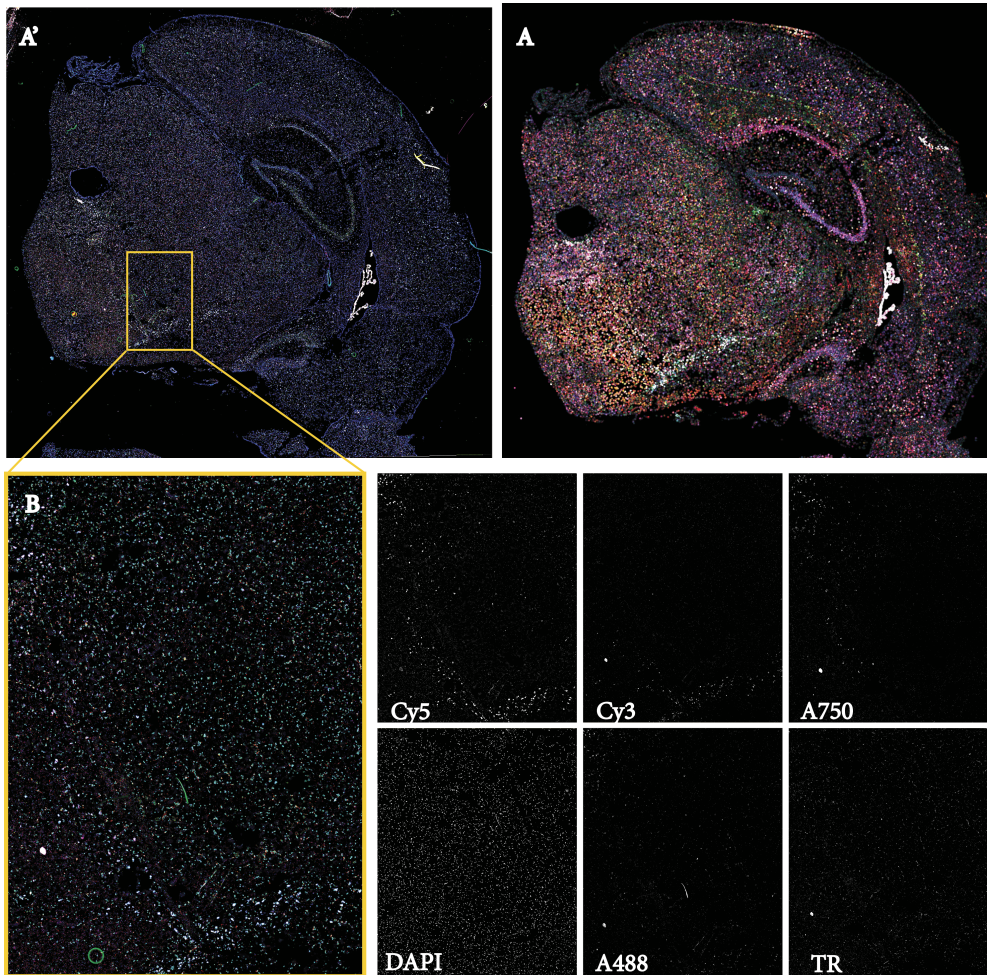


Figure 18: (A) Signal from rolonies formed in a coronal hippocampal section of a rat brain. (A') Tissue segmented based on DAPI stain and colored by the assessment of the cells' rolonies fluorescent signal. (B) Detail of substantia nigra and ventral tegmental area split into channels.

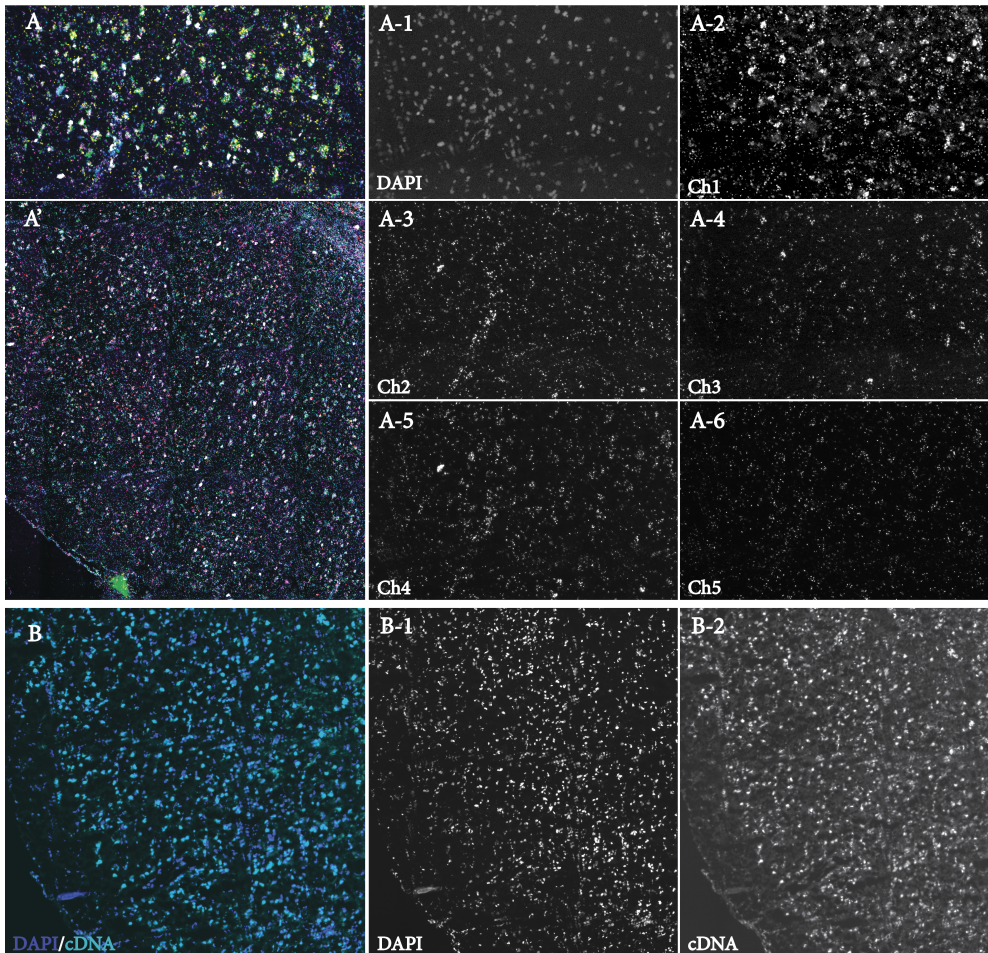


Figure 19: (A) Detailed view of the fluorescent signal from the cortex cells' colonies with all channels presented separately in figures A-1 to A-6. (A') An extended view of the fluorescent signal from a cortical region. (B) The signal from labeled cDNA synthesized from array-amplified primers, DAPI overlay. Channels are shown separately in panels B-1 and B-2.

In the final version of the padlock generation protocol, the cDNA primers and padlock probes were amplified from an array containing thousands of probe sequences targeting the same genes as the previous experiment. Due to the extremely low amount of the input material, the array had to be amplified with 15 cycles of PCR prior to circularization. Afterwards, the process followed as previously. We observed both a strong cDNA signal, showing cDNA synthesis and its crosslinking as expected (figure 19B) and a clear colony signal, with each fluorophore showing a distinct pattern in the cortical tissue as seen in figure 14A.

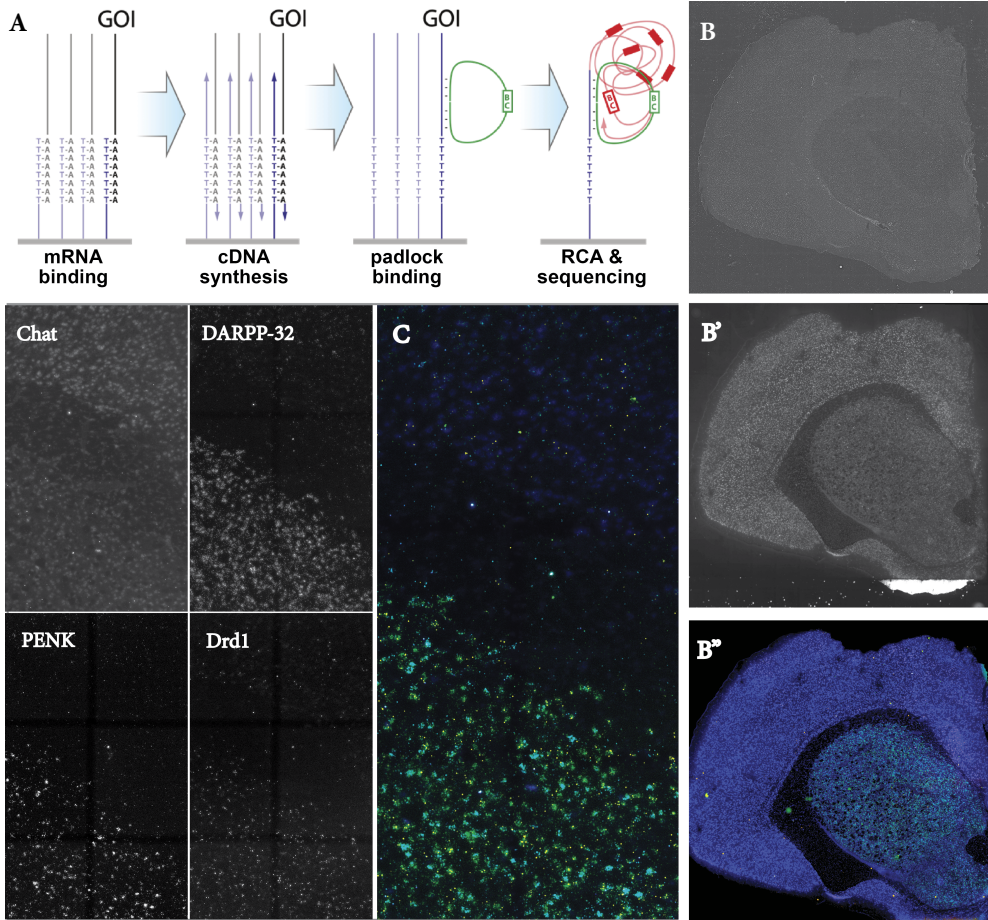


Figure 20: (A) Scheme of Lock-seq workflow. A tissue stained with HE (B), followed by cDNA signal (B') and rolony signal (B'') from *Darpp-32*, *Drd1*, *ChAT* and *Penk*. (C) A detailed view of a striatum-cortex region of tissue is shown in B, with all channels representing unique genes shown separately.

Lock-seq Introduction

We conclude the manuscript with a presentation of a Lock-seq approach, which combines an on-glass mRNA capture used in the original Spatial Transcriptomics studies and a padlock probe transcript detection approach (figure 20A). The immobilization of cDNA on a glass slide allows for complete tissue removal without any detriment to the cDNA (figure 20B-B') and, therefore, significantly improves the accessibility of the DNA to probes and reagents as demonstrated on the detection of 4 striatal genes (figure 20B''-C). While due to the tissue fixation, currently only the

last 200-400 nt of mRNA can be targeted, the 3' end of mRNAs usually provide high diversity, more than capable of analyzing the presence of a gene. Additionally, the increase in sensitivity allows for lower probe concentration while not sacrificing detection capabilities.

Paper III

Animal models are a key part of PD research. In **Paper III**, we present a mouse animal model of PD generated through AAV and utilize it to explore a progression of α Syn pathology, with a focus on its early stages.

In many classic animal models, the Parkinsonian phenotype is achieved by damaging the SN region with a direct injection of a toxic agent, such as in a 6-OHDA injection. This comes with two significant drawbacks. First, this sudden and harsh pathology onset is not in line with the progression of PD in most human patients, where the damage to the dopaminergic neurons comes on gradually, and second, direct injection into the brain region brings on damage on its own. To overcome these, we deliver AAV MNM008 carrying Cre-inducible α Syn cassette through retrograde transport from the striatum to the SN. This approach ensures structurally intact SN, and as the chances of equal delivery of the AAV particles to all cells in SN are low, we obtain cell populations with varying levels of α Syn expression, allowing us to observe molecular changes induced with α Syn overload. In addition to α Syn carrying AAVs, a group of the animals was infected with a viral preparation carrying PFFs, improving our understanding of changes induced with α Syn seeding.

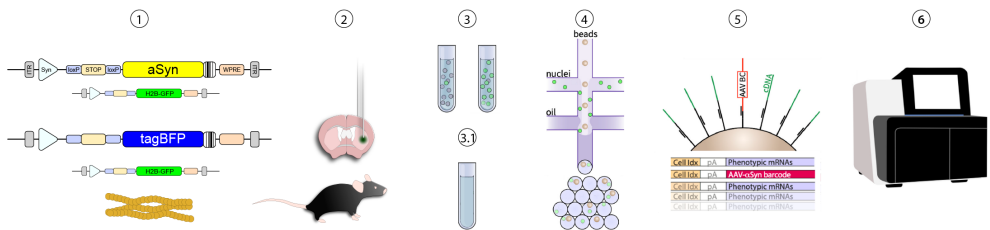


Figure 21: (1) AAV constructs carrying barcoded α Syn and barcoded tagBFP transgenes with a smaller *H2B-GFP* marker construct. STOP sequence CTE preventing transcription without Cre is shown, flanked by two loxP sites. The AAV injection was done in conjunction with PFF injection in a subset of animals. (2) Injection site in the striatum of DAT-Cre mice. (3) Nuclear extraction preparation, followed by GFP enrichment using FANS. (3.1) Supernatant from nuclear preparation, stored for further analysis. (4) 10X Chromium microfluidics system (5) cDNA synthesis at the bead surface with oligodT - barcode primer. (6) Indexing and sequencing of libraries with Illumina NextSeq 2000.

Experimental Setup

To elicit the pathology, experimental animals were infected with a combination of vectors and PFFs, as shown in the study overview in figure 21. Four groups of animals were used in the experimental setup. Three groups consisted of DAT-Cre mice injected with retrogradely-transported AAV-MNM008, with preferential dopamine neuron infectivity (Davidsson et al., 2019), carrying α Syn cassette with or without the addition of PFFs or AAV-MNM008 carrying tagBFP cassette

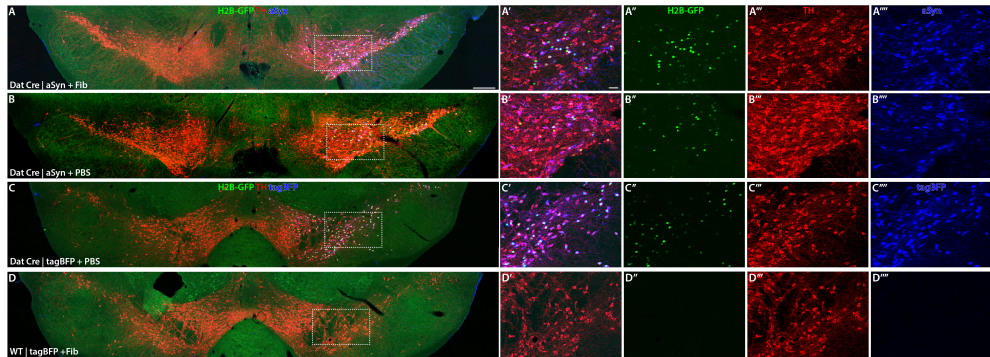


Figure 22: Immunofluorescence stainings validating MNM008 expression in the SN. Representative tissues from all four experimental groups are shown. (A-C) DAT-Cre animals injected ipsilaterally in the striatum with fibrils + α Syn, α Syn + PBS, and *tagBFP* + PBS, respectively. In (D) is shown a WT animal injected with *tagBFP* + fibrils. A detailed view for all animals shows the co-detection of fluorescence from H2B-GFP, TH-targeting antibody, and the MNM008-associated transgene of interest in the highlighted area of the affected SN. Scale bar: (A) 250 μ m, (A'') 50 μ m.

as a control for molecular changes induced by an exogenous protein expression. A separate group of WT mice was also infected with AAV-MNM008 carrying a *tagBFP* cassette with the addition of PFFs.

After 16 weeks, the animals were assessed for behavioral deficits and sacrificed. No significant differences were found among the groups. The spread of AAV vector and the translation of the transgenes they carry into proteins was assessed through an immunohistological (IHC) assay, which confirmed the transgene expression and effective retrograde transport from the striatum to the TH-positive dopaminergic neurons in SN (figure 22). Phosphorylation of α Syn at serine 129 (pSer129) marking α Syn aggregation was also assessed and observed only in cases where PFFs were injected into the animal along the AAVs (figure 23).

Nuclei Extraction and Sorting

Fluorescence-activated nuclei sorting (FANS) was used for all experimental groups to enrich the dopaminergic neuron nuclei. In the case of DAT-Cre animals, AAV-MNM008 delivered H2B-GFP was used as a marker, and dopaminergic neurons from the wt animals were selected through the dopaminergic marker NURR1 (NR4A2) (Kamath et al., 2022) as shown in figure 24.

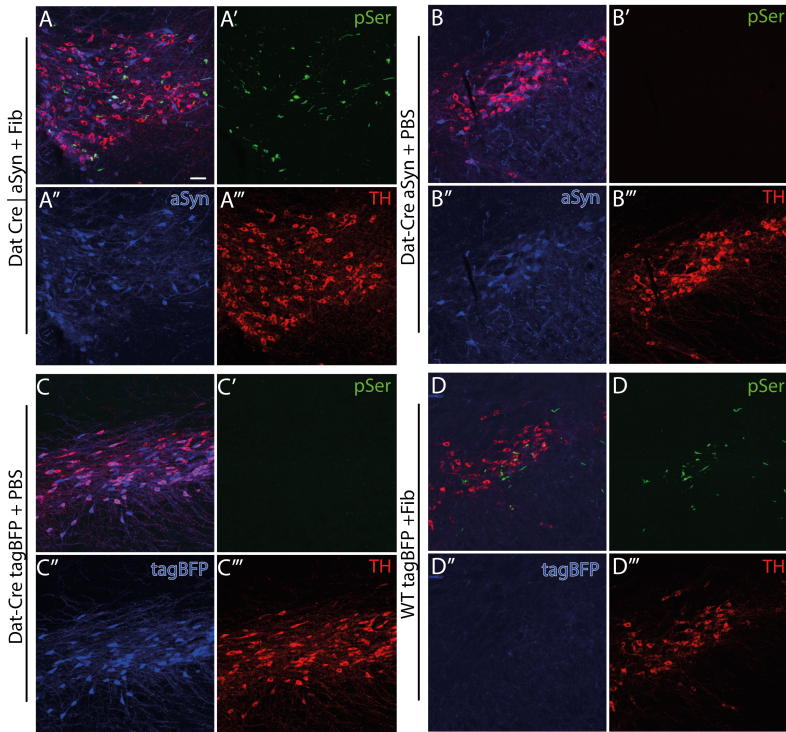


Figure 23: Immunofluorescence stainings validating validating α Syn aggregation. Representative tissues from all four experimental groups are shown. (A-C) show sections from DAT-Cre animals injected ipsilaterally in the striatum with fibrils + α Syn (A), α Syn + PBS (B), and *tagBFP* + PBS (C). In (D) is shown a WT animal injected with *tagBFP* + fibrils. All four groups are shown panels showing the colocalization of TH, transgene, and phospho-serine, indicative of α Syn aggregation. Scale bars in (A) is 50 μ m.

Cell Type Assignment

The enriched nuclei preparations were further supplemented with non-enriched nuclei samples to utilize the sequencing space fully. Following alignment and quality control of the sequencing data, the cellular composition of the sequenced cells was analyzed with the recently published scANVI method (Xu et al., 2021). As a reference cell dataset, we selected cells from SN and VTA from a whole mouse snRNA-seq mouse brain dataset (Langlieb et al., 2023). After the quality control step, normalization, and batch correction, the cells were assigned to a cell type through scANVI label transfer (figure 25A-C). In the final dataset, we could indeed observe a significant dopaminergic population, exceeding the expected yield without additional enrichment (Agarwal et al., 2020) in groups enriched through either marker (figure 25C). Besides dopaminergic cells,

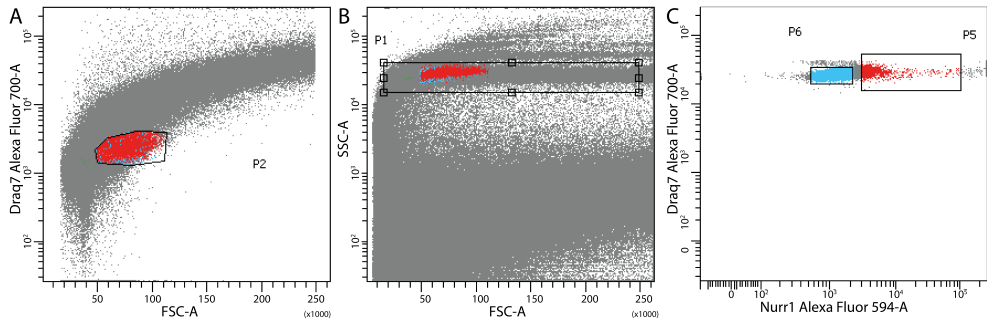


Figure 24: FANS gating strategy for NURR1 stained nuclei extracted from the injected wt animals. (A) SSC-A: side-scattered area vs. FSC-A, forward-scattered area gate. (B) DRAQ7 vs. FSC-A gate. In (C), gates for NURR1+ (in red) and NURR1- (in light blue) are shown.

the dataset contained GABAergic and glutamatergic neurons as well as a smaller number of glial cells.

The TH-positive dopaminergic cells presented a clear SN signature (figure 25D) through the expression of A9 neuron-specific markers and the absence of the A10 DA neuron-specific ones, pointing at excellent SN targeting. Additionally, the transcriptomic information, including the recovered barcode counts (figure 25E) allowed us to dissect changes associated with α Syn expression in the population, which is the most affected *in vivo*.

AAV Gene Expression

Looking closer at the distribution of the four experimental groups and expression of AAV-carried genes throughout the cells, we could observe that while there were no significant differences between groups with and without fibrils, there was a shift in the AAV-tagBFP and AAV- α Syn distributions (figure 25C). While AAV- α Syn groups were heavily enriched in dopaminergic neurons, AAV-tagBFP groups were much more commonly represented within the GABAergic and glutamatergic neuronal clusters despite the identical design of the vectors and expression cassettes.

AAV Barcode Isolation

Due to the design of the cassette, the sequencing library had to be enriched for the AAV barcodes to ensure their capture. Therefore, a small subsection of the library was isolated, and barcodes were amplified separately with PCR to prevent their loss during library fragmentation. Post-sequencing, barcodes were identified with Cutadapt, processed with Starcode, and added to the main dataset. At least one barcode was recovered for almost 1/3 of the cells, significantly improving the chances of sequencing the barcodes without an additional PCR selection.

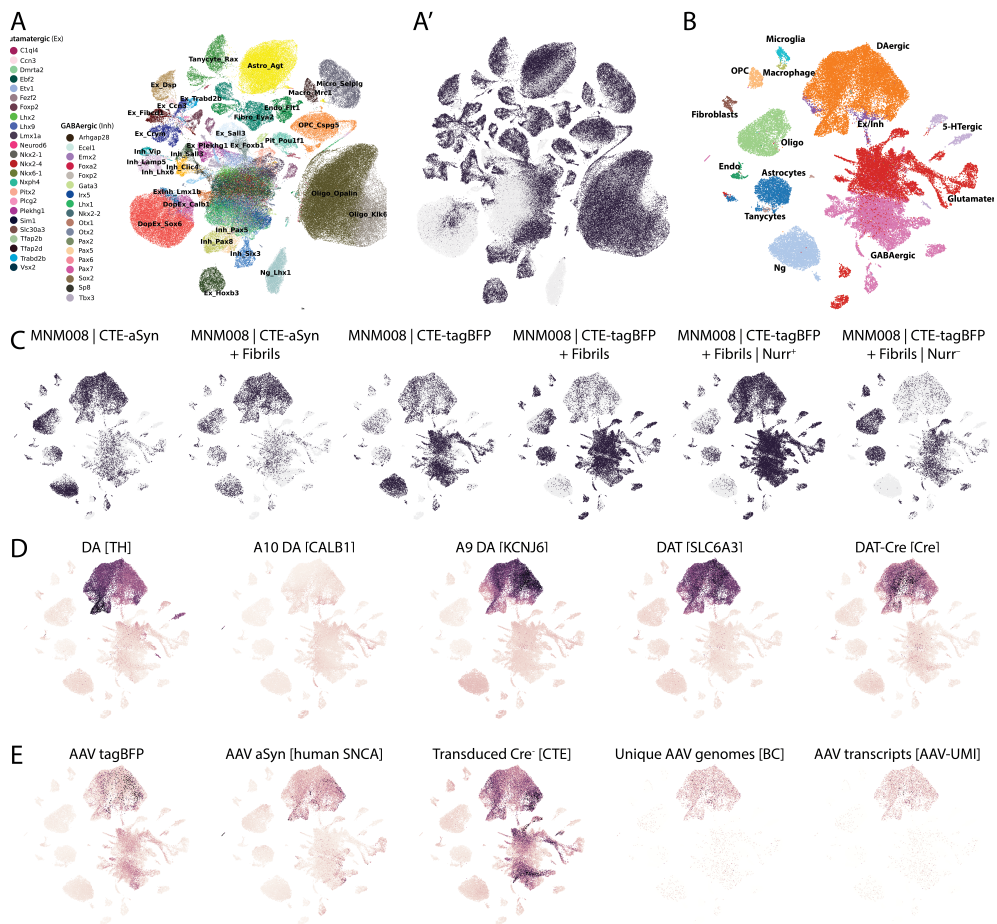


Figure 25: (A) Annotation of the snRNA-seq dataset through integration with an external reference. (B) Distribution of analyzed snRNA-seq (no color) and reference dataset (black) in the UMAP representation. (C) UMAP dimensionality reduction of snRNA-seq, annotated as in panel A. (C) Distribution of the cells from the individual treatment groups projected onto the UMAP representation. (D) Dopaminergic markers, including SNc (A9) and VTA (A10) specific ones and Cre expression. (E) Identification of Cre-induced and non-Cre-induced AAV transcripts through the CTE sequence and plotting of successful AAV infection events based on the number of unique AAV barcoded sequences.

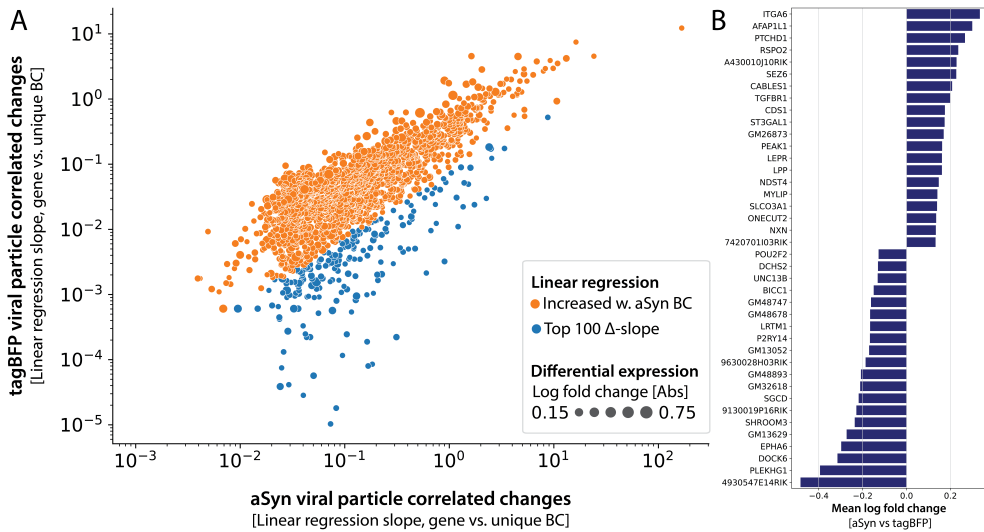


Figure 26: (A) Modeling of correlation between unique viral particles per cell and gene expression using linear regression correlation analysis. (B) Top 40 genes with the highest Δ slope ratio in linear regression ordered by log-fold change.

Regression Analysis of AAV-Related Gene Expression

Differential gene expression was assessed among the experimental groups to analyze the influence of α Syn load on gene expression, and linear regression analysis was performed on all variable genes to detect those correlated with AAV dose in the dopaminergic cells. From the initial 1894 genes, which displayed strong linear correlation regardless of the associated transgene, we looked closer at the top 40 genes, which showed the highest difference in slope between AAV- α Syn and AAV-tagBFP groups (figure 26).

Among the genes positively correlated with α Syn expression was *Itga6*, previously found to be upregulated in brains of mice injected with PFFs (S.-X. Ma et al., 2021). Single nucleotide polymorphisms (SNPs) in another gene, *Afap111*, were previously associated with PD (Lam et al., 2022) and α Syn associated upregulation of *Rspo2* expression was previously reported in another animal PD model (Qin et al., 2016).

Among genes negatively correlated with α Syn load were *Dock6* and *Plekhg1*. *Dock6* and its gene family have been shown to be associated with neurite outgrowth and axon regeneration, and they have been documented to be involved in many brain disorders (Miyamoto et al., 2013; Miyamoto et al., 2007; L. Shi, 2013). *PLEKHG1*, a GTPase regulatory protein (Nakano et al., 2022), has been previously implicated in neurological and hemastasis disorders (Sherva et al., 2014). Overall, the gene association presented here for various transgene loads presents a valuable window into the landscape of molecular changes associated with α Syn induced changes in dopaminergic neurons.

Pseudotime Analysis

Finally, to assess the pseudotime structure of the dopaminergic neuron cluster subset, CellRank analysis was used with the RealTimeKernel as the basis. The number of barcodes has been used as a sign of how far along the α Syn overload axis the cell is. This information allowed us to construct a matrix, estimating the transition probabilities of the cells (figure 27B, E). Modeling of random walks through this transition matrix revealed a high correlation of the walks' endpoints with areas containing cells with the highest barcode number, pointing towards the preservation of the signal (figure 27C, F). Generalized Perron Cluster Cluster Analysis (GPCCA) was used to determine two major states of the cells within the dataset based on the transition matrix, and each of the states was given either the initial or terminal state status based on the transition probabilities as a whole. Within the AAV- α Syn, further exploration of the driver genes associated with the terminal states showed genes previously implicated in PD, such as *Tenm4* (Hor et al., 2015) and *Asic2*, which has been observed in neuroinflammatory states (Ortega-Ramírez et al., 2017) (figure 27G-I). In contrast, tagBFP-carrying AAV vectors did not exhibit a similar pattern of increased pathology-associated gene expression.

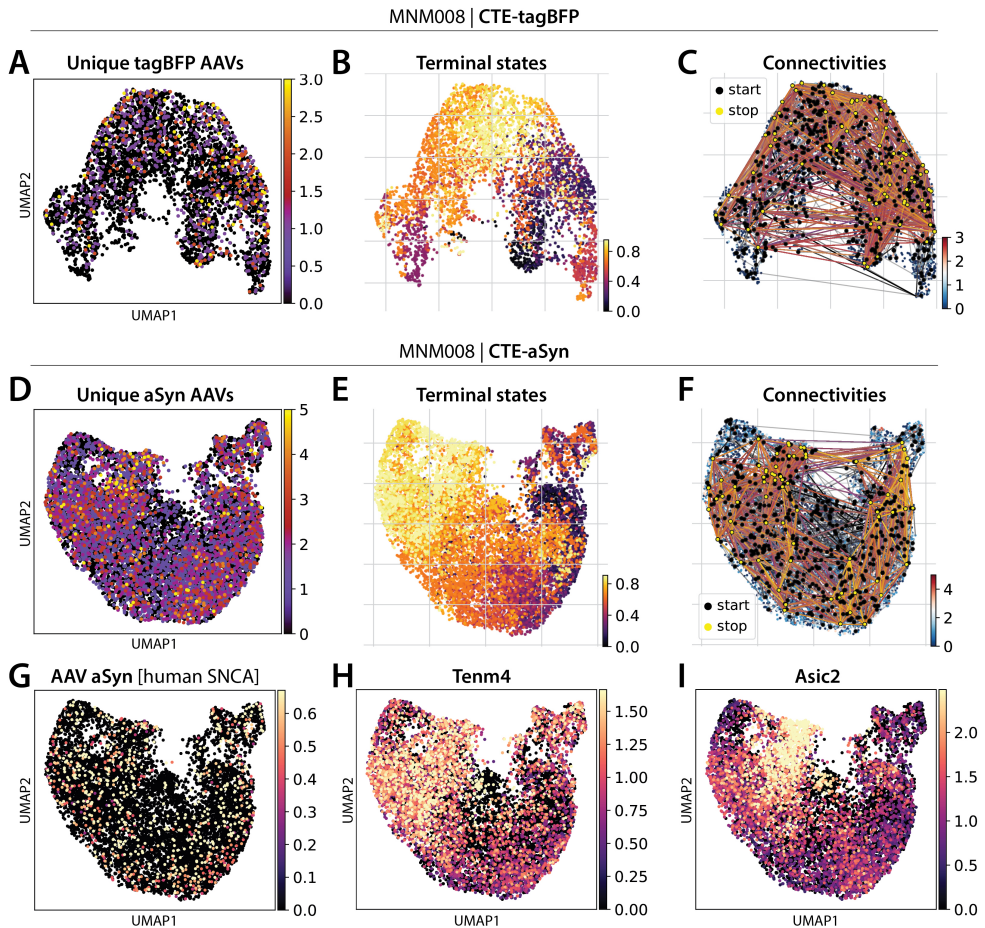


Figure 27: (A-C) UMAP embedding of dopaminergic neurons from tagBFP groups. (A) Number of unique viral barcodes per cell. (B) Probability of cells to belong to the terminal state. (C) Simulated random walks based on the dataset's inferred Markov chain. (D-I) Dopaminergic neurons from α Syn groups. (D) Number of unique viral barcodes per cell. (E) Probability of cells to belong to the terminal state. (F) Simulated random walks based on the dataset's inferred Markov chain. (G-I) Normalized gene expression of selected lineage driver genes.

Paper IV

In 2018, the possibility of a new mode of neuronal communication was introduced in articles by Ashley et al., 2018 and Pastuzyn et al., 2018. This paper reported on the *Arc* gene forming viral-like particles (VLPs) and transferring its mRNA to the neighboring cells. However, proof of this in the mammalian brain has been missing, along with the tools for its monitoring. For this reason, this paper presents a set of tools to investigate the movement of ARC molecules throughout the mouse brain. We start with selecting a suitable knock-in position and move through a fusion mCherry-ARC protein detection to verify its pre- and postsynaptic interactions with proximity ligation assay (PLA).

Targeting HITI System to the *Arc* 5' ORF Leads to In-Frame Knock-in

As the 3' end region is essential for the ARC capsid formation and its neuronal uptake, we focused our efforts on the 5' UTR. AAVs were used to deliver the HITI system (figure 28) carrying either *GFP* or *mCherry* donor template (DT) to be integrated at a selected 2[-] site (figure 29A). Three weeks following the injection, the animals were sacrificed, and the results of the knock-in were evaluated. While we could confirm the expression of the fluorescence reporters (figure 29B-D) and detected a PCR product from both ends of the knock-in (figure 29E), further exploration of the single guide (sgRNA) target site with Sanger and NGS sequencing methods revealed that despite the fluorescent signal, a frameshift mutation at the 3' end of the inserted region caused an out-of-frame expression of *Arc* and a failed fusion attempt (figure 29F). This led to the conclusion that despite the high efficiency of the insertion at the 2[-] site, it was unsuitable for creating a functional fusion protein.

As targeting of the 2[-] position failed to yield a correct product, we theorized targeting the coding strand and staying either in the 5' UTR region (position 1[+]) or moving slightly into the *Arc* ORF (position 9[+]) would be more suitable for functional insertion. This was further supported by a shorter microhomology site at the 3' edit site, which could benefit the knock-in accuracy (figure 30A).

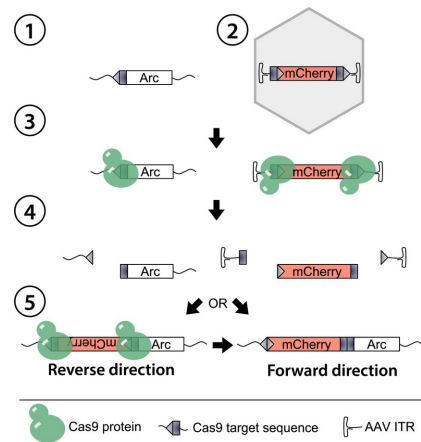


Figure 28: Schematic of HITI gene editing in *Arc*. The targeted genomic *Arc* locus (1), interacts with an AAV-delivered donor template carrying *mCherry* and a sgRNA (2). Following sgRNA-Cas9 assembly, the complex targets the matching sequences in the *Arc* gene and DT (3), resulting in DSBs (4). The insertion is mediated by the NHEJ repair attempts to repair the DSBs. In case of reverse direction integration, the Cas9 target sequence is regenerated, forward direction insertion results in an irreversible knock-in.

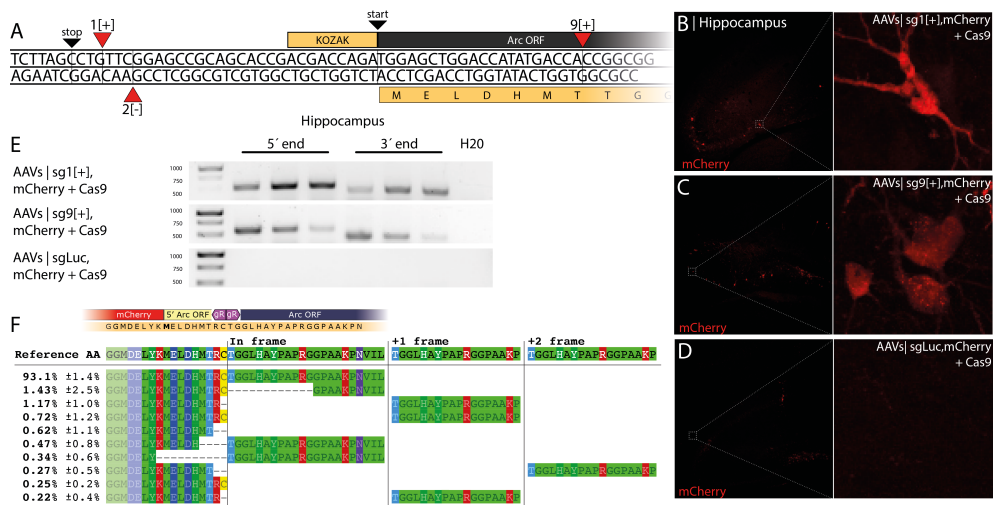


Figure 30: (A) Map of the 5' *Arc* sequence. 1[+] and 9[+] are insertion sites designed for *mCherry* knock-in through the HITI system, 2[-] is an planned insertion site for *mCherry* using the SATI system. (B–C) Confocal images from IHC analysis of the hippocampus in the knock-in groups compared to the control (D). (E) PCR amplicons from bulk DNA extracted from the hippocampus, verifying the knock-in at the 5' and 3' regions of the knocked-in template. (F) Amino acid sequence of the 3' end of the knock-in region translated from the result of NGS analysis of the most common amplicons.

SPs) in the hilar region of the dentate gyrus (figure 31B). The animals were separated into two groups, where the experimental group underwent high-frequency stimulation (HFS) along with low-frequency stimulation (LFS) while the control group only received LFS (Patil et al., 2023). Following HFS, a robust *mCherry* signal was observed, coinciding with HFS-stimulated *Arc* expression in DG as well as the expected early-immediate gene (EIG) *c-Fos* (figure 31C–H”.

A comparison of the prevalence of *ARC*+/*mCherry*+ granule cells in HFS and LFS groups showed that compared to the contralateral side, the ipsilateral side had significantly more double-positive granule cells (one-way ANOVA followed by Tukey HSD, $p < 0.01$)(figure31I). Closer analysis of *c-Fos* expression revealed a non-significant trend of higher values in the HFS group in comparison to the LFS ones (figure 31J). This pattern was repeated in the control LFS animals, with a lower total number of double-positive cells. Notably, the number of *mCherry*+ cells significantly correlated with the number of *Arc*+ cells (figure 31K), further supporting the gene fusion.

ARC-*mCherry* Protein Preserves *ARC*'s Interaction with Synaptic Modules

To evaluate whether the knock-in approach resulted in a fusion *ARC*-*mCherry* protein, a proximity ligation assay (PLA) targeting *mCherry* and *ARC* was employed (figure 32A). PLA signal

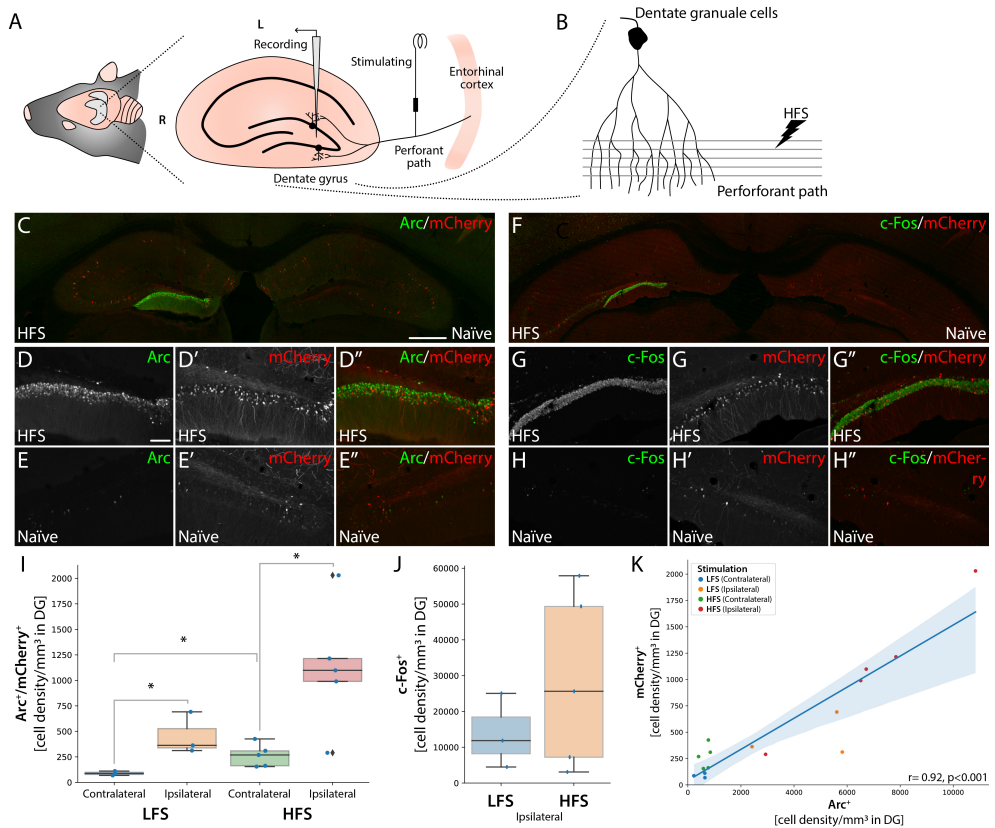


Figure 31: (A) Illustration of electrode placements for recording perforant path-evoked field potentials in the DG. (B) The stimulating electrode on the perforant path projection from the entorhinal cortex, innervating dendrites of granule cells in the DG. (R: rostral, L: lateral). (C-H). IHC-visualized ARC and C-FOS from bilaterally injected mice with AAV-delivered *sg9*[+], *mCherry*, and Cas9 showing the HFS (left) and naïve (right) hippocampus sides. Scale bar in (C): large view - 500 μm , (D) - 100 μm . (I) Cell density box plot quantifying double-positive, ARC, and mCherry cells in the DG; *statistically different (one way ANOVA, $p \leq 0.05$, followed by Tukey's HSD) (LFS $n = 3$, HFS $n = 5$). (J) Box plot showing C-FOS immunoreactive cell density for LFS and HFS in the DG. LFS $n = 3$, HFS $n = 5$. (K) Correlation of densities of mCherry+ and Arc+ cells in the dentate gyrus. Points are separated by the hemisphere (contralateral or ipsilateral) and experimental group (LFS or HFS).

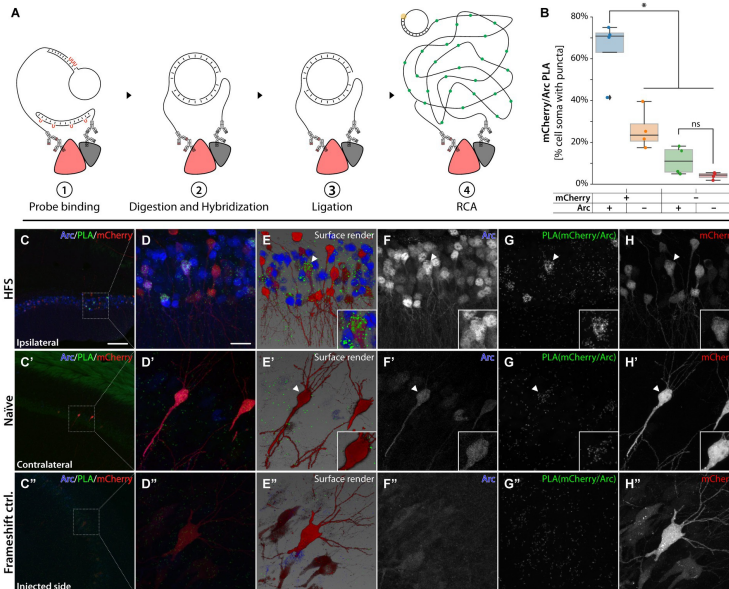


Figure 32: (A) Schematic illustration of the UnFold *in situ* PLA by Navinci technology. (1) Secondary antibodies carrying oligonucleotide probes are added to a sample, with the protein of interest carrying a primary antibody. (2) The interaction of the oligonucleotide probes is enabled by the hydrolysis of the anchoring uracil residues. (3) Gaps in the joined circular template are ligated, creating an RCA template. (4) RCA is initiated and spiked with fluorescently labeled nucleotides. (B) Percentage of cells containing RCA puncta, divided into cell groups positive or negative for mCherry and ARC proteins. *Statistically different (one way ANOVA, $p \leq 0.05$, followed by Tukey's HSD) ($n = 3$). PLA performed in sections from HFS animals. (C–H) HSF-stimulated hippocampal region (ipsilateral, granule cells from DG) (C–H'), naïve hippocampus (contralateral, pyramidal cells from CA1). (E–E'') RCA signal for Arc/mCherry fusion highlighted in green with colocalization with Arc and mCherry positive cells. (C''–H'') PLA signal in CA3 from an animal injected with AAV-carried sg2[-], mCherry, and Cas9. Scale bar: (C) - 100 μm , (D) - 20 μm .

is specific for cases where the two labeled antibodies find themselves nanometers apart, meaning very little to no signal is expected if the fusion fails. This trend was assessed in the HFS animals, and it was indeed observed that the number of positive puncta rose significantly in cells positive for both proteins (figure 32B–H'). Single positive cells did not have more puncta than negative cells. The specificity of the fusion protein detection was further confirmed in animals previously infected with HITI system targeting the 2[-] position. Despite a similar number of mCherry positive neurons in the frameshift control (sg2[-] AAV) and inframe (sg9[+] AAV) group, PLA in the sg2[-] group did not result in any signal, confirming its specificity for the fused protein (figure 32C''–H'').

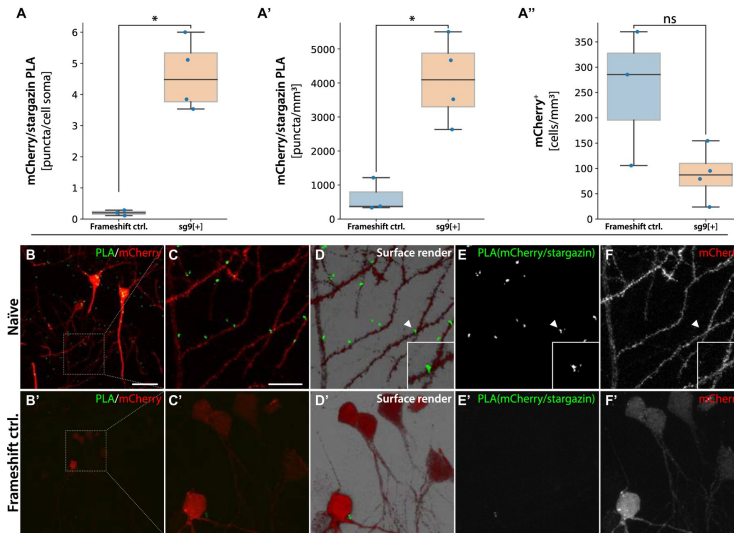


Figure 33: (A) Comparison of the number of puncta per mCherry⁺ neuron in animals injected with sg2^{-/-} (frameshift), and sg9^{+/+} (in frame). (A') Number of RCA puncta over the neuropil. (A'') Number of mCherry⁺ cells detected per mm³, *statistically different, ns = not significant (one-way ANOVA, $p \leq 0.05$, followed by Tukey's HSD), ($n = 3$). Naïve, not HFS stimulated tissue. Pyramidal neurons from the hippocampal region CA1 with PLA targeting ARC-mCherry interaction in sg9^{+/+} animals (B-F) and frameshift animals (B'-F'). (C-C') Detailed view of the area highlighted in B and B'. (D-D') Detail of dendritic spines with a mCherry-Arc PLA signal (more detail showed at the arrowhead). (E-E') PLA signal shown in D-D' separated from mCherry signal (F-F'). Scale bar: (B) - 50 μm , (B') - 20 μm .

We further investigated the maintenance of ARC's biological role. It was previously reported that ARC interacts with the postsynaptic proteins, such as STARGAZIN (Hallin et al., 2018). Due to the proximity that results from this interaction, we reasoned that a positive PLA signal would point to an interaction of the two proteins. Indeed, we were able to show that PLA targeting mCherry and STARGAZIN yielded a significantly more signal in the inframe group than in the frameshift control, supporting the assay validity (figure 33A-C'). We have also observed a strong signal at the neuropil and the predominance of signal on dendritic spines (figure 33D-F'). Together, these results point to the preservation of ARC's biological function in the context of the fusion protein and open new avenues for investigations of synaptic dynamics and protein-protein interactions.

We further focused on previous reports from cultured hippocampal neurons showing inter-neuronal Arc transfer (Pastuzyn et al., 2018). However, up to this date, there has been a lack of proof of this happening in an intact brain. As ARC is primarily found in postsynaptic spines, a transmission route we explored was one from the postsynaptic spines to the presynaptic terminals. This was accomplished through PLA targeting mCherry and BASOON, an abundant presynaptic scaffolding protein. A thorough analysis of the HFS animal group showed a higher percentage of

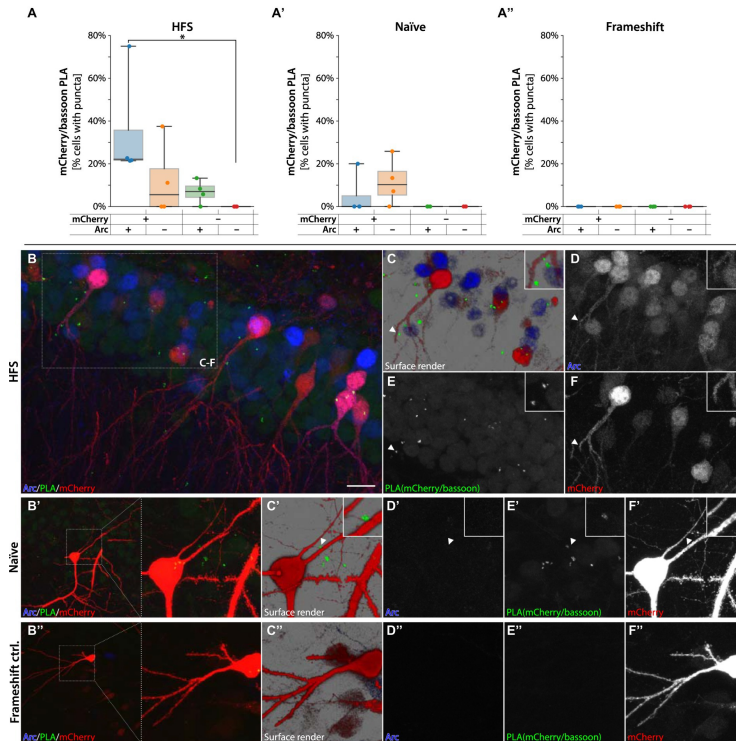


Figure 34: (A,A') quantification of RCA puncta from animals injected with sg9[+] in HFS and naïve tissue. (A'') shows the quantification of RCA puncta from animals injected with the frameshift control sg2[-]. *Statistically different (one-way ANOVA, $p \leq 0.05$, followed by Tukey's HSD). (B–F'') show representative snapshots from the granule cells of DG. Red - mCherry, green - PLA signal for mCherry-BASOON interaction, blue - ARC. (C–C'') Surface render images with detailed views showing mCherry-BASOON PLA signal by a granule cell dendrite in experimental and control groups. (D–D'') ARC signal. (E–E'') PLA signal labeling the proximity of mCherry and BASOON proteins. (F–F'') mCherry labeled cells. The scale bar in (B) shows 20 μm .

cells with PLA puncta by mCherry+/ARC+ cells (figure 34A-A''), with PLA signals concentrating predominantly outside of the dendrites (figure 34C-F). We also detected signals in neurons close to the mCherry-positive cells, often in the vicinity of their dendritic spines (figure 34B-F). In the naïve animals, BASOON-mCherry puncta were sparsely found close-by mCherry positive cells (figure 34B'-F') and importantly, frameshift animals did not result in any signal (figure 34B''-F'').

These results point to the presence of an ARC-mCherry fusion protein and an intact functionality of the Arc protein to the extent it has been described in previous studies. We also show proof of the protein's interaction with pre and postsynaptic modules and present evidence supporting its inter-neuronal transfer.

Key Methodology

This section describes methods essential to the included studies and carried out by the author. A description of the remaining methods is included in the Materials & Methods sections of the thesis-related articles placed in the appendix of this thesis.

Methods for Spatial Transcriptome Analysis

Spatial methods present a major part of **paper I** and **paper II** methods and were also involved in generating results for **paper IV**. Here, we present a subset of the methods available, which were deemed the best choice for the experiments performed in the studies based on their unique properties. Spatial Transcriptomics was selected to analyze the dopaminergic transplants due to its unbiased nature, allowing us to analyze the overall cellular profile of the embryonic stem cell-derived tissue without assumptions. BARseq2 and Lock-seq were used to prove our array-based library amplification method. BARseq2 presents an established method, which allows a comparison of our library to the gold standard and shows the transferability of the method to a published approach. Due to its dependence on cDNA primers, it is not limited to any specific part of mRNA, allowing for the targeting of genes, which might be challenging to detect with 3' region targeting methods. On the other hand, the dependence on 5' amine-modified primers significantly increases its financial demands. Lock-seq targets the polyA end of mRNAs and completely omits the need for cDNA primers. It covalently attaches the mRNA sequence to the slide, allowing for tissue removal and a boost in sensitivity and efficiency. Tissue removal also takes care of tissue-induced fluorescence, and capture of the mRNA on the slide surface confines the signal to two dimensions, both of these making imaging significantly easier and faster.

Spatial Transcriptomics

Spatial Transcriptomics employed in **paper I** was performed according to the original protocol publication (Salmén et al., 2018). Briefly, the brain tissue of nude rats with striatally-placed hESC-derived dopaminergic transplants, fresh frozen and embedded in OCT. 10 µm coronal sections were taken in areas with a noticeable transplant, placed onto an active area of an ST slide, and melted onto it. After placing all six sections, the slide is heated for a minute at 37 °C to allow the tissue to completely melt onto the probe-covered slide area. The tissues are then fixed with 4% paraformaldehyde (PFA), dehydrated with isopropanol, and stained with hematoxylin and eosin.

Imaging of the tissue then provides a histological reference for the sequencing results. Following this step, the cellular interstitial material is digested away with a collagenase pre-permeabilization mixture and further permeabilized with a pepsin-HCl solution for an experimentally validated amount of time, usually between 6-9 minutes. This allows the release of mRNA from the cells and onto the slide, where they bind to the oligo-dT-carrying probes. These act both as the means of capture as well as cDNA primers, carrying a spatial barcode and a unique molecular identifier (UMI) to be incorporated into the cDNA during and overnight synthesis with a reverse transcriptase. After cDNA synthesis, the tissue is digested away, and cDNA can be removed with a uracil-removal enzyme, releasing the probes from the slide into the suspension, where they can be further processed and prepared for sequencing. While this part can be done manually, automatic processing reduces hands-on time and removes human error from the equation. The final library is then easily sequenced with a standard Illumina approach.

As the printed features can, in reality, deviate from the theoretical placement, the probes remaining in the features were visualized through the hybridization of fluorescently labeled probes to get exact positions. The labeled features were imaged with an inverted fluorescence microscope, and the resulting scans were used to correct the theoretical ST features' position.

BARseq2

The BARseq2 protocol was implemented in **paper II** and **paper IV** to visualize transcripts specific to Cas9 expression in **paper IV** and cell type markers in **paper II**. The protocol was implemented as published, starting in a fashion similar to ST protocol, with a fresh frozen tissue sectioned into 10 μm . The tissue is then fixed with 4% PFA for 30 minutes, washed with dPBS, and then dehydrated with an alcohol series with 70% and 85% and 100% ethanol solutions applied for 5 minutes each, followed by an hour wash in 100% ethanol at 4 °C. Following rehydration in dPBS, the sample is embedded in a HybriWell system, where the cDNA synthesis is performed, primed with a collection of 5' end amine-modified targeted oligonucleotides. After an overnight synthesis, amine at the 5' end of the resulting cDNA is crosslinked with the tissue-native proteins, fixing it in its place. With cDNA crosslinked in the sample, a padlock probe library with binding places on the newly synthesized cDNA is added. The original mRNA molecule is digested away, leaving a single-stranded DNA molecule, to which the padlock probes can hybridize and be ligated with Ampligase enzyme. RCA then follows, utilizing cDNA as a primer for the amplification of the circularized padlock probe, with amine-modified deoxyuridine phosphate spiked in to allow for rolony crosslinking. The signal from rolonies can be detected through fluorescent probe hybridization or the various methods of *in situ* sequencing (Gyllborg et al., 2020; Ke et al., 2013; Y.-C. Sun et al., 2021; X. Wang et al., 2018).

Lock-seq

Lock-seq utilizes modified glass slides with a reactive N-hydroxysuccinimide (NHS) group on its surface, to which an amine-modified DNA molecule can be covalently linked. In the case of Lock-seq as presented in **paper II**, the most important part of the DNA probes are the oligo-dT capture sequences, which hybridize to the mRNA polyA tail. As in BARseq2 and ST, fresh-frozen

OCT-embedded tissue is cut into 10 μm sections. These are further placed onto the active areas of the slides and processed in the same manner as ST-processed sections up to the tissue removal step. Following this step, padlock probes targeting 3' end of the gene of interest (GOI) mRNA are added. RNA is digested away to free up hybridizing sequences and padlock probes, which found their targets are ligated with Ampligase. The cDNA itself is used to prime the RCA reaction, and T7 exonuclease is added to further help the removal of non-ligated probes, which could hinder ϕ29 polymerase from forming a product. Compaction oligonucleotides are added to prevent colony stretching and spurious/runaway signals. This is necessary as the colonies in Lock-seq are not as constricted by their environment as in BARseq2. After colony formation, the genes can be identified in a fashion identical to BARseq2.

Molecular Techniques

This section describes some of the molecular methods heavily utilized, especially in **paper II**, encompassing the molecular processing cascades utilized in the generation of cDNA primers and padlock probes with their final modifications.

PCR Template Amplification and Product Processing

In the first part of **paper II**, the padlock probe construct has been amplified with a PCR. In this reaction, Q5U polymerase (NEB) was used together with 0.4 μM of both dUTP-carrying forward and reverse primer and 100 ng of the construct in the Q5U master mix for 45 cycles. All parts of this reaction were optimized to maximize the final product amount. For annealing temperatures, an estimate from the polymerase supplier has been used and further optimized with a temperature gradient. Following PCR amplification, the product was purified with DNA Clean & Concentrator kit (ZYMO Research) and digested first with a BsaI enzyme overnight, followed up by lambda exonuclease assisted removal of sequences with an exposed 5' end phosphate. After the removal of the padlock probe complementary strand, the 5' end of the probe itself was released through the cleavage of uracil embedded in the forward primer, leaving a 5' end phosphorylation, which yields ready-to-use probes after the final purification.

RCA and Product Processing

RCA The starting material for an RCA, performed with a ϕ29 polymerase, is a ssDNA circular molecule. This template is in our application created through the circularization of a synthetic oligonucleotide; its generation from three different sources will be described in detail in the following paragraphs. To maximize the product generation in RCA, we decided to equip EquiPhi29 enzyme from ThermoFisher Scientific, which has been shown to have a higher yield in a shorter time compared to the standard version of the enzyme. RCA for padlock probe library constructs is performed overnight with 1 μM concentration of both primers, 0.1 mM DTT, 2 mM dNTPs and 1 U/ μL EquiPhi29 polymerase. In the case of cDNA primer library RCA, 0.7 μM amino-allyl

dUTP is added to the reaction to ensure the presence of at least one crosslinking amine group in the final product. Longer RCA times, up to 30 hours, have been reported in other studies where extremely high yields are needed (Barreira et al., 2023). To stop RCA, the enzymes are heat-inactivated. As the resulting reaction is extremely viscous, the product is needle-sheared by passing the whole reaction content three times through a 23 G needle and 3 times through a 27 G needle. This makes the DNA more accessible for the restriction enzymes added in the next step.

All restriction and exonuclease reactions that follow are performed in rCutSmart buffer (NEB). First restriction digest happens in a reaction with 15% v/v deactivated and sheared RCA reaction with $0.5 \text{ U } \mu\text{L}^{-1}$ of restriction enzyme (BsaI) and $0.25 \text{ U } \mu\text{L}^{-1}$ alkaline phosphatase in case of padlock probes and $0.75 \text{ U } \mu\text{L}^{-1}$ of restriction enzyme (BbsI, also known as BpiI) $0.5 \text{ U } \mu\text{L}^{-1}$ of alkaline phosphatase for cDNA primers. This reaction is incubated overnight at 37°C while shaking to further help enzymes penetrate the volume. After the reaction concludes, it is inactivated at 95°C for 20 - 30 min to remove all alkaline phosphatase activity. The cut product is purified to remove enzymes, impurities, and any remaining active alkaline phosphatase, as well as sizeable undigested product.

Follows the second restriction digest consisting of $20 \mu\text{g}$ of product from the first restriction digest reaction and $0.5 \text{ U } \mu\text{L}^{-1}$ of BtsI, which is incubated overnight as well. The following day, $0.5 \text{ U } \mu\text{L}^{-1}$ of lambda exonuclease in a volume appropriate to prevent the enzyme contribution to the reaction exceeding 10% is added. During an 1 h incubation at 37°C , the majority of the sequences used for the product amplification is removed, and the resulting library is thereafter purified with a ZYMO Oligo Clean & Concentrator kit (ZYMO Research). In the case of padlock probes, the product is phosphorylated with a reaction composed of $1 \mu\text{M}$ ATP $1 \text{ U } \mu\text{L}^{-1}$ T4 polynucleotide kinase according to the supplier's (NEB) instructions and afterward purified and concentrated with the same Oligo Clean & Concentrator kit (ZYMO Research). Libraries of cDNA primers are used without phosphorylation. In this form, the libraries are used directly in the spatial protocol of choice.

Circular ssDNA Template Generation

In the RCA approach of generating a large amount of oligonucleotide product, three substrates of increasing complexity were used to test the approach.

In the first, least demanding case, we amplify a single construct oligonucleotide. This construct is first phosphorylated and further ligated with T4 ligase with the help of splint oligonucleotide, which brings the 5' and 3' arm together. After an overnight ligation, all oligonucleotides not in a circular form are removed with exonucleases I and III, and the product is purified in a form suitable for RCA amplification.

In the second case, four probes were ordered for each of 63 cell type-specific genes in the form of a $50 \text{ pmol/oligonucleotide}$ pool, already pre-phosphorylated. In this case, an approach identical to a single oligonucleotide library can be taken without sacrificing efficiency.

This was not the case for our final approach, which consists of SurePrint Oligonucleotide Libraries synthesized by Agilent, supplied in the total amount of 10 pmol. A portion of the pool consists of truncated products, which interfere with the RCA at this production scale. To overcome this, full products from the pool have to be first enriched with PCR, where products truncated before the primer site lag behind, and those with incomplete primer sites have their ends repaired. By the manufacturer's instruction, the array is diluted 1:100 in TE pH 8.0 buffer and then further diluted 1:10. 10 fmol of this substrate is then amplified in a 15-cycle PCR with 2 μM of both forward and phosphorylated reverse primer in the Phusion Green Hot Start II master mix (Thermo Fisher Scientific) in a total reaction volume of 50 μL . Amplified library product is then purified with DNA Clean & Concentrator kit (Zymo Research), which removes most undesirable sequences. As the strand complementary to the RCA template now features 5' phosphate, it can be removed with a short lambda incubation (generally 30 min at 37 °C). This reaction is further purified with Oligo Clean & Concentrator kit (ZYMO Research) to get a maximum yield of the ssDNA. The resulting product is phosphorylated with 0.4 U μL^{-1} of T4 polynucleotide kinase in T4 ligase buffer (NEB) and additional 1 mM ATP. The reaction is complete by 1 h mark. The reaction is inactivated at 65 °C for 30 min to prevent further phosphorylation and an equal volume of ligation reagents is added, consisting of 32 U μL^{-1} of T4 ligase (NEB), 1 mM ATP (Thermo Fisher Scientific) 1x T4 ligase buffer (NEB), 4x molar amount of splint oligonucleotide and 30% DMSO for secondary structure disruption. This reaction is incubated at 37 °C overnight, and the non-ligated product and other linear oligonucleotides are removed with exonucleases I and III. The resulting final product is then purified with a ZYMO Oligo Clean & Concentrator kit for maximum recovery and is ready to be used in RCA.

Bioinformatic analyses

Spatial Transcriptome Data Analysis - Normalization and Batch correction

The spatial transcriptome data in the form of gene*features matrices was filtered to only leave genes expressed with more than two transcripts in 4 features and 100 transcripts in total and to leave only features with over 300 transcripts. The normalization method depended on the programming language of the suite. For Scanorama and DESC processing, the total reads per feature were normalized to the median transcript count per feature and then log+1 transformed; for Seurat analysis, the reads were normalized with SCTransform (Hafemeister & Satija, 2019).

Scanorama Scanorama was implemented in integration with the Scanpy module. Scanorama was implemented with 3,000 highly variable genes and a sample assigned as the batch variable, as this is the level where we start to observe the batch effect. Scanpy was used to detect nearest neighbors, calculate the UMAP dimensional reduction, and assign clusters through the Leiden algorithm with resolution 1.

DESC Autoencoder-based DESC was implemented with normalization to 10,000 reads/feature, log+1 transformation and selection of 3,000 highly variable genes. DESC algorithm was applied at the level of tissues with default parameters ([dimensions=len(genes), 32, 16], tolerance=0.005, n_neighbours=3, batch_size=256, learning_rate=300, tSNE_core_number=4) and clustering was done based on the Louvain algorithm with a resolution of 1.

Seurat Integration Seurat approach in its default form was applied after SCTransform normalization based on selected 3,000 integration anchors. UMAP was based on PCs, which explained more than 0.05 variance over the previous component. Clusters were assigned based on the Leiden algorithm with resolution 1.

The most suitable correction has been selected through the comparison of known functionally unique areas and through the quality of tissue/animal mixing.

Anatomical Region Assignment

Anatomical area assignment was done by merging the clustering of gene expression patterns described previously, annotation of areas with a predominance of transcripts from one organism as well as tissue histology.

Only uniquely assigned transcripts from the STAR aligner were used for species transcript assignment. Due to the reads being aligned to a chimeric genome (GRCh38 and Rnor6), this effectively discards any reads present in both organisms. To evaluate the distribution of species-specific transcripts, uniquely aligned transcripts were pooled at the level of organism assignment and projected onto the tissue. These scores for rat and human reads can then be pooled on the assigned cluster level and/or compared to the tissue histology. All three together were able to well delineate the human transplant in contrast with the surrounding rat tissue on all three levels. This species-specific read assignment also helps filter away low-quality tissues, signified by an overall mixing of species-specific reads. Due to the partial volume of many features, the threshold for a "human" cluster was set at 15% of overall reads.

For anatomical regions of the rat brain, the identity was assigned through over-representation of cell type markers specific to the region in question. Regions assigned in our case were white matter tracts, such as corpus callosum and anterior commissure through the expression of *Mbp*, cortical areas through *Cck* and *Kcnc2*, striatum through *Penk*, *Adora2a*, and *Ppp1rb* and finally SN through *Th*, *Pbx1*, *Slc6a3*, *Alhd1a1*, *Ddc* and *Ret*. The cluster was categorized into the corresponding region if the average difference of the mean expressions for the genes was larger than one standard deviation.

Differential Gene Expression

Cluster-based pseudobulk annotated with the assigned region as well as tissue of origin was used for differential gene expression with ribosomal and mitochondrial transcripts excluded from the analysis. The resulting count matrix was analyzed with DESeq2. Four comparisons were made.

Three focus on the human transplants, comparing their transcriptome profile to that of host tissues from the same sections, the surrounding striatal tissue, or the substantia nigra region. Lastly, substantia nigra areas were compared to the remaining midbrain regions. Only genes with a p-value below 0.001 were kept.

Deconvolution

In **paper I**, we present the results of two deconvolution methods, stereoscope (Andersson et al., 2020) and cell2location (Kleshchevnikov et al., 2022). As both datasets need a single-cell RNA sequencing reference, we borrowed a reference from a comprehensive mouse CNS dataset from Zeisel et al., 2018 and filtered it for cells from regions present in both. We performed quality control and discarded cells with less than 1,000 reads. This matrix, together with the spatial dataset sections, was used with stereoscope deconvolution. Stereoscope deconvolution was used as suggested by the method's authors, and 50-500 cells per reference cell type were used. If more cells were present, the subset was selected randomly, and both the reference and spatial composition models were given 75,000 epochs to run. For cell2location, the striatal and midbrain sections were deconvolved separately, with a model for reference being run for 650 epochs and the deconvolution of spatial features for 30,000. Following deconvolution, the Pearson coefficient was used to visualize which cell types most correlated with the human read content of a feature.

scRNA-seq Analysis

To compare the spatial analysis of hESC-derived transplants and the scRNA-seq datasets, scRNA-seq from Tiklová et al., 2020 was adopted. The dataset was processed with SCTranform, and the effect of the sample batch was regressed out. The cell composition analysis was performed with SingleR. This cell type analysis method was chosen as only three clusters were present, with not fully uniform expression patterns (e.g., dopaminergic marker genes were not ubiquitous in the dopaminergic neuron clusters), and marker gene gradients were observed throughout the clusters in 2D UMAP representation. Reference utilized for the spatial dataset deconvolution was provided, normalized with SCTranform, and the sequencing chip ID variable was regressed out. The algorithm was then run unmodified, assigning a probable cell type to each cell of the queried dataset.

Pseudotime Analysis

Pseudotime analysis included in **paper III** was executed through the CellRank v.2 package. The single nuclei RNA-seq dataset was pre-processed with the scvi suite and annotated through scANVI with a reference mouse single nuclei dataset (Langlieb et al., 2023). The viral barcode counts were processed and associated with the cell information through AnnData object observations. As we were primarily interested in changes within the dopaminergic population, we filtered all other cell types away, and the resulting dopaminergic population was further split into the control tag-BFP groups and α Syn group. Lower dimensional representation for this group was visualized with

PCA with 50 PCs followed by a 2-dimensional UMAP (parameters: `min_dist=0.0001`, `spread=1`, `a=0.5`, `b=1.1`).

With the nature of the dataset, the most suitable approach found was through integration of CellRank's (Lange et al., 2022) RealTimeKernel with moscot's (D. Klein et al., 2023) Temporal-Problem, initiated with the following parameters: `epsilon=1e-3`, `tau_a=0.95`, `scale_cost="mean"` and the number of barcodes given as a temporal parameter. The kernel was chosen as the number of viral particles has a similar information value to "time from pathology onset". Due to the restrictions on the processing mode, only time points with 30 or more cells were kept, unfortunately discarding many cells with up to 20 barcodes but present in single digit numbers. The information from moscot was forwarded to the CellRank's RealTimeKernel, which computes the transition matrix (parameters: `self_transitions="connectivities"`, `conn_weight=0.2` and `threshold="auto"`). The transition matrix was visualized by a series of 500 random walks with cells with no detected barcodes being selected as the starting point. A connectivity kernel was also established for the dataset and combined with the RealTimeKernel with a ratio of 1:10,000. The combined kernel was then input into the (GPCCA) estimator. Shur decomposition was computed, and two macrostates were identified. CellRank predicted the initial and terminal macrostate if possible; otherwise, a state with a lower viral barcode load was set as the initial state. Fate probabilities and eigen decomposition were computed with default parameters. As only one lineage was initiated, lineage drivers were computed with the default settings and a GAMR model with `n_knots=1` and smoothing penalty 5. Based on its results, we generated a heatmap of genes whose expression is the most connected to the transition toward the terminal population.

Discussion and Future Perspectives

This thesis's overall goal is to explore tissue transcriptome in spatial and temporal contexts. It begins with **paper I**, introducing a comprehensive transcriptomics characterization of hESC-derived dopaminergic transplant development in an *in vivo* environment with cutting-edge spatial transcriptomics. These stem cell transplants hold great promise for alleviating motor symptoms in PD, and more and more patients are being treated every year. At the same time, while the methods for therapeutic cell generation are being constantly refined, substantial efforts are also being made to standardize the production through extensive screening and GMP-compatible differentiation procedures. Consequently, a need arises for comprehensive methods to monitor the status of these transplants, especially following their integration within the host tissues. This enables a deeper understanding of the tissue itself, the therapeutical impact, and its underlying mechanisms.

While prior studies have frequently reported on dopaminergic transplants, **paper I** distinguishes itself by providing the first comprehensive, unbiased transcriptome analysis of the tissue, free of biases distorting cell-type distributions, such as those associated with tissue dissociation prior to mRNA capture. In this study, we thoroughly analyze the host's (in our case, rat) striatal sections containing the human dopaminergic transplants and provide a comparison with the host SN region. To identify transcriptionally distinct areas, we show the implementation and comparison of several batch correction methods, allowing us to separate the nested batch effects from the underlying gene expression patterns. We identify an approach that nearly ideally separates known anatomically defined regions, is congruent with patterns within deceive, and accesses the histological assignment of the host and graft areas. This allowed us to explore unique expression patterns in the regions of interest, notably the graft-associated region, the surrounding striatum, host SN, and the surrounding ventral midbrain regions. Differential expression analysis between these regions confirmed a significant overrepresentation of dopaminergic markers in the grafted regions compared to the surrounding tissue. Many of them exhibited shared expression patterns with the host SN, supporting the presence of related populations, and their spatial localization showed high enrichment in regions known for high dopaminergic neuron content. However, it is worth noting that while the expression patterns in the native SN and the grafted population were strikingly similar, they were not identical. This discrepancy could stem from compositional differences between the two regions or potentially distinct transcriptional profiles in artificially generated dopaminergic neurons, questions that warrant further investigation.

In the latter part of **paper I**, we aim to bridge the gap between a previously published dopaminergic transplant scRNA-seq study, its spatial counterpart from **paper I**, and an extensive mouse brain profiling reference dataset by Zeisel et al., 2018. Utilizing the same reference dataset for cells analyzed with scRNA-seq and Spatial Transcriptomics (ST) features enables a more straight-

forward comparison of cellular proportions between conditions. Interestingly, while cells within the scRNA-seq dataset could be broadly categorized into glial or neuronal populations, finer type assignments appeared uncertain, and on a more granular level, their transcriptional signatures exhibited similarities to multiple related cell types, such as dopaminergic and cholinergic cells. Comparing cellular proportions between datasets revealed that ST offered a more faithful replication of previous IHC quantification, shedding light on the remaining cell populations.

In summary, **paper I** highlights the promise of ST for mapping cellular communities and provides valuable insights into a tissue of therapeutic significance. As new methodologies emerge, they hold the potential to enhance our understanding of dopaminergic grafts further. In the realm of spatial analysis, countless methods have come onto the scene in recent years, varying in their resolution, transcriptome targeting approaches, and ease of implementation. Further, many methods that capture information not only from the transcriptional layer but also from additional modalities have seen the light of the day. Such a broad toolkit, with many methods optimized for atlas-level efforts, provides a nearly uncountable number of options for the direction of future research.

Many current methods suitable for the analysis of larger tissues rely on gene detection via padlock probes, and this is where **paper II** becomes pertinent. **Paper II** strives to offer an accessible and cost-effective means to custom profile any tissue with unparalleled flexibility. The development of this method unfolds in several stages, progressing from PCR-based padlock probe generation to RCA-based array approach, culminating in the generation of massive pools comprising thousands of unique probes, all from a small amount of highly diverse oligonucleotide material. The study also demonstrates that cDNA primers, often required in abundance, can be produced through this approach with minimal modifications, slashing the assay's cost even more, as unlike padlock probes, they require a 5' end amine modification.

Paper II presents a method for generating padlock and primer libraries and introduces a straightforward transcriptome analysis method focused on ease of use, high efficiency, and quantifiable outcomes. As noted previously, techniques like expansion microscopy show that making tissues more permeable enhances transcriptome capture efficiency. In line with this observation, Lock-seq exhibits a notable increase in sensitivity compared to BARseq while sharing many underlying principles. Moreover, while Lock-seq is limited by the length of mRNA fragments bound to its surface, this heightened sensitivity allows it to detect rare transcripts and significantly reduce the resources required for transcriptome analysis, as it completely eliminates the need for cDNA primers and up to 60% of the padlock probe sequences compared to competing methods. Both BARseq and Lock-seq offer the advantage of a flexible capture field size, practically limited by the size of a microscope slide.

In conclusion, **paper II** represents a significant achievement by providing a robust method for massively amplifying high-variability sequence libraries from femtomole-level starting material. It offers several modifications based on the source of the oligonucleotide template, enabling shorter protocols and a complete omission of PCR for more substantial sources. Parallel to this, Lock-seq enhances efficiency and sensitivity compared to existing padlock probe-based methods and uniquely represents each transcript with only one signal, regardless of the number of targeting probes.

Transitioning to **paper III**, the focus shifts from examining physical space to tracing cellular trajectories through transcriptomic changes. The primary objective of this study is to monitor the early degeneration of dopaminergic populations in a PD animal model by introducing an AAV-vector-based approach for the generation of α Syn-based PD models. The study's innovation lies in its ability to track dose-dependent effects using barcodes intrinsically associated with vector delivery. The study supplies AAV vectors with two distinct cargoes to isolate changes solely attributable to α Syn overexpression. One is carrying the PD-associated α Syn, and a second, control one, carrying benign fluorescent protein tagBFP to the same destination. The study distinguishes changes caused generally by AAV infection and α Syn by splitting the experimental animals into these two groups. To assess the transgene-carrying AAV dose received by each cell, a unique barcode accompanies each transgene copy, quantifying the burden delivered to the cell.

Two complementary mechanisms accomplish targeting of pathological changes to dopaminergic neurons. Specifically, the study employs the AAV-MNM008 vector, which primarily targets dopaminergic neurons and makes use of DAT-Cre mice to ensure that the transgene expression stays limited to the target population. As dopaminergic neurons are usually sparse without enrichment, AAV-MNM008 vectors carrying cassettes with a fluorescent marker were injected alongside the α Syn or tagBFP vectors. This vector combination enables the enrichment of the target cells while also facilitating transduction efficiency assessment due to all groups sharing an identical AAV capsid. This approach allowed for the isolation of thousands of dopaminergic neurons following a four-month incubation period, providing a substantial sample to detect signs of α Syn-associated pathology. While many genes in the dataset exhibited fluctuations related to overall AAV infection load, regardless of the cargo, many genes associated with cellular damage, degeneration, or PD progression were specifically enriched in α Syn-infected cells. Trajectory analysis further supported this finding, linking many PD-associated genes to increasing α Syn doses but not to tagBFP. **Paper III** thus presents an excellent animal model for studying PD progression at the single-cell level. An aspiration for future research is to incorporate methods presented in **paper II** and add another informational layer.

Finally, **paper IV** constitutes a comprehensive effort to investigate claims of the intercellular trafficking of the *Arc* protein and mRNA. The *Arc* gene, originating from an ancient retrovirus, encodes proteins capable of forming capsid-like structures. These structures enclose *Arc* mRNA and can transport it into neighboring cells (Ashley et al., 2018; Pastuzyn et al., 2018). To further explore these claims, the study introduces a suite of tools designed to monitor the protein's spread within the cellular landscape of the mouse brain.

The tracking of ARC molecules is made possible through a combination of AAV-delivered mCherry protein compatible with the HITI method (Suzuki et al., 2016) and the CRISPR/Cas9 system. This approach facilitates the integration of the mCherry protein into the 5' end region of the *Arc* gene without disrupting its functionality (Steward et al., 2014). During this step, we explored some of the top suggestions for CRISPR/Cas9 targeting sites. Although our search for a 5'UTR site did not yield results, we successfully identified a site near the 5' end of the ORF that consistently generated in-frame knock-in molecules.

To validate the functionality of the knock-in, we conducted electrophysiological induction of long-term potentiation. This experiment demonstrated a correlation between *Arc* induction by stimulation and changes in mCherry expression, reinforcing the knock-in's effectiveness and fur-

ther confirming the coupling by PLA. Confirmation of the Arc protein's unchanged functionality was obtained through mCherry's interaction with synaptic proteins. This interaction confirmed the expected interaction with the postsynaptic STARGAZIN protein and revealed a less certain interaction with the presynaptic BASOON protein. A particularly exciting discovery emerged from monitoring interactions between the fusion mCherry-Arc protein and the presynaptic protein BASOON. In this context, we observed signals from unlabeled cells proximal to mCherry-positive cells. While these findings add to the support for the concept of cellular Arc transfer, the inclusion of spatial sequencing methods could provide deeper insights into this process. Further, molecular techniques, such as barcoding, could offer substantial advantages and a more comprehensive understanding.

In conclusion, these papers collectively contribute to our understanding of complex biological processes, offering innovative methodologies and valuable insights that open new avenues for research in the field. The field of spatial transcriptomics as a whole has experienced extensive progress in recent years on both the commercial side and the cutting edge of research. While commercialization on one end brings in the laboratories, which lack the resources to implement more experimental methods and, in doing so, expands spatial transcriptomics to research nooks that would otherwise remain untouched, more intricate, demanding, but also more informative methods are constantly being developed by specialized labs on the other end. All signs point to this dance not slowing down anytime soon, letting us only imagine where the field will be in a decade and further.

References

- Aach, J., Bulyk, M. L., Church, G. M., Comander, J., Derti, A., & Shendure, J. (2001). Computational comparison of two draft sequences of the human genome [Number: 6822 Publisher: Nature Publishing Group]. *Nature*, *409*(6822), 856–859. <https://doi.org/10.1038/35057055>
- Adam, M., Potter, A. S., & Potter, S. S. (2017). Psychrophilic proteases dramatically reduce single-cell RNA-seq artifacts: A molecular atlas of kidney development. *Development*, *144*(19), 3625–3632. <https://doi.org/10.1242/dev.151142>
- Adler, A. F., Cardoso, T., Nolbrant, S., Mattsson, B., Hoban, D. B., Jarl, U., Wahlestedt, J. N., Grealish, S., Björklund, A., & Parmar, M. (2019). hESC-Derived Dopaminergic Transplants Integrate into Basal Ganglia Circuitry in a Preclinical Model of Parkinson's Disease. *Cell Reports*, *28*(13), 3462–3473.e5. <https://doi.org/10.1016/j.celrep.2019.08.058>
- Agarwal, D., Sandor, C., Volpato, V., Caffrey, T. M., Monzón-Sandoval, J., Bowden, R., Alegre-Abarrategui, J., Wade-Martins, R., & Webber, C. (2020). A single-cell atlas of the human substantia nigra reveals cell-specific pathways associated with neurological disorders. *Nature Communications*, *11*, 4183. <https://doi.org/10.1038/s41467-020-17876-0>
- Agbandje-McKenna, M., & Kleinschmidt, J. (2011). AAV capsid structure and cell interactions [ISBN: 1617793698 Publisher: Springer]. *Adeno-associated virus: methods and protocols*, 47–92.
- Aird, D., Ross, M. G., Chen, W.-S., Danielsson, M., Fennell, T., Russ, C., Jaffe, D. B., Nusbaum, C., & Gnirke, A. (2011). Analyzing and minimizing PCR amplification bias in Illumina sequencing libraries. *Genome Biology*, *12*(2), R18. <https://doi.org/10.1186/gb-2011-12-2-r18>
- Albin, R. L., Young, A. B., & Penney, J. B. (1989). The functional anatomy of basal ganglia disorders [ISBN: 0166-2236 Publisher: Elsevier Current Trends]. *Trends in neurosciences*, *12*(10), 366–375.
- Alexander, G. E., & Crutcher, M. D. (1990). Functional architecture of basal ganglia circuits: Neural substrates of parallel processing [ISBN: 0166-2236 Publisher: Elsevier Current Trends]. *Trends in neurosciences*, *13*(7), 266–271.
- Allen, G. S., Burns, R. S., Tulipan, N. B., & Parker, R. A. (1989). Adrenal Medullary Transplantation to the Caudate Nucleus in Parkinson's Disease: Initial Clinical Results in 18 Patients. *Archives of Neurology*, *46*(5), 487–491. <https://doi.org/10.1001/archneur.1989.00520410021016>
- Alon, S., Goodwin, D. R., Sinha, A., Wassie, A. T., Chen, F., Daugharthy, E. R., Bando, Y., Kajita, A., Xue, A. G., Marrett, K., Prior, R., Cui, Y., Payne, A. C., Yao, C.-C., Suk,

- H.-J., Wang, R., Yu, C.-C. (, Tillberg, P., Reginato, P., ... Boyden, E. S. (2021). Expansion sequencing: Spatially precise in situ transcriptomics in intact biological systems [Publisher: American Association for the Advancement of Science]. *Science*, 371(6528), eaax2656. <https://doi.org/10.1126/science.aax2656>
- Alser, M., Rotman, J., Deshpande, D., Taraszka, K., Shi, H., Baykal, P. I., Yang, H. T., Xue, V., Knyazev, S., Singer, B. D., Balliu, B., Koslicki, D., Skums, P., Zelikovsky, A., Alkan, C., Mutlu, O., & Mangul, S. (2021). Technology dictates algorithms: Recent developments in read alignment. *Genome Biology*, 22(1), 249. <https://doi.org/10.1186/s13059-021-02443-7>
- Altman, N., & Krzywinski, M. (2017). Clustering [Number: 6 Publisher: Nature Publishing Group]. *Nature Methods*, 14(6), 545–546. <https://doi.org/10.1038/nmeth.4299>
- Amin, J., Erskine, D., Donaghy, P. C., Surendranathan, A., Swann, P., Kunicki, A. P., Boche, D., Holmes, C., McKeith, I. G., O'Brien, J. T., Teeling, J. L., & Thomas, A. J. (2022). Inflammation in dementia with Lewy bodies. *Neurobiology of Disease*, 168, 105698. <https://doi.org/10.1016/j.nbd.2022.105698>
- Andersson, A., Bergenstr hle, J., Asp, M., Bergenstr hle, L., Jurek, A., Fern ndez Navarro, J., & Lundeberg, J. (2020). Single-cell and spatial transcriptomics enables probabilistic inference of cell type topography. *Communications Biology*, 3(1), 565. <https://doi.org/10.1038/s42003-020-01247-y>
- Andrews, T. S., Atif, J., Liu, J. C., Perciani, C. T., Ma, X.-Z., Thoeni, C., Slyper, M., Eraslan, G., Segerstolpe, A., Manuel, J., Chung, S., Winter, E., Cirilan, I., Khuu, N., Fischer, S., Rozenblatt-Rosen, O., Regev, A., McGilvray, I. D., Bader, G. D., & MacParland, S. A. (2022). Single-Cell, Single-Nucleus, and Spatial RNA Sequencing of the Human Liver Identifies Cholangiocyte and Mesenchymal Heterogeneity. *Hepatology Communications*, 6(4), 821–840. <https://doi.org/10.1002/hep4.1854>
- Arenas, E., Denham, M., & Villaescusa, J. C. (2015). How to make a midbrain dopaminergic neuron. *Development (Cambridge, England)*, 142(11), 1918–1936. <https://doi.org/10.1242/dev.097394>
- Ascherio, A., & Schwarzschild, M. A. (2016). The epidemiology of Parkinson's disease: Risk factors and prevention [Publisher: Elsevier]. *The Lancet Neurology*, 15(12), 1257–1272. [https://doi.org/10.1016/S1474-4422\(16\)30230-7](https://doi.org/10.1016/S1474-4422(16)30230-7)
- Ashley, J., Cordy, B., Lucia, D., Fradkin, L. G., Budnik, V., & Thomson, T. (2018). Retrovirus-like Gag Protein Arc1 Binds RNA and Traffics across Synaptic Boutons. *Cell*, 172(1-2), 262–274.e11. <https://doi.org/10.1016/j.cell.2017.12.022>
- Auer, T. O., Duroure, K., Cian, A. D., Concordet, J.-P., & Bene, F. D. (2014). Highly efficient CRISPR/Cas9-mediated knock-in in zebrafish by homology-independent DNA repair [Company: Cold Spring Harbor Laboratory Press Distributor: Cold Spring Harbor Laboratory Press Institution: Cold Spring Harbor Laboratory Press Label: Cold Spring Harbor Laboratory Press Publisher: Cold Spring Harbor Lab]. *Genome Research*, 24(1), 142–153. <https://doi.org/10.1101/gr.161638.113>
- Azevedo, F. A. C., Carvalho, L. R. B., Grinberg, L. T., Farfel, J. M., Ferretti, R. E. L., Leite, R. E. P., Jacob Filho, W., Lent, R., & Herculano-Houzel, S. (2009). Equal numbers of neuronal and nonneuronal cells make the human brain an isometrically scaled-up primate brain. *The Journal of Comparative Neurology*, 513(5), 532–541. <https://doi.org/10.1002/cne.21974>

- Babcock, B. R., Kosters, A., Yang, J., White, M. L., & Ghosn, E. E. B. (2021). Data Matrix Normalization and Merging Strategies Minimize Batch-specific Systemic Variation in scRNA-Seq Data [Pages: 2021.08.18.456898 Section: New Results]. <https://doi.org/10.1101/2021.08.18.456898>
- Backlund, E. O., Granberg, P. O., Hamberger, B., Knutsson, E., Mårtensson, A., Sedvall, G., Seiger, A., & Olson, L. (1985). Transplantation of adrenal medullary tissue to striatum in parkinsonism. First clinical trials. *Journal of Neurosurgery*, *62*(2), 169–173. <https://doi.org/10.3171/jns.1985.62.2.0169>
- Baichoo, S., & Ouzounis, C. A. (2017). Computational complexity of algorithms for sequence comparison, short-read assembly and genome alignment. *Bio Systems*, *156-157*, 72–85. <https://doi.org/10.1016/j.biosystems.2017.03.003>
- Bais, A. S., & Kostka, D. (2020). Scds: Computational annotation of doublets in single-cell RNA sequencing data. *Bioinformatics*, *36*(4), 1150–1158. <https://doi.org/10.1093/bioinformatics/btz698>
- Bakken, T. E., Jorstad, N. L., Hu, Q., Lake, B. B., Tian, W., Kalmbach, B. E., Crow, M., Hodge, R. D., Krienen, F. M., Sorensen, S. A., Eggermont, J., Yao, Z., Aevermann, B. D., Aldridge, A. I., Bartlett, A., Bertagnolli, D., Casper, T., Castanon, R. G., Crichton, K., ... Lein, E. S. (2021). Comparative cellular analysis of motor cortex in human, marmoset and mouse [Number: 7879 Publisher: Nature Publishing Group]. *Nature*, *598*(7879), 111–119. <https://doi.org/10.1038/s41586-021-03465-8>
- Balasubramanian, S., Klenerman, D., Barnes, C., & Osborne, M. A. (2007). *Arrayed biomolecules and their use in sequencing* (US7232656B2).
- Barker, R. A. (2014). Developing stem cell therapies for Parkinson's disease: Waiting until the time is right. *Cell Stem Cell*, *15*(5), 539–542. <https://doi.org/10.1016/j.stem.2014.09.016>
- Barreira, M., Kerridge, C., Jorda, S., Olofsson, D., Neumann, A., Horton, H., & Smith-Moore, S. (2023). Enzymatically amplified linear dbDNATM as a rapid and scalable solution to industrial lentiviral vector manufacturing. *Gene Therapy*, *30*(1-2), 122–131. <https://doi.org/10.1038/s41434-022-00343-4>
- Bartus, R. T., & Johnson Jr, E. M. (2017). Clinical tests of neurotrophic factors for human neurodegenerative diseases, part 2: Where do we stand and where must we go next? [ISBN: 0969-9961 Publisher: Elsevier]. *Neurobiology of disease*, *97*, 169–178.
- Battich, N., Stoeger, T., & Pelkmans, L. (2013). Image-based transcriptomics in thousands of single human cells at single-molecule resolution. *Nature Methods*, *10*(11), 1127–1133. <https://doi.org/10.1038/nmeth.2657>
- Bennett, E. P., Petersen, B. L., Johansen, I. E., Niu, Y., Yang, Z., Chamberlain, C. A., Met, Ö., Wandall, H. H., & Frödin, M. (2020). INDEL detection, the ‘Achilles heel’ of precise genome editing: A survey of methods for accurate profiling of gene editing induced indels. *Nucleic Acids Research*, *48*(21), 11958–11981. <https://doi.org/10.1093/nar/gkaa975>
- Berbers, B., Saltykova, A., Garcia-Graells, C., Philipp, P., Arella, F., Marchal, K., Winand, R., Vanneste, K., Roosens, N. H. C., & De Keersmaecker, S. C. J. (2020). Combining short and long read sequencing to characterize antimicrobial resistance genes on plasmids applied to an unauthorized genetically modified Bacillus [Number: 1 Publisher: Nature Publishing Group]. *Scientific Reports*, *10*(1), 4310. <https://doi.org/10.1038/s41598-020-61158-0>

- Bergen, V., Lange, M., Peidli, S., Wolf, F. A., & Theis, F. J. (2020). Generalizing RNA velocity to transient cell states through dynamical modeling [Number: 12 Publisher: Nature Publishing Group]. *Nature Biotechnology*, *38*(12), 1408–1414. <https://doi.org/10.1038/s41587-020-0591-3>
- Bertone, P., Stolc, V., Royce, T. E., Rozowsky, J. S., Urban, A. E., Zhu, X., Rinn, J. L., Tongprasit, W., Samanta, M., Weissman, S., Gerstein, M., & Snyder, M. (2004). Global Identification of Human Transcribed Sequences with Genome Tiling Arrays [Publisher: American Association for the Advancement of Science]. *Science*, *306*(5705), 2242–2246. <https://doi.org/10.1126/science.1103388>
- Biancalani, T., Scalia, G., Buffoni, L., Avasthi, R., Lu, Z., Sanger, A., Tokcan, N., Vanderburg, C. R., Segerstolpe, Å., Zhang, M., Avraham-Davidi, I., Vickovic, S., Nitzan, M., Ma, S., Subramanian, A., Lipinski, M., Buenrostro, J., Brown, N. B., Fanelli, D., ... Regev, A. (2021). Deep learning and alignment of spatially resolved single-cell transcriptomes with Tangram [Number: 11 Publisher: Nature Publishing Group]. *Nature Methods*, *18*(11), 1352–1362. <https://doi.org/10.1038/s41592-021-01264-7>
- Björklund, A., Dunnett, S. B., Stenevi, U., Lewis, M. E., & Iversen, S. D. (1980). Reinnervation of the denervated striatum by substantia nigra transplants: Functional consequences as revealed by pharmacological and sensorimotor testing [Place: Netherlands Publisher: Elsevier Science]. *Brain Research*, *199*(2), 307–333. [https://doi.org/10.1016/0006-8993\(80\)90692-7](https://doi.org/10.1016/0006-8993(80)90692-7)
- Björklund, A., & Stenevi, U. (1979). Reconstruction of the nigrostriatal dopamine pathway by intracerebral nigral transplants. *Brain Research*, *177*(3), 555–560. [https://doi.org/10.1016/0006-8993\(79\)90472-4](https://doi.org/10.1016/0006-8993(79)90472-4)
- Boix, J., von Hieber, D., & Connor, B. (2018). Gait analysis for early detection of motor symptoms in the 6-ohda rat model of parkinson's disease. *Frontiers in Behavioral Neuroscience*, *12*. <https://doi.org/10.3389/fnbeh.2018.00039>
- Booeshaghi, A. S., Hallgrímsdóttir, I. B., Gálvez-Merchán, Á., & Pachter, L. (2022). Depth normalization for single-cell genomics count data [Pages: 2022.05.06.490859 Section: New Results]. <https://doi.org/10.1101/2022.05.06.490859>
- Borm, L. E., Mossi Albiach, A., Mannens, C. C. A., Janusauskas, J., Özgün, C., Fernández-García, D., Hodge, R., Castillo, F., Hedin, C. R. H., Villablanca, E. J., Uhlén, P., Lein, E. S., Codeluppi, S., & Linnarsson, S. (2023). Scalable in situ single-cell profiling by electrophoretic capture of mRNA using EEL FISH [Number: 2 Publisher: Nature Publishing Group]. *Nature Biotechnology*, *41*(2), 222–231. <https://doi.org/10.1038/s41587-022-01455-3>
- Bray, N. L., Pimentel, H., Melsted, P., & Pachter, L. (2016). Near-optimal probabilistic RNA-seq quantification. *Nature Biotechnology*, *34*(5), 525–527. <https://doi.org/10.1038/nbt.3519>
- Bronstein, J. M., Tagliati, M., Alterman, R. L., Lozano, A. M., Volkmann, J., Stefani, A., Horak, F. B., Okun, M. S., Foote, K. D., & Krack, P. (2011). Deep brain stimulation for Parkinson disease: An expert consensus and review of key issues [ISBN: 0003-9942 Publisher: American Medical Association]. *Archives of neurology*, *68*(2), 165–165.
- Brundin, P., Nilsson, O. G., Strecker, R. E., Lindvall, O., Astedt, B., & Björklund, A. (1986). Behavioural effects of human fetal dopamine neurons grafted in a rat model of Parkin-

- son's disease. *Experimental Brain Research*, 65(1), 235–240. <https://doi.org/10.1007/BF00243848>
- Brundin, P., Pogarell, O., Hagell, P., Piccini, P., Widner, H., Schrag, A., Kupsch, A., Crabb, L., Odin, P., Gustavii, B., Björklund, A., Brooks, D. J., Marsden, C. D., Oertel, W. H., Quinn, N. P., Rehncrona, S., & Lindvall, O. (2000). Bilateral caudate and putamen grafts of embryonic mesencephalic tissue treated with lazarooids in Parkinson's disease. *Brain: A Journal of Neurology*, 123 (Pt 7), 1380–1390. <https://doi.org/10.1093/brain/123.7.1380>
- Burré, J., Sharma, M., Tsetsenis, T., Buchman, V., Etherton, M. R., & Südhof, T. C. (2010). Alpha-synuclein promotes SNARE-complex assembly in vivo and in vitro. *Science (New York, N.Y.)*, 329(5999), 1663–1667. <https://doi.org/10.1126/science.1195227>
- Butler, A., Hoffman, P., Smibert, P., Papalexi, E., & Satija, R. (2018). Integrating single-cell transcriptomic data across different conditions, technologies, and species. *Nature Biotechnology*, 36(5), 411–420. <https://doi.org/10.1038/nbt.4096>
- Cable, D. M., Murray, E., Zou, L. S., Goeva, A., Macosko, E. Z., Chen, F., & Irizarry, R. A. (2022). Robust decomposition of cell type mixtures in spatial transcriptomics. *Nature Biotechnology*, 40(4), 517–526. <https://doi.org/10.1038/s41587-021-00830-w>
- Caglayan, E., Liu, Y., & Konopka, G. (2022). Neuronal ambient RNA contamination causes misinterpreted and masked cell types in brain single-nuclei datasets. *Neuron*, 110(24), 4043–4056.e5. <https://doi.org/10.1016/j.neuron.2022.09.010>
- Calabresi, P., Mechelli, A., Natale, G., Volpicelli-Daley, L., Di Lazzaro, G., & Ghiglieri, V. (2023). Alpha-synuclein in Parkinson's disease and other synucleinopathies: From overt neurodegeneration back to early synaptic dysfunction [Number: 3 Publisher: Nature Publishing Group]. *Cell Death & Disease*, 14(3), 1–16. <https://doi.org/10.1038/s41419-023-05672-9>
- Callaway, E. M., Dong, H.-W., Ecker, J. R., Hawrylycz, M. J., Huang, Z. J., Lein, E. S., Ngai, J., Osten, P., Ren, B., Tolia, A. S., White, O., Zeng, H., Zhuang, X., Ascoli, G. A., Behrens, M. M., Chun, J., Feng, G., Gee, J. C., Ghosh, S. S., ... Project management. (2021). A multimodal cell census and atlas of the mammalian primary motor cortex [Number: 7879 Publisher: Nature Publishing Group]. *Nature*, 598(7879), 86–102. <https://doi.org/10.1038/s41586-021-03950-0>
- Canzar, S., & Salzberg, S. L. (2017). Short Read Mapping: An Algorithmic Tour. *Proceedings of the IEEE. Institute of Electrical and Electronics Engineers*, 105(3), 436–458. <https://doi.org/10.1109/JPROC.2015.2455551>
- Cao, Y., Lin, Y., Ormerod, J. T., Yang, P., Yang, J. Y., & Lo, K. K. (2019). scDC: Single cell differential composition analysis. *BMC Bioinformatics*, 20(19), 721. <https://doi.org/10.1186/s12859-019-3211-9>
- Carlsson, T., Winkler, C., Burger, C., Muzyczka, N., Mandel, R. J., Cenci, A., Björklund, A., & Kirik, D. (2005). Reversal of dyskinesias in an animal model of Parkinson's disease by continuous l-DOPA delivery using rAAV vectors. *Brain*, 128(3), 559–569. <https://doi.org/10.1093/brain/awh374>
- Carninci, P., Kasukawa, T., Katayama, S., Gough, J., Frith, M. C., Maeda, N., Oyama, R., Ravasi, T., Lenhard, B., Wells, C., Kodzius, R., Shimokawa, K., Bajic, V. B., Brenner, S. E., Batalov, S., Forrest, A. R. R., Zavolan, M., Davis, M. J., Wilming, L. G., ... Hayashizaki, Y. (2005). The Transcriptional Landscape of the Mammalian Genome

- [Publisher: American Association for the Advancement of Science]. *Science*, 309(5740), 1559–1563. <https://doi.org/10.1126/science.1112014>
- Cenci, M. A., & Björklund, A. (2020). Animal models for preclinical Parkinson's research: An update and critical appraisal. *Progress in Brain Research*, 252, 27–59. <https://doi.org/10.1016/bs.pbr.2020.02.003>
- Chambers, S. M., Fasano, C. A., Papapetrou, E. P., Tomishima, M., Sadelain, M., & Studer, L. (2009). Highly efficient neural conversion of human ES and iPS cells by dual inhibition of SMAD signaling. *Nature Biotechnology*, 27(3), 275–280. <https://doi.org/10.1038/nbt.1529>
- Chartier-Harlin, M.-C., Kachergus, J., Roumier, C., Mouroux, V., Douay, X., Lincoln, S., Leveque, C., Larvor, L., Andrieux, J., Hulihan, M., Waucquier, N., Defebvre, L., Amouyel, P., Farrer, M., & Destée, A. (2004). Alpha-synuclein locus duplication as a cause of familial Parkinson's disease. *The Lancet*, 364(9440), 1167–1169. [https://doi.org/10.1016/S0140-6736\(04\)17103-1](https://doi.org/10.1016/S0140-6736(04)17103-1)
- Chaudhuri, K. R., & Schapira, A. H. (2009). Non-motor symptoms of Parkinson's disease: Dopaminergic pathophysiology and treatment [ISBN: 1474-4422 Publisher: Elsevier]. *The Lancet Neurology*, 8(5), 464–474.
- Chen, A., Liao, S., Cheng, M., Ma, K., Wu, L., Lai, Y., Qiu, X., Yang, J., Xu, J., Hao, S., Wang, X., Lu, H., Chen, X., Liu, X., Huang, X., Li, Z., Hong, Y., Jiang, Y., Peng, J., ... Wang, J. (2022). Spatiotemporal transcriptomic atlas of mouse organogenesis using DNA nanoball-patterned arrays. *Cell*, 185(10), 1777–1792.e21. <https://doi.org/10.1016/j.cell.2022.04.003>
- Chen, B., Khodadoust, M. S., Liu, C. L., Newman, A. M., & Alizadeh, A. A. (2018). Profiling tumor infiltrating immune cells with CIBERSORT. *Methods in molecular biology (Clifton, N.J.)*, 1711, 243–259. https://doi.org/10.1007/978-1-4939-7493-1_12
- Chen, F., Wassie, A. T., Cote, A. J., Sinha, A., Alon, S., Asano, S., Daugharthy, E. R., Chang, J.-B., Marblestone, A., Church, G. M., Raj, A., & Boyden, E. S. (2016). Nanoscale imaging of RNA with expansion microscopy. *Nature Methods*, 13(8), 679–684. <https://doi.org/10.1038/nmeth.3899>
- Chen, J., Suo, S., Tam, P. P., Han, J.-D. J., Peng, G., & Jing, N. (2017). Spatial transcriptomic analysis of cryosectioned tissue samples with Geo-seq [Number: 3 Publisher: Nature Publishing Group]. *Nature Protocols*, 12(3), 566–580. <https://doi.org/10.1038/nprot.2017.003>
- Chen, K. H., Boettiger, A. N., Moffitt, J. R., Wang, S., & Zhuang, X. (2015). RNA imaging. Spatially resolved, highly multiplexed RNA profiling in single cells. *Science (New York, N.Y.)*, 348(6233), aaa6090. <https://doi.org/10.1126/science.aaa6090>
- Chen, W., McKenna, A., Schreiber, J., Haeussler, M., Yin, Y., Agarwal, V., Noble, W. S., & Shendure, J. (2019). Massively parallel profiling and predictive modeling of the outcomes of CRISPR/Cas9-mediated double-strand break repair. *Nucleic Acids Research*, 47(15), 7989–8003. <https://doi.org/10.1093/nar/gkz487>
- Chen, X., Sun, Y.-C., Church, G. M., Lee, J. H., & Zador, A. M. (2018). Efficient in situ barcode sequencing using padlock probe-based BaristaSeq. *Nucleic Acids Research*, 46(4), e22. <https://doi.org/10.1093/nar/gkx1206>
- Chen, X., Sun, Y.-C., Zhan, H., Keschull, J. M., Fischer, S., Matho, K., Huang, Z. J., Gillis, J., & Zador, A. M. (2019). High-Throughput Mapping of Long-Range Neuronal Projection

- Using In Situ Sequencing. *Cell*, 179(3), 772–786.e19. <https://doi.org/10.1016/j.cell.2019.09.023>
- Chen, Y., Chen, X., Baserdem, B., Zhan, H., Li, Y., Davis, M. B., Kebschull, J. M., Zador, A. M., Koulakov, A. A., & Albeanu, D. F. (2022). High-throughput sequencing of single neuron projections reveals spatial organization in the olfactory cortex. *Cell*, 185(22), 4117–4134.e28. <https://doi.org/10.1016/j.cell.2022.09.038>
- Chillag-Talmor, O., Giladi, N., Linn, S., Gurevich, T., El-Ad, B., Silverman, B., Friedman, N., & Peretz, C. (2011). Use of a Refined Drug Tracer Algorithm to Estimate Prevalence and Incidence of Parkinson's Disease in a Large Israeli Population [Publisher: IOS Press]. *Journal of Parkinson's Disease*, 1(1), 35–47. <https://doi.org/10.3233/JPD-2011-11024>
- Choi, H. M. T., Beck, V. A., & Pierce, N. A. (2014). Next-generation in situ hybridization chain reaction: Higher gain, lower cost, greater durability. *ACS nano*, 8(5), 4284–4294. <https://doi.org/10.1021/nn405717p>
- Christine, C. W., Richardson, R. M., Laar, A. D. V., Thompson, M. E., Fine, E. M., Khwaja, O. S., Li, C., Liang, G. S., Meier, A., Roberts, E. W., Pfau, M. L., Rodman, J. R., Bankiewicz, K. S., & Larson, P. S. (2022). Safety of AADC Gene Therapy for Moderately Advanced Parkinson Disease: Three-Year Outcomes From the PD-1101 Trial [Publisher: Wolters Kluwer Health, Inc. on behalf of the American Academy of Neurology Section: Research Article]. *Neurology*, 98(1), e40–e50. <https://doi.org/10.1212/WNL.0000000000012952>
- Clevers, H., Rafelski, S., Elowitz, M., Klein, A., Trapnell, C., Shendure, J., Lein, E., Uhlen, M., Lundberg, E., Martinez-Arias, A., Sanes, J. R., Blainey, P., Eberwine, J., Kim, J., & Love, J. C. (2017). What Is Your Conceptual Definition of “Cell Type” in the Context of a Mature Organism? *Cell Systems*, 4(3), 255–259. <https://doi.org/10.1016/j.cels.2017.03.006>
- Codeluppi, S., Borm, L. E., Zeisel, A., La Manno, G., van Lunteren, J. A., Svensson, C. I., & Linnarsson, S. (2018). Spatial organization of the somatosensory cortex revealed by osm-FISH. *Nature Methods*, 15(11), 932–935. <https://doi.org/10.1038/s41592-018-0175-z>
- Cole, M. B., Risso, D., Wagner, A., DeTomaso, D., Ngai, J., Purdom, E., Dudoit, S., & Yosef, N. (2019). Performance Assessment and Selection of Normalization Procedures for Single-Cell RNA-Seq. *Cell Systems*, 8(4), 315–328.e8. <https://doi.org/10.1016/j.cels.2019.03.010>
- Connelly, S., & Manley, J. L. (1988). A functional mRNA polyadenylation signal is required for transcription termination by RNA polymerase II. [Company: Cold Spring Harbor Laboratory Press Distributor: Cold Spring Harbor Laboratory Press Institution: Cold Spring Harbor Laboratory Press Label: Cold Spring Harbor Laboratory Press Publisher: Cold Spring Harbor Lab]. *Genes & Development*, 2(4), 440–452. <https://doi.org/10.1101/gad.2.4.440>
- Connolly, B. S., & Lang, A. E. (2014). Pharmacological treatment of Parkinson disease: A review. *JAMA*, 311(16), 1670–1683. <https://doi.org/10.1001/jama.2014.3654>
- Cooper, O., Hargus, G., Deleidi, M., Blak, A., Osborn, T., Marlow, E., Lee, K., Levy, A., Perez-Torres, E., Yow, A., & Isacson, O. (2010). Differentiation of human ES and Parkinson's disease iPS cells into ventral midbrain dopaminergic neurons requires a high activity form of SHH, FGF8a and specific regionalization by retinoic acid. *Molecular and Cellular Neurosciences*, 45(3), 258–266. <https://doi.org/10.1016/j.mcn.2010.06.017>

- Dalkara, D., Byrne, L. C., Klimczak, R. R., Visel, M., Yin, L., Merigan, W. H., Flannery, J. G., & Schaffer, D. V. (2013). In Vivo-Directed Evolution of a New Adeno-Associated Virus for Therapeutic Outer Retinal Gene Delivery from the Vitreous [Publisher: American Association for the Advancement of Science]. *Science Translational Medicine*, 5(189), 189ra76–189ra76. <https://doi.org/10.1126/scitranslmed.3005708>
- Damier, P., Hirsch, E. C., Agid, Y., & Graybiel, A. M. (1999). The substantia nigra of the human brain: II. Patterns of loss of dopamine-containing neurons in Parkinson's disease. *Brain*, 122(8), 1437–1448. <https://doi.org/10.1093/brain/122.8.1437>
- Danaher, P., Kim, Y., Nelson, B., Griswold, M., Yang, Z., Piazza, E., & Beechem, J. M. (2022). Advances in mixed cell deconvolution enable quantification of cell types in spatial transcriptomic data [Number: 1 Publisher: Nature Publishing Group]. *Nature Communications*, 13(1), 385. <https://doi.org/10.1038/s41467-022-28020-5>
- Das, S., Rai, A., & Rai, S. N. (2022). Differential Expression Analysis of Single-Cell RNA-Seq Data: Current Statistical Approaches and Outstanding Challenges. *Entropy*, 24(7), 995. <https://doi.org/10.3390/e24070995>
- Davidsson, M., Wang, G., Aldrin-Kirk, P., Cardoso, T., Nolbrant, S., Hartnor, M., Mudanayake, J., Parmar, M., & Björklund, T. (2019). A systematic capsid evolution approach performed in vivo for the design of AAV vectors with tailored properties and tropism. *Proceedings of the National Academy of Sciences of the United States of America*, 116(52), 27053–27062. <https://doi.org/10.1073/pnas.1910061116>
- Dean, F. B., Hosono, S., Fang, L., Wu, X., Faruqi, A. F., Bray-Ward, P., Sun, Z., Zong, Q., Du, Y., Du, J., Driscoll, M., Song, W., Kingsmore, S. F., Egholm, M., & Lasken, R. S. (2002). Comprehensive human genome amplification using multiple displacement amplification. *Proceedings of the National Academy of Sciences of the United States of America*, 99(8), 5261–5266. <https://doi.org/10.1073/pnas.082089499>
- Deconinck, L., Cannoodt, R., Saelens, W., Deplancke, B., & Saeyns, Y. (2021). Recent advances in trajectory inference from single-cell omics data. *Current Opinion in Systems Biology*, 27, 100344. <https://doi.org/10.1016/j.coisb.2021.05.005>
- DeLong, M. R. (1990). Primate models of movement disorders of basal ganglia origin [ISBN: 0166-2236 Publisher: Elsevier Current Trends]. *Trends in neurosciences*, 13(7), 281–285.
- Denard, J., Rouillon, J., Leger, T., Garcia, C., Lambert, M. P., Griffith, G., Jenny, C., Camadro, J.-M., Garcia, L., & Svinartchouk, F. (2018). AAV-8 and AAV-9 vectors cooperate with serum proteins differently than AAV-1 and AAV-6 [ISBN: 2329-0501 Publisher: Elsevier]. *Molecular Therapy-Methods & Clinical Development*, 10, 291–302.
- Deng, R., Zhang, K., Wang, L., Ren, X., Sun, Y., & Li, J. (2018). DNA-Sequence-Encoded Rolling Circle Amplicon for Single-Cell RNA Imaging. *Chem*, 4(6), 1373–1386. <https://doi.org/10.1016/j.chempr.2018.03.003>
- Deng, Y.-P., Lei, W.-L., & Reiner, A. (2006). Differential perikaryal localization in rats of D1 and D2 dopamine receptors on striatal projection neuron types identified by retrograde labeling. *Journal of Chemical Neuroanatomy*, 32(2), 101–116. <https://doi.org/10.1016/j.jchemneu.2006.07.001>
- Denisenko, E., Guo, B. B., Jones, M., Hou, R., de Kock, L., Lassmann, T., Poppe, D., Clément, O., Simmons, R. K., Lister, R., & Forrest, A. R. R. (2020). Systematic assessment of tissue dissociation and storage biases in single-cell and single-nucleus RNA-seq work-

- flows [Number: 1 Publisher: BioMed Central]. *Genome Biology*, 21(1), 1–25. <https://doi.org/10.1186/s13059-020-02048-6>
- DePasquale, E. A. K., Schnell, D. J., Camp, P.-J. V., Valiente-Alandí, Í., Blaxall, B. C., Grimes, H. L., Singh, H., & Salomonis, N. (2019). DoubletDecon: Deconvoluting Doublets from Single-Cell RNA-Sequencing Data [Publisher: Elsevier]. *Cell Reports*, 29(6), 1718–1727.e8. <https://doi.org/10.1016/j.celrep.2019.09.082>
- Deuschl, G., & Agid, Y. (2013). Subthalamic neurostimulation for Parkinson's disease with early fluctuations: Balancing the risks and benefits [ISBN: 1474-4422 Publisher: Elsevier]. *The Lancet Neurology*, 12(10), 1025–1034.
- Deverman, B. E., Pravdo, P. L., Simpson, B. P., Kumar, S. R., Chan, K. Y., Banerjee, A., Wu, W.-L., Yang, B., Huber, N., Pasca, S. P., & Gradinaru, V. (2016). Cre-dependent selection yields AAV variants for widespread gene transfer to the adult brain [Number: 2 Publisher: Nature Publishing Group]. *Nature Biotechnology*, 34(2), 204–209. <https://doi.org/10.1038/nbt.3440>
- Dickson, D. W., Braak, H., Duda, J. E., Duyckaerts, C., Gasser, T., Halliday, G. M., Hardy, J., Leverenz, J. B., Tredici, K. D., Wszolek, Z. K., & Litvan, I. (2009). Neuropathological assessment of Parkinson's disease: Refining the diagnostic criteria [Publisher: Elsevier]. *The Lancet Neurology*, 8(12), 1150–1157. [https://doi.org/10.1016/S1474-4422\(09\)70238-8](https://doi.org/10.1016/S1474-4422(09)70238-8)
- Dijkstra, A. A., Voorn, P., Berendse, H. W., Groenewegen, H. J., Bank, N. B., Rozemuller, A. J., & van de Berg, W. D. (2014). Stage-dependent nigral neuronal loss in incidental Lewy body and Parkinson's disease. *Movement Disorders*, 29(10), 1244–1251. <https://doi.org/10.1002/mds.25952>
- Ding, Q., Dimayuga, E., Markesbery, W. R., & Keller, J. N. (2004). Proteasome inhibition increases DNA and RNA oxidation in astrocyte and neuron cultures. *Journal of Neurochemistry*, 91(5), 1211–1218. <https://doi.org/10.1111/j.1471-4159.2004.02802.x>
- Dirkx, M. F., Ouden, H. d., Aarts, E., Timmer, M., Bloem, B. R., Toni, I., & Helmich, R. C. (2016). The Cerebral Network of Parkinson's Tremor: An Effective Connectivity fMRI Study [Publisher: Society for Neuroscience Section: Articles]. *Journal of Neuroscience*, 36(19), 5362–5372. <https://doi.org/10.1523/JNEUROSCI.3634-15.2016>
- Dobin, A., Davis, C. A., Schlesinger, F., Drenkow, J., Zaleski, C., Jha, S., Batut, P., Chaisson, M., & Gingeras, T. R. (2013). STAR: Ultrafast universal RNA-seq aligner. *Bioinformatics (Oxford, England)*, 29(1), 15–21. <https://doi.org/10.1093/bioinformatics/bts635>
- Domínguez Conde, C., Xu, C., Jarvis, L. B., Rainbow, D. B., Wells, S. B., Gomes, T., Howlett, S. K., Suchanek, O., Polanski, K., King, H. W., Mamanova, L., Huang, N., Szabo, P. A., Richardson, L., Bolt, L., Fasouli, E. S., Mahbubani, K. T., Prete, M., Tuck, L., ... Teichmann, S. A. (2022). Cross-tissue immune cell analysis reveals tissue-specific features in humans [Publisher: American Association for the Advancement of Science]. *Science*, 376(6594), eabl5197. <https://doi.org/10.1126/science.abl5197>
- Dorsey, E. R., Constantinescu, R., Thompson, J. P., Biglan, K. M., Holloway, R. G., Kieburtz, K., Marshall, F. J., Ravina, B. M., Schifitto, G., Siderowf, A., & Tanner, C. M. (2007). Projected number of people with Parkinson disease in the most populous nations, 2005 through 2030 [Publisher: Wolters Kluwer Health, Inc. on behalf of the American Academy of Neurology Section: Articles]. *Neurology*, 68(5), 384–386. <https://doi.org/10.1212/01.wnl.0000247740.47667.03>

- Doyle, J. J. (2022). Cell types as species: Exploring a metaphor. *Frontiers in Plant Science*, *13*.
- Drmanac, R., Sparks, A. B., Callow, M. J., Halpern, A. L., Burns, N. L., Kermani, B. G., Carnevali, P., Nazarenko, I., Nilsen, G. B., Yeung, G., Dahl, F., Fernandez, A., Staker, B., Pant, K. P., Baccash, J., Borcharding, A. P., Brownley, A., Cedeno, R., Chen, L., ... Reid, C. A. (2010). Human Genome Sequencing Using Unchained Base Reads on Self-Assembling DNA Nanoarrays [Publisher: American Association for the Advancement of Science]. *Science*, *327*(5961), 78–81. <https://doi.org/10.1126/science.1181498>
- Du, Y., Huang, Q., Arisdakessian, C., & Garmire, L. X. (2020). Evaluation of STAR and Kallisto on Single Cell RNA-Seq Data Alignment. *G3: Genes|Genomes|Genetics*, *10*(5), 1775–1783. <https://doi.org/10.1534/g3.120.401160>
- Edwards, K. J., Reid, A. L., Coghill, J. A., Berry, S. T., & Barker, G. L. A. (2009). Multiplex single nucleotide polymorphism (SNP)-based genotyping in allohexaploid wheat using padlock probes [eprint: <https://onlinelibrary.wiley.com/doi/pdf/10.1111/j.1467-7652.2009.00413.x>]. *Plant Biotechnology Journal*, *7*(4), 375–390. <https://doi.org/10.1111/j.1467-7652.2009.00413.x>
- Elbaz, A., Carcaillon, L., Kab, S., & Moisan, F. (2016). Epidemiology of Parkinson's disease. *Revue Neurologique*, *172*(1), 14–26. <https://doi.org/10.1016/j.neurol.2015.09.012>
- Elson, J. L., Yates, A., & Pienaar, I. S. (2016). Pedunculopontine cell loss and protein aggregation direct microglia activation in parkinsonian rats. *Brain Structure and Function*, *221*(4), 2319–2341. <https://doi.org/10.1007/s00429-015-1045-4>
- Eng, C.-H. L., Lawson, M., Zhu, Q., Dries, R., Koulena, N., Takei, Y., Yun, J., Cronin, C., Karp, C., Yuan, G.-C., & Cai, L. (2019). Transcriptome-scale super-resolved imaging in tissues by RNA seqFISH+ [Number: 7751 Publisher: Nature Publishing Group]. *Nature*, *568*(7751), 235–239. <https://doi.org/10.1038/s41586-019-1049-y>
- Eng, C.-H. L., Shah, S., Thomassie, J., & Cai, L. (2017). Profiling the transcriptome with RNA SPOTs. *Nature Methods*, *14*(12), 1153–1155. <https://doi.org/10.1038/nmeth.4500>
- English, A. C., Richards, S., Han, Y., Wang, M., Vee, V., Qu, J., Qin, X., Muzny, D. M., Reid, J. G., Worley, K. C., & Gibbs, R. A. (2012). Mind the Gap: Upgrading Genomes with Pacific Biosciences RS Long-Read Sequencing Technology [Publisher: Public Library of Science]. *PLOS ONE*, *7*(11), e47768. <https://doi.org/10.1371/journal.pone.0047768>
- Eraslan, G., Drokhljansky, E., Anand, S., Fiskin, E., Subramanian, A., Slyper, M., Wang, J., Van Wittenberghe, N., Rouhana, J. M., Waldman, J., Ashenberg, O., Lek, M., Dionne, D., Win, T. S., Cuoco, M. S., Kuksenko, O., Tsankov, A. M., Branton, P. A., Marshall, J. L., ... Regev, A. (2022). Single-nucleus cross-tissue molecular reference maps toward understanding disease gene function [Publisher: American Association for the Advancement of Science]. *Science*, *376*(6594), eabl4290. <https://doi.org/10.1126/science.abl4290>
- Espa, E., Clemensson, E. K., Luk, K. C., Heuer, A., Björklund, T., & Cenci, M. A. (2019). Seeding of protein aggregation causes cognitive impairment in rat model of cortical synucleinopathy. *Movement Disorders*, *34*(11), 1699–1710. <https://doi.org/10.1002/mds.27810>
- Fan, Y., Andrusivová, Ž., Wu, Y., Chai, C., Larsson, L., He, M., Luo, L., Lundeberg, J., & Wang, B. (2023). Expansion spatial transcriptomics [Number: 8 Publisher: Nature Publishing Group]. *Nature Methods*, *20*(8), 1179–1182. <https://doi.org/10.1038/s41592-023-01911-1>

- Faustini, G., Longhena, F., Varanita, T., Bubacco, L., Pizzi, M., Missale, C., Benfenati, F., Björklund, A., Spano, P., & Bellucci, A. (2018). Synapsin III deficiency hampers alpha-synuclein aggregation, striatal synaptic damage and nigral cell loss in an AAV-based mouse model of Parkinson's disease. *Acta Neuropathologica*, *136*(4), 621–639. <https://doi.org/10.1007/s00401-018-1892-1>
- Fearnley, J. M., & Lees, A. J. (1991). Ageing and Parkinson's Disease: Substantia nigra regional selectivity. *Brain*, *114*(5), 2283–2301. <https://doi.org/10.1093/brain/114.5.2283>
- Ferreira, J. J., Lees, A., Rocha, J.-F., Poewe, W., Rascol, O., & Soares-da-Silva, P. (2016). Opi-capone as an adjunct to levodopa in patients with Parkinson's disease and end-of-dose motor fluctuations: A randomised, double-blind, controlled trial [ISBN: 1474-4422 Publisher: Elsevier]. *The Lancet Neurology*, *15*(2), 154–165.
- Foltynie, T., Magee, C., James, C., Webster, G. J. M., Lees, A. J., & Limousin, P. (2013). Impact of Duodopa on Quality of Life in Advanced Parkinson's Disease: A UK Case Series. *Parkinson's Disease*, *2013*, 362908. <https://doi.org/10.1155/2013/362908>
- Fong, Y. W., & Zhou, Q. (2001). Stimulatory effect of splicing factors on transcriptional elongation [Number: 6866 Publisher: Nature Publishing Group]. *Nature*, *414*(6866), 929–933. <https://doi.org/10.1038/414929a>
- Fox, S. H., Katzenschlager, R., Lim, S.-Y., Ravina, B., Seppi, K., Coelho, M., Poewe, W., Rascol, O., Goetz, C. G., & Sampaio, C. (2011). The Movement Disorder Society evidence-based medicine review update: Treatments for the motor symptoms of Parkinson's disease [ISBN: 0885-3185 Publisher: Wiley Online Library]. *Movement Disorders*, *26*(S3), S2–S41.
- Francardo, V., Recchia, A., Popovic, N., Andersson, D., Nissbrandt, H., & Cenci, M. A. (2011). Impact of the lesion procedure on the profiles of motor impairment and molecular responsiveness to L-DOPA in the 6-hydroxydopamine mouse model of Parkinson's disease. *Neurobiology of Disease*, *42*(3), 327–340. <https://doi.org/10.1016/j.nbd.2011.01.024>
- Frank, M. J., Samanta, J., Moustafa, A. A., & Sherman, S. J. (2007). Hold Your Horses: Impulsivity, Deep Brain Stimulation, and Medication in Parkinsonism [Publisher: American Association for the Advancement of Science]. *Science*, *318*(5854), 1309–1312. <https://doi.org/10.1126/science.1146157>
- Freed, C. R., Greene, P. E., Breeze, R. E., Tsai, W.-Y., DuMouchel, W., Kao, R., Dillon, S., Winfield, H., Culver, S., Trojanowski, J. Q., Eidelberg, D., & Fahn, S. (2001). Transplantation of Embryonic Dopamine Neurons for Severe Parkinson's Disease. *New England Journal of Medicine*, *344*(10), 710–719. <https://doi.org/10.1056/NEJM200103083441002>
- Freed, W. J., Poltorak, M., & Becker, J. B. (1990). Intracerebral adrenal medulla grafts: A review. *Experimental Neurology*, *110*(2), 139–166. [https://doi.org/10.1016/0014-4886\(90\)90026-o](https://doi.org/10.1016/0014-4886(90)90026-o)
- Fusco, G., De Simone, A., Gopinath, T., Vostrikov, V., Vendruscolo, M., Dobson, C. M., & Veglia, G. (2014). Direct observation of the three regions in α -synuclein that determine its membrane-bound behaviour. *Nature Communications*, *5*, 3827. <https://doi.org/10.1038/ncomms4827>
- Gaedcke, S., Sinning, J., Dittrich-Breiholz, O., Haller, H., Soerensen-Zender, I., Liao, C. M., Nordlohne, A., Sen, P., von Vietinghoff, S., DeLuca, D. S., & Schmitt, R. (2022). Single cell versus single nucleus: Transcriptome differences in the murine kidney af-

ter ischemia-reperfusion injury [Publisher: American Physiological Society]. *American Journal of Physiology-Renal Physiology*, 323(2), F171–F181. <https://doi.org/10.1152/ajprenal.00453.2021>

- Gagnon, J., Pi, L., Ryals, M., Wan, Q., Hu, W., Ouyang, Z., Zhang, B., & Li, K. (2022). Recommendations of scRNA-seq Differential Gene Expression Analysis Based on Comprehensive Benchmarking. *Life*, 12(6), 850. <https://doi.org/10.3390/life12060850>
- Gebert, N., Rahman, S., Lewis, C. A., Ori, A., & Cheng, C.-W. (2021). Identifying Cell-Type-Specific Metabolic Signatures Using Transcriptome and Proteome Analyses [eprint: <https://onlinelibrary.wiley.com/doi/pdf/10.1002/cpz1.245>]. *Current Protocols*, 1(9), e245. <https://doi.org/10.1002/cpz1.245>
- Genovese, P., Schirolli, G., Escobar, G., Tomaso, T. D., Firrito, C., Calabria, A., Moi, D., Mazzieri, R., Bonini, C., Holmes, M. C., Gregory, P. D., van der Burg, M., Gentner, B., Montini, E., Lombardo, A., & Naldini, L. (2014). Targeted genome editing in human repopulating haematopoietic stem cells. *Nature*, 510(7504), 235–240. <https://doi.org/10.1038/nature13420>
- Gerfen, C. R., Engber, T. M., Mahan, L. C., Susel, Z., Chase, T. N., Monsma, F. J., & Sibley, D. R. (1990). D1 and D2 Dopamine Receptor-regulated Gene Expression of Striatonigral and Striatopallidal Neurons [Publisher: American Association for the Advancement of Science]. *Science*, 250(4986), 1429–1432. <https://doi.org/10.1126/science.2147780>
- Ghanegolmohammadi, F., Ohnuki, S., & Ohya, Y. (2022). Assignment of unimodal probability distribution models for quantitative morphological phenotyping. *BMC Biology*, 20(1), 81. <https://doi.org/10.1186/s12915-022-01283-6>
- González-Hernández, T., Barroso-Chinea, P., De La Cruz Muros, I., Del Mar Pérez-Delgado, M., & Rodríguez, M. (2004). Expression of dopamine and vesicular monoamine transporters and differential vulnerability of mesostriatal dopaminergic neurons. *The Journal of Comparative Neurology*, 479(2), 198–215. <https://doi.org/10.1002/cne.20323>
- Gordon, P. H., Mehal, J. M., Holman, R. C., Rowland, A. S., & Cheek, J. E. (2012). Parkinson's disease among American Indians and Alaska natives: A nationwide prevalence study [eprint: <https://onlinelibrary.wiley.com/doi/pdf/10.1002/mds.25153>]. *Movement Disorders*, 27(11), 1456–1459. <https://doi.org/10.1002/mds.25153>
- Grealish, S., Diguët, E., Kirkeby, A., Mattsson, B., Heuer, A., Bramoulle, Y., Van Camp, N., Perrier, A. L., Hantraye, P., Björklund, A., & Parmar, M. (2014). Human ESC-Derived Dopamine Neurons Show Similar Preclinical Efficacy and Potency to Fetal Neurons when Grafted in a Rat Model of Parkinson's Disease [Publisher: Elsevier]. *Cell Stem Cell*, 15(5), 653–665. <https://doi.org/10.1016/j.stem.2014.09.017>
- Grealish, S., Heuer, A., Cardoso, T., Kirkeby, A., Jönsson, M., Johansson, J., Björklund, A., Jakobsson, J., & Parmar, M. (2015). Monosynaptic Tracing using Modified Rabies Virus Reveals Early and Extensive Circuit Integration of Human Embryonic Stem Cell-Derived Neurons. *Stem Cell Reports*, 4(6), 975–983. <https://doi.org/10.1016/j.stemcr.2015.04.011>
- Griffiths, J. A., Scialdone, A., & Marioni, J. C. (2018). Using single-cell genomics to understand developmental processes and cell fate decisions. *Molecular Systems Biology*, 14(4), e8046. <https://doi.org/10.15252/msb.20178046>
- Gross, R. E., Watts, R. L., Hauser, R. A., Bakay, R. A., Reichmann, H., von Kummer, R., Ondo, W. G., Reissig, E., Eisner, W., Steiner-Schulze, H., Siedentop, H., Fichte, K., Hong,

- W., Cornfeldt, M., Beebe, K., Sandbrink, R., & Spheramine Investigational Group. (2011). Intrastriatal transplantation of microcarrier-bound human retinal pigment epithelial cells versus sham surgery in patients with advanced Parkinson's disease: A double-blind, randomised, controlled trial. *The Lancet. Neurology*, *10*(6), 509–519. [https://doi.org/10.1016/S1474-4422\(11\)70097-7](https://doi.org/10.1016/S1474-4422(11)70097-7)
- Guo, J. L., & Lee, V. M. Y. (2014). Cell-to-cell transmission of pathogenic proteins in neurodegenerative diseases. *Nature Medicine*, *20*(2), 130–138. <https://doi.org/10.1038/nm.3457>
- Gyllborg, D., Langseth, C. M., Qian, X., Choi, E., Salas, S. M., Hilscher, M. M., Lein, E. S., & Nilsson, M. (2020). Hybridization-based in situ sequencing (HybISS) for spatially resolved transcriptomics in human and mouse brain tissue. *Nucleic Acids Research*, *48*(19), e112. <https://doi.org/10.1093/nar/gkaa792>
- Hafemeister, C., & Satija, R. (2019). Normalization and variance stabilization of single-cell RNA-seq data using regularized negative binomial regression. *Genome Biology*, *20*(1), 296. <https://doi.org/10.1186/s13059-019-1874-1>
- Hahn, O., Foltz, A. G., Atkins, M., Kedir, B., Moran-Losada, P., Guldner, I. H., Munson, C., Kern, F., Pálovics, R., Lu, N., Zhang, H., Kaur, A., Hull, J., Huguenard, J. R., Grönke, S., Lehallier, B., Partridge, L., Keller, A., & Wyss-Coray, T. (2023). Atlas of the aging mouse brain reveals white matter as vulnerable foci [Publisher: Elsevier]. *Cell*, *0*(0). <https://doi.org/10.1016/j.cell.2023.07.027>
- Hallett, P. J., Cooper, O., Sadi, D., Robertson, H., Mendez, I., & Isacson, O. (2014). Long-term health of dopaminergic neuron transplants in Parkinson's disease patients. *Cell Reports*, *7*(6), 1755–1761. <https://doi.org/10.1016/j.celrep.2014.05.027>
- Halliday, G. M., Holton, J. L., Revesz, T., & Dickson, D. W. (2011). Neuropathology underlying clinical variability in patients with synucleinopathies. *Acta Neuropathologica*, *122*(2), 187–204. <https://doi.org/10.1007/s00401-011-0852-9>
- Hallin, E. I., Eriksen, M. S., Baryshnikov, S., Nikolaienko, O., Grødem, S., Hosokawa, T., Hayashi, Y., Bramham, C. R., & Kursula, P. (2018). Structure of monomeric full-length ARC sheds light on molecular flexibility, protein interactions, and functional modalities. *Journal of Neurochemistry*, *147*(3), 323–343. <https://doi.org/10.1111/jnc.14556>
- Harrison, P. R., Conkie, D., Paul, J., & Jones, K. (1973). Localisation of cellular globin messenger RNA by in situ hybridisation to complementary DNA. *FEBS letters*, *32*(1), 109–112. [https://doi.org/10.1016/0014-5793\(73\)80749-5](https://doi.org/10.1016/0014-5793(73)80749-5)
- Hashimshony, T., Wagner, F., Sher, N., & Yanai, I. (2012). CEL-Seq: Single-Cell RNA-Seq by Multiplexed Linear Amplification. *Cell Reports*, *2*(3), 666–673. <https://doi.org/10.1016/j.celrep.2012.08.003>
- Herculano-Houzel, S., Mota, B., & Lent, R. (2006). Cellular scaling rules for rodent brains [Publisher: Proceedings of the National Academy of Sciences]. *Proceedings of the National Academy of Sciences*, *103*(32), 12138–12143. <https://doi.org/10.1073/pnas.0604911103>
- Heumos, L., Schaar, A. C., Lance, C., Litinetskaya, A., Drost, F., Zappia, L., Lücken, M. D., Strobl, D. C., Henao, J., Curion, F., Schiller, H. B., & Theis, F. J. (2023). Best practices for single-cell analysis across modalities [Number: 8 Publisher: Nature Publishing Group]. *Nature Reviews Genetics*, *24*(8), 550–572. <https://doi.org/10.1038/s41576-023-00586-w>

- Hicks, S. C., Townes, F. W., Teng, M., & Irizarry, R. A. (2018). Missing data and technical variability in single-cell RNA-sequencing experiments. *Biostatistics*, *19*(4), 562–578. <https://doi.org/10.1093/biostatistics/kxx053>
- Hie, B., Bryson, B., & Berger, B. (2019). Efficient integration of heterogeneous single-cell transcriptomes using Scanorama [Number: 6 Publisher: Nature Publishing Group]. *Nature Biotechnology*, *37*(6), 685–691. <https://doi.org/10.1038/s41587-019-0113-3>
- Hinton, G. E., & Roweis, S. (2002). Stochastic neighbor embedding. *Advances in neural information processing systems*, *15*.
- Hirose, Y., & Manley, J. L. (2000). RNA polymerase II and the integration of nuclear events [Company: Cold Spring Harbor Laboratory Press Distributor: Cold Spring Harbor Laboratory Press Institution: Cold Spring Harbor Laboratory Press Label: Cold Spring Harbor Laboratory Press Publisher: Cold Spring Harbor Lab]. *Genes & Development*, *14*(12), 1415–1429. <https://doi.org/10.1101/gad.14.12.1415>
- Ho, C. K., Van Etten, J. L., & Shuman, S. (1997). Characterization of an ATP-dependent DNA ligase encoded by Chlorella virus PBCV-1. *Journal of Virology*, *71*(3), 1931–1937. <https://doi.org/10.1128/JVI.71.3.1931-1937.1997>
- Hoban, D. B., Shrigley, S., Mattsson, B., Breger, L. S., Jarl, U., Cardoso, T., Nelander Wahlestedt, J., Luk, K. C., Björklund, A., & Parmar, M. (2020). Impact of a-synuclein pathology on transplanted hESC-derived dopaminergic neurons in a humanized alpha-synuclein rat model of PD. *Proceedings of the National Academy of Sciences of the United States of America*, *117*(26), 15209–15220. <https://doi.org/10.1073/pnas.2001305117>
- Hocquemiller, M., Giersch, L., Audrain, M., Parker, S., & Cartier, N. (2016). Adeno-Associated Virus-Based Gene Therapy for CNS Diseases. *Human Gene Therapy*, *27*(7), 478–496. <https://doi.org/10.1089/hum.2016.087>
- Hor, H., Francescato, L., Bartesaghi, L., Ortega-Cubero, S., Kousi, M., Lorenzo-Betancor, O., Jiménez-Jiménez, F. J., Gironell, A., Clarimón, J., Drechsel, O., Agúndez, J. A. G., Kenzelmann Broz, D., Chiquet-Ehrismann, R., Lleó, A., Coria, F., García-Martin, E., Alonso-Navarro, H., Martí, M. J., Kulisevsky, J., ... Estivill, X. (2015). Missense mutations in TENM4, a regulator of axon guidance and central myelination, cause essential tremor. *Human Molecular Genetics*, *24*(20), 5677–5686. <https://doi.org/10.1093/hmg/ddv281>
- Hsu, H.-L., Brown, A., Loveland, A., Lotun, A., Xu, M., Luo, L., Xu, G., Li, J., Ren, L., Su, Q., Gessler, D., Wei, Y., Tai, P., Korostelev, A., & Gao, G. (2020). Structural characterization of a novel human adeno-associated virus capsid with neurotropic properties. *Nature Communications*, *11*(1). <https://doi.org/10.1038/s41467-020-17047-1>
- Huang, L., Kebschull, J. M., Fürth, D., Musall, S., Kaufman, M. T., Churchland, A. K., & Zador, A. M. (2020). BRICseq Bridges Brain-wide Interregional Connectivity to Neural Activity and Gene Expression in Single Animals. *Cell*, *182*(1), 177–188.e27. <https://doi.org/10.1016/j.cell.2020.05.029>
- Hurtig, H., Joyce, J., Sladek, J. R., & Trojanowski, J. Q. (1989). Postmortem analysis of adrenal-medulla-to-caudate autograft in a patient with Parkinson's disease. *Annals of Neurology*, *25*(6), 607–614. <https://doi.org/10.1002/ana.410250613>
- Iacono, D., Geraci-Erck, M., Rabin, M. L., Adler, C. H., Serrano, G., Beach, T. G., & Kurlan, R. (2015). Parkinson disease and incidental Lewy body disease: Just a question of time? [Publisher: Wolters Kluwer Health, Inc. on behalf of the American Academy of Neurol-

- ogy Section: Article]. *Neurology*, 85(19), 1670–1679. <https://doi.org/10.1212/WNL.0000000000002102>
- Ilicic, T., Kim, J. K., Kolodziejczyk, A. A., Bagger, F. O., McCarthy, D. J., Marioni, J. C., & Teichmann, S. A. (2016). Classification of low quality cells from single-cell RNA-seq data. *Genome Biology*, 17, 29. <https://doi.org/10.1186/s13059-016-0888-1>
- Illumina reports financial results for fourth quarter and fiscal year 2022. (n.d.).
- Islam, S., Kjällquist, U., Moliner, A., Zajac, P., Fan, J.-B., Lönnerberg, P., & Linnarsson, S. (2011). Characterization of the single-cell transcriptional landscape by highly multiplex RNA-seq. *Genome Research*, 21(7), 1160–1167. <https://doi.org/10.1101/gr.110882.110>
- Iyama, T., & Wilson, D. M. (2013). DNA repair mechanisms in dividing and non-dividing cells. *DNA Repair*, 12(8), 620–636. <https://doi.org/10.1016/j.dnarep.2013.04.015>
- Jaitin, D. A., Kenigsberg, E., Keren-Shaul, H., Elefant, N., Paul, F., Zaretsky, I., Mildner, A., Cohen, N., Jung, S., Tanay, A., & Amit, I. (2014). Massively Parallel Single-Cell RNA-Seq for Marker-Free Decomposition of Tissues into Cell Types [Publisher: American Association for the Advancement of Science]. *Science*, 343(6172), 776–779. <https://doi.org/10.1126/science.1247651>
- Jang, M. J., Coughlin, G. M., Jackson, C. R., Chen, X., Chuapoco, M. R., Vendemiatti, J. L., Wang, A. Z., & Gradinaru, V. (2023). Spatial transcriptomics for profiling the tropism of viral vectors in tissues [Publisher: Nature Publishing Group]. *Nature Biotechnology*, 1–15. <https://doi.org/10.1038/s41587-022-01648-w>
- Jankovic, J., Grossman, R., Goodman, C., Pirozzolo, F., Schneider, L., Zhu, Z., Scardino, P., Garber, A. J., Jhingan, S. G., & Martin, S. (1989). Clinical, biochemical, and neuropathologic findings following transplantation of adrenal medulla to the caudate nucleus for treatment of Parkinson's disease. *Neurology*, 39(9), 1227–1234. <https://doi.org/10.1212/wnl.39.9.1227>
- Jarraya, B., Boulet, S., Scott Ralph, G., Jan, C., Bonvento, G., Azzouz, M., Miskin, J. E., Shin, M., Delzescaux, T., Drouot, X., Hérard, A.-S., Day, D. M., Brouillet, E., Kingsman, S. M., Hantraye, P., Mitrophanous, K. A., Mazarakis, N. D., & Palfi, S. (2009). Dopamine Gene Therapy for Parkinson's Disease in a Nonhuman Primate Without Associated Dyskinesia [Publisher: American Association for the Advancement of Science]. *Science Translational Medicine*, 1(2), 2ra4–2ra4. <https://doi.org/10.1126/scitranslmed.3000130>
- Jin, J., Vaud, S., Zhelkovsky, A. M., Posfai, J., & McReynolds, L. A. (2016). Sensitive and specific miRNA detection method using SplintR Ligase. *Nucleic Acids Research*, 44(13), e116. <https://doi.org/10.1093/nar/gkw399>
- Jones, R. N., Coons, A. H., & Creech, H. J. (1941). Immunological Properties of an Antibody Containing a Fluorescent Group. [Publisher: Society for Experimental Biology and Medicine]. *Experimental biology and medicine*. <https://doi.org/10.3181/00379727-47-13084P>
- Kalia, L. V., & Lang, A. E. (2015). Parkinson's disease [ISBN: 0140-6736 Publisher: Elsevier]. *The Lancet*, 386(9996), 896–912.
- Kamath, T., Abdulraouf, A., Burris, S. J., Langlieb, J., Gazestani, V., Nadaf, N. M., Balderrama, K., Vanderburg, C., & Macosko, E. Z. (2022). Single-cell genomic profiling of human dopamine neurons identifies a population that selectively degenerates in Parkinson's dis-

ease [Number: 5 Publisher: Nature Publishing Group]. *Nature Neuroscience*, 25(5), 588–595. <https://doi.org/10.1038/s41593-022-01061-1>

- Karin, M. (1990). Too many transcription factors: Positive and negative interactions. *The New Biologist*, 2(2), 126–131.
- Ke, R., Mignardi, M., Pacureanu, A., Svedlund, J., Botling, J., Wählby, C., & Nilsson, M. (2013). In situ sequencing for RNA analysis in preserved tissue and cells. *Nature Methods*, 10(9), 857–860. <https://doi.org/10.1038/nmeth.2563>
- Kebschull, J. M., Garcia da Silva, P., Reid, A. P., Peikon, I. D., Albeanu, D. F., & Zador, A. M. (2016). High-Throughput Mapping of Single-Neuron Projections by Sequencing of Barcoded RNA. *Neuron*, 91(5), 975–987. <https://doi.org/10.1016/j.neuron.2016.07.036>
- Kefalopoulou, Z., Politis, M., Piccini, P., Mencacci, N., Bhatia, K., Jahanshahi, M., Widner, H., Rehncrona, S., Brundin, P., Björklund, A., Lindvall, O., Limousin, P., Quinn, N., & Foltynie, T. (2014). Long-term clinical outcome of fetal cell transplantation for Parkinson disease: Two case reports. *JAMA neurology*, 71(1), 83–87. <https://doi.org/10.1001/jamaneurol.2013.4749>
- Kiely, A. P., Murray, C. E., Foti, S. C., Benson, B. C., Courtney, R., Strand, C., Lashley, T., & Holton, J. L. (2018). Immunohistochemical and Molecular Investigations Show Alteration in the Inflammatory Profile of Multiple System Atrophy Brain. *Journal of Neuropathology and Experimental Neurology*, 77(7), 598–607. <https://doi.org/10.1093/jnen/nly035>
- Kikuchi, T., Morizane, A., Doi, D., Onoe, H., Hayashi, T., Kawasaki, T., Saiki, H., Miyamoto, S., & Takahashi, J. (2011). Survival of human induced pluripotent stem cell-derived midbrain dopaminergic neurons in the brain of a primate model of Parkinson's disease. *Journal of Parkinson's Disease*, 1(4), 395–412. <https://doi.org/10.3233/JPD-2011-11070>
- Kirik, D., Rosenblad, C., Burger, C., Lundberg, C., Johansen, T. E., Muzyczka, N., Mandel, R. J., & Björklund, A. (2002). Parkinson-Like Neurodegeneration Induced by Targeted Overexpression of α -Synuclein in the Nigrostriatal System [Publisher: Society for Neuroscience Section: ARTICLE]. *Journal of Neuroscience*, 22(7), 2780–2791. <https://doi.org/10.1523/JNEUROSCI.22-07-02780.2002>
- Kirkeby, A., Grealish, S., Wolf, D. A., Nelander, J., Wood, J., Lundblad, M., Lindvall, O., & Parmar, M. (2012). Generation of regionally specified neural progenitors and functional neurons from human embryonic stem cells under defined conditions. *Cell Reports*, 1(6), 703–714. <https://doi.org/10.1016/j.celrep.2012.04.009>
- Kirkeby, A., Nolbrant, S., Tiklova, K., Heuer, A., Kee, N., Cardoso, T., Ottosson, D. R., Lelos, M. J., Rifés, P., Dunnnett, S. B., Grealish, S., Perlmann, T., & Parmar, M. (2017). Predictive Markers Guide Differentiation to Improve Graft Outcome in Clinical Translation of hESC-Based Therapy for Parkinson's Disease. *Cell Stem Cell*, 20(1), 135–148. <https://doi.org/10.1016/j.stem.2016.09.004>
- Klein, A. M., Mazutis, L., Akartuna, I., Tallapragada, N., Veres, A., Li, V., Peshkin, L., Weitz, D. A., & Kirschner, M. W. (2015). Droplet Barcoding for Single-Cell Transcriptomics Applied to Embryonic Stem Cells [Publisher: Elsevier]. *Cell*, 161(5), 1187–1201. <https://doi.org/10.1016/j.cell.2015.04.044>

- Klein, C., & Westenberger, A. (2012). Genetics of Parkinson's Disease [Publisher: Cold Spring Harbor Laboratory Press]. *Cold Spring Harbor Perspectives in Medicine*, 2(1), a008888. <https://doi.org/10.1101/cshperspect.a008888>
- Klein, D., Palla, G., Lange, M., Klein, M., Piran, Z., Gander, M., Meng-Papaxanthos, L., Sterr, M., Bastidas-Ponce, A., Tarquis-Medina, M., Lickert, H., Bakhti, M., Nitzan, M., Cuturi, M., & Theis, F. J. (2023). Mapping cells through time and space with moscot [Pages: 2023.05.11.540374 Section: New Results]. <https://doi.org/10.1101/2023.05.11.540374>
- Kleshchevnikov, V., Shmatko, A., Dann, E., Aivazidis, A., King, H. W., Li, T., Elmentaite, R., Lomakin, A., Kedlian, V., Gayoso, A., Jain, M. S., Park, J. S., Ramona, L., Tuck, E., Arutyunyan, A., Vento-Tormo, R., Gerstung, M., James, L., Stegle, O., & Bayraktar, O. A. (2022). Cell2location maps fine-grained cell types in spatial transcriptomics. *Nature Biotechnology*, 40(5), 661–671. <https://doi.org/10.1038/s41587-021-01139-4>
- Konieczny, J., Czarnecka, A., Lenda, T., Kamińska, K., & Lorenc-Koci, E. (2014). Chronic l-DOPA treatment attenuates behavioral and biochemical deficits induced by unilateral lactacystin administration into the rat substantia nigra. *Behavioural Brain Research*, 261, 79–88. <https://doi.org/10.1016/j.bbr.2013.12.019>
- Konstantakos, V., Nentidis, A., Krithara, A., & Paliouras, G. (2022). CRISPRpredict: A CRISPR-Cas9 web tool for interpretable efficiency predictions. *Nucleic Acids Research*, 50(W1), W191–W198. <https://doi.org/10.1093/nar/gkac466>
- Kordower, J. H., & Bjorklund, A. (2013). Trophic Factor Gene Therapy for Parkinson's Disease: Trophic Factors For Pd. *Movement Disorders*, 28(1), 96–109. <https://doi.org/10.1002/mds.25344>
- Kordower, J. H., Herzog, C. D., Dass, B., Bakay, R. A., Stansell III, J., Gasmi, M., & Bartus, R. T. (2006). Delivery of neurturin by AAV2 (CERE-120)-mediated gene transfer provides structural and functional neuroprotection and neurorestoration in MPTP-treated monkeys [ISBN: 0364-5134 Publisher: Wiley Online Library]. *Annals of Neurology: Official Journal of the American Neurological Association and the Child Neurology Society*, 60(6), 706–715.
- Korsunsky, I., Millard, N., Fan, J., Slowikowski, K., Zhang, F., Wei, K., Baglaenko, Y., Brenner, M., Loh, P.-r., & Raychaudhuri, S. (2019). Fast, sensitive and accurate integration of single-cell data with Harmony [Number: 12 Publisher: Nature Publishing Group]. *Nature Methods*, 16(12), 1289–1296. <https://doi.org/10.1038/s41592-019-0619-0>
- Kozłowska, M., Kotarba, S., Tambor, J., Winiarski, M., Moczulska, H., Pietrusiński, M., & Borowiec, M. (2023). Parkinson's disease gene therapy: A comparative effectiveness review of completed clinical trials in terms of their possible implementation in treatment [ISBN: 2544-1620 Publisher: Index Copernicus]. *Medical Science Pulse*, 17(1), 24–31.
- Krzywkowski, T., Kühnemund, M., Wu, D., & Nilsson, M. (2018). Limited reverse transcriptase activity of phi29 DNA polymerase. *Nucleic Acids Research*, 46(7), 3625–3632. <https://doi.org/10.1093/nar/gky190>
- Krzywkowski, T., & Nilsson, M. (2017). Fidelity of RNA templated end-joining by chlorella virus DNA ligase and a novel iLock assay with improved direct RNA detection accuracy. *Nucleic Acids Research*, 45(18), e161. <https://doi.org/10.1093/nar/gkx708>

- Krzywkowski, T., & Nilsson, M. (2018). Padlock Probes to Detect Single Nucleotide Polymorphisms. *Methods in Molecular Biology (Clifton, N.J.)*, 1649, 209–229. https://doi.org/10.1007/978-1-4939-7213-5_14
- Kühn, A. A., Kempf, F., Brücke, C., Doyle, L. G., Martinez-Torres, I., Pogosyan, A., Trottenberg, T., Kupsch, A., Schneider, G.-H., Hariz, M. I., Vandenberghe, W., Nuttin, B., & Brown, P. (2008). High-Frequency Stimulation of the Subthalamic Nucleus Suppresses Oscillatory β Activity in Patients with Parkinson's Disease in Parallel with Improvement in Motor Performance [Publisher: Society for Neuroscience Section: Articles]. *Journal of Neuroscience*, 28(24), 6165–6173. <https://doi.org/10.1523/JNEUROSCI.0282-08.2008>
- Kuter, K. Z., Cenci, M. A., & Carta, A. R. (2020). Chapter 5 - The role of glia in Parkinson's disease: Emerging concepts and therapeutic applications. In A. Björklund & M. A. Cenci (Eds.), *Progress in Brain Research* (pp. 131–168). Elsevier. <https://doi.org/10.1016/bs.pbr.2020.02.004>
- La Manno, G., Siletti, K., Furlan, A., Gyllborg, D., Vinsland, E., Mossi Albiach, A., Mattsson Langseth, C., Khven, I., Lederer, A. R., Dratva, L. M., Johnsson, A., Nilsson, M., Lönnnerberg, P., & Linnarsson, S. (2021). Molecular architecture of the developing mouse brain. *Nature*, 596(7870), 92–96. <https://doi.org/10.1038/s41586-021-03775-x>
- La Manno, G., Soldatov, R., Zeisel, A., Braun, E., Hochgerner, H., Petukhov, V., Lidschreiber, K., Kastrioti, M. E., Lönnnerberg, P., Furlan, A., Fan, J., Borm, L. E., Liu, Z., van Bruggen, D., Guo, J., He, X., Barker, R., Sundström, E., Castelo-Branco, G., ... Kharchenko, P. V. (2018). RNA velocity of single cells. *Nature*, 560(7719), 494–498. <https://doi.org/10.1038/s41586-018-0414-6>
- Lake, B. B., Codeluppi, S., Yung, Y. C., Gao, D., Chun, J., Kharchenko, P. V., Linnarsson, S., & Zhang, K. (2017). A comparative strategy for single-nucleus and single-cell transcriptomes confirms accuracy in predicted cell-type expression from nuclear RNA [Number: 1 Publisher: Nature Publishing Group]. *Scientific Reports*, 7(1), 6031. <https://doi.org/10.1038/s41598-017-04426-w>
- Lam, S., Arif, M., Song, X., Uhlén, M., & Mardinoglu, A. (2022). Machine Learning Analysis Reveals Biomarkers for the Detection of Neurological Diseases. *Frontiers in Molecular Neuroscience*, 15, 889728. <https://doi.org/10.3389/fnmol.2022.889728>
- Lander, E. S., Linton, L. M., Birren, B., Nusbaum, C., Zody, M. C., Baldwin, J., Devon, K., Dewar, K., Doyle, M., FitzHugh, W., Funke, R., Gage, D., Harris, K., Heaford, A., Howland, J., Kann, L., Lehoczky, J., LeVine, R., McEwan, P., ... International Human Genome Sequencing Consortium. (2001). Initial sequencing and analysis of the human genome. *Nature*, 409(6822), 860–921. <https://doi.org/10.1038/35057062>
- Lane, E. L., Winkler, C., Brundin, P., & Cenci, M. A. (2006). The impact of graft size on the development of dyskinesia following intrastriatal grafting of embryonic dopamine neurons in the rat. *Neurobiology of Disease*, 22(2), 334–345. <https://doi.org/10.1016/j.nbd.2005.11.011>
- Lang, A. E., Gill, S., Patel, N. K., Lozano, A., Nutt, J. G., Penn, R., Brooks, D. J., Hotton, G., Moro, E., & Heywood, P. (2006). Randomized controlled trial of intraputamenal glial cell line-derived neurotrophic factor infusion in Parkinson disease [ISBN: 0364-5134 Publisher: Wiley Online Library]. *Annals of neurology*, 59(3), 459–466.

- Lange, M., Bergen, V., Klein, M., Setty, M., Reuter, B., Bakhti, M., Lickert, H., Ansari, M., Schniering, J., Schiller, H. B., Pe'er, D., & Theis, F. J. (2022). CellRank for directed single-cell fate mapping. *Nature Methods*, *19*(2), 159–170. <https://doi.org/10.1038/s41592-021-01346-6>
- Langer-Safer, P. R., Levine, M., & Ward, D. C. (1982). Immunological method for mapping genes on Drosophila polytene chromosomes. *Proceedings of the National Academy of Sciences of the United States of America*, *79*(14), 4381–4385.
- Langlieb, J., Sachdev, N. S., Balderrama, K. S., Nadaf, N. M., Raj, M., Murray, E., Webber, J. T., Vanderburg, C., Gazestani, V., Tward, D., Mezas, C., Li, X., Cable, D. M., Norton, T., Mitra, P., Chen, F., & Macosko, E. Z. (2023). The cell type composition of the adult mouse brain revealed by single cell and spatial genomics [Pages: 2023.03.06.531307 Section: New Results]. <https://doi.org/10.1101/2023.03.06.531307>
- Langmead, B., & Salzberg, S. L. (2012). Fast gapped-read alignment with Bowtie 2. *Nature methods*, *9*(4), 357–359. <https://doi.org/10.1038/nmeth.1923>
- Langston, J. W., Ballard, P., Tetrud, J. W., & Irwin, I. (1983). Chronic Parkinsonism in Humans Due to a Product of Meperidine-Analog Synthesis [Publisher: American Association for the Advancement of Science]. *Science*, *219*(4587), 979–980. <https://doi.org/10.1126/science.6823561>
- Latchman, D. S. (1993). Transcription factors: An overview. *International Journal of Experimental Pathology*, *74*(5), 417–422.
- Lautenschläger, J., Stephens, A. D., Fusco, G., Ströhl, F., Curry, N., Zacharopoulou, M., Michel, C. H., Laine, R., Nespovitaya, N., Fantham, M., Pinotsi, D., Zago, W., Fraser, P., Tandon, A., St George-Hyslop, P., Rees, E., Phillips, J. J., De Simone, A., Kaminski, C. F., & Schierle, G. S. K. (2018). C-terminal calcium binding of a-synuclein modulates synaptic vesicle interaction. *Nature Communications*, *9*(1), 712. <https://doi.org/10.1038/s41467-018-03111-4>
- Lee, H., Marco Salas, S., Gyllborg, D., & Nilsson, M. (2022). Direct RNA targeted in situ sequencing for transcriptomic profiling in tissue [Number: 1 Publisher: Nature Publishing Group]. *Scientific Reports*, *12*(1), 7976. <https://doi.org/10.1038/s41598-022-11534-9>
- Lee, J. H., Daugharthy, E. R., Scheiman, J., Kalhor, R., Yang, J. L., Ferrante, T. C., Terry, R., Jeanty, S. S. F., Li, C., Amamoto, R., Peters, D. T., Turczyk, B. M., Marblestone, A. H., Inverso, S. A., Bernard, A., Mali, P., Rios, X., Aach, J., & Church, G. M. (2014). Highly Multiplexed Subcellular RNA Sequencing in Situ [Publisher: American Association for the Advancement of Science]. *Science*, *343*(6177), 1360–1363. <https://doi.org/10.1126/science.1250212>
- Lein, E. S., Hawrylycz, M. J., Ao, N., Ayres, M., Bensinger, A., Bernard, A., Boe, A. F., Boguski, M. S., Brockway, K. S., Byrnes, E. J., Chen, L., Chen, L., Chen, T.-M., Chi Chin, M., Chong, J., Crook, B. E., Czaplinska, A., Dang, C. N., Datta, S., ... Jones, A. R. (2007). Genome-wide atlas of gene expression in the adult mouse brain [Number: 7124 Publisher: Nature Publishing Group]. *Nature*, *445*(7124), 168–176. <https://doi.org/10.1038/nature05453>
- LeWitt, P. A., & Fahn, S. (2016). Levodopa therapy for Parkinson disease: A look backward and forward [ISBN: 0028-3878 Publisher: AAN Enterprises]. *Neurology*, *86*(14 Supplement 1), S3–S12.

- Li, H., Zhou, J., Li, Z., Chen, S., Liao, X., Zhang, B., Zhang, R., Wang, Y., Sun, S., & Gao, X. (2023). A comprehensive benchmarking with practical guidelines for cellular deconvolution of spatial transcriptomics [Number: 1 Publisher: Nature Publishing Group]. *Nature Communications*, *14*(1), 1548. <https://doi.org/10.1038/s41467-023-37168-7>
- Li, H., & Durbin, R. (2009). Fast and accurate short read alignment with Burrows-Wheeler transform. *Bioinformatics (Oxford, England)*, *25*(14), 1754–1760. <https://doi.org/10.1093/bioinformatics/btp324>
- Li, J., Zhang, B.-b., Ren, Y.-g., Gu, S.-y., Xiang, Y.-h., Huang, C., & Du, J.-l. (2015). Intron targeting-mediated and endogenous gene integrity-maintaining knockin in zebrafish using the CRISPR/Cas9 system [Number: 5 Publisher: Nature Publishing Group]. *Cell Research*, *25*(5), 634–637. <https://doi.org/10.1038/cr.2015.43>
- Li, J.-Y., Englund, E., Holton, J. L., Soulet, D., Hagell, P., Lees, A. J., Lashley, T., Quinn, N. P., Rehncrona, S., Björklund, A., Widner, H., Revesz, T., Lindvall, O., & Brundin, P. (2008). Lewy bodies in grafted neurons in subjects with Parkinson's disease suggest host-to-graft disease propagation. *Nature Medicine*, *14*(5), 501–503. <https://doi.org/10.1038/nm1746>
- Li, J.-Y., Englund, E., Widner, H., Rehncrona, S., Björklund, A., Lindvall, O., & Brundin, P. (2010). Characterization of Lewy body pathology in 12- and 16-year-old intrastriatal mesencephalic grafts surviving in a patient with Parkinson's disease. *Movement Disorders: Official Journal of the Movement Disorder Society*, *25*(8), 1091–1096. <https://doi.org/10.1002/mds.23012>
- Li, X., Wang, K., Lyu, Y., Pan, H., Zhang, J., Stambolian, D., Susztak, K., Reilly, M. P., Hu, G., & Li, M. (2020). Deep learning enables accurate clustering with batch effect removal in single-cell RNA-seq analysis [Number: 1 Publisher: Nature Publishing Group]. *Nature Communications*, *11*(1), 2338. <https://doi.org/10.1038/s41467-020-15851-3>
- Li, X.-Y., Du, Y.-C., Zhang, Y.-P., & Kong, D.-M. (2017). Dual functional Phi29 DNA polymerase-triggered exponential rolling circle amplification for sequence-specific detection of target DNA embedded in long-stranded genomic DNA [Number: 1 Publisher: Nature Publishing Group]. *Scientific Reports*, *7*(1), 6263. <https://doi.org/10.1038/s41598-017-06594-1>
- Liao, X., Li, M., Zou, Y., Wu, F.-X., Yi-Pan, & Wang, J. (2019). Current challenges and solutions of de novo assembly. *Quantitative Biology*, *7*(2), 90–109. <https://doi.org/10.1007/s40484-019-0166-9>
- Lieber, M. R. (2010). The Mechanism of Double-Strand DNA Break Repair by the Nonhomologous DNA End-Joining Pathway. *Annual Review of Biochemistry*, *79*(1), 181–211. <https://doi.org/10.1146/annurev.biochem.052308.093131>
- Limousin, P., Pollak, P., Benazzouz, A., Hoffmann, D., Le Bas, J.-F., Perret, J. E., Benabid, A. L., & Broussolle, E. (1995). Effect on parkinsonian signs and symptoms of bilateral subthalamic nucleus stimulation [ISBN: 0140-6736 Publisher: Elsevier]. *The Lancet*, *345*(8942), 91–95.
- Lindholm, P., Voutilainen, M. H., Laurén, J., Peränen, J., Leppänen, V.-M., Andressoo, J.-O., Lindahl, M., Janhunen, S., Kalkkinen, N., Timmusk, T., Tuominen, R. K., & Saarna, M. (2007). Novel neurotrophic factor CDNF protects and rescues midbrain dopamine neurons in vivo. *Nature*, *448*(7149), 73–77. <https://doi.org/10.1038/nature05957>

- Lindvall, O., Rehnström, S., Brundin, P., Gustavii, B., Astedt, B., Widner, H., Lindholm, T., Björklund, A., Leenders, K. L., Rothwell, J. C., Frackowiak, R., Marsden, D., Johnels, B., Steg, G., Freedman, R., Hoffer, B. J., Seiger, A., Bygdeman, M., Strömberg, I., & Olson, L. (1989). Human fetal dopamine neurons grafted into the striatum in two patients with severe Parkinson's disease. A detailed account of methodology and a 6-month follow-up. *Archives of Neurology*, *46*(6), 615–631. <https://doi.org/10.1001/archneur.1989.00520420033021>
- Lindvall, O., Sawle, G., Widner, H., Rothwell, J. C., Björklund, A., Brooks, D., Brundin, P., Frackowiak, R., Marsden, C. D., & Odin, P. (1994). Evidence for long-term survival and function of dopaminergic grafts in progressive Parkinson's disease. *Annals of Neurology*, *35*(2), 172–180. <https://doi.org/10.1002/ana.410350208>
- Lindvall, O., Brundin, P., Widner, H., Rehnström, S., Gustavii, B., Frackowiak, R., Leenders, K. L., Sawle, G., Rothwell, J. C., Marsden, C. D., & Björklund, M. (1990). Grafts of Fetal Dopamine Neurons Survive and Improve Motor Function in Parkinson's Disease. *Science*, *247*(4942), 574–577. <https://doi.org/10.1126/science.2105529>
- Liu, S., Punthambaker, S., Iyer, E. P. R., Ferrante, T., Goodwin, D., Fürth, D., Pawlowski, A. C., Jindal, K., Tam, J. M., Mifflin, L., Alon, S., Sinha, A., Wassie, A. T., Chen, F., Cheng, A., Willocq, V., Meyer, K., Ling, K.-H., Camplisson, C. K., ... Church, G. M. (2021). Barcoded oligonucleotides ligated on RNA amplified for multiplexed and parallel in situ analyses. *Nucleic Acids Research*, *49*(10), e58. <https://doi.org/10.1093/nar/gkab120>
- Liu, X., Wang, S., & Ai, D. (2022). Predicting CRISPR/Cas9 Repair Outcomes by Attention-Based Deep Learning Framework. *Cells*, *11*(11), 1847. <https://doi.org/10.3390/cells11111847>
- Liu, Y., Huang, J., Pandey, R., Liu, P., Therani, B., Qiu, Q., Rao, S., Geurts, A. M., Cowley, A. W., Greene, A. S., & Liang, M. (2023). Robustness of single-cell RNA-seq for identifying differentially expressed genes. *BMC Genomics*, *24*(1), 371. <https://doi.org/10.1186/s12864-023-09487-y>
- Logan, J., Falck-Pedersen, E., Darnell, J. E., & Shenk, T. (1987). A poly(A) addition site and a downstream termination region are required for efficient cessation of transcription by RNA polymerase II in the mouse beta maj-globin gene. [Publisher: Proceedings of the National Academy of Sciences]. *Proceedings of the National Academy of Sciences*, *84*(23), 8306–8310. <https://doi.org/10.1073/pnas.84.23.8306>
- Lohoff, T., Ghazanfar, S., Missarova, A., Kouloua, N., Pierson, N., Griffiths, J. A., Bardot, E. S., Eng, C.-H. L., Tyser, R. C. V., Argelaguet, R., Guibentif, C., Srinivas, S., Briscoe, J., Simons, B. D., Hadjantonakis, A.-K., Göttgens, B., Reik, W., Nichols, J., Cai, L., & Marioni, J. C. (2022). Integration of spatial and single-cell transcriptomic data elucidates mouse organogenesis [Number: 1 Publisher: Nature Publishing Group]. *Nature Biotechnology*, *40*(1), 74–85. <https://doi.org/10.1038/s41587-021-01006-2>
- Loman, N. J., Misra, R. V., Dallman, T. J., Constantinidou, C., Gharbia, S. E., Wain, J., & Pallen, M. J. (2012). Performance comparison of benchtop high-throughput sequencing platforms [Number: 5 Publisher: Nature Publishing Group]. *Nature Biotechnology*, *30*(5), 434–439. <https://doi.org/10.1038/nbt.2198>
- Lopez, R., Li, B., Keren-Shaul, H., Boyeau, P., Kedmi, M., Pilzer, D., Jelinski, A., Yofe, I., David, E., Wagner, A., Ergen, C., Addadi, Y., Golani, O., Ronchese, F., Jordan, M. I., Amit, I., & Yosef, N. (2022). DestVI identifies continuums of cell types in spatial transcriptomics

- data [Number: 9 Publisher: Nature Publishing Group]. *Nature Biotechnology*, 40(9), 1360–1369. <https://doi.org/10.1038/s41587-022-01272-8>
- Lu, H., Giordano, F., & Ning, Z. (2016). Oxford Nanopore MinION Sequencing and Genome Assembly. *Genomics, Proteomics & Bioinformatics*, 14(5), 265–279. <https://doi.org/10.1016/j.gpb.2016.05.004>
- Lubeck, E., Coskun, A. F., Zhiyentayev, T., Ahmad, M., & Cai, L. (2014). Single-cell in situ RNA profiling by sequential hybridization. *Nature Methods*, 11(4), 360–361. <https://doi.org/10.1038/nmeth.2892>
- Luecken, M. D., & Theis, F. J. (2019). Current best practices in single-cell RNA-seq analysis: A tutorial. *Molecular Systems Biology*, 15(6), e8746. <https://doi.org/10.15252/msb.20188746>
- Luk, K. C., Kehm, V., Carroll, J., Zhang, B., O'Brien, P., Trojanowski, J. Q., & Lee, V. M.-Y. (2012). Pathological alpha-Synuclein Transmission Initiates Parkinson-like Neurodegeneration in Nontransgenic Mice [Publisher: American Association for the Advancement of Science]. *Science*, 338(6109), 949–953. <https://doi.org/10.1126/science.1227157>
- Lun, A. T. L., Riesenfeld, S., Andrews, T., Dao, T. P., Gomes, T., Marioni, J. C., & participants in the 1st Human Cell Atlas Jamboree. (2019). EmptyDrops: Distinguishing cells from empty droplets in droplet-based single-cell RNA sequencing data. *Genome Biology*, 20(1), 63. <https://doi.org/10.1186/s13059-019-1662-y>
- Ma, S.-X., Seo, B. A., Kim, D., Xiong, Y., Kwon, S.-H., Brahmachari, S., Kim, S., Kam, T.-I., Nirujogi, R. S., Kwon, S. H., Dawson, V. L., Dawson, T. M., Pandey, A., Na, C. H., & Ko, H. S. (2021). Complement and Coagulation Cascades are Potentially Involved in Dopaminergic Neurodegeneration in alpha-Synuclein-Based Mouse Models of Parkinson's Disease. *Journal of Proteome Research*, 20(7), 3428–3443. <https://doi.org/10.1021/acs.jproteome.0c01002>
- Ma, Y., Feigin, A., Dhawan, V., Fukuda, M., Shi, Q., Greene, P., Breeze, R., Fahn, S., Freed, C., & Eidelberg, D. (2002). Dyskinesia after fetal cell transplantation for parkinsonism: A PET study. *Annals of Neurology*, 52(5), 628–634. <https://doi.org/10.1002/ana.10359>
- Ma, Y., & Zhou, X. (2022). Spatially informed cell-type deconvolution for spatial transcriptomics. *Nature Biotechnology*, 40(9), 1349–1359. <https://doi.org/10.1038/s41587-022-01273-7>
- Macosko, E. Z., Basu, A., Satija, R., Nemeshe, J., Shekhar, K., Goldman, M., Tirosh, I., Bialas, A. R., Kamitaki, N., Martersteck, E. M., Trombetta, J. J., Weitz, D. A., Sanes, J. R., Shalek, A. K., Regev, A., & McCarroll, S. A. (2015). Highly Parallel Genome-wide Expression Profiling of Individual Cells Using Nanoliter Droplets. *Cell*, 161(5), 1202–1214. <https://doi.org/10.1016/j.cell.2015.05.002>
- Madrazo, I., Drucker-Colín, R., Díaz, V., Martínez-Mata, J., Torres, C., & Becerril, J. J. (1987). Open Microsurgical Autograft of Adrenal Medulla to the Right Caudate Nucleus in Two Patients with Intractable Parkinson's Disease [Publisher: Massachusetts Medical Society _eprint: <https://doi.org/10.1056/NEJM198704023161402>]. *New England Journal of Medicine*, 316(14), 831–834. <https://doi.org/10.1056/NEJM198704023161402>
- Marks, W. J., Bartus, R. T., Siffert, J., Davis, C. S., Lozano, A., Boulis, N., Vitek, J., Stacy, M., Turner, D., Verhagen, L., Bakay, R., Watts, R., Guthrie, B., Jankovic, J., Simpson, R., Tagliati, M., Alterman, R., Stern, M., Baltuch, G., ... Olanow, C. W. (2010). Gene

- delivery of AAV2-neurturin for Parkinson's disease: A double-blind, randomised, controlled trial. *The Lancet. Neurology*, 9(12), 1164–1172. [https://doi.org/10.1016/S1474-4422\(10\)70254-4](https://doi.org/10.1016/S1474-4422(10)70254-4)
- Marks, W. J., Ostrem, J. L., Verhagen, L., Starr, P. A., Larson, P. S., Bakay, R. A., Taylor, R., Cahn-Weiner, D. A., Stoessl, A. J., Olanow, C. W., & Bartus, R. T. (2008). Safety and tolerability of intraputaminally delivered CERERE-120 (adeno-associated virus serotype 2-neurturin) to patients with idiopathic Parkinson's disease: An open-label, phase I trial. *The Lancet. Neurology*, 7(5), 400–408. [https://doi.org/10.1016/S1474-4422\(08\)70065-6](https://doi.org/10.1016/S1474-4422(08)70065-6)
- Martelotto, L. G., Baslan, T., Kendall, J., Geyer, F. C., Burke, K. A., Spraggon, L., Piscuoglio, S., Chadalavada, K., Nanjangud, G., Ng, C. K. Y., Moody, P., D'Italia, S., Rodgers, L., Cox, H., da Cruz Paula, A., Stepansky, A., Schizas, M., Wen, H. Y., King, T. A., ... Reis-Filho, J. S. (2017). Whole-genome single-cell copy number profiling from formalin-fixed paraffin-embedded samples [Number: 3 Publisher: Nature Publishing Group]. *Nature Medicine*, 23(3), 376–385. <https://doi.org/10.1038/nm.4279>
- Maxam, A. M., & Gilbert, W. (1977). A new method for sequencing DNA. *Proceedings of the National Academy of Sciences of the United States of America*, 74(2), 560–564.
- McCarty, D., Fu, H., Monahan, P., Toulson, C., Naik, P., & Samulski, R. (2003). Adeno-associated virus terminal repeat (TR) mutant generates self-complementary vectors to overcome the rate-limiting step to transduction in vivo. *Gene Therapy*, 10(26), 2112–2118. <https://doi.org/10.1038/sj.gt.3302134>
- McGinnis, C. S., Murrow, L. M., & Gartner, Z. J. (2019). DoubletFinder: Doublet Detection in Single-Cell RNA Sequencing Data Using Artificial Nearest Neighbors [Publisher: Elsevier]. *Cell Systems*, 8(4), 329–337.e4. <https://doi.org/10.1016/j.cels.2019.03.003>
- McGregor, M. M., & Nelson, A. B. (2019). Circuit Mechanisms of Parkinson's Disease. *Neuron*, 101(6), 1042–1056. <https://doi.org/10.1016/j.neuron.2019.03.004>
- McInnes, L., Healy, J., & Melville, J. (2020). UMAP: Uniform Manifold Approximation and Projection for Dimension Reduction [arXiv:1802.03426 [cs, stat]]. <https://doi.org/10.48550/arXiv.1802.03426>
- Mendell, J., Al-Zaidy, S., Shell, R., Arnold, W., Rodino-Klapac, L., Prior, T., Lowes, L., Alfano, L., Berry, K., Church, K., Kissel, J., Nagendran, S., L'Italien, J., Sproule, D., Wells, C., Cardenas, J., Heitzer, M., Kaspar, A., Corcoran, S., ... Kaspar, B. (2017). Single-dose gene-replacement therapy for spinal muscular atrophy. *New England Journal of Medicine*, 377(18), 1713–1722. <https://doi.org/10.1056/NEJMoa1706198>
- Mendez, I., Sanchez-Pernaute, R., Cooper, O., Viñuela, A., Ferrari, D., Björklund, L., Dagher, A., & Isacson, O. (2005). Cell type analysis of functional fetal dopamine cell suspension transplants in the striatum and substantia nigra of patients with Parkinson's disease. *Brain: A Journal of Neurology*, 128(Pt 7), 1498–1510. <https://doi.org/10.1093/brain/awh510>
- Miao, Z., Moreno, P., Huang, N., Papatheodorou, I., Brazma, A., & Teichmann, S. A. (2020). Putative cell type discovery from single-cell gene expression data. *Nature Methods*, 17(6), 621–628. <https://doi.org/10.1038/s41592-020-0825-9>
- Miller, B. F., Huang, F., Atta, L., Sahoo, A., & Fan, J. (2022). Reference-free cell type deconvolution of multi-cellular pixel-resolution spatially resolved transcriptomics data [Number:

- 1 Publisher: Nature Publishing Group]. *Nature Communications*, 13(1), 2339. <https://doi.org/10.1038/s41467-022-30033-z>
- Min, Y.-L., Li, H., Rodriguez-Caycedo, C., Mireault, A. A., Huang, J., Shelton, J. M., McAnally, J. R., Amoasii, L., Mammen, P. P. A., Bassel-Duby, R., & Olson, E. N. (2019). CRISPR-Cas9 corrects Duchenne muscular dystrophy exon 44 deletion mutations in mice and human cells. *Science Advances*, 5(3), eaav4324. <https://doi.org/10.1126/sciadv.aav4324>
- Mínguez-Castellanos, A., Escamilla-Sevilla, F., Hotton, G. R., Toledo-Aral, J. J., Ortega-Moreno, A., Méndez-Ferrer, S., Martín-Linares, J. M., Katati, M. J., Mir, P., Villadiego, J., Meersmans, M., Pérez-García, M., Brooks, D. J., Arjona, V., & López-Barneo, J. (2007). Carotid body autotransplantation in Parkinson disease: A clinical and positron emission tomography study. *Journal of Neurology, Neurosurgery, and Psychiatry*, 78(8), 825–831. <https://doi.org/10.1136/jnnp.2006.106021>
- Mitra, R. D., Shendure, J., Olejnik, J., Edyta-Krzymanska-Olejnik, n., & Church, G. M. (2003). Fluorescent in situ sequencing on polymerase colonies. *Analytical Biochemistry*, 320(1), 55–65. [https://doi.org/10.1016/s0003-2697\(03\)00291-4](https://doi.org/10.1016/s0003-2697(03)00291-4)
- Mittermeyer, G., Christine, C. W., Rosenbluth, K. H., Baker, S. L., Starr, P., Larson, P., Kaplan, P. L., Forsayeth, J., Aminoff, M. J., & Bankiewicz, K. S. (2012). Long-Term Evaluation of a Phase 1 Study of AADC Gene Therapy for Parkinson's Disease. *Human Gene Therapy*, 23(4), 377–381. <https://doi.org/10.1089/hum.2011.220>
- Miyamoto, Y., Torii, T., Yamamori, N., Ogata, T., Tanoue, A., & Yamauchi, J. (2013). Akt and PP2A reciprocally regulate the guanine nucleotide exchange factor Dock6 to control axon growth of sensory neurons. *Science Signaling*, 6(265), ra15. <https://doi.org/10.1126/scisignal.2003661>
- Miyamoto, Y., Yamauchi, J., Sanbe, A., & Tanoue, A. (2007). Dock6, a Dock-C subfamily guanine nucleotide exchanger, has the dual specificity for Rac1 and Cdc42 and regulates neurite outgrowth. *Experimental Cell Research*, 313(4), 791–804. <https://doi.org/10.1016/j.yexcr.2006.11.017>
- Moffitt, J. R., Bambah-Mukku, D., Eichhorn, S. W., Vaughn, E., Shekhar, K., Perez, J. D., Rubinstein, N. D., Hao, J., Regev, A., Dulac, C., & Zhuang, X. (2018). Molecular, Spatial and Functional Single-Cell Profiling of the Hypothalamic Preoptic Region. *Science (New York, N.Y.)*, 362(6416), eaau5324. <https://doi.org/10.1126/science.aau5324>
- Monaco, G., Lee, B., Xu, W., Mustafah, S., Hwang, Y. Y., Carré, C., Burdin, N., Visan, L., Ceccarelli, M., Poidinger, M., Zippelius, A., Magalhães, J. P. d., & Larbi, A. (2019). RNA-Seq Signatures Normalized by mRNA Abundance Allow Absolute Deconvolution of Human Immune Cell Types [Publisher: Elsevier]. *Cell Reports*, 26(6), 1627–1640.e7. <https://doi.org/10.1016/j.celrep.2019.01.041>
- Moore, R., & Bloom, F. (1978). Central catecholamine neuron systems: Anatomy and physiology of the dopamine systems. *Annual review of neuroscience*, 1, 129–169. <https://doi.org/10.1146/annurev.ne.01.030178.001021>
- Morens, D. M., Davis, J. W., Grandinetti, A., Ross, G. W., Popper, J. S., & White, L. R. (1996). Epidemiologic observations on Parkinson's disease: Incidence and mortality in a prospective study of middle-aged men [Publisher: Wolters Kluwer Health, Inc. on behalf of the American Academy of Neurology Section: ARTICLES]. *Neurology*, 46(4), 1044–1050. <https://doi.org/10.1212/WNL.46.4.1044>

- Muñoz-Castañeda, R., Zingg, B., Matho, K. S., Chen, X., Wang, Q., Foster, N. N., Li, A., Narasimhan, A., Hirokawa, K. E., Huo, B., Bannerjee, S., Korobkova, L., Park, C. S., Park, Y.-G., Bienkowski, M. S., Chon, U., Wheeler, D. W., Li, X., Wang, Y., ... Dong, H.-W. (2021). Cellular anatomy of the mouse primary motor cortex [Number: 7879 Publisher: Nature Publishing Group]. *Nature*, 598(7879), 159–166. <https://doi.org/10.1038/s41586-021-03970-w>
- Muskovic, W., & Powell, J. E. (2021). DropletQC: Improved identification of empty droplets and damaged cells in single-cell RNA-seq data. *Genome Biology*, 22(1), 329. <https://doi.org/10.1186/s13059-021-02547-0>
- Nagalakshmi, U., Wang, Z., Waern, K., Shou, C., Raha, D., Gerstein, M., & Snyder, M. (2008). The Transcriptional Landscape of the Yeast Genome Defined by RNA Sequencing. *Science (New York, N.Y.)*, 320(5881), 1344–1349. <https://doi.org/10.1126/science.1158441>
- Nakano, S., Nishikawa, M., Kobayashi, T., Harlin, E. W., Ito, T., Sato, K., Sugiyama, T., Yamakawa, H., Nagase, T., & Ueda, H. (2022). The Rho guanine nucleotide exchange factor PLEKHG1 is activated by interaction with and phosphorylation by Src family kinase member FYN. *The Journal of Biological Chemistry*, 298(2), 101579. <https://doi.org/10.1016/j.jbc.2022.101579>
- Nalls, M. A., Pankratz, N., Lill, C. M., Do, C. B., Hernandez, D. G., Saad, M., DeStefano, A. L., Kara, E., Bras, J., Sharma, M., Schulte, C., Keller, M. F., Arepalli, S., Letson, C., Edsall, C., Stefansson, H., Liu, X., Pliner, H., Lee, J. H., ... Singleton, A. B. (2014). Large-scale meta-analysis of genome-wide association data identifies six new risk loci for Parkinson's disease [Number: 9 Publisher: Nature Publishing Group]. *Nature Genetics*, 46(9), 989–993. <https://doi.org/10.1038/ng.3043>
- Nambu, A., Tokuno, H., Hamada, I., Kita, H., Imanishi, M., Akazawa, T., Ikeuchi, Y., & Hasegawa, N. (2000). Excitatory Cortical Inputs to Pallidal Neurons Via the Subthalamic Nucleus in the Monkey [Publisher: American Physiological Society]. *Journal of Neurophysiology*, 84(1), 289–300. <https://doi.org/10.1152/jn.2000.84.1.289>
- Naso, M. F., Tomkowicz, B., Perry, W. L., & Strohl, W. R. (2017). Adeno-Associated Virus (AAV) as a Vector for Gene Therapy. *BioDrugs: Clinical Immunotherapeutics, Biopharmaceuticals and Gene Therapy*, 31(4), 317–334. <https://doi.org/10.1007/s40259-017-0234-5>
- Negrini, M., Tomasello, G., Davidsson, M., Fenyi, A., Adant, C., Hauser, S., Espa, E., Gubinelli, F., Manfredsson, F. P., Melki, R., & Heuer, A. (2022). Sequential or Simultaneous Injection of Preformed Fibrils and AAV Overexpression of Alpha-Synuclein Are Equipotent in Producing Relevant Pathology and Behavioral Deficits. *Journal of Parkinson's Disease*, 12(4), 1133–1153. <https://doi.org/10.3233/JPD-212555>
- Nielsen, M. S., Vorum, H., Lindersson, E., & Jensen, P. H. (2001). Ca²⁺ binding to alpha-synuclein regulates ligand binding and oligomerization. *The Journal of Biological Chemistry*, 276(25), 22680–22684. <https://doi.org/10.1074/jbc.M101181200>
- Niethammer, M., Tang, C. C., LeWitt, P. A., Rezai, A. R., Leehey, M. A., Ojemann, S. G., Flaherty, A. W., Eskandar, E. N., Kostyk, S. K., Sarkar, A., Siddiqui, M. S., Tatter, S. B., Schwalb, J. M., Poston, K. L., Henderson, J. M., Kurlan, R. M., Richard, I. H., Sapan, C. V., Eidelberg, D., ... Feigin, A. (2017). Long-term follow-up of a randomized AAV2-GAD gene therapy trial for Parkinson's disease. *JCI insight*, 2(7), e90133. <https://doi.org/10.1172/jci.insight.90133>

- Nikolov, D. B., & Burley, S. K. (1997). RNA polymerase II transcription initiation: A structural view [Publisher: Proceedings of the National Academy of Sciences]. *Proceedings of the National Academy of Sciences*, 94(1), 15–22. <https://doi.org/10.1073/pnas.94.1.15>
- Nolbrant, S., Heuer, A., Parmar, M., & Kirkeby, A. (2017). Generation of high-purity human ventral midbrain dopaminergic progenitors for in vitro maturation and intracerebral transplantation [Number: 9 Publisher: Nature Publishing Group]. *Nature Protocols*, 12(9), 1962–1979. <https://doi.org/10.1038/nprot.2017.078>
- Nyren, P., Pettersson, B., & Uhlen, M. (1993). Solid Phase DNA Minisequencing by an Enzymatic Luminometric Inorganic Pyrophosphate Detection Assay. *Analytical Biochemistry*, 208(1), 171–175. <https://doi.org/10.1006/abio.1993.1024>
- O’Carroll, S. J., Cook, W. H., & Young, D. (2021). AAV Targeting of Glial Cell Types in the Central and Peripheral Nervous System and Relevance to Human Gene Therapy. *Frontiers in Molecular Neuroscience*, 13.
- Odekerken, V. J., Boel, J. A., Schmand, B. A., de Haan, R. J., Figees, M., van den Munckhof, P., Schuurman, P. R., de Bie, R. M., & Group, N. S. (2016). GPi vs STN deep brain stimulation for Parkinson disease: Three-year follow-up [ISBN: 0028-3878 Publisher: AAN Enterprises]. *Neurology*, 86(8), 755–761.
- Olanow, C. W., Goetz, C. G., Kordower, J. H., Stoessl, A. J., Sossi, V., Brin, M. F., Shannon, K. M., Nauert, G. M., Perl, D. P., Godbold, J., & Freeman, T. B. (2003). A double-blind controlled trial of bilateral fetal nigral transplantation in Parkinson’s disease. *Annals of Neurology*, 54(3), 403–414. <https://doi.org/10.1002/ana.10720>
- Olanow, C. W., Kieburtz, K., Odin, P., Espay, A. J., Standaert, D. G., Fernandez, H. H., Vanaganas, A., Othman, A. A., Widnell, K. L., Robieson, W. Z., Pritchett, Y., Chatamra, K., Benesh, J., Lenz, R. A., & Antonini, A. (2014). Double-Blind, Double-Dummy, Randomized Study of Continuous Intrajejunal Infusion of Levodopa-Carbidopa Intestinal Gel in Advanced Parkinson’s Disease. *The Lancet. Neurology*, 13(2), 141–149. [https://doi.org/10.1016/S1474-4422\(13\)70293-X](https://doi.org/10.1016/S1474-4422(13)70293-X)
- Orphanides, G., & Reinberg, D. (2002). A Unified Theory of Gene Expression [Publisher: Elsevier]. *Cell*, 108(4), 439–451. [https://doi.org/10.1016/S0092-8674\(02\)00655-4](https://doi.org/10.1016/S0092-8674(02)00655-4)
- Ortega-Ramírez, A., Vega, R., & Soto, E. (2017). Acid-Sensing Ion Channels as Potential Therapeutic Targets in Neurodegeneration and Neuroinflammation. *Mediators of Inflammation*, 2017, 3728096. <https://doi.org/10.1155/2017/3728096>
- Orthwein, A., Noordermeer, S. M., Wilson, M. D., Landry, S., Enchev, R. I., Sherker, A., Munro, M., Pinder, J., Salsman, J., Dellaire, G., Xia, B., Peter, M., & Durocher, D. (2015). A mechanism for the suppression of homologous recombination in G1 cells [Number: 7582 Publisher: Nature Publishing Group]. *Nature*, 528(7582), 422–426. <https://doi.org/10.1038/nature16142>
- Ortiz, C., Navarro, J. F., Jurek, A., Märtin, A., Lundeberg, J., & Meletis, K. (2020). Molecular atlas of the adult mouse brain [Publisher: American Association for the Advancement of Science]. *Science Advances*, 6(26), eabb3446. <https://doi.org/10.1126/sciadv.abb3446>
- Osterberg, V. R., Spinelli, K. J., Weston, L. J., Luk, K. C., Woltjer, R. L., & Unni, V. K. (2015). Progressive Aggregation of Alpha-Synuclein and Selective Degeneration of Lewy Inclusion-Bearing Neurons in a Mouse Model of Parkinsonism. *Cell Reports*, 10(8), 1252–1260. <https://doi.org/10.1016/j.celrep.2015.01.060>

- Palfi, S., Gurruchaga, J. M., Ralph, G. S., Lepletit, H., Lavisse, S., Buttery, P. C., Watts, C., Miskin, J., Kelleher, M., Deeley, S., Iwamuro, H., Lefaucheur, J. P., Thiriez, C., Fenelon, G., Lucas, C., Brugières, P., Gabriel, I., Abhay, K., Drouot, X., ... Mitrophanous, K. A. (2014). Long-term safety and tolerability of ProSavin, a lentiviral vector-based gene therapy for Parkinson's disease: A dose escalation, open-label, phase 1/2 trial [Publisher: Elsevier]. *The Lancet*, *383*(9923), 1138–1146. [https://doi.org/10.1016/S0140-6736\(13\)61939-X](https://doi.org/10.1016/S0140-6736(13)61939-X)
- Park, C.-H., Minn, Y.-K., Lee, J.-Y., Choi, D. H., Chang, M.-Y., Shim, J.-W., Ko, J.-Y., Koh, H.-C., Kang, M. J., Kang, J. S., Rhie, D.-J., Lee, Y.-S., Son, H., Moon, S. Y., Kim, K.-S., & Lee, S.-H. (2005). In vitro and in vivo analyses of human embryonic stem cell-derived dopamine neurons. *Journal of Neurochemistry*, *92*(5), 1265–1276. <https://doi.org/10.1111/j.1471-4159.2004.03006.x>
- Parkinson, J. (2002). An essay on the shaking palsy. 1817. *The Journal of Neuropsychiatry and Clinical Neurosciences*, *14*(2), 223–236, discussion 222. <https://doi.org/10.1176/jnp.14.2.223>
- Pastuzyn, E. D., Day, C. E., Kearns, R. B., Kyrke-Smith, M., Taibi, A. V., McCormick, J., Yoder, N., Belnap, D. M., Erlendsson, S., Morado, D. R., Briggs, J. A. G., Feschotte, C., & Shepherd, J. D. (2018). The Neuronal Gene Arc Encodes a Repurposed Retrotransposon Gag Protein that Mediates Intercellular RNA Transfer [Publisher: Elsevier]. *Cell*, *172*(1), 275–288.e18. <https://doi.org/10.1016/j.cell.2017.12.024>
- Patil, S., Chalkiadaki, K., Mergiya, T. F., Krimbacher, K., Amorim, I. S., Akerkar, S., Gkogkas, C. G., & Bramham, C. R. (2023). eIF4E phosphorylation recruits beta-catenin to mRNA cap and promotes Wnt pathway translation in dentate gyrus LTP maintenance. *iScience*, *26*(5), 106649. <https://doi.org/10.1016/j.isci.2023.106649>
- Patro, R., Duggal, G., Love, M. I., Irizarry, R. A., & Kingsford, C. (2017). Salmon provides fast and bias-aware quantification of transcript expression. *Nature Methods*, *14*(4), 417–419. <https://doi.org/10.1038/nmeth.4197>
- Paul, K. C., Krolewski, R. C., Lucumi Moreno, E., Blank, J., Holton, K. M., Ahfeldt, T., Furlong, M., Yu, Y., Cockburn, M., Thompson, L. K., Kreymerman, A., Ricci-Blair, E. M., Li, Y. J., Patel, H. B., Lee, R. T., Bronstein, J., Rubin, L. L., Khurana, V., & Ritz, B. (2023). A pesticide and iPSC dopaminergic neuron screen identifies and classifies Parkinson-relevant pesticides [Number: 1 Publisher: Nature Publishing Group]. *Nature Communications*, *14*(1), 2803. <https://doi.org/10.1038/s41467-023-38215-z>
- Paumier, K. L., Luk, K. C., Manfredsson, F. P., Kanaan, N. M., Lipton, J. W., Collier, T. J., Steece-Collier, K., Kemp, C. J., Celano, S., Schulz, E., Sandoval, I. M., Fleming, S., Dirr, E., Polinski, N. K., Trojanowski, J. Q., Lee, V. M., & Sortwell, C. E. (2015). Intrastriatal injection of pre-formed mouse alpha-synuclein fibrils into rats triggers alpha-synuclein pathology and bilateral nigrostriatal degeneration. *Neurobiology of Disease*, *82*, 185–199. <https://doi.org/10.1016/j.nbd.2015.06.003>
- Pearson, K. (1901). LIII. On lines and planes of closest fit to systems of points in space [Publisher: Taylor & Francis _eprint: <https://doi.org/10.1080/14786440109462720>]. *The London, Edinburgh, and Dublin Philosophical Magazine and Journal of Science*, *2*(11), 559–572. <https://doi.org/10.1080/14786440109462720>
- Peelaerts, W., Bousset, L., Van der Perren, A., Moskalyuk, A., Pulizzi, R., Giugliano, M., Van den Haute, C., Melki, R., & Baekelandt, V. (2015). Alpha-Synuclein strains cause distinct

synucleinopathies after local and systemic administration [Number: 7556 Publisher: Nature Publishing Group]. *Nature*, 522(7556), 340–344. <https://doi.org/10.1038/nature14547>

- Peikon, I. D., Kebschull, J. M., Vagin, V. V., Ravens, D. I., Sun, Y.-C., Brouzes, E., Corrêa, I. R., Bressan, D., & Zador, A. M. (2017). Using high-throughput barcode sequencing to efficiently map connectomes. *Nucleic Acids Research*, 45(12), e115. <https://doi.org/10.1093/nar/gkx292>
- Peng, H., Xie, P., Liu, L., Kuang, X., Wang, Y., Qu, L., Gong, H., Jiang, S., Li, A., Ruan, Z., Ding, L., Yao, Z., Chen, C., Chen, M., Daigle, T. L., Dalley, R., Ding, Z., Duan, Y., Feiner, A., ... Zeng, H. (2021). Morphological diversity of single neurons in molecularly defined cell types. *Nature*, 598(7879), 174–181. <https://doi.org/10.1038/s41586-021-03941-1>
- Piccini, P., Lindvall, O., Björklund, A., Brundin, P., Hagell, P., Ceravolo, R., Oertel, W., Quinn, N., Samuel, M., Rehncrona, S., Widner, H., & Brooks, D. J. (2000). Delayed recovery of movement-related cortical function in Parkinson's disease after striatal dopaminergic grafts. *Annals of Neurology*, 48(5), 689–695.
- Picelli, S., Björklund, Å. K., Faridani, O. R., Sagasser, S., Winberg, G., & Sandberg, R. (2013). Smart-seq2 for sensitive full-length transcriptome profiling in single cells [Number: 11 Publisher: Nature Publishing Group]. *Nature Methods*, 10(11), 1096–1098. <https://doi.org/10.1038/nmeth.2639>
- Piovesan, A., Antonaros, F., Vitale, L., Strippoli, P., Pelleri, M. C., & Caracausi, M. (2019). Human protein-coding genes and gene feature statistics in 2019. *BMC Research Notes*, 12(1), 315. <https://doi.org/10.1186/s13104-019-4343-8>
- Poewe, W., & Antonini, A. (2015). Novel formulations and modes of delivery of levodopa [ISBN: 0885-3185 Publisher: Wiley Online Library]. *Movement Disorders*, 30(1), 114–120.
- Politis, M., Wu, K., Loane, C., Quinn, N. P., Brooks, D. J., Rehncrona, S., Björklund, A., Lindvall, O., & Piccini, P. (2010). Serotonergic neurons mediate dyskinesia side effects in Parkinson's patients with neural transplants. *Science Translational Medicine*, 2(38), 38ra46. <https://doi.org/10.1126/scitranslmed.3000976>
- Polymeropoulos, M., Lavedan, C., Leroy, E., Ide, S., Dehejia, A., Dutra, A., Pike, B., Root, H., Rubenstein, J., Boyer, R., Stenroos, E., Chandrasekharappa, S., Athanassiadou, A., Papapetropoulos, T., Johnson, W., Lazzarini, A., Duvoisin, R., Di Iorio, G., Golbe, L., & Nussbaum, R. (1997). Mutation in the alpha-synuclein gene identified in families with Parkinson's disease. *Science*, 276(5321), 2045–2047. <https://doi.org/10.1126/science.276.5321.2045>
- Pontén, F., Gry, M., Fagerberg, L., Lundberg, E., Asplund, A., Berglund, L., Oksvold, P., Björling, E., Hober, S., Kampf, C., Navani, S., Nilsson, P., Ottosson, J., Persson, A., Wernérus, H., Wester, K., & Uhlén, M. (2009). A global view of protein expression in human cells, tissues, and organs [Publisher: John Wiley & Sons, Ltd]. *Molecular Systems Biology*, 5(1), 337. <https://doi.org/10.1038/msb.2009.93>
- Powers, R., Lei, S., Anandhan, A., Marshall, D. D., Worley, B., Cerny, R. L., Dodds, E. D., Huang, Y., Panayiotidis, M. I., Pappa, A., & Franco, R. (2017). Metabolic Investigations of the Molecular Mechanisms Associated with Parkinson's Disease [Number: 2 Publisher: Multidisciplinary Digital Publishing Institute]. *Metabolites*, 7(2), 22. <https://doi.org/10.3390/metabo7020022>

- Pringsheim, T., Jette, N., Frolkis, A., & Steeves, T. D. (2014). The prevalence of Parkinson's disease: A systematic review and meta-analysis. *Movement Disorders*, 29(13), 1583–1590. <https://doi.org/10.1002/mds.25945>
- Publications. (n.d.).
- Qin, W., Liu, C., Sodhi, M., & Lu, H. (2016). Meta-analysis of sex differences in gene expression in schizophrenia. *BMC Systems Biology*, 10(Suppl 1), 9. <https://doi.org/10.1186/s12918-015-0250-3>
- Rahmani, E., Schweiger, R., Rhead, B., Criswell, L. A., Barcellos, L. F., Eskin, E., Rosset, S., Sankararaman, S., & Halperin, E. (2019). Cell-type-specific resolution epigenetics without the need for cell sorting or single-cell biology [Number: 1 Publisher: Nature Publishing Group]. *Nature Communications*, 10(1), 3417. <https://doi.org/10.1038/s41467-019-11052-9>
- Regev, A., Teichmann, S. A., Lander, E. S., Amit, I., Benoist, C., Birney, E., Bodenmiller, B., Campbell, P., Carninci, P., Clatworthy, M., Clevers, H., Deplancke, B., Dunham, I., Eberwine, J., Eils, R., Enard, W., Farmer, A., Fugger, L., Götting, B., ... Human Cell Atlas Meeting Participants. (2017). The Human Cell Atlas (T. R. Gingeras, Ed.) [Publisher: eLife Sciences Publications, Ltd]. *eLife*, 6, e27041. <https://doi.org/10.7554/eLife.27041>
- Reiner, A., Medina, L., & Veenman, C. L. (1998). Structural and functional evolution of the basal ganglia in vertebrates. *Brain Research Reviews*, 28(3), 235–285. [https://doi.org/10.1016/S0165-0173\(98\)00016-2](https://doi.org/10.1016/S0165-0173(98)00016-2)
- Rey, N. L., Steiner, J. A., Maroof, N., Luk, K. C., Madaj, Z., Trojanowski, J. Q., Lee, V. M.-Y., & Brundin, P. (2016). Widespread transneuronal propagation of alpha-synucleinopathy triggered in olfactory bulb mimics prodromal Parkinson's disease. *Journal of Experimental Medicine*, 213(9), 1759–1778. <https://doi.org/10.1084/jem.20160368>
- Rey, N. L., Wesson, D. W., & Brundin, P. (2018). The olfactory bulb as the entry site for prion-like propagation in neurodegenerative diseases. *Neurobiology of Disease*, 109, 226–248. <https://doi.org/10.1016/j.nbd.2016.12.013>
- Riggs, A. D., Bourgeois, S., & Cohn, M. (1970). The lac repressor-operator interaction: III. Kinetic studies. *Journal of Molecular Biology*, 53(3), 401–417. [https://doi.org/10.1016/0022-2836\(70\)90074-4](https://doi.org/10.1016/0022-2836(70)90074-4)
- Rodrigues, S. G., Stickels, R. R., Goeva, A., Martin, C. A., Murray, E., Vanderburg, C. R., Welch, J., Chen, L. M., Chen, F., & Macosko, E. Z. (2019). Slide-seq: A scalable technology for measuring genome-wide expression at high spatial resolution. *Science (New York, N.Y.)*, 363(6434), 1463–1467. <https://doi.org/10.1126/science.aaw1219>
- Ronaghi, M., Karamohamed, S., Pettersson, B., Uhlén, M., & Nyren, P. (1996). Real-Time DNA Sequencing Using Detection of Pyrophosphate Release. *Analytical Biochemistry*, 242(1), 84–89. <https://doi.org/10.1006/abio.1996.0432>
- Rotman, A., & Creveling, C. R. (1976). A rationale for the design of cell-specific toxic agents: The mechanism of action of 6-hydroxydopamine. *FEBS Letters*, 72(2), 227–230. [https://doi.org/10.1016/0014-5793\(76\)80974-X](https://doi.org/10.1016/0014-5793(76)80974-X)
- Roy, N. S., Cleren, C., Singh, S. K., Yang, L., Beal, M. F., & Goldman, S. A. (2006). Functional engraftment of human ES cell-derived dopaminergic neurons enriched by coculture with telomerase-immortalized midbrain astrocytes. *Nature Medicine*, 12(11), 1259–1268. <https://doi.org/10.1038/nm1495>

- Rusk, N. (2011). Torrents of sequence [Number: 1 Publisher: Nature Publishing Group]. *Nature Methods*, 8(1), 44–44. <https://doi.org/10.1038/nmeth.f.330>
- Sack, B., & Herzog, R. (2009). Evading the immune response upon in vivo gene therapy with viral vectors. *Current Opinion in Molecular Therapeutics*, 11(5), 493–503.
- Sahlin, K., & Medvedev, P. (2021). Error correction enables use of Oxford Nanopore technology for reference-free transcriptome analysis [Number: 1 Publisher: Nature Publishing Group]. *Nature Communications*, 12(1), 2. <https://doi.org/10.1038/s41467-020-20340-8>
- Salmén, F., Ståhl, P. L., Mollbrink, A., Navarro, J. F., Vickovic, S., Frisé, J., & Lundeberg, J. (2018). Barcoded solid-phase RNA capture for Spatial Transcriptomics profiling in mammalian tissue sections. *Nature Protocols*, 13(11), 2501–2534. <https://doi.org/10.1038/s41596-018-0045-2>
- Sánchez-Pernaute, R., Harvey-White, J., Cunningham, J., & Bankiewicz, K. S. (2001). Functional effect of adeno-associated virus mediated gene transfer of aromatic L-amino acid decarboxylase into the striatum of 6-OHDA-lesioned rats. *Molecular Therapy: The Journal of the American Society of Gene Therapy*, 4(4), 324–330. <https://doi.org/10.1006/mthe.2001.0466>
- Sanger, F., Nicklen, S., & Coulson, A. R. (1977). DNA sequencing with chain-terminating inhibitors. *Proceedings of the National Academy of Sciences of the United States of America*, 74(12), 5463–5467.
- Santiago, C. P., Gimmen, M. Y., Lu, Y., McNally, M. M., Duncan, L. H., Creamer, T. J., Orzolek, L. D., Blackshaw, S., & Singh, M. S. (2023). Comparative Analysis of Single-cell and Single-nucleus RNA-sequencing in a Rabbit Model of Retinal Detachment-related Proliferative Vitreoretinopathy. *Ophthalmology Science*, 3(4), 100335. <https://doi.org/10.1016/j.xops.2023.100335>
- Santiago-Ortiz, J., Ojala, D., Westesson, O., Weinstein, J., Wong, S., Steinsapir, A., Kumar, S., Holmes, I., & Schaffer, D. (2015). AAV ancestral reconstruction library enables selection of broadly infectious viral variants. *Gene Therapy*, 22(12), 934–946. <https://doi.org/10.1038/gt.2015.74>
- Savica, R., Grossardt, B. R., Bower, J. H., Ahlskog, J. E., & Rocca, W. A. (2013). Incidence and Pathology of Synucleinopathies and Tauopathies Related to Parkinsonism. *JAMA Neurology*, 70(7), 859–866. <https://doi.org/10.1001/jamaneurol.2013.114>
- Schapira, A. H. (2011). Monoamine oxidase B inhibitors for the treatment of Parkinson's disease: A review of symptomatic and potential disease-modifying effects [ISBN: 1172-7047 Publisher: Springer]. *CNS drugs*, 25, 1061–1071.
- Schumacher, J. M., Ellias, S. A., Palmer, E. P., Kott, H. S., Dinsmore, J., Dempsey, P. K., Fischman, A. J., Thomas, C., Feldman, R. G., Kassissieh, S., Raineri, R., Manhart, C., Penney, D., Fink, J. S., & Isacson, O. (2000). Transplantation of embryonic porcine mesencephalic tissue in patients with PD. *Neurology*, 54(5), 1042–1050. <https://doi.org/10.1212/wnl.54.5.1042>
- Shah, S., Lubeck, E., Zhou, W., & Cai, L. (2016). In Situ Transcription Profiling of Single Cells Reveals Spatial Organization of Cells in the Mouse Hippocampus. *Neuron*, 92(2), 342–357. <https://doi.org/10.1016/j.neuron.2016.10.001>
- Shen, H., Pirruccello, M., & De Camilli, P. (2012). SnapShot: Membrane Curvature Sensors and Generators. *Cell*, 150(6), 1300–1300.e2. <https://doi.org/10.1016/j.cell.2012.08.017>

- Shendure, J., Porreca, G. J., Reppas, N. B., Lin, X., McCutcheon, J. P., Rosenbaum, A. M., Wang, M. D., Zhang, K., Mitra, R. D., & Church, G. M. (2005). Accurate Multiplex Polony Sequencing of an Evolved Bacterial Genome [Publisher: American Association for the Advancement of Science]. *Science*, *309*(5741), 1728–1732. <https://doi.org/10.1126/science.1117389>
- Sherva, R., Tripodis, Y., Bennett, D. A., Chibnik, L. B., Crane, P. K., de Jager, P. L., Farrer, L. A., Saykin, A. J., Shulman, J. M., Naj, A., Green, R. C., & The GENAROAD Consortium, The Alzheimer's Disease Neuroimaging Initiative, and The Alzheimer's Disease Genetics Consortium. (2014). Genome-wide association study of the rate of cognitive decline in Alzheimer's disease. *Alzheimer's & Dementia*, *10*(1), 45–52. <https://doi.org/10.1016/j.jalz.2013.01.008>
- Shi, H., He, Y., Zhou, Y., Huang, J., Wang, B., Tang, Z., Tan, P., Wu, M., Lin, Z., Ren, J., Thapa, Y., Tang, X., Liu, A., Liu, J., & Wang, X. (2022). Spatial Atlas of the Mouse Central Nervous System at Molecular Resolution [Pages: 2022.06.20.496914 Section: New Results]. <https://doi.org/10.1101/2022.06.20.496914>
- Shi, L. (2013). Dock protein family in brain development and neurological disease. *Communicative & Integrative Biology*, *6*(6), e26839. <https://doi.org/10.4161/cib.26839>
- Shi, Z., Wang, F., Cui, Y., Liu, Z., Guo, X., Zhang, Y., Deng, Y., Zhao, H., & Chen, Y. (2015). Heritable CRISPR/Cas9-mediated targeted integration in *Xenopus tropicalis*. *FASEB journal: official publication of the Federation of American Societies for Experimental Biology*, *29*(12), 4914–4923. <https://doi.org/10.1096/fj.15-273425>
- Siletti, K., Hodge, R., Albiach, A. M., Hu, L., Lee, K. W., Lönnerberg, P., Bakken, T., Ding, S.-L., Clark, M., Casper, T., Dee, N., Gloe, J., Keene, C. D., Nyhus, J., Tung, H., Yanny, A. M., Arenas, E., Lein, E. S., & Linnarsson, S. (2022). Transcriptomic diversity of cell types across the adult human brain. *bioRxiv*. <https://doi.org/10.1101/2022.10.12.511898>
- Slyper, M., Porter, C. B. M., Ashenberg, O., Waldman, J., Drokhllyansky, E., Wakiro, I., Smillic, C., Smith-Rosario, G., Wu, J., Dionne, D., Vigneau, S., Jané-Valbuena, J., Tickle, T. L., Napolitano, S., Su, M.-J., Patel, A. G., Karlstrom, A., Gritsch, S., Nomura, M., ... Regev, A. (2020). A single-cell and single-nucleus RNA-Seq toolbox for fresh and frozen human tumors [Number: 5 Publisher: Nature Publishing Group]. *Nature Medicine*, *26*(5), 792–802. <https://doi.org/10.1038/s41591-020-0844-1>
- Soldner, F., Hockemeyer, D., Beard, C., Gao, Q., Bell, G. W., Cook, E. G., Hargus, G., Blak, A., Cooper, O., Mitalipova, M., Isacson, O., & Jaenisch, R. (2009). Parkinson's disease patient-derived induced pluripotent stem cells free of viral reprogramming factors. *Cell*, *136*(5), 964–977. <https://doi.org/10.1016/j.cell.2009.02.013>
- Somogyi, P., & Klausberger, T. (2005). Defined types of cortical interneurone structure space and spike timing in the hippocampus. *The Journal of Physiology*, *562*(Pt 1), 9–26. <https://doi.org/10.1113/jphysiol.2004.078915>
- Song, Q., & Su, J. (2021). DSTG: Deconvoluting spatial transcriptomics data through graph-based artificial intelligence. *Briefings in Bioinformatics*, *22*(5), bbaa414. <https://doi.org/10.1093/bib/bbaa414>
- Sountoulidis, A., Liontos, A., Nguyen, H. P., Firsova, A. B., Fysikopoulos, A., Qian, X., Seeger, W., Sundström, E., Nilsson, M., & Samakovlis, C. (2020). SCRINSHOT enables spatial mapping of cell states in tissue sections with single-cell resolution [Publisher: Public

Library of Science]. *PLOS Biology*, 18(11), e3000675. <https://doi.org/10.1371/journal.pbio.3000675>

- Squair, J. W., Gautier, M., Kathe, C., Anderson, M. A., James, N. D., Hutson, T. H., Hudelle, R., Qaiser, T., Matson, K. J. E., Barraud, Q., Levine, A. J., La Manno, G., Skinnider, M. A., & Courtine, G. (2021). Confronting false discoveries in single-cell differential expression [Number: 1 Publisher: Nature Publishing Group]. *Nature Communications*, 12(1), 5692. <https://doi.org/10.1038/s41467-021-25960-2>
- Stahl, P. L., Salmén, F., Vickovic, S., Lundmark, A., Navarro, J. F., Magnusson, J., Giacomello, S., Asp, M., Westholm, J. O., Huss, M., Mollbrink, A., Linnarsson, S., Codeluppi, S., Borg, Å., Pontén, F., Costea, P. I., Sahlén, P., Mulder, J., Bergmann, O., ... Frisén, J. (2016). Visualization and analysis of gene expression in tissue sections by spatial transcriptomics. *Science (New York, N.Y.)*, 353(6294), 78–82. <https://doi.org/10.1126/science.aaf2403>
- Steen, C. B., Liu, C. L., Alizadeh, A. A., & Newman, A. M. (2020). Profiling Cell Type Abundance and Expression in Bulk Tissues with CIBERSORTx. *Methods in molecular biology (Clifton, N.J.)*, 2117, 135–157. https://doi.org/10.1007/978-1-0716-0301-7_7
- Steward, O., Farris, S., Pirbhoy, P. S., Darnell, J., & Driesche, S. J. V. (2014). Localization and local translation of Arc/Arg3.1 mRNA at synapses: Some observations and paradoxes. *Frontiers in Molecular Neuroscience*, 7, 101. <https://doi.org/10.3389/fnmol.2014.00101>
- Stickels, R. R., Murray, E., Kumar, P., Li, J., Marshall, J. L., Di Bella, D. J., Arlotta, P., Macosko, E. Z., & Chen, F. (2021). Highly sensitive spatial transcriptomics at near-cellular resolution with Slide-seqV2 [Number: 3 Publisher: Nature Publishing Group]. *Nature Biotechnology*, 39(3), 313–319. <https://doi.org/10.1038/s41587-020-0739-1>
- Stoeckius, M., Hafemeister, C., Stephenson, W., Houck-Loomis, B., Chattopadhyay, P. K., Swerdlow, H., Satija, R., & Smibert, P. (2017). Large-scale simultaneous measurement of epitopes and transcriptomes in single cells. *Nature methods*, 14(9), 865–868. <https://doi.org/10.1038/nmeth.4380>
- Stokholm, M. G., Iranzo, A., Østergaard, K., Serradell, M., Otto, M., Svendsen, K. B., Garrido, A., Vilas, D., Borghammer, P., Santamaria, J., Møller, A., Gaig, C., Brooks, D. J., Tolosa, E., & Pavese, N. (2017). Assessment of neuroinflammation in patients with idiopathic rapid-eye-movement sleep behaviour disorder: A case-control study. *The Lancet Neurology*, 16(10), 789–796. [https://doi.org/10.1016/S1474-4422\(17\)30173-4](https://doi.org/10.1016/S1474-4422(17)30173-4)
- Sun, D., Liu, Z., Li, T., Wu, Q., & Wang, C. (2022). STRIDE: Accurately decomposing and integrating spatial transcriptomics using single-cell RNA sequencing. *Nucleic Acids Research*, 50(7), e42. <https://doi.org/10.1093/nar/gkac150>
- Sun, Y.-C., Chen, X., Fischer, S., Lu, S., Zhan, H., Gillis, J., & Zador, A. M. (2021). Integrating barcoded neuroanatomy with spatial transcriptional profiling enables identification of gene correlates of projections [Number: 6 Publisher: Nature Publishing Group]. *Nature Neuroscience*, 24(6), 873–885. <https://doi.org/10.1038/s41593-021-00842-4>
- Suzuki, K., Tsunekawa, Y., Hernandez-Benitez, R., Wu, J., Zhu, J., Kim, E. J., Hatanaka, F., Yamamoto, M., Araoka, T., Li, Z., Kurita, M., Hishida, T., Li, M., Aizawa, E., Guo, S., Chen, S., Goebel, A., Soligalla, R. D., Qu, J., ... Belmonte, J. C. I. (2016). In vivo genome editing via CRISPR/Cas9 mediated homology-independent targeted integration [Number: 7631 Publisher: Nature Publishing Group]. *Nature*, 540(7631), 144–149. <https://doi.org/10.1038/nature20565>

- Svedlund, J., Strell, C., Qian, X., Zilkens, K. J. C., Tobin, N. P., Bergh, J., Siewerts, A. M., & Nilsson, M. (2019). Generation of in situ sequencing based OncoMaps to spatially resolve gene expression profiles of diagnostic and prognostic markers in breast cancer. *EBioMedicine*, *48*, 212–223. <https://doi.org/10.1016/j.ebiom.2019.09.009>
- Svensson, V., da Veiga Beltrame, E., & Pachter, L. (2020). A curated database reveals trends in single-cell transcriptomics. *Database*, *2020*, baaa073. <https://doi.org/10.1093/database/baaa073>
- Tabar, V., & Studer, L. (2014). Pluripotent stem cells in regenerative medicine: Challenges and recent progress. *Nature Reviews. Genetics*, *15*(2), 82–92. <https://doi.org/10.1038/nrg3563>
- Tafvizi, A., Mirny, L. A., & van Oijen, A. M. (2011). Dancing on DNA: Kinetic Aspects of Search Processes on DNA [Publisher: John Wiley & Sons, Ltd]. *ChemPhysChem*, *12*(8), 1481–1489. <https://doi.org/10.1002/cphc.201100112>
- Takahashi, K., Okita, K., Nakagawa, M., & Yamanaka, S. (2007). Induction of pluripotent stem cells from fibroblast cultures. *Nature Protocols*, *2*(12), 3081–3089. <https://doi.org/10.1038/nprot.2007.418>
- Tang, F., Barbacioru, C., Wang, Y., Nordman, E., Lee, C., Xu, N., Wang, X., Bodeau, J., Tuch, B. B., Siddiqui, A., Lao, K., & Surani, M. A. (2009). mRNA-Seq whole-transcriptome analysis of a single cell [Number: 5 Publisher: Nature Publishing Group]. *Nature Methods*, *6*(5), 377–382. <https://doi.org/10.1038/nmeth.1315>
- Tasic, B., Yao, Z., Graybuck, L. T., Smith, K. A., Nguyen, T. N., Bertagnolli, D., Goldy, J., Garren, E., Economo, M. N., Viswanathan, S., Penn, O., Bakken, T., Menon, V., Miller, J., Fong, O., Hirokawa, K. E., Lathia, K., Rimorin, C., Tieu, M., ... Zeng, H. (2018). Shared and distinct transcriptomic cell types across neocortical areas [Number: 7729 Publisher: Nature Publishing Group]. *Nature*, *563*(7729), 72–78. <https://doi.org/10.1038/s41586-018-0654-5>
- Temin, H. M., & Mizutani, S. (1970). Viral RNA-dependent DNA Polymerase: RNA-dependent DNA Polymerase in Virions of Rous Sarcoma Virus [Number: 5252 Publisher: Nature Publishing Group]. *Nature*, *226*(5252), 1211–1213. <https://doi.org/10.1038/2261211a0>
- Thakur, P., Breger, L., Lundblad, M., Wan, O., Mattsson, B., Luk, K., Lee, V., Trojanowski, J., & Björklund, A. (2017). Modeling Parkinson's disease pathology by combination of fibril seeds and alpha-synuclein overexpression in the rat brain. *Proceedings of the National Academy of Sciences of the United States of America*, *114*(39), E8284–E8293. <https://doi.org/10.1073/pnas.1710442114>
- The Tabula Sapiens Consortium. (2022). The Tabula Sapiens: A multiple-organ, single-cell transcriptomic atlas of humans [Publisher: American Association for the Advancement of Science]. *Science*, *376*(6594), eabl4896. <https://doi.org/10.1126/science.abl4896>
- Thomsen, M. B., Ferreira, S. A., Schacht, A. C., Jacobsen, J., Simonsen, M., Betzer, C., Jensen, P. H., Brooks, D. J., Landau, A. M., & Romero-Ramos, M. (2021). PET imaging reveals early and progressive dopaminergic deficits after intra-striatal injection of preformed alpha-synuclein fibrils in rats. *Neurobiology of Disease*, *149*, 105229. <https://doi.org/10.1016/j.nbd.2020.105229>
- Thrupp, N., Sala Frigerio, C., Wolfs, L., Skene, N. G., Fattorelli, N., Poovathingal, S., Fourné, Y., Matthews, P. M., Theys, T., Mancuso, R., de Strooper, B., & Fiers, M. (2020). Single-

Nucleus RNA-Seq Is Not Suitable for Detection of Microglial Activation Genes in Humans. *Cell Reports*, 32(13), 108189. <https://doi.org/10.1016/j.celrep.2020.108189>

- Tiklová, K., Nolbrant, S., Fiorenzano, A., Björklund, Å. K., Sharma, Y., Heuer, A., Gillberg, L., Hoban, D. B., Cardoso, T., Adler, A. F., Birtele, M., Lundén-Miguel, H., Volakakis, N., Kirkeby, A., Perlmann, T., & Parmar, M. (2020). Single cell transcriptomics identifies stem cell-derived graft composition in a model of Parkinson's disease [Number: 1 Publisher: Nature Publishing Group]. *Nature Communications*, 11(1), 2434. <https://doi.org/10.1038/s41467-020-16225-5>
- Trapnell, C. (2015). Defining cell types and states with single-cell genomics. *Genome Research*, 25(10), 1491–1498. <https://doi.org/10.1101/gr.190595.115>
- Travers, K. J., Chin, C.-S., Rank, D. R., Eid, J. S., & Turner, S. W. (2010). A flexible and efficient template format for circular consensus sequencing and SNP detection. *Nucleic Acids Research*, 38(15), e159. <https://doi.org/10.1093/nar/gkq543>
- Truong, D. D., Lamhamedi-Cherradi, S.-E., Porter, R. W., Krishnan, S., Swaminathan, J., Gibson, A., Lazar, A. J., Livingston, J. A., Gopalakrishnan, V., Gordon, N., Daw, N. C., Navin, N. E., Gorlick, R., & Ludwig, J. A. (2023). Dissociation protocols used for sarcoma tissues bias the transcriptome observed in single-cell and single-nucleus RNA sequencing. *BMC Cancer*, 23(1), 488. <https://doi.org/10.1186/s12885-023-10977-1>
- Tsukahara, T., Takeda, M., Shimohama, S., Ohara, O., & Hashimoto, N. (1995). Effects of brain-derived neurotrophic factor on 1-methyl-4-phenyl-1,2,3,6-tetrahydropyridine-induced parkinsonism in monkeys. *Neurosurgery*, 37(4), 733–739, discussion 739–741. <https://doi.org/10.1227/00006123-199510000-00018>
- Twelves, D., Perkins, K. S., & Counsell, C. (2003). Systematic review of incidence studies of Parkinson's disease. *Movement Disorders*, 18(1), 19–31. <https://doi.org/10.1002/mds.10305>
- Uhlen, M. (1989). Magnetic separation of DNA [Number: 6236 Publisher: Nature Publishing Group]. *Nature*, 340(6236), 733–734. <https://doi.org/10.1038/340733a0>
- Ungerstedt, U. (1968). 6-hydroxy-dopamine induced degeneration of central monoamine neurons. *European Journal of Pharmacology*, 5(1), 107–110. [https://doi.org/10.1016/0014-2999\(68\)90164-7](https://doi.org/10.1016/0014-2999(68)90164-7)
- Vallejos, C. A., Risso, D., Scialdone, A., Dudoit, S., & Marioni, J. C. (2017). Normalizing single-cell RNA sequencing data: Challenges and opportunities [Number: 6 Publisher: Nature Publishing Group]. *Nature Methods*, 14(6), 565–571. <https://doi.org/10.1038/nmeth.4292>
- Vamvaca, K., Volles, M. J., & Lansbury, P. T. (2009). The first N-terminal amino acids of alpha-synuclein are essential for alpha-helical structure formation in vitro and membrane binding in yeast. *Journal of Molecular Biology*, 389(2), 413–424. <https://doi.org/10.1016/j.jmb.2009.03.021>
- Van den Berge, K., Roux de Bézieux, H., Street, K., Saelens, W., Cannoodt, R., Saeys, Y., Dudoit, S., & Clement, L. (2020). Trajectory-based differential expression analysis for single-cell sequencing data [Number: 1 Publisher: Nature Publishing Group]. *Nature Communications*, 11(1), 1201. <https://doi.org/10.1038/s41467-020-14766-3>
- Van Den Eeden, S. K., Tanner, C. M., Bernstein, A. L., Fross, R. D., Leimpeter, A., Bloch, D. A., & Nelson, L. M. (2003). Incidence of Parkinson's Disease: Variation by Age,

- Gender, and Race/Ethnicity. *American Journal of Epidemiology*, 157(11), 1015–1022. <https://doi.org/10.1093/aje/kwg068>
- Vandereyken, K., Sifrim, A., Thienpont, B., & Voet, T. (2023). Methods and applications for single-cell and spatial multi-omics [Number: 8 Publisher: Nature Publishing Group]. *Nature Reviews Genetics*, 24(8), 494–515. <https://doi.org/10.1038/s41576-023-00580-2>
- Venter, J. C., Adams, M. D., Myers, E. W., Li, P. W., Mural, R. J., Sutton, G. G., Smith, H. O., Yandell, M., Evans, C. A., Holt, R. A., Gocayne, J. D., Amanatides, P., Ballew, R. M., Huson, D. H., Wortman, J. R., Zhang, Q., Kodira, C. D., Zheng, X. H., Chen, L., ... Zhu, X. (2001). The Sequence of the Human Genome [Publisher: American Association for the Advancement of Science]. *Science*, 291(5507), 1304–1351. <https://doi.org/10.1126/science.1058040>
- Vernon, A. C., Crum, W. R., Johansson, S. M., & Modo, M. (2011). Evolution of Extra-Nigral Damage Predicts Behavioural Deficits in a Rat Proteasome Inhibitor Model of Parkinson's Disease [Publisher: Public Library of Science]. *PLOS ONE*, 6(2), e17269. <https://doi.org/10.1371/journal.pone.0017269>
- Vicari, M., Mirzazadeh, R., Nilsson, A., Shariatgorji, R., Bjärterot, P., Larsson, L., Lee, H., Nilsson, M., Foyer, J., Ekvall, M., Czarnewski, P., Zhang, X., Svenningsson, P., Andrén, P. E., & Lundeberg, J. (2023). Spatial Multimodal Analysis of Transcriptomes and Metabolomes in Tissues [Pages: 2023.01.26.525195 Section: New Results]. <https://doi.org/10.1101/2023.01.26.525195>
- Vickaryous, M. K., & Hall, B. K. (2006). Human cell type diversity, evolution, development, and classification with special reference to cells derived from the neural crest. *Biological Reviews of the Cambridge Philosophical Society*, 81(3), 425–455. <https://doi.org/10.1017/S1464793106007068>
- Vickovic, S., Lötstedt, B., Klughammer, J., Mages, S., Segerstolpe, Å., Rozenblatt-Rosen, O., & Regev, A. (2022). SM-Omics is an automated platform for high-throughput spatial multi-omics. *Nature Communications*, 13(1), 795. <https://doi.org/10.1038/s41467-022-28445-y>
- Vickovic, S., Eraslan, G., Salmén, F., Klughammer, J., Stenbeck, L., Schapiro, D., Äijö, T., Bonneau, R., Bergensträhle, L., Navarro, J. F., Gould, J., Griffin, G. K., Borg, Å., Ronaghi, M., Frisén, J., Lundeberg, J., Regev, A., & Ståhl, P. L. (2019). High-definition spatial transcriptomics for in situ tissue profiling. *Nature methods*, 16(10), 987–990. <https://doi.org/10.1038/s41592-019-0548-y>
- Vinsland, E., & Linnarsson, S. (2022). Single-cell RNA-sequencing of mammalian brain development: Insights and future directions. *Development*, 149(10), dev200180. <https://doi.org/10.1242/dev.200180>
- Volpicelli-Daley, L. A. (2017). Effects of a-synuclein on axonal transport. *Neurobiology of Disease*, 105, 321–327. <https://doi.org/10.1016/j.nbd.2016.12.008>
- Volpicelli-Daley, L. A., Gamble, K. L., Schultheiss, C. E., Riddle, D. M., West, A. B., & Lee, V. M.-Y. (2014). Formation of alpha-synuclein Lewy neurite-like aggregates in axons impedes the transport of distinct endosomes. *Molecular Biology of the Cell*, 25(25), 4010–4023. <https://doi.org/10.1091/mbc.E14-02-0741>
- Volpicelli-Daley, L. A., Luk, K. C., Patel, T. P., Tanik, S. A., Riddle, D. M., Stieber, A., Meaney, D. F., Trojanowski, J. Q., & Lee, V. M. -. (2011). Exogenous alpha-Synuclein Fibrils

Induce Lewy Body Pathology Leading to Synaptic Dysfunction and Neuron Death. *Neuron*, 72(1), 57–71. <https://doi.org/10.1016/j.neuron.2011.08.033>

- Wang, L., Qu, L., Yang, L., Wang, Y., & Zhu, H. (2020). NanoReviser: An Error-Correction Tool for Nanopore Sequencing Based on a Deep Learning Algorithm. *Frontiers in Genetics*, 11.
- Wang, X., Allen, W. E., Wright, M. A., Sylwestrak, E. L., Samusik, N., Vesuna, S., Evans, K., Liu, C., Ramakrishnan, C., Liu, J., Nolan, G. P., Bava, F.-A., & Deisseroth, K. (2018). Three-dimensional intact-tissue sequencing of single-cell transcriptional states. *Science (New York, N.Y.)*, 361(6400), eaat5691. <https://doi.org/10.1126/science.aat5691>
- Wang, Z., Ma, H.-I., Li, J., Sun, L., Zhang, J., & Xiao, X. (2003). Rapid and highly efficient transduction by double-stranded adeno-associated virus vectors in vitro and in vivo. *Gene Therapy*, 10(26), 2105–2111. <https://doi.org/10.1038/sj.gt.3302133>
- Watson, J. D., & Crick, F. H. C. (1953). Molecular Structure of Nucleic Acids: A Structure for Deoxyribose Nucleic Acid [Number: 4356 Publisher: Nature Publishing Group]. *Nature*, 171(4356), 737–738. <https://doi.org/10.1038/171737a0>
- Wei, X., Fu, S., Li, H., Liu, Y., Wang, S., Feng, W., Yang, Y., Liu, X., Zeng, Y.-Y., Cheng, M., Lai, Y., Qiu, X., Wu, L., Zhang, N., Jiang, Y., Xu, J., Su, X., Peng, C., Han, L., ... Gu, Y. (2022). Single-cell Stereo-seq reveals induced progenitor cells involved in axolotl brain regeneration [Publisher: American Association for the Advancement of Science]. *Science*, 377(6610), eabp9444. <https://doi.org/10.1126/science.abp9444>
- Weintraub, D., Koester, J., Potenza, M. N., Siderowf, A. D., Stacy, M., Voon, V., Whetteckey, J., Wunderlich, G. R., & Lang, A. E. (2010). Impulse Control Disorders in Parkinson Disease: A Cross-Sectional Study of 3090 Patients. *Archives of Neurology*, 67(5), 589–595. <https://doi.org/10.1001/archneurol.2010.65>
- Wen, F., Tang, X., Xu, L., & Qu, H. (2022). Comparison of single-nucleus and single-cell transcriptomes in hepatocellular carcinoma tissue. *Molecular Medicine Reports*, 26(5), 339. <https://doi.org/10.3892/mmr.2022.12855>
- Wenger, A. M., Peluso, P., Rowell, W. J., Chang, P.-C., Hall, R. J., Concepcion, G. T., Ebler, J., Functammasan, A., Kolesnikov, A., Olson, N. D., Töpfer, A., Alonge, M., Mahmoud, M., Qian, Y., Chin, C.-S., Phillippy, A. M., Schatz, M. C., Myers, G., DePristo, M. A., ... Hunkapiller, M. W. (2019). Accurate circular consensus long-read sequencing improves variant detection and assembly of a human genome [Number: 10 Publisher: Nature Publishing Group]. *Nature Biotechnology*, 37(10), 1155–1162. <https://doi.org/10.1038/s41587-019-0217-9>
- Wenning, G. K., Odin, P., Morrish, P., Rehncrona, S., Widner, H., Brundin, P., Rothwell, J. C., Brown, R., Gustavii, B., Hagell, P., Jahanshahi, M., Sawle, G., Björklund, A., Brooks, D. J., Marsden, C. D., Quinn, N. P., & Lindvall, O. (1997). Short- and long-term survival and function of unilateral intrastriatal dopaminergic grafts in Parkinson's disease. *Annals of Neurology*, 42(1), 95–107. <https://doi.org/10.1002/ana.410420115>
- Wolf, F. A., Angerer, P., & Theis, F. J. (2018). SCANPY: Large-scale single-cell gene expression data analysis. *Genome Biology*, 19(1), 15. <https://doi.org/10.1186/s13059-017-1382-0>
- Wolock, S. L., Lopez, R., & Klein, A. M. (2019). Scrublet: Computational Identification of Cell Doublets in Single-Cell Transcriptomic Data [Publisher: Elsevier]. *Cell Systems*, 8(4), 281–291.e9. <https://doi.org/10.1016/j.cels.2018.11.005>

- Workman, R. E., Tang, A. D., Tang, P. S., Jain, M., Tyson, J. R., Razaghi, R., Zuzarte, P. C., Gilpatrick, T., Payne, A., Quick, J., Sadowski, N., Holmes, N., de Jesus, J. G., Jones, K. L., Soulette, C. M., Snutch, T. P., Loman, N., Paten, B., Loose, M., ... Timp, W. (2019). Nanopore native RNA sequencing of a human poly(A) transcriptome [Number: 12 Publisher: Nature Publishing Group]. *Nature Methods*, 16(12), 1297–1305. <https://doi.org/10.1038/s41592-019-0617-2>
- Wu, X., Zhang, Q., Gong, L., & He, M. (2021). Sequencing-Based High-Throughput Neuroanatomy: From Mapeq to Briceq and Beyond. *Neuroscience Bulletin*, 37(5), 746–750. <https://doi.org/10.1007/s12264-021-00646-3>
- Xia, C., Fan, J., Emanuel, G., Hao, J., & Zhuang, X. (2019). Spatial transcriptome profiling by MERFISH reveals subcellular RNA compartmentalization and cell cycle-dependent gene expression. *Proceedings of the National Academy of Sciences of the United States of America*, 116(39), 19490–19499. <https://doi.org/10.1073/pnas.1912459116>
- Xie, W., Li, X., Li, C., Zhu, W., Jankovic, J., & Le, W. (2010). Proteasome inhibition modeling nigral neuron degeneration in Parkinson's disease. *Journal of Neurochemistry*, 115(1), 188–199. <https://doi.org/10.1111/j.1471-4159.2010.06914.x>
- Xilouri, M., Brekk, O. R., & Stefanis, L. (2013). Alpha-synuclein and Protein Degradation Systems: A Reciprocal Relationship. *Molecular Neurobiology*, 47(2), 537–551. <https://doi.org/10.1007/s12035-012-8341-2>
- Xu, C., Lopez, R., Mehlman, E., Regier, J., Jordan, M. I., & Yosef, N. (2021). Probabilistic harmonization and annotation of single-cell transcriptomics data with deep generative models [Publisher: John Wiley & Sons, Ltd]. *Molecular Systems Biology*, 17(1), e9620. <https://doi.org/10.15252/msb.20209620>
- Yan, L., & Sun, X. (2023). Benchmarking and integration of methods for deconvoluting spatial transcriptomic data. *Bioinformatics*, 39(1), btac805. <https://doi.org/10.1093/bioinformatics/btac805>
- Yang, S., Corbett, S. E., Koga, Y., Wang, Z., Johnson, W. E., Yajima, M., & Campbell, J. D. (2020). Decontamination of ambient RNA in single-cell RNA-seq with DecontX. *Genome Biology*, 21(1), 57. <https://doi.org/10.1186/s13059-020-1950-6>
- Yao, K., Rochman, N. D., & Sun, S. X. (2019). Cell Type Classification and Unsupervised Morphological Phenotyping From Low-Resolution Images Using Deep Learning [Number: 1 Publisher: Nature Publishing Group]. *Scientific Reports*, 9(1), 13467. <https://doi.org/10.1038/s41598-019-50010-9>
- Yao, Z., Velthoven, C. T. J. v., Kunst, M., Zhang, M., McMillen, D., Lee, C., Jung, W., Goldy, J., Abdelhak, A., Baker, P., Barkan, E., Bertagnolli, D., Campos, J., Carey, D., Casper, T., Chakka, A. B., Chakrabarty, R., Chavan, S., Chen, M., ... Zeng, H. (2023). A high-resolution transcriptomic and spatial atlas of cell types in the whole mouse brain [Pages: 2023.03.06.531121 Section: New Results]. <https://doi.org/10.1101/2023.03.06.531121>
- Yasuhara, T., Shingo, T., Kobayashi, K., Takeuchi, A., Yano, A., Muraoka, K., Matsui, T., Miyoshi, Y., Hamada, H., & Date, I. (2004). Neuroprotective effects of vascular endothelial growth factor (VEGF) upon dopaminergic neurons in a rat model of Parkinson's disease. *The European Journal of Neuroscience*, 19(6), 1494–1504. <https://doi.org/10.1111/j.1460-9568.2004.03254.x>

- Young, M. D., & Behjati, S. (2020). SoupX removes ambient RNA contamination from droplet-based single-cell RNA sequencing data. *GigaScience*, 9(12), giaa151. <https://doi.org/10.1093/gigascience/giaa151>
- Yuan, L., Chen, X., Zhan, H., Gilbert, H. L., & Zador, A. M. (2023). Massive Multiplexing of Spatially Resolved Single Neuron Projections with Axonal BARseq [Pages: 2023.02.18.528865 Section: New Results]. <https://doi.org/10.1101/2023.02.18.528865>
- Zeisel, A., Hochgerner, H., Lönnerberg, P., Johnsson, A., Memic, F., Zwan, J. v. d., Häring, M., Braun, E., Borm, L. E., Manno, G. L., Codeluppi, S., Furlan, A., Lee, K., Skene, N., Harris, K. D., Hjerling-Leffler, J., Arenas, E., Ernfors, P., Marklund, U., & Linnarsson, S. (2018). Molecular Architecture of the Mouse Nervous System [Publisher: Elsevier]. *Cell*, 174(4), 999–1014.e22. <https://doi.org/10.1016/j.cell.2018.06.021>
- Zeng, H., Huang, J., Zhou, H., Meilandt, W. J., Dejanovic, B., Zhou, Y., Bohlen, C. J., Lee, S.-H., Ren, J., Liu, A., Tang, Z., Sheng, H., Liu, J., Sheng, M., & Wang, X. (2023). Integrative in situ mapping of single-cell transcriptional states and tissue histopathology in a mouse model of Alzheimer's disease [Number: 3 Publisher: Nature Publishing Group]. *Nature Neuroscience*, 26(3), 430–446. <https://doi.org/10.1038/s41593-022-01251-x>
- Zhang, G., Taneja, K. L., Singer, R. H., & Green, M. R. (1994). Localization of pre-mRNA splicing in mammalian nuclei [Number: 6508 Publisher: Nature Publishing Group]. *Nature*, 372(6508), 809–812. <https://doi.org/10.1038/372809a0>
- Zhang, H., Hunter, M. V., Chou, J., Quinn, J. F., Zhou, M., White, R. M., & Tansey, W. (2023). BayesTME: An end-to-end method for multiscale spatial transcriptional profiling of the tissue microenvironment. *Cell Systems*, 14(7), 605–619.e7. <https://doi.org/10.1016/j.cels.2023.06.003>
- Zhang, Y., Ma, Y., Huang, Y., Zhang, Y., Jiang, Q., Zhou, M., & Su, J. (2020). Benchmarking algorithms for pathway activity transformation of single-cell RNA-seq data. *Computational and Structural Biotechnology Journal*, 18, 2953–2961. <https://doi.org/10.1016/j.csbj.2020.10.007>
- Ziegenhain, C., Hendriks, G.-J., Hagemann-Jensen, M., & Sandberg, R. (2022). Molecular spikes: A gold standard for single-cell RNA counting [Number: 5 Publisher: Nature Publishing Group]. *Nature Methods*, 19(5), 560–566. <https://doi.org/10.1038/s41592-022-01446-x>
- Zrimec, J., Buric, F., Kokina, M., Garcia, V., & Zelezniak, A. (2021). Learning the Regulatory Code of Gene Expression. *Frontiers in Molecular Biosciences*, 8.

Acknowledgement

Finally, this thesis comes to an end. In this last section, I would like to thank all of you who made this thesis a feat more feasible, enjoyable, and eventful. During my nearly five years of working on the material on these pages, there were many ups and downs. And as on any reputable roller coaster ride, you can't be sure of what awaits you behind the next turn. I could not have finished or enjoyed this ride without you.

First and foremost, **Tomas**, thank you for taking me on as a student on a single cold email basis. I have learned many things from you in the half a decade I have spent in MNM, possibly more than I could have learned in most places. Looking back, I can clearly see how I grew as a scientist. I believe you have played a significant part in this development. You have definitely inspired my thinking about science and helped me many times to get my thoughts and plans, at times slightly scattered, into a neat line. I still have yet to meet another researcher who puts together a server in the morning, troubleshoots an AAV production in the afternoon, catches up on the spatial sequencing in the evening, and reads up on the newest research in the gaps of time in between.

I'm looking forward to our continuing collaboration and pushing the remaining projects together over the finish line!

I would like to express my thanks to my co-supervisors, **Malin P.** and **Malin Å.** for not only technical support during my Ph.D. but also for all the inspiring conversations with many moments that clarified questions I had not yet managed to pose. **Malin Å.**, I am very grateful we got to sit back-to-back in the office. You have been my rock in many moments, and I will always appreciate your willingness to have a conversation or share advice that a 30-year-old woman should definitely already live by. Ever since your arrival, you have inspired me to take more care of my life outside of the lab.

Without a steady supply of all my "urgent" reagents from **Susanne**, my lab work would be impossible. Thank you for being so helpful with the everyday orders as well as with the obscure corners of the reagent re-re-re-distribution networks. My thanks also belong to **Olga G.** and **Lisette E.** You keep this land of academia a lawful place, and I am very thankful for all the care you give to the EMV Ph.D. students.

The past and present MNM members are some of the main people who made my journey at BMC enjoyable. Starting from the OGs, **Marcus**, you have been a great Master's thesis supervisor and a great lab mate. On the professional side, I cannot imagine a better person to help me with my sequencing (and re-sequencing) runs. I appreciate all the banter in the lab; it always lifted my mood that someone enjoys a little bit of sardonic humor as much as I do. My thanks also belong to

Morgan, my lab mate during my thesis. How well integrated some people are never fails to amaze me; thank you for providing that inspiration and also for the illustrations you have contributed. **Martino** - as you mention in your thesis, we were in this together from the beginning till the end, and that's a damn long time! I'm very glad we got to share this journey. You have inspired the nearly non-existent extrovert within me to interact more with strangers and appreciate parts of life (food is one example I can think of) I hadn't paid much attention to. **Janitha**, thank you for all your help in the beginning and for the after-work drinks. You were a pleasure to work with! **Sara**. Are you lost baby girl? You have made my time in BMC infinitely better over the years. I would say that we have made quite the friendship journey, from me supervising your separating sludge and the slightly less disgusting (a.k.a. "purified") water to having "most horrible movies of all times" evenings. You are probably my largest respite in the BMC from the world of science, and I hope that I contribute to your well-being as much as you do to mine. The latest addition to the MNM gang, **Joquin**. You never cease to surprise me. You are such a hard worker, yet you always seem to look at life from such a light angle (for an eastern... ehm, central European, at least). I don't remember ever seeing you visibly tired. It must be all the yerba mate!

Maria S., thank you for your thoughtfulness. For always taking such good care of students and never forgetting a dessert for the floor's vegans! I sincerely appreciate all the small gestures you have made over the years. **Elna**, thank you for all the kind words and helpful conversations and for being such a straightforward person. I hope to see you at the next DnD evening! **Andreas**, tack för allt. För alla samtalen och för att du inte bytte till engelska varje gång jag stötte på min svenska! Jag ber om ursäkt att jag missade Miracle, men jag hoppas att vi fortsätter med A10 filmkvällar! **Lautaro**, thank you for all the thought-provoking discussions we have had. You are such a well-read person, and you have inspired me to take up other printed material besides research papers again. I cannot forget **Kajsa**, the other bioinformatician at A10, unfortunately belonging to the enemy R team (kidding!). You have made my office days much brighter, especially during the long, dreary, and slushy Skåne winters. You are my go-to person when it comes to information I should definitely know but do not. It has been a pleasure sharing an office with you, and I am glad we will share it for my remaining time in BMC! **Filip**, you have been, together with Kajsa and Malin, an inspiration for a well-balanced life; I hope some of it will rub off on me after your return to BMC. **Carolina**, I am very happy we got to know each other and even acted in a (PhD) movie together. Why have you stopped having the parties in your apartment (above mine)? **Alex S.**, to me, you are the pinnacle of scientific curiosity; I could swear that there is no topic in the world you find uninteresting. You are such a kind and joyful person, and I hope you're delving into some mind-exploding science over in the great 'Murica. **Laura**, you are a BMC spirit of joy. I have honestly never met anyone as optimistic as you in my life. **Edoardo**, your post-PhD transformation has been an inspiration and hope to me, especially in recent weeks. And **Robert**, thank you for the A10 spirit and the company around the lunch table!

To my Åre and MedBioInfo gang. Thank you all for turning this part of my Ph.D. into some of my best times. I hope we will get the whole Cruë de la Åre together again, be it at a conference or outside! **Haris**, you have been a fantastic friend since we met all those years ago. You are someone I can share so much of my humor with, as well as the more serious conversations. It has been a privilege to gain you as a friend and a fellow bioinformatic struggler! **Patrick**, you have inspired me to take my social skills and gym training to a new level. **Isabelle**, having your company on our skiing trip has been a pleasure. And **Alrik**, you were the MedBioInfo-BMC bridge I had kept

hoping for since starting the program. Thank you for your company, for (not only) scientific discussions, as well as for introducing me to the Copenhagen tea scene!

And finally, to my friends and family. Kära **Oskar**, du har varit min bästa vän i Sverige i så många år nu! Tack för alla möjliga och omöjliga diskussioner vi har haft och för att ha stött mig genom mina bästa och sämsta tider. Jag vet att vi har många äventyr framför oss, och jag lovar att äntligen läsa din bok nu när jag är klar med min doktorsexamen! **Magnus**, thank you for sharing hundreds of kilometers of pedalling with me and for always being up for new adventures. **Andre**, you are the cultural hub of the group and I aspire to get my Swedish to your level one day! **Amina**, thank you for being the best corridor-mate and co-traumatized Slavic soul one can ask for. **Samed**, and **Tilda**, my many thanks belong to you for the many hours we spent on the disc-golf court. Let's crush this years championship! **Miklas**, you are probably one of my most productive friends, I will never forget driving hours to check out houses, crawling with you underneath a house ladden with a billion of spider nests, hammering down planks in a dusty attic, and the illegal joint Swedish sessions our small group had during the pandemic (and sorry about the drama). **Cornelia** and **Victoria**, thank you for opening my world with your amazing book club choices. **Juhan**, **Paola** and the whole NYD ensemble, thank you for all the fun and back-breaking times by the pole.

Moje díky patří také mým **rodičům**, **bráchovi** a celé **rodině**, za útočiště, když se mi stýská po Čechách, za každoroční zdravotní údržbu a hlavně za všechnu podporu, co se mi za ty léta dostalo. Bez Vás bych se do Švédska stěhovala horko těžko. **Brácha**, tvoje společnost se nikdy neomrzí a bez tvých řidičských schopností bychom byli v Itálii ztraceni! Ráda bych také poděkovala **Marušce**, za jeden z mých nejoblíbenějších hrníčků, který mi udržoval stálou hladinku kofeinu a dobré nálady a za to, že nám všem ukázala, co znamená správná turistická výbava, když my ostatní jsme chodili po horách v kolekci pantoflí, sandalů a kroksů.

Finally, a big thanks belongs to **Leo**. You have done so much to keep me sane and grounded through the past years. We went through some tough times together but always came out on the other end, having understood each other better. You are the best running mate one can ask for, and I can't fully express how thankful I am to have you in my life!

And last but not least, **Jim**. I don't know where I (and the cover of this thesis) would be without you. You have been my comrade through many questionable adventures, a very responsible dog dad, and someone alongside whom I became a better person. I aspire to have the passion and dedication to intellectual endeavors you have shown throughout our years together, as well as your skills of cutting through bullshit while (occasionally) putting up with a (teensy) bit of mine. Thank you for going through this journey with me, and helping me not trip over myself too much.

APPENDIX (Papers I-IV)

About the author

JANA RÁJOVÁ has previously studied biotechnology at LTH in Lund. She joined the Molecular Neuromodulation group in 2018 under the supervision of Tomas Björklund. During her Ph.D. studies, Jana has been working on developing and applying advanced spatial transcriptomics tools. On the 23rd of October 2023, Jana will defend her thesis titled "Development of Spatial Sequencing Methods and Applications for Brain Circuit Repair in Parkinson's Disease" at Segerfalksalen, Wallenberg Neuroscience Center at Lund University.

